Synthesis and Properties of Polymer/Layered Silicate Clay Nanocomposites

A thesis submitted to the

University of Pune

For the degree of

DOCTOR OF PHILOSOPHY

in

CHEMISTRY

by

S. R. MALLIKARJUNA

Division of Polymer Science and Engineering
National Chemical Laboratory
PUNE 411 008

January 2009

DECLARATION

I hereby declare that the thesis entitled **"Synthesis and properties of polymer/layered silicate clay nanocomposites"** submitted for Ph. D. degree to the University of Pune has been carried out at National Chemical Laboratory, Pune, India under the supervision of **Dr. S. Sivaram,** Division of Polymer Science and Engineering, National Chemical Laboratory, Pune-411008. The work is original and has not been submitted in part or full by me for any degree or diploma to this or any other University.

January 2009   (**S. R. Mallikarjuna**)

Pune

CERTIFICATE

Certified that the work incorporated in this thesis entitled **"Synthesis and properties of polymer/layered silicate clay nanocomposites"** submitted by **Mr. S. R. Mallikarjuna** was carried out by the candidate at National Chemical Laboratory, Pune-08, under my supervision. Such materials as obtained from other sources have been duly acknowledged.

January 2009

Pune

Dr. S. Sivaram

(Research Supervisor)

Dedicated to

My Family

ACKNOWLEDGEMENT

*I am deeply and thoroughly indebted to my family members for their sacrifices, patience, and kind support throughout my upbringing. I am deeply indebted to my **Doddappa** and Dr. Thatha for their values in life that I have had the good fortune to see, experience and learn, and wish to specifically thank them for being instrumental in shaping my career in education.*

Finally, my acknowledgement would not be complete without thanking the Almighty, for the strength and determination to put my chin up when faced with hardships in life.

(S. R. Mallikarjuna)

Table of Contents

Chapter 1: Introduction

Chapter 2: Scope and objectives

Chapter 3: Poly(urethane)/Clay Nanocomposites via *in-situ* Solution Polymerization

Chapter 4: Poly(carbonate)/Clay Nanocomposites via *in-situ* Melt Polymerization

Chapter 5: Syndiotactic Poly(styrene)/Clay Nanocomposites via Solvent Casting

Chapter 6: Poly(propylene)/Clay Nanocomposites via Melt Mixing

Chapter 7: Summary and Conclusions

Synthesis and properties of polymer/layered silicate clay nanocomposites

Abstract

Polymer nanocomposites are a novel class of composites that are particle-filled polymers, in which at least one dimension of the dispersed particles is in the nanometer range. Amongst all the potential nanocomposite precursors, those based on clay and layered silicates have been more widely investigated. Large improvements in properties are achieved when the clay layers are thoroughly dispersed and exfoliated in the polymer matrix. Therefore, in this thesis various strategies were explored to obtain better dispersion of clay layers in selected polymers and to study the property enhancements of the resultant nanocomposites.

The present thesis is organized and presented in seven chapters. A brief overview of preparation, properties and application of polymer clay nanocomposites are discussed in the first chapter. The scope and objectives of the thesis are described the second chapter. In third chapter, various factors that affect the structure and dispersion of clay in the PU were established. A thermoplastic poly(urethane)/clay nanocomposites based on poly(caprolactone) diol were prepared and dynamic mechanical properties of the thermoplastic poly(urethane)s were correlated with the organoclay used. Fourth chapter describes the preparation and properties of exfoliated polycarbonate/clay nanocomposites via *in-situ* polymerization using a novel modifier for the clay, which contain a reactive bisphenol group that can be incorporated in poly(carbonate) backbone during in-situ polymerization. Interaction between the poly(carbonate) chains and the clay layers were enhanced due to enchainment and attachment of the polymer to clay surface through electrostatic forces. In the fifth chapter, the effect of ionomer content and cation type on the intercalation/exfoliation efficiency of the sulfonated syndiotactic polystyrene ionomer/organoclay nanocomposites is described. It was found that ionomers with higher degree of sulfonation, larger size and polarizability of cations in ionomer lead to better dispersion of clay in the polymer matrix. Their crystallization behavior was correlated

with the dispersion of the clay. In sixth chapter, the efficiency of potassium succinate-*g*-polypropylene as compatibilizer for dispersion of clay in a higher molecular weight poly(propylene) matrix was evaluated and compared with maleic anhydride-*g*-polypropylene. The mechanical and crystallization behavior were correlated with the dispersion of organoclay in the PP matrix.

Thus, it has been demonstrated that when the interaction of the polymer chains with the layered silicate clay improved either by modifying the surface of the clay to suitably interact with polymer or modify the polymer by functionalization results in better dispersion. The properties of the nanocomposites obtained were correlated with the structure of the clay dispersion in the polymer matrix.

Glossary

ABS	Poly(acrylonitrile-butadiene-styrene)
APS	Aminopropyl siloxane
ATRP	Atom transfer radical polymerization
BPA	Bisphenol-A
BPAIMI	12,12-bis(4-hydroxyphenyl) tridecyl-2,3-dimethylimidazolium bromide
BPAIM-MMT	12,12-bis(4-hydroxyphenyl) tridecyl-2,3-dimethylimidazolium ion exchanged montmorillonite
BPAP-MMT	12,12-bis(4-hydroxyphenyl) tridecyltriphenylphosphonium ion exchanged montmorillonite
C16IM-MMT	Hexadecyl-2,3-dimethylimidazolium ion exchanged montmorillonite
C16P-MMT	Hexadecyltriphenylphosphonium ion exchanged montmorillonite
CEC	Cation exchange capacity
DBA	Dibutyl amine
DBTDL	Dibutyl tin dilaurate
DGEBA	Diglycidyl ether of bisphenol A
DMA	Dynamic mechanical analysis
DSC	Differential scanning calorimetry
DPC	Diphenyl carbonate
FTIR	Fourier Transform-Infra Red spectrum
HDT	Heat distorsion temperature
IPDI	Isophorone diisocyanate
KPPSA	Potassium succinate-g-polypropylene ionomer
KSsPS	Potassium salt of sulfonated syndiotactic polystyrene
LAH	Lithium aluminum hydride
LOI	Loss on ignition
MDI	4,4'-diphenylmethane diisocyanate

MMT	Montmorillonite
N-6	Nylon-6
NaSsPS	Sodium salt of Sulfonated syndiotactic polystyrene
NMR	Nuclear Magnetic Resonance
1-OH(MMT)	N-(2-hydroxyethyl-N,N-dimethyl-N-hexadecylammonium cation modified montmorillonite
2-OH(MMT)	N,N-bis(2-hydroxyethyl-N-methyl-N-hexadecylammonium cation modified montmorillonite
3-OH(MMT)	N,N-bis(2-hydroxyethyl-N-methyl-N-(hydroxymethyl)octadecyl ammonium cation modified montmorillonite
PBO	Polybenzoxazole
PBS	Polybutylene succinate
PC	Polycarbonate
PCL	Polycarolactone
PCN	Polymer clay nanocomposites
PEO	Polyethylene oxide
PET	Poly(ethylene terepthalate)
PHA	Polyhydroxamide
PLA	Polylactic acid
PMMA	Poly(methyl methacrylate)
PNC	Polymer nanocomposites
PP	Polypropylene
PPG	Poly(propylene glycol)
PPMA	Maleated polypropylene
PS	Polystyrene
PtBA	Poly(t-butyl acrylate)
PTMG	Poly(tetramethylene glycol)
PTFE	Polytetrafluroethylene
PU	Polyurethane
PVDF	Polyvinylidene fluoride

RbSsPS	Rubidium salt of sulfonated syndiotactic polystyrene
SEC	Size exclusion chromatography
sPS	Syndiotactic polystyrene
SsPS	Sulfonated syndiotactic polystyrene
T_{CC}	Crystallization peak temperature on cooling
TCE	1,1,2-Trichloroethane
TDI	Toluene diisocyanate
TEM	Transmission electron micrograph
TMAH	Tetramethylammonium hydroxide
TMS	Tetramethylsilane
TMP	Trimethylol propane
T_g	Glass transition temperature
TGA	Thermogravimetric analysis
TPU	Thermoplasic polyurethane
WAXD	Wide angle X-ray diffraction

List of Figures

List of Tables

List of Schemes

Chapter 1

Introduction

1. Introduction

1.1 Polymer Nanocomposites

Materials are key components of our civilization. We ascribe the major historical landmarks of our society to materials with epithets, such as, the stone age, bronze age, iron age, steel age (the industrial revolution), polymer age, silicon age, etc. This reflects the importance of materials in the evolution of our society. As the 21st century unfolds, it is becoming even more apparent that the next technological frontiers will unfold through a better understanding of structure-property relationship in materials and their functions. The emerging importance of nanoscale and the associated excitement surrounding nanoscience and technology affords unique opportunities to create novel materials with unique and useful properties. These novel materials promise new applications by exploiting the unique synergisms between constituents that only occur when the length scale of the morphology and the critical length associated with the fundamental physics of a given property coincide.

Polymer nanocomposites (PNC) are a novel class of composites that are particle-filled polymers in which, at least, one dimension of the dispersed particles is in the nanometer range. Polymer nanocomposites have been an area of intense industrial and academic research for the past twenty years. PNCs represent an alternative to conventional filled polymers or polymer blends– a staple of the modern plastics industry. In contrast to conventional composites, where the reinforcement is of the order of microns, PNCs are exemplified by discrete constituents of the order of a few nanometers.

One can distinguish three types of nanocomposites depending on how many dimensions of the dispersed particles are in the nanometer range. When the three dimensions are in the order of nanometers, we are dealing with isodimensional nanoparticles, such as spherical silica nanoparticles obtained by *in-situ* sol gel methods[1,2] or by polymerization promoted directly from their surface[3], but also can include semiconductor nanoclusters[4] and others . When two dimensions are in the nanometer scale and the third is larger, forming an elongated structure, we speak about nanotubes or whiskers as, for example,

carbon nanotubes[5] or cellulose whiskers[6,7] which are extensively studied as reinforcing nanofillers yielding materials with exceptional properties. The third type of nanocomposites is characterized by only one dimension in the nanometer range. In this case the filler is present in the form of sheets of one to a few nanometer thick to hundreds to thousands nanometers long. This family of composites can be gathered under the name of polymer-layered nanocomposites.

Amongst all the potential nanocomposite precursors, those based on clay and layered silicates have been more widely investigated probably because the starting clay materials are easily available and their intercalation chemistry has been studied for a long time[8,9]. The important characteristics pertinent to application of clay minerals in polymer nanocomposites are their rich intercalation chemistry, high strength and stiffness and higher aspect ratio of individual platelets, abundance in nature and low cost. First, their unique layered structure and high intercalation capabilities allow them to be chemically modified to be compatible with polymers, which make them particularly attractive in the development of clay-based polymer nanocomposites. In addition, their relatively low layer charge (x = 0.2–0.6) implies a relatively weak force between adjacent layers, making the interlayer cations exchangeable. Therefore, intercalation of inorganic and organic cations and other molecules into the interlayer space are facile, which is an important aspect in the preparation of polymer nanocomposites. Among the smectite clays, MMT and hectorite are the most commonly used while others are sometimes useful depending on the targeted applications. Moreover, smectite clays are naturally not nanoparticles; however, they can be exfoliated or delaminated into nanometer platelets with a thickness of about 1 nm and an aspect ratio of 100–1500 and surface areas of 700–800 m^2/g. Each platelet has very high strength and stiffness and can be regarded as a rigid inorganic polymer whose molecular weight (ca.1.3×10^8) is much larger than that of a typical polymer. Therefore, very low loading of clays is required to achieve equivalent properties compared to the conventional composites. Finally, and importantly, they are ubiquitous in nature and, therefore, inexpensive. Owing to the nanometer-size particles obtained by dispersion, these nanocomposites exhibit markedly improved mechanical, thermal, optical and physico-chemical properties when compared with the pure polymer

or conventional (microscale) composites. There are several reviews and books published highlighting the major developments in this area of polymer/clay nanocomposites and discuss various preparation techniques, characterization and the properties that those materials can display; their potential and commercial applications[10-25]. In this chapter, a brief overview of preparation, properties and application of polymer clay nanocomposites is discussed with a special emphasis on choice of the organoclay and organo-modification for the preparation of various polymer clay nanocomposites.

1.2   Structure of clay and the organoclay

Layered silicates commonly used in nanocomposites belong to the structural family known as the 2:1 phyllosilicates. Their crystal lattice consists of two-dimensional layers where a central octahedral sheet of alumina or magnesia is fused to two external silica tetrahedron by the tip so that the oxygen ions of the octahedral sheet also belong to the tetrahedral sheets. The layer thickness is around 1 nm and the lateral dimensions of these layers may vary from 300 Å to several microns and even larger depending on the particular silicate. These layers organize themselves to form stacks with a regular van der Walls gap in between them called the interlayer or the gallery. Isomorphic substitution within the layers (for example, Al^{3+} replaced by Mg^{2+} or by Fe^{2+} or Mg^{2+} replaced by Li.) generates negative charges that are counterbalanced by alkali or alkaline earth cations situated in the interlayer. As the forces that hold the stacks together are relatively weak, the intercalation of small molecules between the layers becomes easier[8].

In order to mix these hydrophilic layered silicates with polymers, it has to be modified in to organophilic (organoclay) by exchanging the cations of the interlayer with organic cationic surfactants such as alkylammonium or alkylphosphonium (onium) salts. The maximum extent to which these cations can be exchanged is called cation exchange capacity (CEC), and generally expressed in mequiv/100 g. Montmorillonites, hectorite and saponite are the most commonly used layered silicates. The organoclays prepared are generally characterized by WAXD and TGA. Depending on the chain length of the onium cations, and the way in which it aligns in the interlayer gallery, the interlayer distance changes and can be characterized by observing the characteristic shift for the

001 peak by WAXD. The organic content in the organoclay can be obtained from thermogravimetric analysis by measuring the weight loss at 900 °C. In some of the studies, for reducing the hydrophilicity of the clays, the hydroxyl groups at the edges of the platelets are reacted with silane coupling agents[26,27]

Nowadays, several pristine and organoclays are available commercially. Commercial organoclays include Cloisite 10A, 15A, 20A and 30B produced from Southern Clay Products (U.S.A.)[28], Bentone 107, 108, 109 and 2010 from Elementis Specialties Company[29], Nanomer 1.30P, 1.31PS, 1.44P, 1.44PS, 1.44PT and 1.28E from Nanocor, Inc. (U.S.A.)[32], Nanofil 2, 5, 9, SE 3000 and SE 3010 from Sud-Chemie (Germany)[33] as well as Dellite 72T from Laviosa Chimica Mineraria (Italy). Synthetic fluoromica clays (Somasif ME100) are supplied to Asian customers by Co-op Chemicals, Japan. Most of these commercially available organoclays are modified with ammonium cations and few of them are with silane modification.

1.3   Types of polymers used for nanocomposites preparation with layered silicates

Although the intercalation chemistry of polymers when mixed with appropriately modified layered silicates has long been known [32, 8], the field of polymer/clay nanocomposites has gained momentum only recently. Two major findings have stimulated the revival of interest in these materials: first the report from the Toyota research group of a nylon-6 (PA-6)/montmorillonite nanocomposite[33], which showed pronounced improvements in thermal and mechanical properties; and second the observation by Vaia *et al* that it is possible prepare nanocomposite by melt mixing the polymers with layered silicates[34]. The large variety of polymer systems used in nanocomposites preparation with layered silicate can be conveniently classified into vinyl polymers, condensation polymers, polyolefins, specialty polymers and biodegradable polymers and are thoroughly reviewed elsewhere[15].

1.4   Structure of nanocomposites and their characterization

Nanocomposites can be classified into three types depending on the structure and arrangement of the clay in the polymer matrix. They are (a) intercalated nanocomposites, in which the polymer chains are inserted in the interlayer gallery and increases the interlayer distance resulting in a well ordered multi-layer morphology built up with alternating polymeric and inorganic layers (b) flocculated nanocomposites which are similar to intercalated nanocomposites wherein the clay platelet sizes have been increased by flocculation due to hydroxylated edge-edge interaction and (c) exfoliated or delaminated nanocomposites, where the individual clay layers are separated and uniformly distributed in a continuous polymer matrix.
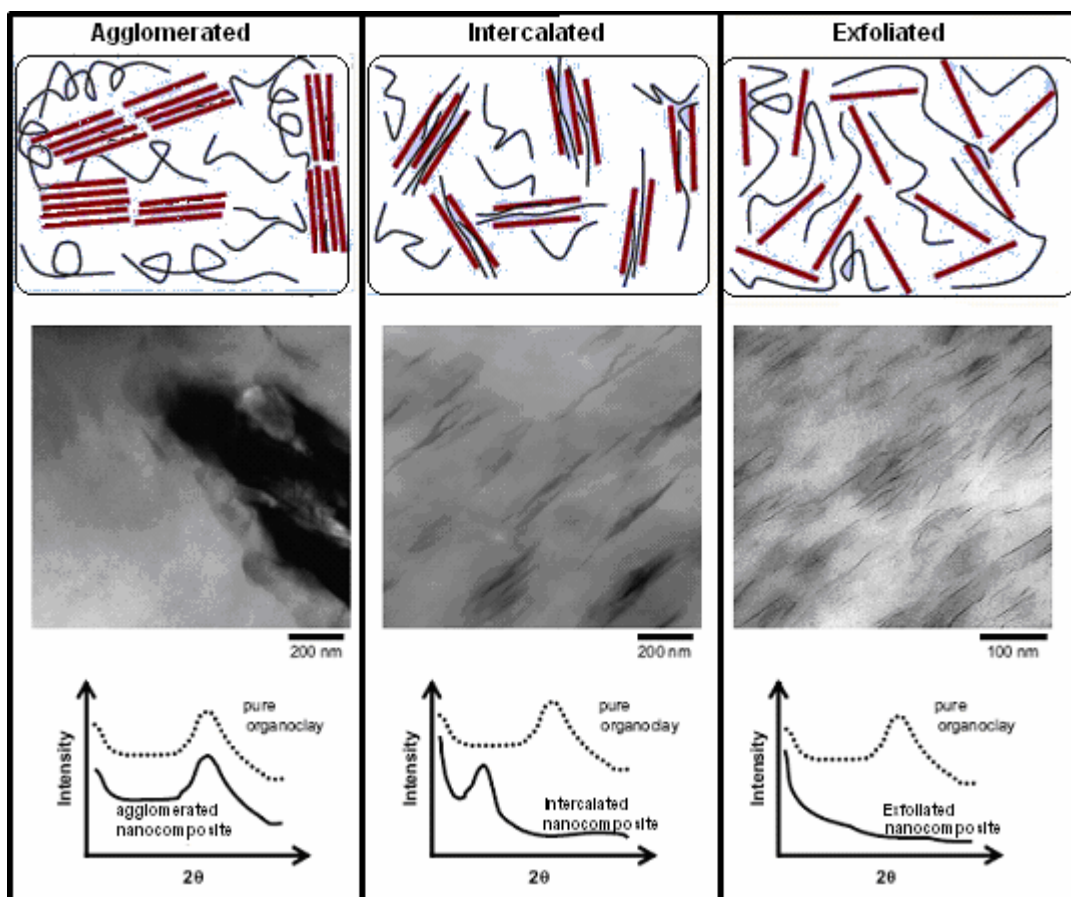
Figure 1.1: Structure of clay in nanocomposites with corresponding WAXS and TEM results.

WAXD is commonly used for the characterization of the structure of nanocomposites. For an intercalated structure, the (0 0 1) characteristic peak for the organoclay tends to

shift to lower angle regime due to the expansion of the basal spacing as shown in Figure 1.1. Although the layer spacing increases, there still exists an attractive force between the silicate layers to stack them in an ordered structure. In contrast, no peaks are observed in the WAXD pattern of exfoliated polymer nanocomposites due to loss of the structural registry of the layers. The absence of Bragg diffraction peaks in the nanocomposites may indicate that the clay has been completely exfoliated or delaminated as shown in Figure 1.1 [35].

The absence of Bragg diffraction peaks in the WAXD patterns should not be used as the sole evidence for the formation of an exfoliated structure. Morgan and Gilman[36] and Eckel *et al*[37] pointed out that WAXD analysis alone could lead to false interpretation of the extent of exfoliation. Several factors such as clay dilution, peak broadening and preferred orientation make WAXD characterization of polymer nanocomposites susceptible to errors. WAXD does not yield the information relating to the spatial distribution of the silicate in the polymer matrix because all its data are averaged over the whole regions of the specimen. Transmission electron microscopic (TEM) observations are needed to confirm the formation of exfoliated nanocomposites [37]. TEM can provide useful information in a localized area on the morphology, structure and spatial distribution of the dispersed phase of the nanocomposites. Vaia *et al* showed that the features of the local microstructures from TEM give useful information which is complementary to that obtained from WAXD[38]. Besides these two well defined structures, other intermediate organizations can exist presenting partial intercalation and exfoliation. For such intermediate structures, TEM offers a qualitative understanding of the internal structure, spatial distribution of various phases, and defect structure through direct visualization.

1.5   Methods of preparation of nanocomposites

Several strategies have been used for the preparation of polymer-layered silicate nanocomposites. These are described in the following paragraphs.

1.5.1   Intercalation of polymer or prepolymer from solution

When the polymer solution is mixed with a dispersion of clay the polymer chains intercalate and displace the solvent within the interlayer of the silicate. Upon solvent removal, the intercalated structure remains resulting in the nanocomposites formation. The entropy gained by desorption of small molecules of solvent compensates for the decrease in conformational entropy of larger size of intercalated polymers and acts as the driving force for the formation of nanocomposites. Requirement of large quantities of solvents and non-availability of many compatible polymer-clay solvent systems limits the use of this method.

1.5.2   In-situ intercalative polymerization method

In this method, the layered silicates are swollen within the liquid monomer or a monomer solution so that the polymer formation can occur in between the intercalated sheets. Polymerization can be initiated either by heat, radiation, by the diffusion of a suitable initiator or by an organic initiator/catalyst fixed via cation exchange inside the interlayer before the swelling step.

1.5.3   Melt intercalation method

This method involves annealing, statically or under shear, a mixture of the polymer and organoclay above the softening point of the polymer. This method has great advantages over either *in-situ* intercalative polymerization or polymer solution intercalation. First, this method is environmentally benign due to the absence of organic solvents. Second, it is compatible with current industrial process such as extrusion and injection molding.

The enhancement of the mechanical properties depends on the interaction of the polymer chains on the clay platelet surface. This is mainly affected by the amount of clay loading and the extent of dispersion so as to allow maximum platelet surface available to interact. Therefore, the key issue in the design of polymer–clay nanocomposites is to monitor the dispersion of clay platelets on nanometer scale in a polymer matrix. Accordingly, it is necessary to understand the interaction between the clay surface and the intercalants to

prepare the desired morphology of (exfoliated) clay–polymer nanocomposites. In other words, understanding the structure of organoclays and the interaction of surfactant–clay is of crucial importance to the design, fabrication and characterization of nanocomposites.

1.6   Choice of the organoclay

Proper selection of organoclays depends mainly on the type of polymer matrix used. Fornes *et al*[39] investigated the effect of the structure of alkylammonium compounds on the dispersion of MMT in a polar polymer, polyamide-6(PA-6), during melt compounding. They found that the alkylammonium compound consisting of one alkyl tail is more effective than the quaternary cation having two alkyl tails in forming exfoliated nanocomposites. This was further explained in terms of the competition between the effects of platelet–platelet interaction and the polymer-platelet interaction. PA-6, because of its polarity or strong hydrogen-bonding characteristic, has some affinity for the pristine surface of the clay. In this case, the organic modifier consisting of two alkyl tails shields more silicate surface than one alkyl tail, thereby, precluding desirable interactions between the polyamide and the clay surface[39]. On the other hand, nanocomposites made from a non-polar polymer like linear low-density polyethylene (LLDPE) showed an opposite behaviour. In that case, the two-tailed organoclay formed nanocomposites exhibit better exfoliation and mechanical properties than a one-tailed organoclay[40]. Manias *et al* demonstrated that the polypropylene(PP)–MMT nanocomposite formation can be achieved by two ways, i.e. either by using neat PP and semi-fluorinated surfactants for the silicates, or by using functionalized PP and common organo-montmorillonites[41,42]. In the first case, a semi fluorinated alkyltrichlorosilane (CF_3–$(CF_2)_5$–$(CH_2)_2$–Si–Cl_3) was used to modify C18-MMT, rendering it miscible with neat or unfunctionalised PP. This surfactant was tethered to the MMT surface through a reaction of the trichlorosilane groups with hydroxyls in the cleavage plane of the MMT. In the second case, several functional groups were grafted to PP in a random-copolymer fashion. The functionalized PP samples were aimed to render the polymer–MMT interactions more thermodynamically favorable than the surfactant– MMT interactions.

As mentioned above, interactions between the PA6 chains and pristine MMT via hydrogen bonding facilitate the intercalation of PA6 molecules into the galleries of MMT. In general, organic molecules can intercalate the galleries of the clays by interacting with the clay surface via ion–dipole, dipole–dipole and hydrogen bonding [43-45]. Recently, Hansen solubility parameters, $(\delta_t^2 = \delta_d^2 + \delta_p^2 + \delta_h^2)$ [46,47] has been adopted by the researchers to characterize the dispersion of organoclays in organic solvents [43-45]. The parameters take the dispersive (δ_d), polar (δ_p) and hydrogen-bonding (δ_h) forces acting together to disperse MMT in various solvents into account. It is noted that Hildebrand and Scott proposed the original definition of solubility parameter, $\delta = (E/V)^{1/2}$, where E is the molar cohesive energy and V is the molar volume. The cohesive energy is the energy associated with the net attractive interactions of the material. This is a well established approach for characterizing the inorganic powder (e.g. carbon black) dispersion in solvents [48]. Hansen then extended the Hildebrand parameter to polymer–solvent systems, particularly for polar and hydrogen bonding interactions [45-47]. Ho *et al* demonstrated that Cloisite 15A dispersed in chloroform was fully exfoliated, whereas, it formed tactoids in benzene, toluene and p-xylene, which possess different values of solvent solubility parameter [43]. They further concluded that the polar (δ_p) and hydrogen bonding (δ_h) forces affect primarily the exfoliated structure or tactoid formation of the suspended platelets in particular solvents [44]. Similarly, Choi *et al* reported that that δ_h is an important factor for the dispersion state of Na-MMT in a liquid or solvent. The polar components (δ_p) and hydrogenbonding components (δ_h) of organic liquids determined the dispersion and basal spacings of Na-MMT in various solvents and monomers [45-47]. The Hansen solubility parameters are particularly useful for the preparation of polymer–clay nanocomposites via the solution intercalation route [49].

1.6.1   Thermal stability of the modifiers

Quaternary ammonium ion is nominally chosen to compatibilize the layered silicate with a given polymer. However, the molecular structure, such as alkyl chain length, number of alkyl chains and unsaturations, is also a determining factor for the thermal stability of the polymer/MMT nanocomposites [50,51]. Although these modification agents have been gaining significant success in the preparation of polymer/MMT nanocomposites, their

common shortcoming is the poor thermal stability. Thermal stability of the organoclay component is of major importance since many polymer composites are either melt-blended or intercalated at high temperatures. If the processing temperature is higher than the thermal stability of the organoclay, then decomposition occurs, and the interface between the filler and the matrix polymer is effectively altered. Substantial work has been reported on the degradation process of organoclays and nanocomposites[18,19]. Significant successes in identifying thermally stable organic modifiers for compatibilizing the clay and polymer matrix has been achieved. However many questions still remain unanswered.

To circumvent the detrimental effect of the lower thermal stability of alkyl ammonium-treated MMT, alkyl-imidazolium molten salts treated MMT clays *via* ion exchange of the Na$^+$-MMT with imidazolium salts have been widely studied[52,53]. Ngo *et al*[54] and Begg *et al*[55] found that imidazole is resistant to ring fission during thermal rearrangements of 1-alkyl- and 1-aryl-imidazoles at temperatures as high as 600 °C. Earlier research indicated that the facility with which various groups are cleaved from quaternary salts involves S_N1 or S_N2 mechanisms[56,57]. Pyrolysis of the imidazolium quaternary salt proceeds most likely *via* S_N2 process (Figure 1.2).
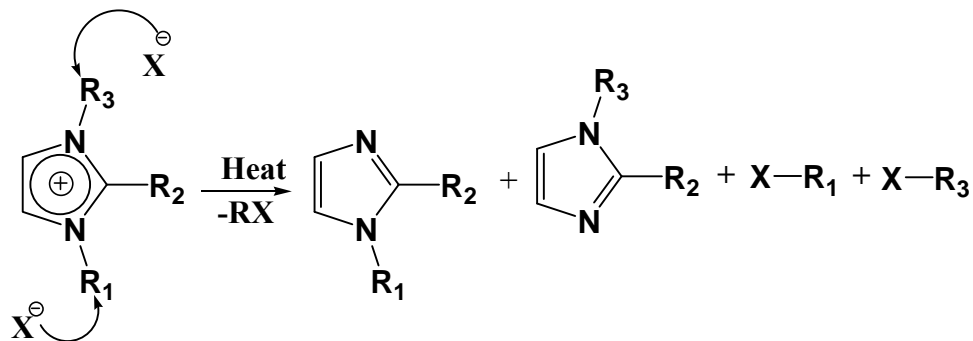
Figure 1.2: S_N2 mechanism for degradation of the quaternary imidazolium salt

Awad *et al*[52] studied the influence of the anion type on thermal stability of the imidazolium salts. The hexafluorophosphate, tetrafluoroborate and bis(trifluoromethylsulfonyl)imide salts showed more than 100 °C increase in the onset decomposition temperature compared to the halide salts. The thermal stability increased in the order: PF_6 > $N(SO_2CF_3)_2$ > BF_4 > Cl, Br. Additionally, the thermal stability of

imidazolium cation was affected by the type of isomeric structure of the alkyl side group. This was evidenced by the observation that both 1-butyl-2,3-dimethyl-imidazolium tetrafluoroborate and hexafluorophosphate salts had higher onset decomposition temperature than 1,2-dimethyl-3-isobutyl-imidazolium tetrafluoroborate and hexafluorophosphate salts, respectively. The degradation reaction presumably proceeds via a two-step S_N1 reaction since the cleavage of the tertiary carbon atom is likely to occur (Figure 1.3). Further, methyl substitution in the 2-position (i.e. between the two N atoms) has been reported to enhance the thermal stability[58]. This is evident from the increase in the onset decomposition temperature of both 1-butyl-2,3-dimethyl-imidazolium chloride and 1,2-dimethyl-3-hexadecyl-imidazolium chloride compared to 1-butyl-3-methyl-imidazolium chloride and 1-hexadecyl-3- methyl-imidazolium chloride, respectively; this effect may be due to the high acidic character of the C2 proton.
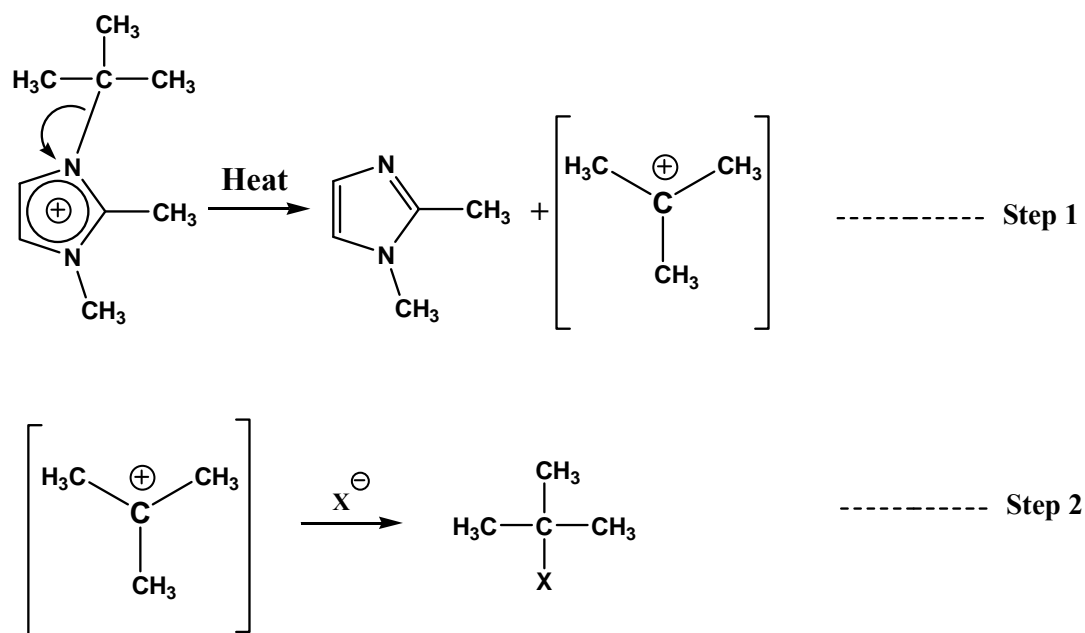
Figure 1.3: S_N1 mechanism for degradation of the quaternary imidazolium salt.

Thermal stability of imidazolium intercalated MMT was superior to ammonium-modified MMT. Moreover, higher thermal stability was observed for dimethyl hexadecyl–imidazolium-intercalated MMT compared to dimethyl hexadecyl–imidazolium chloride and bromide salts. This was ascribed to the absence of halide. However, it was observed that there was no significant improvement in the thermal stability of the intercalated tetrafluoroborate and hexafluorophosphate compounds compared to molten salts due to

the weak nucleophilicity of the BF_4^- and PF_6^- anions. The results also indicated that the thermo-oxidative stability of imidazolium-treated MMT decreased as the chain length of the alkyl group attached to the nitrogen atom increased. FTIR analysis of the decomposition products showed that water, carbon dioxide and hydrocarbons are the main degradation products[52].

Xie and coworkers[50] studied the degradation mechanism for the organoclay obtained by phosphonium ion modification. According to their study, due to the greater steric tolerance of the phosphorus atom and the participation of its low-lying d-orbitals in the processes of making and breaking chemical bonds, phosphonium salts are generally capable of undergoing a wider range of reactions and behave differently than their ammonium counterparts toward an external base (B). The following types of reactions have been established for tetraalkyl phosphonium salts under appropriate conditions; (1) nucleophilic substitution reaction at the α-carbon center, [S_N(C)]: where the attendant nucleophilic anion (e.g., a halide) displaces a triphenylphosphine group. This is effectively the reverse of the quaternization reaction. Because there is a change in oxidation state from the reactant (P at +5 oxidation state) to the product (P at +3 oxidation state), this reaction can also be regarded as a reductive elimination process. (2) β-elimination, E_β: where the β-proton is abstracted by a base in concert with the expulsion of triphenylphosphine from the α-carbon; (3) substitution at phosphorus, [S_N(P)]: where a hydroxyl anion attacks the phosphorus center to form a five-coordinate intermediate, followed by concomitant separation of a phosphone oxide and an alkane. This reaction is primarily driven by the formation of a strong phosphoryl (P=O) bond; (4) α-elimination, E_α: which is actually an α-proton abstraction process and the basis for the synthetically useful reaction for converting carbonyl compounds to olefins (Wittig reaction). However, this reaction typically requires a strong base such as alkyllithium or aryllithium reagents. Thus, reactions 1-3 are most likely to occur as the primary processes during the thermal decomposition of quaternary phosphonium compounds either in neat state or intercalated within montmorillonite.
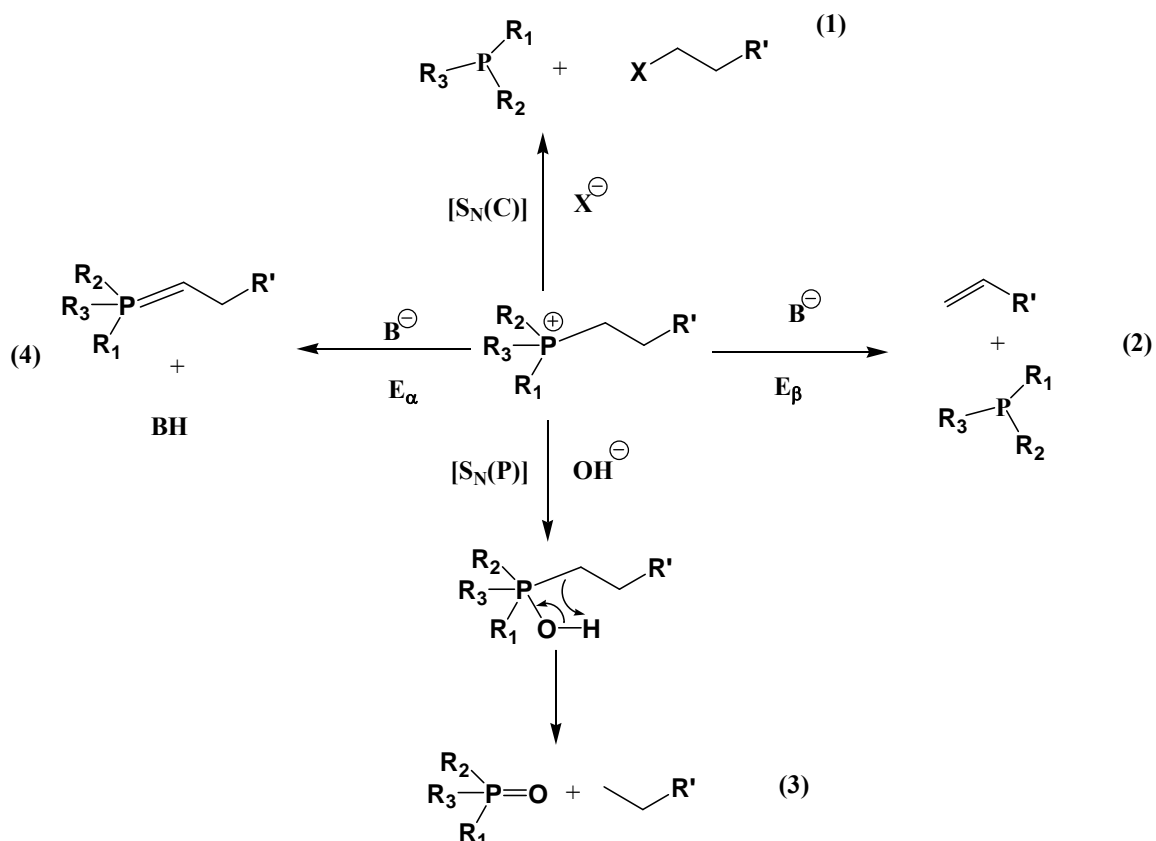
Figure 1.4: Degradation mechanism of alkyl phosphonium halides

Indeed, the pyrolysis/GC-MS of neat phosphonium salts indicated that both $[S_N(C)]$ and E_β elimination reactions are involved, confirmed by the presence of both alkenes and alkyl (or aryl) halides in the pyrolysis products. However, the $[S_N(C)]$ reaction is probably more favored in neat phosphonium salts at lower temperatures, considering the initial attack of the halide anion on the β-hydrogen is unfavored. Similar to the pristine salts, tertiary phosphine and long-chain olefins are observed as the decomposition products from the alkyl P-MMTs but at lower temperatures (250 vs 300°C). This indicates the occurrence of a β-elimination mechanism upon degradation of P-MMT. Additionally, phosphine oxide and octadecane are also detected from P-C18, consistent with the $[S_N(P)]$ pathway associated with hydroxyls along the sheet edge. Absence of alkyl halides indicates that the $[S_N(C)]$ reaction is suppressed by the removal of the bromide anion and replacement by the aluminosilicate sheet. The neat negative charge of the aluminosilicate is dispersed over numerous bridging oxygen, depending on the

crystallographic location of the isomorphic substitution. The weak Lewis basicity of the siloxane surface is thought to be insufficient to drive the $S_N(C)$ reaction.

Thermal stability of phosphonium ion modified montmorillonites was studied by TGA and pyrolysis/GC-MS[50]. Thermal degradation behavior of phosphonium ions such as triphenyldodecyl phosphonium(P-C12), tributyltetradecyl phosphonium(P-C14), tributyllhexadecyl phosphonium(P-C16), tributyloctadecyl phosphonium(P-C18), tetraphenyl phosphonium(P-4Ph), tetraoctyl phosphonium(P-4C8) and ammonium ion such as tetraoctylammonium(N-4C8) was studied. It was shown that the thermal decomposition process of phosphonium cations within montmorillonite follows multiple reaction pathways due to catalytic and morphological effects of the aluminosilicate matrix. In general, nonisothermal decomposition behaviour of P-MMT and N-MMT share similar characteristics such as β- elimination and nucleophilic substitution which occur in both the cases. In contrast to the studies on N-MMTs, the structure of the phosphonium cation is reflected in the thermal stability of the P-MMTs. Comparison of P-C14, P-C16, and P-C18 indicates that the alkyl chain length does not influence the thermal stability of corresponding P-MMTs, paralleling previous observation from alkyl N-MMTs and in agreement with the anticipated decomposition reactions. However, the stability of a longer chain, symmetric alkyl P-MMT, such as P-4C8, is ~30 °C greater than that of tributyl alkyl phosphonium MMTs, even though the stability of the salt is only slightly greater (0-5 °C). Similar dependence on structure is not observed for N-MMTs. The initial decomposition temperature for tetraoctyl quaternary ammonium modified montmorillonite (N-4C8) and the corresponding salt is similar to that of other trimethyl alkylammonium MMTs and salts. However, the increased stability of P-4C8 probably reflects increased steric resistance around the P center inhibiting the bimolecular reactions at the P. Substantially greater stability of the tetraaryl phosphonium arises from the alternative decomposition pathways. When aryl akyl phosphonium is present, such as triphenyl alkyl montmorillonite (P-C12), lower stability (~20 °C) relative to tetraaryl phosphonium is observed. Nonetheless, the stability is ~15 °C greater than tetraalkyl P-MMTs. The steric hindrance provided by the phenyl group is probably the major contributor to this behavior. Alternatively, the possibility of pπ-dπ interactions

between the P and phenyl groups, resulting in the delocalization of the positive charge can also diminish the susceptibility of the alkyl chain to β-elimination, increasing the thermal stability of P-C12.

1.6.2 *In-situ* polymerization and reactive modifiers for clay

It is strongly believed that the dispersion of the clay layers in the polymer matrix and the interaction of the clay layers with the matrix affect the nanocomposite properties. The enhancements in the properties are maximum when the clay layers are completely exfoliated and the interactions of the polymer chain with the clay layers are strongest. It can be understood that when the interactions are stronger the dispersion is also improved. Therefore, for improving the interaction of the polymer chains with clay surface, the polymer chains are anchored on to the clay surface via ionic bonding. This can be achieved by incorporating suitable functional groups in the clay modifier which can react with the polymer chains either during initiation of polymerization or during the polymerization process or post polymerization process. This approach has been exemplified in the literature with ring opening polymerization, radical polymerization including living radical polymerization, olefin polymerization, and condensation polymerization. The polymer can also be anchored to the clay surface through use of reactive modifiers during melt processing. It was shown that in the absence of the reactive anchoring group in the modifier resulted in poor dispersion of the clay. Another approach is to design the locus of polymerization to be at the interlayer gallery so that the polymer chain grows inside the interlayer gallery.

1.6.2.1 Ring opening polymerization

The Toyota research group reported the ability of α, ω-amino acids (COOH-$(CH_2)_{n-1}$-NH_2^+, with n=2,3,4,5,6,8,11,12,18), modified Na^+-MMT to be swollen by ε-caprolactam monomer at 100 °C to initiate the polymerization resulting in PA-6/MMT nanocomposites[59]. For the intercalation of ε-caprolactam, they chose the ammonium cation of ω-amino acids because these acids efficiently initiate the ring opening polymerization of ε-caprolactam. During this process they can anchor the polymer chains on to the clay surface through the formation of amide bonds. It was shown that the chain

length of the modifier amino acid plays a critical role in the swelling behavior of the organoclay with the monomer.

Reichert *et al*[60] also used the same method for the preparation of nylon12/MMT nanocomposites by *in-situ* ring opening polymerization of ω-lauryllactam. In a similar attempt to prepare polycaprolactone/clay nanocomposites, Messersmith and Giannelis [61] have used protonated ω-aminolauric acid to modify clay and prepare nanocomposites *via in-situ* ring opening polymerization of caprolactone. Uniformly dispersed and fully exfoliated nanocomposites were obtained.

1.6.2.2 Radical polymerization

Akelah and Moet[62,63] used the *in-situ* intercalative polymerization technique for the preparation of poly(styrene) (PS) based nanocomposites. They used Na$^+$MMT and Ca$^+$MMT modified with vinylbenzyl trimethylammonium cation for the preparation of nanocomposites. The resulting nanocomposites were found to have intercalated structures, and the extent of intercalation depending on the solvent used. Although PS anchors on to the clay surface through copolymerization with the vinyl group in the modifier, it did not result in exfoliation of clay. This may be because sufficient styrene monomer could not penetrate into the clay gallery during polymerization, since the clay was not sufficiently organophilic. Zhu *et al*[64] prepared the nanocomposites PS using organoammonium (*N,N*-dimethyl-*n*-hexadecyl-(4-vinylbenzyl)ammonium chloride(VB-16), *N,N,*-dimethyl-*n*-hexadecyl-(4-hydroxymethylbenzyl)ammonium chloride(OH-16),) and phosphonium (*n*-hexadecyl triphenylphosphonium chloride (P-16)) salts as modifiers. They found that the exfoliated nanocomposites can be obtained when the clay modifier possesses, in addition to a long alkyl chain a vinylbenzyl group which can copolymerize with styrene.

1.6.2.3 Condensation polymerization

The dispersability of the clay by using polar monomers or the precursor (prepolymers) for the polymers has been exploited by dispersing the clay using the monomers or prepolymers with or without the use of suitable solvents followed by polymerization.

There are several reports on the synthesis of poly(ethylene terepthalate) (PET)/clay nanocomposites. Ke *et al*[65] have prepared PET/clay nanocomposite via *in-situ* polymerization by dispersing the organoclay in water along with the monomers. Another novel route reported by Nanocor, Inc.[66] is based on the exfoliation of clays into ethylene glycol using suitable modifiers for the clay followed by *in-situ* polymerization. Imai *et al*[67] reported the preparation of high modulus PET/expandable fluorine mica nanocomposites with a novel reactive compatibilizer, which can copolymerize during the synthesis. An *in-situ* intercalative polymerization technique was successfully used by Hsu and Chang [68] in order to prepare polybenzoxazole (PBO)/clay nanocomposite from its polymer precursor polyhydroxyamide (PHA) and an organoclay. PHA/organoclay nanocomposite film was first prepared by solvent casting method in which dimethylacetamide was used as solvent. Finally, the exfoliated PBO/clay nanocomposite was obtained by curing the film to form benzoxazole ring.

A large number of reports discuss the preparation of various polyurethane (PU)/clay nanocomposite by *in-situ* polymerization. In some of the reports the PU/clay nanocomposites were prepared by dispersing the organoclay with the polyol followed by addition of a diisocyanate monomer and a diol[69-71]. In other reports, the nanocomposites were prepared by first mixing the organoclay containing hydroxyl group with isocyanate terminated prepolymers followed by addition of short chain diols for chain extension[72-79]. Presence of the reactive hydroxyl groups in the modifier for the clay resulted in improved properties for the nanocomposites obtained. In another report, organoclay/polyol nanocomposites was prepared in the first step by *in-situ* ring opening polymerization of caprolactone followed by chain extension with diisocynates[80].

Leu *et al*[81] prepared covalently bonded layered silicate/polyimide nanocomposites. Amino functionalized –layered silicate (APTS-kenyaite) was mixed with poly(amic acid) (BTDA-ODA type) containing an anhydride end group, so that the amino groups of APTS-kenyaite react with the anhydride end group of poly(amic acid) to form covalently bonded polymer tethered silicates. The sequence of reactions leading to polymer tethered APTS-kenyaite is presented in Figure 1.5.
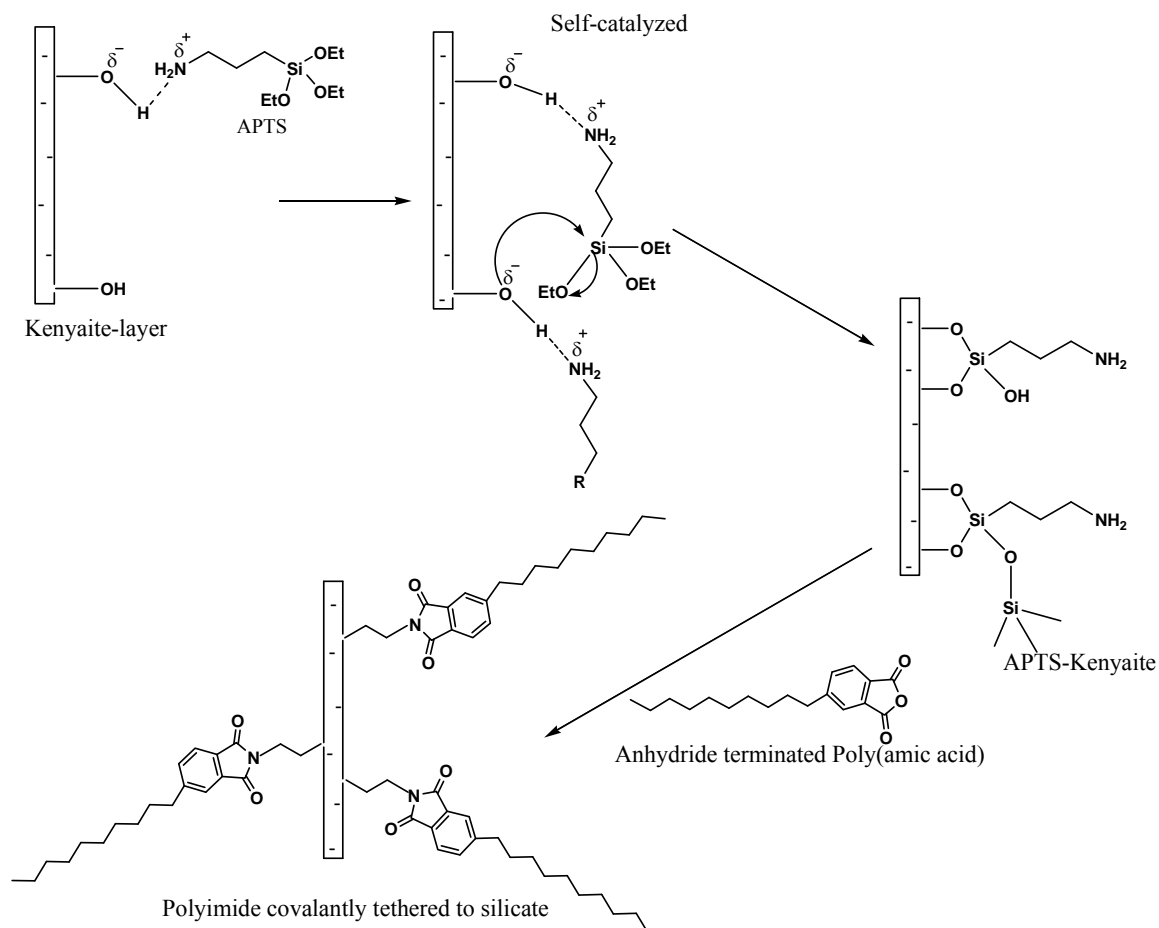
Figure 1.5: A schematic drawing showing the reactions leading to polymer tethered APTS-kenyaite

1.6.2.4 Olefin polymerization

For the preparation of polyolefin nanocomposites, Tudor *et al*[82] first used *in-situ* polymerization method. Metallocene catalyst, ([Zr(η-C$_5$H$_5$)Me(THF)]$^+$, was intercalated into methylaluminoxane (MAO) treated layered silicate, by cation exchange reactions.Polymerization of propylene with the intercalated catalyst caused the polymer to grow in the interlayer gallery and delaminate the clay layers to give exfoliated PP/clay nanocomposites. Bergman[83] intercalated the clay with aliphatic 1-tetradecylammonium cations to make an organically modified fluorohectorite. The exchanged fluorohectorite was mixed in toluene with a Brookhardt-type Pd catalyst [{2,6-iPr$_2$C$_6$H$_3$N=C(Me)C(Me)=NC$_6$H$_3$iPr$_2$}Pd(CH$_2$)$_3$CO$_2$-Me][B(C$_6$H$_3$(CF$_3$)$_2$-3,5)$_4$]. Perfluoroborates were then used as an activator to initiate polymerization with ethylene at

5.6 Kg/cm^2 and 22 °C. The recovered dry solid was a rubbery poly(ethylene)/clay nanocomposites. The catalyst had a turnover frequency of 162 h^{-1}. The X-ray powder diffraction of the nanocomposites showed disappearance of ordering in the clay structure during polymerization indicating that the clay was exfoliated or became totally disordered. Using a MAO activator and quaternary ammonium modified clay fillers, Mulhaupt *et al*[68] made high-density polyethylene (PE)/montmorillonite nanocomposites with high catalyst efficiency. They showed that by decreasing the aliphatic hydrocarbon chain length in the alkylammonium cations from 18 to 4, the catalyst efficiency increases suggesting a homogeneous polymerization process. Ray *et al* studied the preparation and properties of polyethylene/clay nanocomposites by *in-situ* polymerization using a late transition metal complex, 2,6-bis[1-(2,6-diisopropylphenylimino)ethyl] pyridine iron(II) dichloride, as catalyst which was supported on MAO treated modified montmorillonite[85]. They showed that parameters such as catalyst concentration, MAO/catalyst ratio and the specific manner of supporting the catalyst on the clay interlayer surface were the determining parameters to obtain exfoliated nanocomposites. Sun and Garces[86] reported the preparation of PP/clay nanocomposites by *in-situ* intercalative polymerization with metallocene/clay catalyst under mild conditions. Jin *et al*[87] developed an *in-situ* exfoliation method during the polymerization by fixing a Ti-based Ziegler–Natta catalyst at the inner surface of MMT. They have used organic salts with hydroxyl groups for the modification of MMT since hydroxyl groups in intercalation agents offer facile reactive sites for anchoring catalysts in between silicate layers.

1.6.2.5   Living or controlled polymerization

Nanocomposites based on homo and copolymers of butadiene were prepared by *in-situ* living anionic polymerization in presence of organoclay which were modified by exchanging with quaternary ammonium ions[88-90]. Dispersion of the organoclay improved by addition of toluene in the solvent medium or when the styrene content in the copolymer was increased. The living nature of the reaction is suspect because the molecular weight distribution of the polymer obtained were quite broad. The molecular weight distribution of the polymer matrix in the nanocomposites was narrower when the edge hydroxyl groups on the clay were reacted with titanium coupling agents[91].
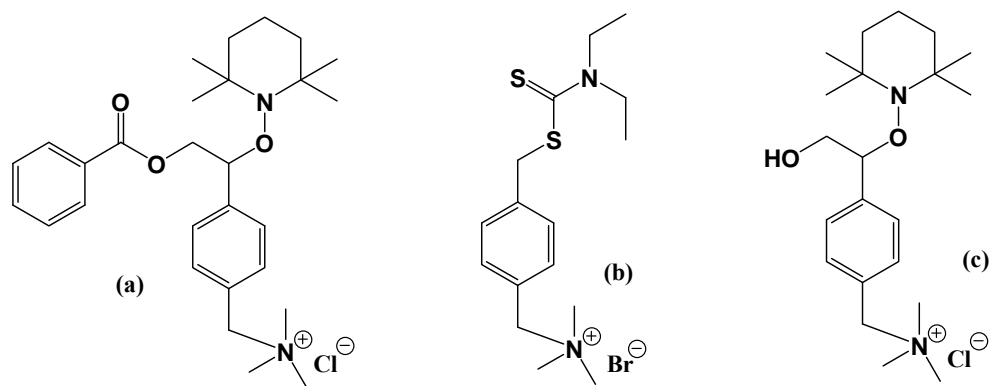
Figure 1.6: Structure of clay modifiers containing the initiator moiety.

Sogah *et al*[92] prepared fully dispersed polystyrene clay nanocomposite by intra-gallery nitroxide mediated living free radical polymerization via silicate-anchored initiators. The structure of the organo-modifier used for the clay containing initiator moiety is shown in Figure 1.6(a). Dispersed polymer silicate nanocomposite via *in-situ* living polymerization from silicate anchored initiators was prepared using a dithiocarbomate photoiniferter-modified silicate (Figure 1.6(b)). Subsequent living free radical polymerization of variety of monomers gave dispersed polymer silicate nanocomposites of PS, poly(methyl methacrylate) (PMMA), poly-(*t*-butyl acrylate) (PtBA) with controlled molecular weight and narrow molecular weight distribution[93]. By employing sequential monomer addition, poly(styrene)-*b*-poly(methylmethacrylate)/silicate nanocomposites could be prepared. Exfoliated nanocomposites with very high silicate content (above 20 wt %) could readily be prepared which, in turn, can be used as masterbatches for the preparation of other nanocomposites by simple melt blending. The same authors in an another report showed that fully exfoliated poly(styrene-b-caprolactone)/silicate nanocomposites could be prepared via one pot, one step *in-situ* living polymerization from silicate-anchored bifunctional initiator[94]. The structure of the initiator is shown in Figure 1.6(c). The polymer chains were attached to the surface of the silicate layers at the junction between the two blocks. Molecular weights of the polymer and the concentration of clay in nanocomposite were controlled by diluting the initiator with non-initiating salt. Atom transfer radical polymerization (ATRP) has been extensively studied for the preparation of polymer nanocomposites using a copper catalyst and an initiator. Shipp *et al* [95,96] showed that block copolymer brushes based on poly(styrene-b-butyl acrylate) can be

grown on the surface of exfoliated and intercalated clay layers by exchanging with organocations containing initiator moiety. The schematic representation showing the exchange of cations in clay with organocations containing initiator moiety for *in-situ* ATRP is shown in Figure 1.7. The homopolymer clay nanocomposites of MMA, styrene and n-butyl acrylate were prepared by *in-situ* ATRP with predictable molecular weights and low polydispersities, both characteristics of living radial polymerization[97].

1.23 nm   1.96 nm

NaBr

Na-MMT   Organoclay with modifier having initiator moiety

ATRP   1) Styrene+ Cu Catalyst

2) Butyl acrylate

PBA block

PS block
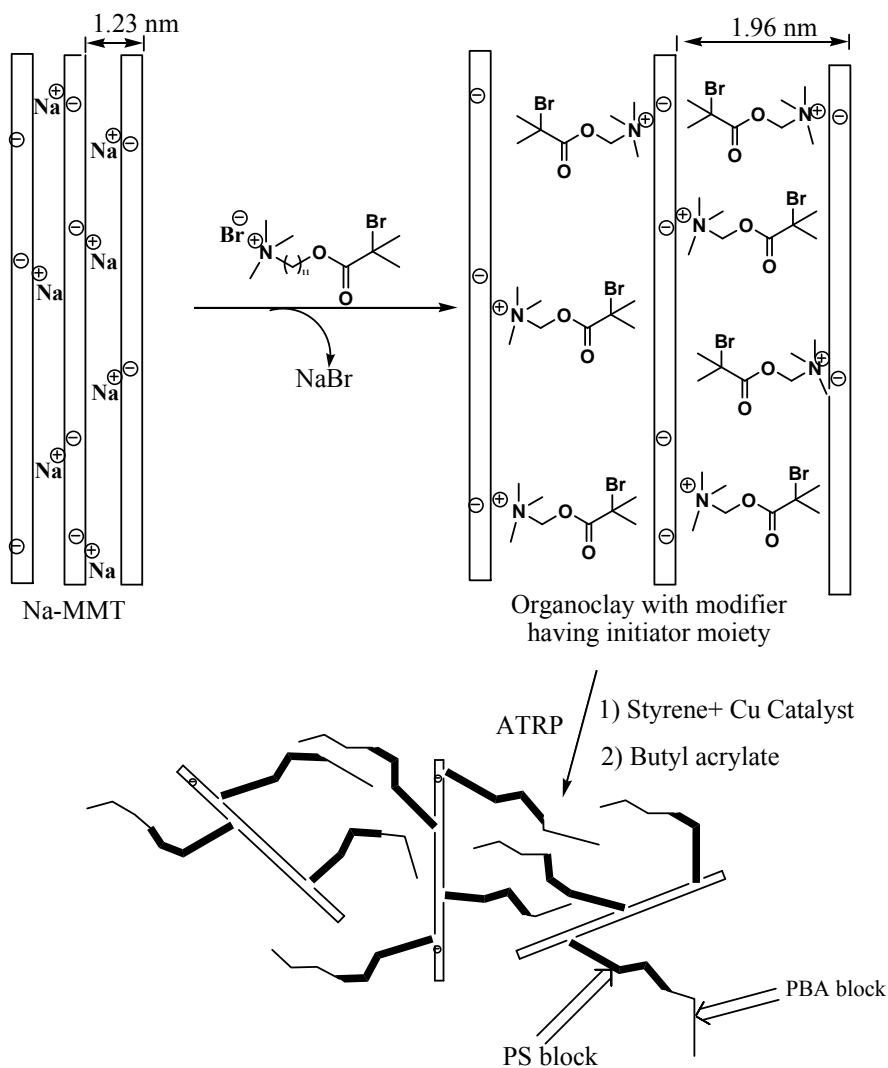
Figure 1.7: Schematic representation showing the exchange of cations in clay with organocations containing initiator moiety for *in-situ* ATRP

Mathias *et al*[98] prepared covalently functionalized laponite clay through a condensation reaction of the clay silanol groups with mono and trifunctional alkoxy silanes. The work

focused on pimary amine containing modification through aminopropyltrimethoxy silane (APS) treatment. Attaching primary amines to the edges of clay opens up a wide range of possible functionalization reactions. Thus APS treated clay was reacted to give attached methacrylate, benzophenone and tertiary bromine groups capable of polymerization, photoinitiation, ATRP initiation respectively. Reaction schemes are shown in Figure 1.8. Covalently bonded layered silicate/polystyrene nanocomposites were synthesized via ATRP in presence of initiator modified layered silicate based on megadite[99]. Wang *et al*[100] showed that exfoliated PS-PMMA-PS triblock copolymer/clay nanocomposites could be prepared by *in-situ* ATRP. Bhowmick *et al*[101,102] prepared poly(ethyl acrylate)/clay nanocomposites by *in-situ* ATRP and showed that the rate of ATRP improved in presence of organoclay. This can be attributed to the interaction of carbonyl of the monomer with the clay surface.
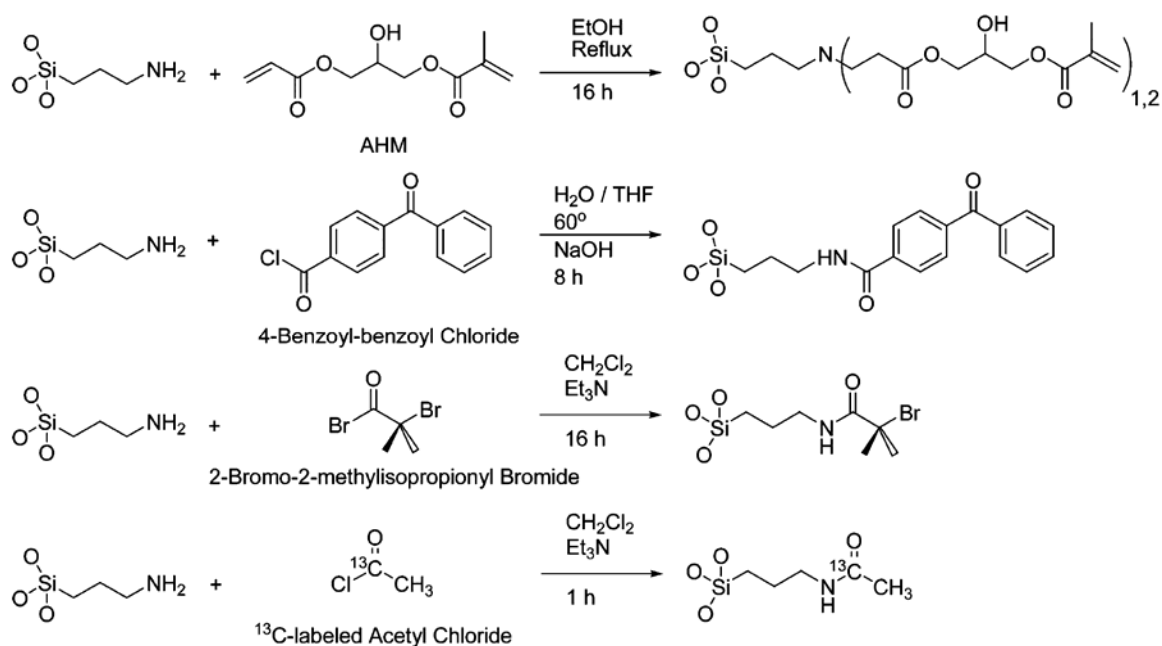
Figure 1.8: Functionalization of Laponite modified by APS.

1.6.2.6   Thermoset polymers

Messersmith and Giannelis[103] first reported the preparation of epoxy resin based nanocomposites with clay. They analyzed the effects of different curing agents and curing conditions on the formation of nanocomposites based on the diglycidyl ether of

nanocomposites based on the diglycidyl ether of bisphenol A (DGEBA), and Cloisite 30B. Subsequently, Pinnavaia *et al*[104], extensively studied the effect of various parameters on the preparation and properties of the epoxy/clay nanocomposites. The effect of acidity of the organoclay used for the preparation of nanocomposite based on DGEBA was studied by using modifiers for the clay with a series of acidic cations and found that with decreasing acidity of the modifier cation, the epoxy-clay delamination increased. The effect of alkyl chain length of the modified MMT was studied and shown that the structures obtained such as an intercalated, partially exfoliated or fully exfoliated depends on the alkyl chain length of the modifier[105]. Several reports exist on the effect of CEC of the organoclay, type of modifiers on the preparation of nanocomposites based on DGEBA, which are cured with different amines [106-108]. Simon *et al*[109] reported the morphology, thermal relaxation and mechanical properties the clay nanocomposites based on epoxies with varying epoxy functionalities. Three different types of resins were used: bifunctional DGEBA, trifunctional triglycidyl p-aminophenol (TGAP), and tetrafunctional tetraglycidyl diaminodiphenylmethane (TGDDM). All were cured with diethyltoluenediamine. MMT modified with octadecylammonium cation was used for the preparation of nanocomposites. Nanocomposites based on higher functionalities showed poor dispersion of clay as compared to those based on DGEBA. Chen *et al* [110] studied the exfoliation mechanism and thermal–mechanical properties of surface-initiated epoxy nanocomposites. Time-resolved high-temperature X-ray diffraction, DSC, and isothermal rheological analyses revealed that the interlayer expansion mechanism might be separated into three stages. These stages relate to the initial interlayer expansion, the steady-state interlayer expansion and the cessation of interlayer expansion. It was found that differences in the activation energies of interlayer expansion and of curing influence the final nanostructures of the materials. This was ascribed to the evolving modulus of the extragallery polymer such that the interlayer expansion stopped when the modulus of the extragallery polymer became equal to or exceeded the modulus of the intragallery polymer. Variations in ultimate properties were attributed to the formation of an interphase layer, where the interphase was hypothesized to be the epoxy matrix plasticized by surfactant chains.

1.6.3   Polymeric surfactant modifiers

A variety of polymeric surfactant modifiers, namely, one-end terminated, α–ω two-end terminated, and multiple-cation containing polymeric surfactants have been used for the modification of layered silicates and clays. This area has been thoroughly reviewed[111]. These polymeric surfactant modified clays are usually highly expanded compared to the common organo-clays based on cationic surfactants such as alkyl ammoniums. The polymeric surfactant modified clays show outstanding thermal stability and may be directly melt compounded with various polymers, i.e., a compatibilizer or a masterbatch is not required even for poly(olefin)s. Polymeric surfactant modified clay and polymer matrices are frequently immiscible, but with proper choice of the surfactant and the processing conditions, formation of clay clusters can be significantly reduced in size. In addition, polymeric surfactants as organic modifications for clay offer unparalleled opportunities to incorporate additional functionalities that target specific property improvements, beyond the dispersion of the fillers in the polymer matrix. For example, incorporating phosphate moieties in polymeric surfactants for clays can further significantly reduce the flammability of the nanocomposite.

1.7   Properties of nanocomposites

1.7.1   Mechanical properties

Polymer–clay nanocomposites exhibit extremely large interfacial area due to the confinement of polymer chains within the galleries of clay platelets of large surface area per unit volume. It is believed that the confinement of polymer in clay galleries would affect the local chain dynamics to a certain extent. Since several chemical and physical interactions are governed by surfaces, polymer-clay nanocomposites can have substantially different properties from conventional polymer microcomposites. Several micromechanical models, e.g., Halpin-Tsai[112-114], Mori-Tanaka[115], have been developed to predict the macroscopic behavior of polymer microcomposites. The models generally include a simple route for evaluating individual contributions of component properties such as the matrix and the filler modulus, the volume fraction, the filler aspect ratio, the filler orientation, etc.

Halpin and Tsai developed a well-known composite theory for predicting the stiffness of unidirectional composites as a function of aspect ratio[112-114]. This theory is based on the early micromechanical works of Hermans[116] and Hill[117]. Hermans generalized the form of Hill's self-consistent theory by considering a single fiber encased in a cylindrical shell of the matrix that is embedded in an infinite medium assumed to possess the average properties of the composite. Halpin and Tsai reduced Herman's results into a simpler analytical form adapted for a variety of reinforcement geometries, including discontinuous filler reinforcement. The overall composite moduli E_c can be predicated by:

$$\frac{E_c}{E_m} = \frac{1 + \zeta\eta\phi_f}{1 - \eta\phi_f}$$

where η is given by

$$\eta = \frac{E_f/E_m - 1}{E_f/E_m + \zeta},$$

where E_c, E_f, and E_m represent the overall Young's modulus of the composite, filler, and matrix, respectively, ϕ_f is the volume fraction of the filler, ζ is a shape parameter dependent upon the geometry of the filler and the loading direction, which is a function of aspect ratio L/t:

$$\zeta = f\left(\frac{L}{t}\right)$$

To calculate the aspect ratio of filler in intercalated nanocomposites, where the polymer chains have penetrated in the interlayer gallery and the particle is swollen, the whole intercalant cluster can be considered as the filler particle and the stiffness ratio is also obtained by considering the whole cluster. The theory predicts that the dependency of various parameters on the ratio of modulus of the nanocomposite to the matrix polymer. Particles with large aspect ratio **L/t** or high stiffness ratio E_f/E_m prove to be more efficient in enhancing stiffness of the nanocomposite. Therefore, The results show that exfoliation is favored over intercalation as far as the enhancement of the composite modulus is concerned. Of course, for all composite theories the properties of the matrix

and filler are considered to be identical to those of the pure components. Therefore, numerous complexities arise when comparing the composite theory to the experimental composite data, particularly for polymer-layered silicate nanocomposites, as the interaction of the polymer chain with filler interface is ignored.

The importance of the interfacial strength and the nanofiller structure in polymer-clay nanocomposites has been demonstrated using a designed polymer and nanocomposite synthesis. Interfacial interaction determines how the polymer chain interacts with the clay sheet, how an effective nanophase is formed, and how effective the new nanophase constrains the surrounding polymers. In the studied polymer-clay nanocomposites, the matrix chain mobility is largely decreased. The modulus enhancement strongly relates to the volume of the added clay as well as to the volume of the constrained polymer. It has been shown that the significant modulus enhancement of the polymer-clay nanocomposites follows a power law with the content of the clay and can be modeled well by modified Mooney's equation.

$$\ln \frac{E}{E_1} = \frac{k_E \phi_2}{1 - \phi_2/\phi_m}$$

where E is the modulus of the nanocomposite, $E1$ is the modulus of the matrix, k_E is the Einstein coefficient, ϕ_2 is the volume fraction of the filler, and ϕ_m is the maximum volume fraction that the filler can have. k_E is a function of the interaction between the filler and the matrix as well as the aspect ratio of the filler. The stronger the interaction and the higher the aspect ratio of the filler, the higher the k_E is. The strong interaction between the clay and the polymer ensures a non-slippage interface. Under the nonslippage condition:

$$K_E = 2.5 \cdot (L/t)^{0.645}$$

An excellent fit is achieved when this Mooney power function is used to describe the observed modulus change with the amount of added clay. The modulus enhancement is dominated by the high aspect ratio of the clay platelet and the interfacial strength, through the Einstein coefficient, K, when the modulus of the matrix phase is much lower than that of the clay, i.e., $E_f/E_m > 100$. The study also suggests that the structure of clay

nanocomposites with strong interfacial interaction is analogous to that of semicrystalline polymers. Here, in this clay nanocomposite, the intercalated clay phase serves as an unmeltable crystalline phase to result in the improvement of mechanical properties.

Thus, enhancement in mechanical properties of polymer nanocomposites can be attributed to the high rigidity and aspect ratio together with the good affinity between polymer and organoclay. For instance, stronger interface interactions significantly reduce the stress concentration point upon repeated distortion which easily occurs in conventional composites reinforced by glass fibers and thus lead to weak fatigue strength. The unprecedented mechanical properties of PA-6/clay nanocomposite synthesized by *in-situ* polymerization were first demonstrated by researchers at the Toyota Central Research Laboratories[118]. Such nanocomposites exhibit significant improvement in strength and modulus, namely, 40% in tensile strength, 60% in flexural strength, 68% in tensile modulus, and 126% in flexural modulus. RTP Company has reported equivalent property enhancement of PA-6/clay nanocomposites synthesized by direct melt intercalation [119]. The increase in modulus is believed to be directly related to the high aspect ratio of clay layers as well as the ultimate nanostructure. Moreover, a dramatic increase was also observed in exfoliated nanostructures such as MMT based thermoset amine-cured epoxy nanocomposite and magadiite-based elastomeric epoxy nanocomposite[120]. Figures 1.9 and 1.10 show the effect of clay loading on tensile modulus[118,120-122] and yield strength[123] of some polymer nanocomposites. In contrast, a relatively small increase was reported for the intercalated nanocomposites such as those from clay and PMMA[124] and PS[125].
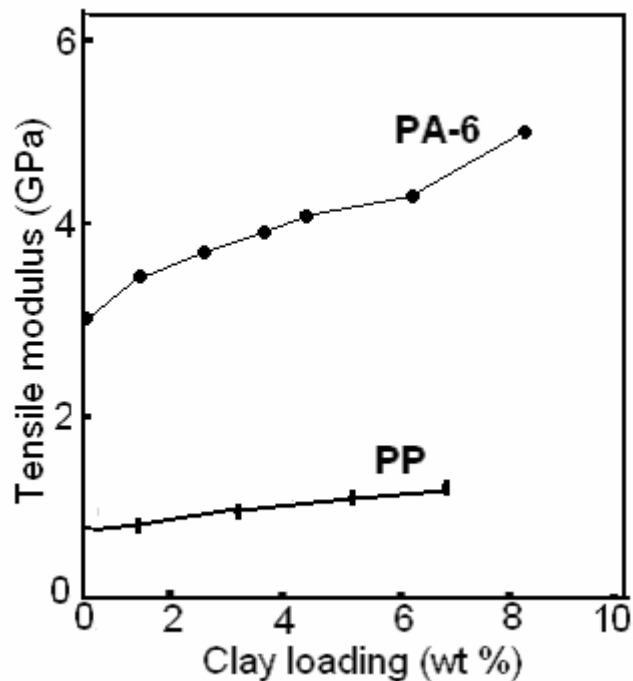
Figure 1.9: Effect of clay loading on tensile modulus for different clay based polymer nanocomposites.
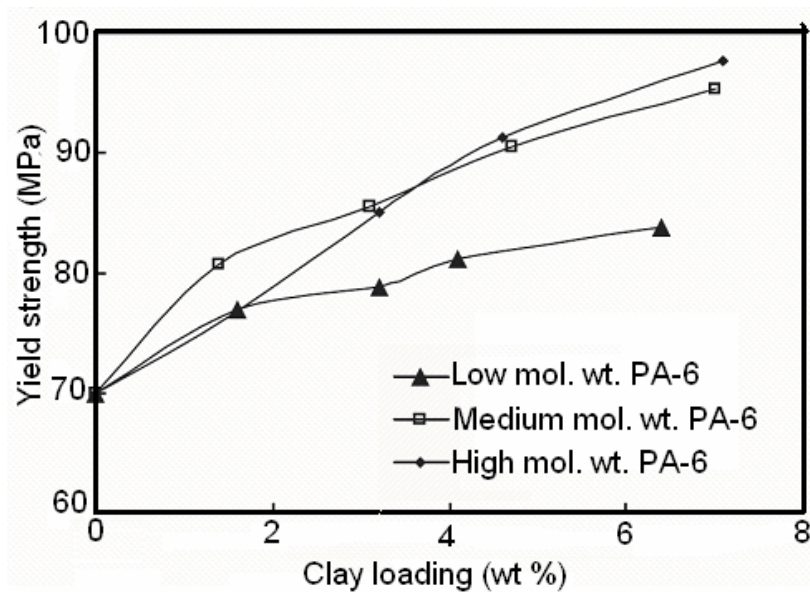
Figure 1.10: Effect of clay loading on yield strength for different clay-based PA-6 nanocomposites.

The thermodyanamics of interaction at the interface significantly affect the mechanical properties of polymer nanocomposites. For example, polar PMMA and ionic PA-6 interact favorably with clay layers which may explain the stress increase for intercalated PMMA nanocomposites and exfoliated PA-6 nanocomposites, respectively. Impact properties measured for PA-6 nanocomposites showed that it was not affected by the extent of exfoliation[121]. In the case of PP nanocomposites[126], a slight enhancement in tensile stress was attributed partially to the lack of interfacial adhesion between apolar PP and polar clays, which may be improved by adding maleic anhydride modified PP to the matrix. The tensile stress is even lower in PS intercalated nanocomposites due to the weak interaction at PS and clay interface[63]. In thermoset nanocomposites, the exfoliation of clay minerals can result in substantial property improvement, including enhanced mechanical properties, dimensional stability, thermal stability, chemical stability, resistance to solvent swelling, excellent transparency, together with high barrier property and reduced flammability of polymer nanocomposites[127-129].

1.7.2   Barrier property

Polymer nanocomposites exhibit excellent barrier properties against gases (e.g., oxygen, nitrogen and carbon dioxide), water and hydrocarbons. Studies have showed that such reduction in permeability strongly depends on the aspect ratio of clay platelets, with high ratios dramatically enhancing gaseous barrier properties. Water permeability of exfoliated polyimide (PI) nanocomposites is reported to decrease with increase in the aspect ratio of clay (Figure 1.11)[130]. The barrier properties were enhanced when the clay was fully exfoliated. Moreover, the aspect ratio of clay platelets was observed to affect greatly the relative permeability coefficient for PI filled with 2% of organoclay. Permeability to water vapor of exfoliated poly(caprolactone) (PCL) nanocomposites also showed a dramatic decrease in the relative permeability with the increase in the size of clay platelets[131]. The effect of clay loading on relative permeability coefficienct of several polymer nanocomposites is shown in Figure 1.12.[132-135]
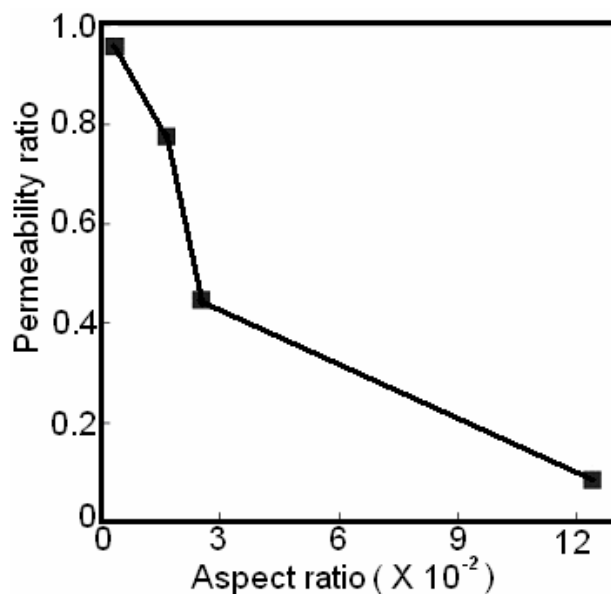
Figure 1.11: Effect of clay aspect ratio on relative permeability coefficienct of polyimide nanocomposites.
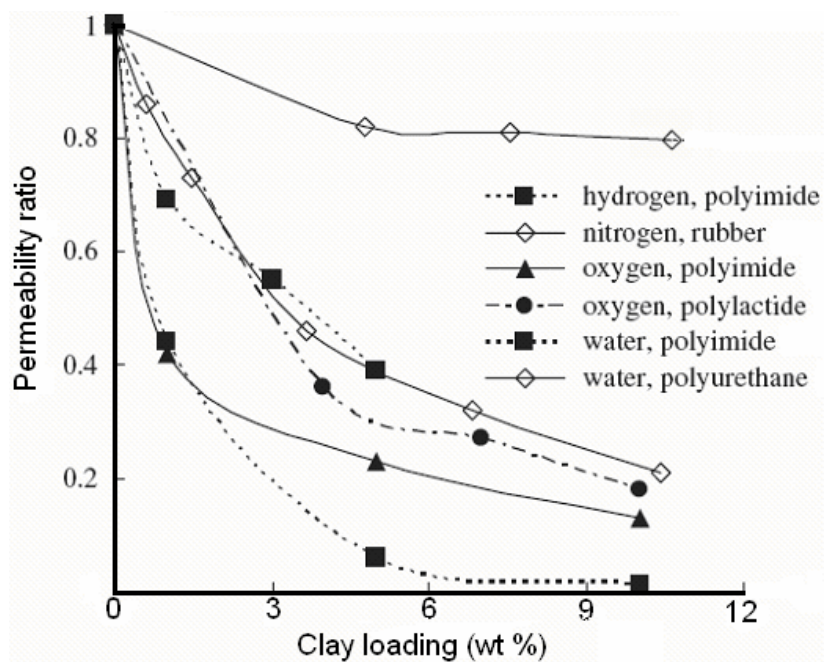
Figure 1.12: Effect of clay loading on relative permeability coefficients of polymer nanocomposites.

In addition, polymer nanocomposites also show better barrier properties against organic solvents such as alcohol, toluene and chloroform. This is attributed to the labyrinth or

tortuous pathway model as proposed in Figure 1.13[130]. When a film of polymer nanocomposites is formed, the sheet-like clay layers orient in parallel with the film surface. As a result, gas molecules have to take a long way around the impermeable clay layers in polymer nanocomposite than in pristine polymer matrix when they traverse an equivalent film thickness. It is interesting to note that the enhancement of barrier properties does not arise from the chemical interactions since it does not depend on the type of gas or liquid molecules.
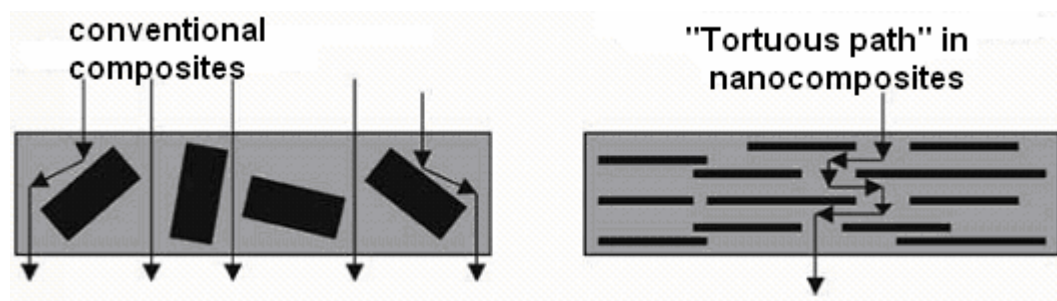
Figure 1.13: Formation of tortuous path in polymer/clay nanocomposites.

1.7.3   Thermal properties of nanocomposites

The thermal stability of polymer composites is generally estimated from the weight loss upon heating which results in the formation of volatile products. Blumstein[32] first reported the thermal stability improvement in PMMA nanocomposite, which showed that intercalated PMMA containing 10% clay degraded at about 40–50 °C higher than unfilled PMMA. Several reports have appeared on the improved thermal stability of nanocomposites made with various organoclays and polymer matrices[64,136-138]. For example, improvement in thermal stability is reported for cross-linked polydimethylsiloxane exfoliated with 10% of orango-montmorillonite[139] and intercalated nanocomposites made from the polymerization of methyl methacrylate[124], styrene[64,125,140] and epoxy precursors[141]. The layered structure of nanocomposites as well as their shape and and dimensions of the dispersed phase causes several changes in thermal properties. Experimental results have shown that layers of MMT are impermeable for gases meaning that both intercalated and exfoliated structure get created in a labyrinth for gas penetrating the polymer bulk. Thus, the effect of 'labyrinth' limits the oxygen diffusion

inside the nanocomposite sample. Similarly in the samples exposed to high temperature the MMT layers restrain the diffusion of gases evolved during degradation. Moreover, MMT layers are thought to reduce heat conduction. When MMT layers strongly interact with the polymer matrix the motions of polymer chains are limited. This effect brings additional stabilization in the case of polymer/MMT nanocomposites. Nanocomposites exhibit more intensive char formation on the surface of sample exposed to heat. It protects the bulk of sample from heat and decreases the rate of mass loss during thermal decomposition of polymeric nanocomposite material. More intensive formation of a char in comparison with pristine polymers can be indicative of improved flame resistance. The char formed in a case of nanocomposites performs higher mechanical resistance and therefore nanocomposites are considered as a potential ablative. The phenomena mentioned above are thought to retard the thermal decomposition processes through reducing the rate of mass loss. Unfortunately, few studies have been reported on the study of gases evolved from nanocomposites during thermal and thermo-oxidative degradation. The heat barrier effect could also provide superheated conditions inside the polymer melt leading to extensive random scission of polymer chain and evolution of numerous chemical species which, trapped between clay layers, have more opportunity to undergo secondary reactions. As a result, some degradation pathways could be promoted leading to enhanced charring. It is also suggested that the effect of more effective char production during thermal decomposition of polymer–clay nanocomposites may be derived from a chemical interaction between the polymer matrix and the clay layer surface during thermal degradation. Some authors indicated that catalytic effect of nano-dispersed clay is effective in promoting char-forming reactions. Nano-dispersed MMT layers were also found to interact with polymer chains in a way that forces the arrangement of macrochains and restricts the thermal motions of polymer domains. Generally, the thermal stability of polymeric nanocomposites containing MMT is related to the organoclay content and the dispersion. Synthesis methods also influence the thermal stability of polymer/MMT nanocomposites. Currently, extensive research is devoted to the synthesis of novel thermally stable modifiers (including oligomeric compounds) that can ensure good compatibility and improve the nanocomposite thermal stability due to low migration characteristics.

Another thermal property of interest is the heat resistance upon external loading, which can be measured from the heat distortion temperature (HDT). The HDT of PA-6 nanocomposites increased from 65 °C of pristine nylon to 145 °C. The increase in HDT has also been observed in clay-based nanocomposites for other polymer systems such as PP [142] and poly-lactide (PLA)[143]. Such an increase in HDT is very difficult to achieve in conventional polymer composites reinforced by micro-particles.

Finally, flame retardancy and mechanical properties are both improved in clay-based polymer nanocomposites while the mechanical properties are always degraded in polymer composites with conventional flame-retardants. Such fire resistance of polymer nanocomposites is attributed to the carbonaceous char layers formed when burnt and the structure of clay minerals. A schematic representation of combustion mechanism and ablative reassembly of a nanocomposite during cone calorimeter experiments is shown in Figure 1.14.
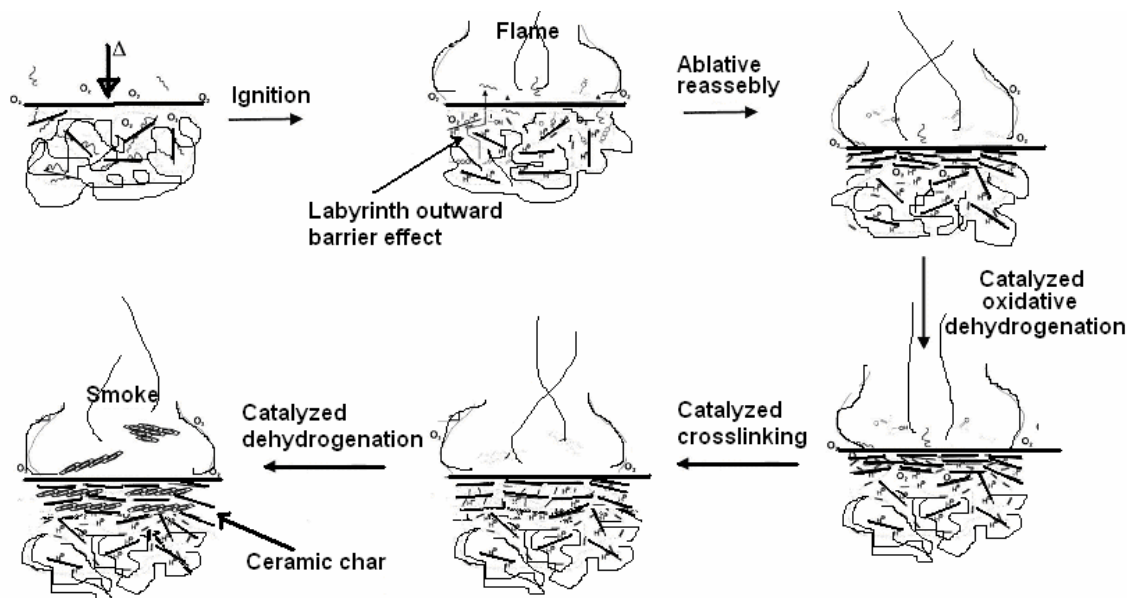
Figure 1.14: Schematic representation of combustion mechanism and ablative reassembly of a nanocomposite during cone calorimeter experiments.

The multi-layered clay structure acts as an excellent insulator and mass transport barrier. Char formation and clay structure impede the escape of the decomposed volatiles from the interior of a polymer matrix[144]. Gilman[137] has recently reviewed the flame retardancy

properties of nanocomposites. Flame retardancy is normally evaluated by the reduction of the peak of heat release rate (HRR).

1.7.4 Crystallization behaviour

Crystallinity and crystallization behaviour of a polymer affects the structure and property of the material. In the polymer–clay nanocomposites, the dispersed clay particles in a polymer matrix invariably act as a heterogeneous nucleating agent for the spherulite growth. However, such nucleating effect of nanoclays is more pronounced at very low loading levels, ca. 1–5 wt.%. Above these levels, nanoclays may hinder the motion of polymers, thus retarding the crystallization rates. The restricted mobility of the chains imposed by higher clay content would not allow the growth of well developed lamellar crystals[145]. Nanoclays, thus, play two roles in the crystallization process, i.e. a nucleating agent to facilitate the crystallization and a physical hindrance to retard the crystallization[146]. For nanocomposites with low loading levels of fillers, the crystallization process can be either enhanced or inhibited depending on the nature or property of polymer employed. Literature reports enhanced crystallization rates of polymer due to clay addition in case of PA-6[147,148], PP [149,150], poly(ethylene) [151,152], poly(ethylene terepthalate)[153], poly(butylene terepthalate)[154,155], syndiotactic PS[156], and polyvinylidene fluoride (PVDF)[137-159], etc. The introduction of MMT hinders the crystallization of poly(ethylene oxide) (PEO). This is evidenced by a decrease of the spherulite growth and crystallization temperature on the basis of optical microscopy and DSC observations[160].

Apart from enhancing the crystallization rate nanoclay platelets with large surface areas also enhance polymer–silicate interactions. In this regard, the addition of MMT fillers to polymers can stabilize a metastable phase and induce polymorphism. Typical examples are nanoclays which stabilize the γ-phase in polyamides [161-163] and the β-phase in PVDF [157-159]. Pure PA6 crystallize in α-phase while in presence of clay it crystallizes in an otherwise a metastable γ-phase at room temperature. Giannelis and coworkers have recently reported on the remarkable enhancement in the toughness of PVDF filled with organoclay (Cloisite 30B)[158]. They attributed this behavior to the structural and

morphological changes induced by the organoclay particles. In general, there are five crystalline forms or polymorphs of PVDF, i.e. α, β, γ, δ and ε[164]. The α-phase is the dominant crystalline form when the polymer crystallizes from the melt. It was shown from XRD and FTIR studies that organo-MMT induces a phase transition from ordered α-crystallites to disordered, fiber-like β-phase crystallites. The formation of β-phase is also shown to be beneficial to the improvements of stiffness and toughness of PVDF. The fiber-like β-phase is considered to be much more conducive to plastic flow under applied stress. This could give rise to a more efficient energy-dissipation in the nanocomposites, thereby delaying crack formation.

1.7.5 Rheological behavior

The linear dynamic mechanical properties of several nanocomposites have been examined in the melt state for wide range of polymer matrices including PA-6 [165] PS[166], polystyrene-polyisoprene block copolymers[167,168], poly(caprolactone)[169], PP [170-172], poly(lactic acid)[143,173], poly(butylene succinate)[174-176], etc. Rheological behavior of the nanocomposite show peculiar characteristics as compared to conventional composites. The PP/clay nanocomposites showed solid like rheological behaviour at lower frequencies which was shown to be due to frictional interactions between the silicate layers[170]. This behavior depends on the concentration of clay in the composite. It was shown that above a critical concentration of the clay, nanocomposites form percolated structure with the clay layers and show solid like behavior. Studies on the steady shear rheological behavior of poly(butylenes succinate)/clay nanocomposites show that for very low shear rates, clay platelets take a longer time to attain planar alignment along the flow direction, and hence, show a rheopexy behavior. At higher shear rates, the nanocomposite show time independent shear viscosity [175].

1.7.6 Dynamics of polymer chains confined in the clay gallery

Dynamics of polymer chains in intercalated polymer/layered silicate nanocomposites have been extensively studied as they offer a unique system to study the behavior of macromolecules in nanoscopic confinement utilizing macroscopic samples and conventional analytical techniques[177-182]. The equivalence in the behavior between

polymer nanocomposites and thin polymer films has recently been quantitatively verified for silica/polystyrene nanocomposites[183]. Dielectric relaxation behavior by dielectric spectroscopy[184], relaxation behavior due to chain mobility by NMR measurements[180, 181], mean square displacement measurements through quasi-elastic neutron scattering experiments[182], have been employed to study the dynamics of the polymer chains intercalated in the clay galleries. Using quasielastic neutron scattering measurements on polymer dynamics of intercalated poly(methyl phenyl siloxane)/clay nanocomposites, Chrissopoulou *et al*[185], observed that the segmental motion is strongly coupled to the motion of the surfactant chains at temperatures above the calorimetric glass transition temperature of the bulk polymer. However, the mean square displacement data have shown that the segmental motion in confinement is faster than that of the bulk polymer even after the contribution of the surfactant chains is taken into consideration. Vaia *et al*[178] examined the glass transition phenomena using thermally stimulated current technique (TSC thermal sampling technique) to estimate the extent of cooperativity of chain motions and found that the motions of the intercalated PEO chains are inherently non-cooperative relative to the cooperative T_g motions in the amorphous portion of the bulk polymer. It has been recognized that a free surface and/or a non wetting hard interface play the key role in these effects, whereas a strongly attractive surface may alter the behavior[186,187].

On the other hand, the glass transition in thin polymer films can show different behavior depending on the material and the specific experimental technique used. The results generally show a dependence of the glass transition on the film thickness below 50–80 nm. The sign of the shift in T_g depends on the interaction between the surface and the substrate. In the case of constrained films where there is a strong interaction between the polymer and the substrate, an increase in T_g was reported for different polymers[188,189]. In the case of free-standing films, where the interaction between the polymer and the hard surface is less, a decrease in T_g was observed for different polymers[190,191].

Alcoutlabi and McKenna[192] reviewed the effects of confinement of molecules at the nanometre size scale on material behavior. Several theoretical models were proposed to

explain the dynamics of the macromolecules confined in the nano-regime. The effect of confinement on the motion of macromolecules is far less understood at the present time.

1.7.7 Other properties

Polymer nanocomposites show several other improvements in polymer properties. For example, they exhibit transparency similar to pristine polymer materials when the clay layers are completely delaminated and exfoliated in the polymer matrix and when the clay platelets are about one nanometer thickness[14]. Scratch resistance, abrasion resistance is strongly enhanced by the incorporation of layered silicates in the polymer matrix[142]. Biodegradability characteristics of nanocomposites made from organoclay and biodegradable polymers show significant improvements. This is attributed to the presence of terminal hydroxylated edge groups in the clay layers and the catalytic role of the organoclay[193]. Nanocomposites based on the intercalation of polymer electrolyte (e.g., PEO) into clay minerals are an attractive substitute of conventional polymer-salt compounds[194]. This nanocomposite has shown to enhance the stability of the ionic conductivity at lower temperature when compared to more conventional $PEO/LiBF_4$ mixture. Nanocomposites with conjugated conducting polymers have also been reported including polymers such as PANI, polypyrrole, and polythiophene which exhibit a significant increase in the electrical conductivity.

1.8 Applications and commercial developments

Many applications of polymer nanocomposites based on clays have emerged owing to their markedly improved performance in mechanical, thermal, barrier, optical, electrical, and other physical and chemical properties. Increasing number of commercial products has become available. Current and potential commercial applications of nanocomposites have been described in the literature[195, 196]. Some of the commercial products available in the market, their characteristics and their applications are listed in the Table 1.1. The first commercial product of a clay-based polymer nanocomposite is the timing belt cover made from PA-6 nanocomposites introduced by Toyota Motors in the early 1990s[197]. These polymer nanocomposites offer high performance with significant weight reduction and affordable materials for applications in automotive and aerospace industry.

Table 1.1: Commercially available products based on polymer – clay nanocomposites.

Polymer matrix	Property enhancement	Application	Developer / Trade name of product
Polyamide 6	Stiffness, and low density	Timing belt cover, bumpers in automotive	Toyaota / Ube
Nylon MXD6, PP	Barrier property	Beverage containers	Imperm™; Nanocor
nylon 6, 66, 12	Barrier property	Auto fuel systems	Ube, USA
Thermoplastic polyolefins (TPO)	Stiffness / Strength	Exterior step assist	General Motors
Polyisobutylene	Permeability barrier	Tennis balls, tires soccer balls	InMat LLC
Nylon nanocomposite	Modulus	Medical tubing	Foster -Miller
Pouch with helium insert	Barrier property	Basket ball shoe pouch	Converse/Triton system
Nanoclay additives	Flame retardant	Flame retardant additives	Sud chemie
PP	Antic scratch property	Body work in automotives	Dow plastics/Magma
PP	Aesthetics, recyclability, low density	Panes of doors, consoles and interior decoration	Ford, Volvo
Nylon, Acetal	Flame retardecy	cables	Showa denko
Ultra High Molecular Weight Polyethylene	Strength/stiffness	Earth quake resistance pipes	Yantai Haili Ind. & Commerce of China
Aegis NC, Aegis OX (nylon 6)	Stiffness, HDT, clarity, Barrier property	Bottles and films	Honeywell Polymer
Forte nanocomposite	Temperature resistance, stiffness and impact properties	Automotive, furniture, appliance	Noble Polymer
Durethane KU2-2601 (nylon 6)	Stiffness, gloss, clarity, barrier properties	Films and coatings	Bayer

Polymer nanocomposites offer a promising alternative to the commonly employed flame resistant materials containing halogen/phosphorous flame retardants. Polymer nanocomposites can be used to improve the ablative properties of materials. Excellent barrier and optical properties of the films made from clay based polymer nanocomposites

offer advantages in packaging industries as wrapping films and beverage containers for processed meats, cheese, confectionary, cereals, fruit juice, dairy products, beer and carbonated drinks bottles and improves the shelf life for many types of packaged food. Nano-pigments or PlanoColors, developed by TNO Materials, made from clays and organic dyes are believed to be environment friendly substitutes for toxic inorganic pigments. PlanoColors can be readily dispersed on a nanoscale in polymer matrix, which can be used in coatings. An improved oxygen, ultraviolet and temperature stability combined with high brilliance and color efficiency has been displayed due to the surface area of the nano-pigments. The property enhancements, especially on thermal responsivity, swelling-deswelling rate and molecular diffusion, are expected to extend clay-based nanocomposites to such applications as artificial muscles and actuators. Thermo-responsive hydrogels based on poly(N-isopropyl acrylamide)/clay nanocomposites were developed by Liang *et al*[198] and Messersmith and Znidarsich[199]. Manias and coworkers have shown that clay nanocomposites based on poly(urethane-urea) can be used in biomedical applications such as blood sacs in ventricular assist devices and total artificial hearts with improved properties such as reduced gas permeability and increased mechanical properties[200]. O' Neil el al studied the potential design of nylon 12 nanocomposites for catheter shafts which require varying mechanical properties along their length to allow for manipulation of the device[200].

Apart from medical device applications, polymer nanocomposites have recently been extensively investigated for controlled drug delivery (Table 1.2)[159]. The remarkable electrochemical behavior of conducting polymers associated with clay minerals has attracted potential applications such as modified electrodes, biosensors, solid-state batteries, smart windows and other electrochemical devices. For instance, polypyrrole nanocomposites has been developed for modified electrodes useful as sensors or as devices for electrocatalysis. PEO nanocomposites could become novel electrolyte materials because of their relatively higher ambient conductivity and weak temperature dependence over conventional $LiBF_4$/PEO electrolyte as well as their single ionic conduction character.

Table 1.2: Potential biomedical and bioengineering applications of clay-based polymer nanocomposites.

Clay/Organoclay	Polymer	Behaviors/Applications
MMT	poly(*N*-isopropylacrylamide)	swelling-deswelling behaviors
MMT	polyacrylamide	swelling-deswelling behaviors
TDTMA-MMT	poly(*N*-sopropylacrylamide)	thermal response and controlled release rate
Cloisite 20A, Somasif-MAE, Somasif-MAE300	poly(ethylene-co-vinyl acetate)	drug delivery for dexamethasone
Cloisite 30B AAPTMA-MMT	poly(*N*-sopropylacrylamide)	drug release behaviors for caffeine, crystal violet and phenol red
Halloysite	chitosan/polyethyleneimine	drug release for diltriazem hydrochloride and propranolol hydrochloride
Halloysite	chitosan/poloxamer 407	drug delivery for tetracycline
DDTMA-Kanemite and its microporous derivative		drug loading and release of diphenydramine hydrochloride

1.9   Conclusions

The fact that polymeric nanocomposites show substantial improvement in various material properties at very low filler content together with the ease of preparation through simple processes opens a new opportunity for property tailoring. Clay based polymer nanocomposites have been produced as energy-saving and environment-friendly automotive parts and packaging materials. Their future markets will further expand from current automotive, packaging and containers, coatings and pigments to other industries such as appliances and tools, electromaterials, building and construction. Moreover, clay-based polymer nanocomposites have shown promising applications in the biomedical and bioengineering fields. However, in spite of the substantial body of work and some commercial successes, the design and manufacturing of nanocomposites are often empirical. The majority of scientific studies and commercial successes are largely restricted to polar polymers, such as poly(amide)s, epoxies and poly(aniline)s. Only polypropylene has been studied widely as a non-polar polymer. This is indicative of

difficulties in tailoring clay surface for compatibility with non-polar polymers. Additionally most hydrophobic modifiers employed are derived from quaternary ammonium compounds which degrade thermally well below the processing temperature of most of the thermoplastics. There are several unmet challenges in the area of polymer/clay nanocomposites. These are, design of more thermally stable hydrophobic modifiers for clay, a better understanding of the factors controlling miscibility of clay with the polymer and the effect of polymer structure and modifier structure on the structure and property of nanocomposites. For example, whereas it is relatively easier to obtain property improvements (modulus) for nanocomposites with polypropylene, no unambiguous property enhancements have been reported for polyethylene clay nanocomposites. Similarly, in case of polypropylene, whereas, property improvements are generally observed with high MFI (lower molecular weight) polymers, no property enhancements are observed with low MFI PP. Often, with polyolefins, external modifiers (maleated PP) are also used. The relative importance of external and internal modifiers is also poorly understood. Unless significant advances in fundamental understanding of these problems are made widespread applications of polymer-nanocomposites will not become a reality.

References

1.   Mark, J. E. *Polym. Eng. Sci.* **1996**, *36*, 2905.

2.   Reynaud, E.; Gauthier, C.; Perez, J. *Rev. Metall./Cah. Inf. Tech*. **1999**, *96*, 169.

3.   von Werne, T.; Patten, T. E. *J. Am. Chem. Soc*. **1999**, *121*, 7409.

4.   Herron, N.; Thorn, D. L. *Adv. Mater*. **1998**, *10*, 1173.

5.   Calvert, P., *Potential applications of nanotubes*, in: Ebbesen T. W. (Ed.), *Carbon Nanotube*s, CRC Press, Boca Raton, FL, **1997**, pp 277.

6.   Favier, V.; Canova, G. R.; Shrivastava, S. C.; Cavaille, J. Y. *Polym. Eng. Sci.* **1997**, *37,* 1732.

7.   Chazeau, L.; Cavaille, J. Y.; Canova, G.; Dendievel, R.; Boutherin, B. *J. Appl. Polym. Sci.* **1999**, *71*, 1797.

8.   Theng, B. K. G. *Formation and Properties of Clay-Polymer Complexes*, Elsevier Scientific Publishing Co., Amsterdam, The Netherlands, **1979**.

9.   Ogawa, M.; Kuroda, K. *Bull. Chem. Soc. Jpn.* **1997**, *70*, 2593.

10.   Pinnavaia, T. J.; Beall, G. W. *Polymer clay nanocomposites,* John Wiley & Sons Ltd, New York, **2000**.

11.   Koo, J. H. *Polymer Nanocomposites: Processing, Characterization and Applications*, McGraw-Hill Publications, **2006**.

12.   Mai, Y.-W.; Yu, Z.-Z. *Polymer Nanocomposites*, Woodhead Publishing in Materials, CRC, **2006**.

13.   LeBaron, P. C.; Wang, Z.; Pinnavaia, T. J. *Appl. Clay Science*, **1999**, *15*, 11.

14.   Alexandre, M.; Dubois, P. *Mater. Sci. Engg. R: Reports,* **2000**, *28*, 1.

15.   Ray, S. S.; Okamoto, M. *Prog. Polym. Sci.* **2003**, *28*, 1539.

16.   Viswanathan, V.; Laha, T.; Balani, K.; Agarwal, A.; Seal, S. *Mater. Sci. Engg. R: Reports* **2006**, *54*, 121.

17.   Nguyen, Q. T.; Baird D. G. *Adv. Polym. Tech.* **2006**, *25*, 270.

18.   Leszynska, A.; Njuguna, J.; Pielichowski, K.; Banerjee, J. R. *Thermochim. Acta*, **2007**, *453*, 75.

19.   Leszynska, A.; Njuguna, J.; Pielichowski, K.; Banerjee, J. R. *Thermochim. Acta*, **2007**, *454*, 1.

20. Vaia, R. A.; Maguire, J. F. *Chem. Mater*. **2007**, *19*, 2736.

21. Chen, B.; Evans, J. R. G.; Greenwell, H. C.; Boulet, P.; Coveney, P. V.; Bowden, A. A.; Whiting, A. *Chem. Soc. Rev.* **2008**, *37*, 568.

22. Esfandiari, A.; Nazokdast, H.; Rashidi, A.-S.; Yazdanshenas, M.-E. *J. Appl. Polym. Sci*. **2008**, *8*, 545.

23. Yeh, J.-M.; Chang, K.-C. *J. Ind & Eng Chem.* **2008**, *14*, 275.

24. Ciardelli, F.; Coiai, S.; Passaglia, E.; Pucci, A.; Ruggeri, G. *Polym. Int.* **2008**, *57*, 805.

25. Paul, D. R.; Robson, L. M. *Polymer* **2008**, *49*, 3187.

26. Herrera, N. N.; Letoffe, J.-M.; Putaux, J.-L.; David, L.; Bourgeat-Lami, E. *Langmuir* **2004**, *20*, 1564.

27. Kornmann, X.; Berglund, L. A.; Sterte, J. *Polym. Eng. Sci.* **1998**, *38*, 1351.

28. http://www.nanoclay.com

29. http://www.rheox.com

30. http://www.nanocor.com

31. http://www.sud-chemie.com

32. Blumstein, A. *J. Polym. Sci., Part A: Polym. Chem.* **1965**, *3,* 2665.

33. Okada, A.; Kawasumi, M.; Usuki, A.; Kojima, Y.; Kurauchi, T.; Kamigaito, O. In: Schaefer, D. W.; Mark, J. E. *Eds*. *Polymer based molecular composites.* MRS Symposium Proceedings, Pittsburgh, **1990**, *171*, 45.

34. Vaia, R. A.; Ishii, H.; Giannelis, E. P. *Chem. Mater*. **1993**, *5,* 1694.

35. Vaia, R. A.; Giannelis, E. P. *Macromolecules* **1997**, *30*, 8000.

36. Morgan, A. B.; Gilman, J. F. *J. Appl. Polym. Sci.* **2003**, *87*, 1327.

37. Eckel, D. F.; Balogh, M. P.; Fasulo, P. D.; Rodgers, W. R. *J. Appl. Polym. Sci.* **2004**, *93*, 1110.

38. Vaia, R. A.; Jandt, K. D.; Kramer, E. J.; Giannelis, E. P. *Chem. Mater.* **1996**, *8*, 2628.

39. Fornes, T. D.; Yoon, P. J.; Paul, D. R. *Polymer* **2003**, *44*, 7545.

40. Hotta, S.; Paul, D. R. *Polymer* **2004**, *45*, 7639.

41. Manias, E.; Touny, A.; Wu, L.; Strawhecker, K.; Lu, B.; Chung, T. C. *Chem. Mater.* **2001**, *13,* 3516.

42.   Wang, Z. M.; Nagajima, H.; Manias, E.; Chung, T. C. *Macromolecules* **2003**, 36, 8919.

43.   Ho, D. L.; Briber, R. M.; Glinka, C. J. *Chem. Mater*. **2001**, 13, 1923.

44.   Ho, D. L.; Glinka, C. J. *Chem. Mater.* **2003**, *15*, 1309.

45.   Choi, Y. S.; Ham, H. T.; Chung, I. J. *Chem. Mater.* **2004**, *16,* 2522.

46.   Hansen, C. M. *J. Paint Technol.* **1967**, *39*, 104.

47.   Hansen, C. M. *J. Paint Technol.* **1967**, *39*, 505.

48.   Lin, H. M.; Nash, R. A. *J. Pharm. Sci.* **1993**, *82*, 1018.

49.   Li, Y.; Ishida, H. *Polymer* **2003**, *44*, 6571.

50.   Xie, W.; Xie, R.; Pan, W.-P.; Hunter, D.; Koene, B.; Tan, L.-S.; Vaia, R. *Chem. Mater.* **2002**, *14*, 4837.

51.   Xie, W.; Gao, Z.; Liu, K.; Pan, W.-P.; Vaia, R.; Hunter, D.; Singh, A. *Thermochim. Acta* **2001**, *339*, 367.

52.   Awad, W. H.; Gilman, J. W.; Nydena, M.; Harris Jr., R. H.; Sutto, T. E.; Callahan, J.; Trulove, P. C.; DeLongc, H. C.; Fox, D. M. *Thermochim. Acta* **2004**, *409*, 3.

53.   Gilman, J. W.; Awad, W. H.; Davis, R. D.; Shields, J.; Harris Jr., R. H.; Davis, C.; Morgan, A. B.; Sutto, T. E.; Callahan, J.; Trulove, P. C.; Delong, H. C. *Chem. Mater.* **2002**, *14*, 3776.

54.   Ngo, H.; Le Compte, K.; Hargens, L.; McEwen, A. B. *Thermochim. Acta* **2000**, *97*, 357.

55.   Begg, C. G.; Grimmett, M. R.; Wethey, P. D. *Aust. J. Chem.* **1973**, *26*, 2435.

56.   Chan, B. K. M.; Chang, N.-H.; Grimmett, M. R. *Aust. J. Chem.* **1977**, *30*, 2005.

57.   Kost, A. N.; Grandberg, I. I. *Adv. Heterocycl. Chem.* **1966**, *6*, 417.

58.   Carlin, R. T.; Fuller, J., in: Gaune-Escard M. (Ed.), *Molten Salts: From Fundamentals to Applications,* in NATO Science Series, Kluwer, Dordrecht, **2002**.

59.   Usuki, A.; Kawasumi, M.; Kojima, Y.; Okada, A.; Kurauchi, T.; Kamigaito, O. *J. Mater. Res.* **1993**, *8*, 1174.

60.   Reichert, P.; Kressler, J.; Tliomann, R.; Mulhaupf, R.; Stöppelmann, G. *Acta Polym.* **1998**, *49*, 116-123.

61.   Messersmith, P. B.; Giannelis, E. P. *Chem. Mater.* **1993**, *5*, 1064.

62.   Akelah, A. *Polystyrene/clay nanocomposites. In*: Prasad P.N.; Mark J. E.; Ting F. J.; Eds. *Polymers and other advanced materials. Emerging technologies and business opportunities.* New York: Plenum Press; **1995**. p.625.

63.   Akelah, A.; Moet, M. *J. Mater. Sci.* **1996**, *31*, 3589.

64.   Zhu, J.; Morgan, A. B.; Lamelas, F. J.; Wilkie C. A. *Chem. Mater.* **2001**, *13*, 3774.

65.   Ke, Y. C.; Long, C.; Qi, Z. *J. Appl. Polym. Sci.* **1999**, *71*, 1139.

66.   Tsai, T. Y. *Polyethylene terephthalate–clay nanocomposites.* In: Pinnavaia T. J.; Beall, G. W., Eds. *Polymer–clay nanocomposites.* Wiley, London; **2000**. p.173.

67.   Imai, Y.; Nishimura, S.; Abe, E.; Tateyama, H.; Abiko, A.; Yamaguchi, A.; Aoyama, T.; Taguchi, H. *Chem. Mater.* **2002**, *14*, 477.

68.   Hsu, S. L. C.; Chang, K. C. *Polymer* **2002**, *43*, 4097.

69.   Xia, H. S.; Song, M. *Polym. Int.* **2006**, *55*, 229.

70.   Wang, Z.; Pinnavaia, T. J. *Chem. Mater*. **1998**, *10*, 3769.

71.   Xia, H. S.; Song, M. *Polym. Int.* **2006**, *55*, 229.

72.   Pattanayak, A.; Jana, S. C. *Polymer* **2005**, *46*, 3275.

73.   Pattanayak, A.; Jana, S. C. *Polymer* **2005**, *46*, 3394.

74.   Pattanayak, A.; Jana, S. C. *Polymer* **2005**, *46*, 5183.

75.   Pattanayak, A.; Jana, S. C. *Polym. Eng. and Sci*. **2005**, *45*, 1532.

76.   Ni, P.; Li, J.; Suo, J. S.; Li, S. B. *J. Appl. Polym. Sci*. **2004**, *94,* 534.

77.   Ni, P.; Wang, Q. L.; Li, J.; Suo, J.S.; Li, S. B. *J. Appl. Polym. Sci.,* **2006**, *99*, 6.

78.   Tien, Y. I.; Wei, K. H. *Macromolecules* **2001**, *34*, 9045.; Tien, Y. I.; Wei, K. H. *Polymer* **2001**, *42,* 3213.

79.   Moon, S.-Y.; Kim, J.-K.; Nah, C.; Lee, Y.-S. *European Polym. J.* **2004**, *40*, 1615.

80.   Chen, T. K.; Tien, Y. I.; Wei, K. H. *J. Polym. Sci. Part A: Polym. Chem*. **1999**, *37*, 2225.

81.   Leu, C. M.; Wu, Z. W.; Wei, K. H. *Chem. Mater.* **2002**, *14*, 3016.

82.   Tudor, J.; Willington, L.; O'Hare, D.; Royan, B. *Chem. Commun.* **1996**, 2031.

83.   Bergman, J. S.; Chen, H.; Giannelis, E. P.; Thomas, M. G.; Coates, G. W. *J. Chem. Soc.: Chem. Commun.* **1999**, *21*, 2179.

84.   Heinemann, J.; Reichert, P.; Thomann, R.; Mulhaupt, R. *Macromol. Rapid Commun.* **1999**, *20*, 423.

85.   Ray, S.; Galgali, G.; Lele, A.; Sivaram, S. *J. Polym. Sci. Part A: Polym Chem.* **2005**, *43*, 304–318.

86.   Sun, T.; Garces, J. M. *Adv. Mater.* **2002**, *14,* 128.

87.   Jin, Y-H.; Park, H-J.; Im, S-S.; Kwak, S-Y.; Kwak, S. *Macromol. Rapid Commun.* **2002**, *23*, 135.

88.   Zhang, Z.; Zhang, L.; Li, Y.; Xu, H. *Polymer,* **2005**, *46*, 129.

89.   Zhang, Z.; Zhang, L.; Li, Y. *Macromol. Mater. Eng.* **2005**, *290,* 430.

90.   Zhang, Z.; Zhang, L.; Li, Y. *J. Appl. Poly. Sci.* **2006**, *102*, 1167.

91.   Qian, X.; Liao, M.; Zhang. *Polym. Int.* **2007**, *56,* 399.

92.   Weimer, M. W.; Chen, H.; Giannelis, E. P.; Sogah, D. Y. *J. Am. Chem. Soc.* **1999**, *121*, 1615.

93.   Di, J.; Sogah, D. Y. *Macromolecules* **2006**, *39*, 1020.

94.   Di, J.; Sogah, D. Y. *Macromolecules* **2006**, *39*, 5052.

95.   Zhao, H.; Shipp, D. A. *Chem. Mater.* **2003**, *15*, 2693.

96.   Zhao, H.; Farrell, B. P.; Shipp, D. A. *Polymer* **2004**, *45*, 4473.

97.   Zhao, H.; Dayana, A. S.; Farrell, B. P.; Shipp, D. A. *J. Polym. Sci. Part A. Poly. Chem.* **2004**, *42*, 916.

98.   Wheeler, P. A.; Wang, J.; Baker, J.; Mathias, L. J. *Chem. Mater.* **2005**, *17*, 3012.

99.   Li, C-P.; Huang, C-M.; Hsieh, M-T.; Wei, K-H. *J. Polym. Sci. Part A, Poly. Chem.* **2005**, *43,* 534.

100.   Wang, Y.-P.; Pei, X-W.; Liu, X-J.; Yuan, K.; Zhang, D-X.; Li, Q-L.; Wang, Y-F. *Polym. Composit.* **2005**, *26,* 465.

101.   Datta, H.; Bhowmick, A. K.; Singha, N. K. *J. Polym. Sci. Part A: Polym. Chem.* **2008**, *46*, 5014.

102.   Datta, H.; Singha, N. K.; Bhowmick, A. K. Macromolecules **2008**, *41*, 50.

103.   Messersmith, P. B.; Giannelis, E. P. *Chem. Mater.* **1994**, *6*, 1719.

104.   Wang, M. S.; Pinnavaia, T. J. *Chem. Mater.* **1994**, 6, 468.

105.   Lan, T.; Pinnavaia, T. J. *Chem. Mater.* **1994**, *6,* 2216.

106.   Lan, T.; Kaviratna, P. D.; Pinnavaia, T. J. *Chem. Mater.* **1995**, *7*, 2144.

107.   Zilg, C.; Mulhaupt, R.; Finter, J. *Macromol Chem Phys* **1999**, *200,* 661.

108.   Kornmann, X.; Thomann, R.; Mulhaupt, R.; Finter, J.; Berglund, L. A. *Polym. Eng. Sci* **2002**, *42*, 1815.

109.   Becker, O.; Varley, R.; Simon, G. *Polymer* **2002**, *43*, 4365.

110.   Chen, J.-S.; Poliks, M.D.; Ober, C.K.; Zhang, Y.; Wiesner, U.; Giannelis, E. *Polymer* **2002**, *43*, 4895-4904.

111.   Zhang, J.; Manias, E.; Wilkie, C. A. *J. Nanosci. and Nanotechnol.* **2008**, *8*, 1.

112.   Halpin, J. C. *J. Compos. Mater.* **1969**, *3,* 732.

113.   Halpin, J. C.; Kardos, J. L. *Polym. Eng. Sci.,* **1976**, *16,* 344.

114.   Ashton, J. E.; Halpin, J. C.; Petit, P. H., *Primer on Composite Materials: Analysis,* Conn: Techomic Pub. Co, Stamford, **1969.**

115.   T. Mori.; K. Tanaka, *Acta Metallurgica* **1973**, *21*, 571-574.

116.   Hermans, J. *Proc Kon Ned Akad v Wetensch B,* **1967**, *65*, 1–9.

117.   Hill, R. *J. Mech. Phys. Solids,* **1964**, *12*, 119.

118.   Kojima, Y.; Usuki, A.; Kawasumi, M.; Okada, A.; Fukushima, Y.; Kurauchi, T.; Kamigaito, O. *J. Mater. Res.* **1993**, *8*, 1185.

119.   Sherman, L., *Plast. Technol.* **1999**, *45*, 52.

120.   Wang, Z.; Pinnavaia, T. J., *Chem. Mater.* **1998**, *10*, 1820.

121.   Liu, L. M.; Qi, Z. N.; Zhu X. G. *J. Appl. Polym. Sci.* **1999**, *71*, 1133.

122.   Liu, X. H.; Wu, Q. J. *Polymer* **2001**, *42*, 10013.

123.   Fornes, T. D.; Yoon, P. J.; Keskkula, H.; Paul, D. R. *Polymer* **2001**, *42*, 9929.

124.   Lee, D. C.; Jang, L. W. *J. Appl. Polym. Sci.* **1996**, *61*, 1117.

125.   Noh, M. W.; Lee, D. C., *Polym. Bull.* **1999**, *42,* 619.

126.   Chung, M. J.; Jang, L. W.; Shim, J. H.; Yoon J. S. *J. Appl. Polym. Sci.* **2005**, *95*, 307.

127.   Pinnavaia, T. J.; Beall, G. W. *Polymer-Clay Nanocomposites*, Wiley, London, **2000**.

128.   Krishnamoorti, R.; Vaia, R. A. *Polymer Nanocomposites: Synthesis, Characterization, and Modeling,* American Chemical Society, Washington, DC **2001**.

129. Komarneni, S. *Nanophase and Nanocomposite Materials IV: Symposium held November 26–29, 2001, Boston, Massachusetts, USA,* Materials Research Society, Warrendale, Pennsylvania. **2002.**

130. Yano, K.; Usuki, A.; Okada, A., *J. Polym. Sci., Part A: Poly. Chem.* **1997**, *35*, 2289.

131. Messersmith, P. B.; Giannelis, E. P. *J. Polym. Sci., Part A: Polym.Chem.* **1995**, *33,* 1047.

132. Yeh, J. M.; Chen, C. L.; Kuo, T. H.; Su, W. F.; Huang, H. Y.; Liaw, D. J.; Lu, H. Y.; Liu, C. F.; Yu, Y. H. *J. Appl. Polym. Sci.* **2004**, *92*, 1072.

133. Liang, Y. R.; Wang, Y. Q.; Wu, Y. P.; Lu, Y. L.; Zhang, H. F.; Zhang, L. Q. *Polym. Test.* **2005**, *24*, 12.

134. Ray, S. S.; Yamada, K.; Okamoto, M.; Ueda, K. *Nano Lett.* **2002**, *2*, 1093.

135.   Xu, R. J.; Manias, E.; Snyder, A. J.; Runt, J. *J. Biomed. Mater.Res. Part A* **2003**, *64*, 114.

136. Lim, S. T.; Hyun, Y. H.; Choi, H. J.; Jhon, M. S., *Chem. Mater.* **2002**, *14,* 1839.

137. Gilman, J. W. *Appl. Clay Sci.* **1999**, *15*, 31.

138. Zanetti, M.; Camino, G.; Thomann, R.; Mullhaupt, R. *Polymer* **2001**, *42*, 4501.

139. Burnside, S. D.; Giannelis, E. P., *Chem. Mater.* **1995**, *7,* 1597.

140. Doh, J. G.; Cho, I. *Polym. Bull.* **1998**, *41*, 511.

141. Lee, D. C.; Jang, L. W., *J. Appl. Polym. Sci.* **1998**, *68*, 1997.

142. Nam, P. H.; Maiti, P.; Okamoto, M.; Kotaka, M.; Ohshima M.; Hasegawa, N.; Usuki A. in *The First World Congress of Nanocomposites*, Chicago, USA **2001**, p.281.

143. Ray, S. S.; Yamada, K.; Okamoto, M.; Ueda, K. *Polymer* **2003**, *44*, 857.

144. Gilman, J. W.; Kashiwagi, T.; Brown, J. E. T.; Lomakin, S.; Giannelis, E. P.; Manias, E. *Int. SAMPE Symposium and Exhibition.*, **1998**, *43*, 1053.

145. Maio E. D.; Iannace, S.; Sorrentino, L.; Nicolais, L., *Polymer* **2004**, *45*, 8893.

146. Zhang, G.; Yan, D., *J. Appl. Polym. Sci.* **2003**, *88*, 2181.

147. Fornes, T. D.; Paul, D. R. *Polymer* **2003**, *44*, 3945.

148. Lincoln, D. M.; Vaia, R. A.; Krishnamoorti, R. *Macromolecules* **2004**, *37*, 4554.

149. Hambir S.; Bulakh N.; Jog, J. P. *Polym. Eng. Sci.* **2002**, *42,* 1800.

150.   Nam, P. H.; Maiti, P.; Okamoto, M.; Kotaka, T.; *Polym. Eng. Sci.* **2002**, *42,* 1864.

151.   Tjong, S. C.; Bao, S. P.; *J. Polym. Sci. Part B: Polym. Phys.* **2005**, *43,* 253.

152.   Gopakumar, T. G.; Lee, J. A.; Kontopolou, M.; Parent, J. S. *Polymer* **2002**, *43*, 5483.

153.   Ke, Y.; Long, C.; Qi, Z. *J. Appl. Polym. Sci.* **1999**, *71*, 1139.

154.   Chisholm, B. J.; Moore, R. B.; Barber, G.; Khouri, F.; Hempstead, A.; Larsen, M. *Macromolecules* **2002**, *35*, 5508.

155.   Wu, D. F.; Zhou, C. X.; Xie, F.; Mao, D. L.; Zhang, B. *J. Appl. Polym. Sci.* **2006**, *99*, 3257.

156.   Wu, H. D.; Tseng, C. R.; Chang, F. C. *Macromolecules* **2001**, *34*, 2992.

157.   Priya, L.; Jog, J. P. *J. Polym. Sci. Part B: Polym. Phys.* **2002**, *40*, 1682.

158.   Shah, D.; Maiti, P.; Gunn, E.; Schnidt, D. F.; Jiang, D. D.; Batt, C. A.; Giannelis E. P. *Adv. Mater.* **2004**, *16*, 1173

159.   Dillon, D. R.; Tenneti, K. K.; Li, C. Y.; Ko, F. K.; Sics, I.; Hsiao, B. S. *Polymer* **2006**, *47*, 1678.

160.   Strawhecker, K. E.; Manias, E. *Chem. Mater.* **2003**, *15*, 844.

161.   Tjong, S. C.; Bao, S. P. *J. Polym. Sci. Part B: Polym. Phys.* **2004**, *42*, 2878.

162.   Lincoln, D. M.; Vaia, R. A.; Wang, Z.; Hsiao B.S.; *Polymer* **2001**, *42*, 1621.

163.   Incarnato, L.; Scarfato, P.; Russo, G. M.; Maio, L. D.; Iannelli, P.; Arcierno, D., *Polymer* **2003**, *44,* 4625.

164.   Guerra, G.; Karasz, F. E.; MacKnight, W. J. *Macromolecules* **1986**, *19,* 1935.

165.   Fornes, T. D.; Yoon, P. J.; Keskkula, H.; Paul D.R. *Polymer* **2001**, *42*, 9929.

166.   Hoffman, B.; Dietrich, C.; Thomann, R.; Friedrich, C.; Mulhaupt, R. *Macromol. Rapid. Commun.* **2000**, *21,* 57.

167.   Ren, J.; Silva, A. S.; Krishnamoorti, R. *Macromolecules* **2000**, *33*, 3739.

168.   Mitchell, C. A.; Krishnamoorti, R. *J. Polym. Sci., Part B: Polym Phys.* **2002**, *40,* 1434.

169.   Lepoittevin, B.; Devalckenaere, M.; Pantoustier, N.; Alexandre, M.; Kubies, D.; Calberg, C.; Jerome, R.; Dubois, P. *Polymer* **2002**, *43,* 4017.

170.   Galgali, G.; Ramesh, C.; Lele, A. *Macromolecules* **2001**, *34,* 852.

171.   Solomon, M. J.; Almusallam A.S.; Seefeldt K.F.; Somwangthanaroj A.; Varadan P. *Macromolecules* **2001**, *34*, 1864.

172.   Lele, A.; Mackley, M.; Galgali, G.; Ramesh, C. *J. Rheol.* **2002**, *46*, 1091.

173.   Ray, S. S.; Maiti, P.; Okamoto, M.; Yamada, K.; Ueda, K. *Macromolecules* **2002**, *35,* 3104.

174.   Ray, S. S.; Okamoto, K, Maiti, P.; Okamoto, M. *J. Nanosci. Nanotechnol.* **2002**, *2*, 171.

175.   Ray, S. S.; Okamoto, K.; Okamoto, M. *Macromolecules* **2003**, *36*, 2355.

176.   Kornmann, X.; Berglund, L. A.; Sterete, J.; Giannelis, E. P. *Polym. Eng. Sci.* **1998**, *38,* 1351.

177.   Wong, S.; Vaia, R. A.; Giannelis, E. P.; Zax, D. B. *Solid State Ionics* **1996**, *86*, 547.

178.   Vaia, R.; Sauer, B. B.; Tse, O. K.; Giannelis, E. P. *J. Polym. Sci., Part B: Polym. Phys.* **1997**, *35*, 59.

179.   Anastasiadis, S. H.; Karatasos, K.; Vlachos, G.; Manias, E.; Giannelis, E. P. *Phys. Rev. Lett.* **2000**, *84*, 915.

180.   Zax, D. B.; Yang, D.-K.; Santos, R. A.; Hegemann, H.; Giannelis, E. P.; Manias, E. *J. Chem. Phys.* **2000**, *112*, 2945.

181.   Manias, E.; Giannelis, E. P.; Zax, D. B.; Anastasiadis, S. H. *Polym. Mater. Sci. Eng.* **2000**, *82*, 59.

182.   Frick, B.; Alba-Simionesco, C.; Dosseh, G.; Le Quellec, C. Moreno, A. J.; Colmenero, J.; Schonhals, A.; Zorn, R.; Chrissopoulou, K.; Anastasiadis, S.H.; Dalnoki-Veress, K. *J. Non-Cryst. Solids* **2005**, *351*, 2657.

183.   Bansal, A.; Yang, H.; Li, C.; Cho, K.; Benicewicz, B. C.; Kumar, S. K.; and Schadler, L. *Nat. Mater.* **2005**, *4*, 693.

184.   Elmahdy, M. M.; Chrissopoulou, K.; Afratis, A.; Floudas, G.; Anastasiadis S. H. *Macromolecules* **2006**, *39,* 5170-5173.

185.   Chrissopoulou, K.; Anastasiadis, S. H.; Giannelis, E. P.; Frick, B. *The J. Chem. Phys.* **2007**, *127,* 144910.

186.   Sharp, J. S.; Forrest, J. A. *Phys. Rev. Lett.* **2003**, *91*, 235701.

187.   Ellison, C. J.; Torkelson, J. M. *Nat. Mater.* **2003**, *2*, 695.

188.   Keddie, J. L.; Jones, R. A. L.; Cory, R. A. *Faraday Discuss.* **1994**, *98*, 219

189.   Keddie, J. L.; Jones, R. A. L. *I. S. R. Chem. Soc.* **1995**, *35,* 21.

190.   Forrest, J. A.; Dalnoki-Veress, K.; Dutcher, J. R. *Phys. Rev.* **1997**, *E 56***, 5705.

191.   Dalnoki-Veress, K.; Forrest, J. A.; Murray, C.; Gigault, C.; Dutcher, J. R. *Phys. Rev. E* **2001**, *63*, 31801.

192.   Alcoutlabi, M.; McKenna, G. B. *J. Phys.: Condens. Matter* **2005**, *17*, R461.

193.   Ray, S. S.; Yamada, K.; Okamoto, M.; Ueda, K. *Polymer* **2003**, *44*, 857.

194.   Vaia, R. A.; Vasudevan, S.; Krawiec, W.; Scanlon, L. G.; Giannelis, E. P. *Adv. Mater.* **1995**, *7,* 154.

195.   Sanchez, C.; Julian, B.; Belleville, P.; Popall, M. *J. Mater. Chem.* **2005**, *15*, 3559.

196.   Zeng, Q. H.; Yu, A. B.; Lu, G. Q. (M).; Paul D. R. *J. Nanosci. Nanotech.* **2005**, *5,* 1574.

197.   Okada, A.; Fukumori, K.; Usuki, A.; Kojima, Y.; Sato, N.; Kurauchi, T.; Kamigaito, O. *Polym. Prepr*. **1991**, *32*, 540.

198.   Liang, L.; Liu, J.; Gong, X. *Langmuir* **2000**, *16*, 9895.

199.   Messersmith, P. B.; Znidarsich, F., *Mater. Res. Soc. Symp. – Proceedings* **1997**, *457,* 507.

200.   Xu, R.; Manias, E.; Snyder, A. J.; Runt, J. *Macromolecules* **2001**, *34*, 337

201.   O'Neil, C. J.; Acquarulo Jr., L. A.; Jain, N. R.; Faucher, J. *Annual Technical Conference - ANTEC, Conference Proceedings* **2003**, *3,* 2593.

Chapter 2

Scope and Objectives

2. Scope and Objectives

Polymer nanocomposites have been an area of intense industrial and academic research for the past twenty years. Amongst all the potential nanocomposite precursors, those based on clay and layered silicates have been more widely investigated, presumably, because the starting clay materials are easily available and their intercalation chemistry has been a subject of research over a long period of time. Further development of polymer nanocomposite materials depends largely on our understanding of the fundamentals with respect to their formation, processing, property prediction and design. It has been well established that stronger the interaction of the polymer chains with the clay surface better the dispersion of the clay layers in the polymer matrix. Significant improvements in properties are achieved when the clay layers are thoroughly dispersed and exfoliated in the polymer matrix. Dispersion of clay depends on the method of preparation of the nanocomposite and the nature and properties of polymer used. Therefore, the objective of this thesis is to explore various strategies to obtain better dispersion of clay layers in chosen polymers and to examine relationship between structure and property of nanocomposites.

In spite of several prior efforts in the literature no clear understanding has emerged on the structure of poly(urethane)s/clay nanocomposites and its dependence on the nature of modifiers and polyols. *Therefore, to understand the dispersion of clay in the polyurethane matrix, the focus of the present work i) to study the effect of branching agent on the structure of the polyurethane/clay nanocomposites and ii) to study the effect of degree of functionality of the organic modifier of the clay on the structure of the polyurethane/clay nanocomposites.*

For the dispersion of clay in poly(carbonate)s matrix most of the studies reported use organoclays modified with quaternary ammonium salts which are known to degrade at the temperatures normally encountered during the preparation and processing of the polymer. *The objective of the present work is to prepare poly(carbonate)s/clay*

nanocomposites via in-situ melt polycondensation using organoclays which were modified using more thermally stable modifiers. A further goal was to improve the interaction of the polymer with the clay surface by introducing a reactive bisphenol functionality into the modifier.

Studies on the synthesis of syndiotactic poly(styrene)s (sPS)/clay nanocomposites are very scarce mainly because of the high melting and processing temperatures and poor dispersion of clay in the sPS matrix due to the low surface energy and non-polar nature of the polymer. *Therefore, the objective of the present work is to improve the surface energy of the sPS by sulfonation to form an ionomer and to study the effect of degree of sulfonation and nature of cation in ionomer (H^+, Na^+, K^+ and Rb^+) on intercalation/exfoliation of sPS ionomers/organoclay nanocomposites.*

Maleic anhydride-g-polypropylene has been extensively used as compatibilizer for the preparation of polypropylene/clay nanocomposites via melt mixing. Nanocomposites obtained with lower molecular weight PP showed better dispersion and property enhancements compared to higher molecular weight PP. *Therefore an objective of the present study was to evaluate the dispersion of organoclay in relatively higher molecular weight PP using potassium succinate-g-PP as compatibilizer and study the enhancement in properties including crystallization behaviour, thermal and mechanical properties.*

Chapter 3

Poly(urethane)/Clay Nanocomposites via *in-situ* Solution Polymerization

3. Poly(urethane)/clay nanocomposites via *in-situ* solution polymerization

3.1 Introduction

Polyurethanes (PU) are versatile polymeric materials exhibiting a wide range of physical and chemical properties with well designed combinations of monomeric materials which can be tailored to meet the diversified demands in applications such as coatings, adhesives, and reaction injection molding plastics, fibers, foams, rubbers, thermoplastic elastomers and composites[1-3]. However PU also suffer from some weakneses such as low thermal stability and poor mechanical strength. Chemical modifications of PU or use of inorganic filler may in specific instances mitigate these problems. Many properties of PU are reported to be improved by incorporation of fillers. Calcium carbonate, aluminum hydroxide, kaolin, titanium dioxide, zinc oxide, were used to improve mechanical properties[4-9]. However, use of inorganic particulate fillers also has a deleterious effect on the fatigue property of PU and reduces its elongation at break[10].

Nanostructured PU/clay composites have been explored in recent years. Wang and Pinnavaia[11] reported preparation of nanocomposites of elastomeric PU based on a polyol, poly(glycerol propoxylate), and Rubinate methylene diphenyl diisocyanate prepolymer (Mn: 1050) with a functionality of two. They found that clays exchanged with long chain onium ions (carbon number $\geq$ 12) have good compatibility with several polyols commonly used for the synthesis of PU. The PU nanocomposites obtained exhibited large enhancement in tensile strength and tensile modulus when compared to the pristine polymer. This initial result triggered a spate of research activities on the synthesis of thermoplastic polyurethanes (TPU)/clay nanocomposites via solvent mixing; melt mixing, *in-situ* solution and bulk polymerization methods. In general, tensile strength and thermal stability of PU-nanocomposites showed improvements without loss of high elongation at break of the pristine polymer[12-30] except for one study where a decrease of tensile modulus was observed[12]. In the case of *in-situ* polymerization studies, similar to the successful *in-situ* polymerization of PA-6/clay nanocomposites, clay particles were

intercalated either by soft polyols prior to reaction with diisocyanates, or prepolymer terminated with diisocyanates were mixed with organoclay followed by chain extension with short chain diols.[31, 32]. For e.g. Hu *et al*[20], prepared nanocomposites by synthesis of prepolymer terminated with diisocyante, in presence of organoclay using poly(propylene oxide) (PPG) and toluene diisocyanate (TDI) in the first step, followed by curing with glycerol and diglycol. Ni *et al*[33,34], mixed the dispersion of organoclay with prepolymer terminated isocyanate, which was prepared from poly(tetramethylene glycol) (PTMG) and 4,4'-diphenylmethane diisocyanate (MDI), followed by addition of the curing agent 1,2-diamino propane.

Self-consistent field theory calculations were performed by Balazs[35] *et al* to investigate the effect of composition of the polymer on the miscibility of polymer/organoclay mixture. A combination of functional groups on the surfactant modifier and larger number of branches in the polymer leads to better interaction of clay with the polymer chains leading to exfoliated structures. Only branching in the polymer results in intercalated structures. Enhanced miscibility of the organoclay with the polymer containing branched structure was attributed to the compactness of the macromolecule. The radius of gyration decreases as the number of branches increases with a given molecular weight and the more compact polymer can better interact and interpenetrate the short grafted layer. It should be noted that exfoliated PU/clay nanocomposites, based on polyether polyol and hydrogenated MDI, were obtained whenever the functionality of the polyol used was greater than two[36]. It has been shown that the exfoliation process takes place during mixing with the polyol prior to urethane formation step.

It is generally recognized that the properties of the nanocomposites are better when the interaction of the polymer chains with the surface of the clay layers are improved. This can be achieved by tethering the polymer onto the surface of the clay layers, which are completely delaminated and fully exfoliated through out the polymer matrix[37]. Tien and Wei[18], showed that PU based on PTMG and MDI can be ionically tethered to the surface of the clay by choosing modifiers having reactive hydroxyl groups. They used short chain hydroxyl containing modifiers based on protonated 3-aminopropanol (NH_2-CH_2-CH_2-

CH_2-OH), 3-amino-1,2-propanediol (NH_2-CH_2-(CHOH)-CH_2-OH) and tris(hydroxy methyl)aminomethane ((HO-CH_2)$_3$-C-NH_2) (THAM) having hydroxyl functionalities of 1, 2, and 3 respectively. The hydroxyl groups in the modifier of the clay were reacted with isocyanate terminated PU-prepolymer. The presence of 3 hydroxyl groups per modifier favored formation of exfoliated PU nanocomposites. Moon *et al*[38] utilized the organoclay modified with protonated THAM to prepare PU nanocomposites based on poly(butylene succinate) (PBS). Poly(ethylene glycol) was employed as the soft segment and 1,4-butanediol and hydrogenated MDI as hard segments. The nanocomposites obtained exhibited an intercalated structure even at 1-3 wt % of organoclay. Inability to form exfoliated structures was attributed to the poorer swelling of organoclay by PBS over PTMG. Chavarria and Paul[39] studied the effect of organoclay structure on the dispersion of thermoplastic polyurethane nanocomposites prepared by melt mixing. It was shown that the ammonium ion having one alkyl tail rather than two, presence of hydroxyethyl groups rather than methyl groups on the nitrogen and a longer alkyl tail along with hydroxyethyl group rather than shorter alkyl chain along with hydroxyethyl group leads to better clay dispersion. The study also showed that PU with more hard segments, i.e., with more polar functionalities, favors better interaction. Pattanayak and Jana[40-43] utilized a combination of tethering reaction and melt shear force to disperse the clay in PU matrix. The PU was derived from polypropylene glycol, 1,4-butanediol and MDI. They showed that partially exfoliated structures could be obtained by adding the organoclay during bulk polymerization. The extent of dispersion of clay depends on the polarity of polyol used. However, bulk polymerization method has its own limitations such as (i) poor diffusion of reactants that hinder the rate of the reaction (ii) exotherm resulting in steep rise in temperature during polymerization leading to the formation of biurets and allophanates.

In spite of several prior studies, the dependence of the structure of nanocomposites obtained on the structure and composition of the poly(urethane)s are poorly understood. An exfoliated nanocomposite results when a branched polyol is used. Similarly when a modifier containing three methylol groups was ionically anchored to the clay and reacted

with an isocyanate terminated prepolymer, based on PTMG and MDI, an exfoliated structure was reported to be obtained[18].

To better understand the nature of modifiers, its functionality and structure on the structure of PU nanocomposites the present study was undertaken. In the first study, two commercially available organomodified clay, one without any hydroxyl functionality and the other with two primary hydroxyl groups were chosen. In the second study, a series of quaternary ammonium cations bearing modifiers were synthesized bearing respectively, one, two or three primary hydroxyl groups. In addition these modifiers contained a long chain hexadecyl group, which could presumably improve miscibility with less polar monomers used for PU preparation.

For the first study, PU nanocomposites were prepared via *in-situ* solution polymerization using 2-ethyl-1, 3-hexanediol and toluenediisocyanate (TDI) as monomers and trimethylolpropane (TMP) as a branching agent. Organically modified montmorillonite clays Cloisite 30 B, (in which the modifier has a long alkyl chain and two hydroxy ethyl groups) and Cloisite 25 A (in which the modifier have only long alkyl chain and no hydroxyl groups) were chosen for the study (Table 3.1). For the second study, organoclays were prepared by exchanging the Na^+ ions in pristine sodium montmorillonite with three different quaternary ammonium bromides namely *N*-(2-hydroxyethyl)-*N,N*-dimethylhexadecyl-1-ammonium bromide (**1**), N,N-bis(2-hydroxyethyl)-N-methylhexadecyl-1-ammonium bromide (**2**) and N,N-bis(2-hydroxyethyl)-N-methyl-2-(hydroxymethyl)octadecyl-1-ammonium bromide (**3**), having 1, 2 or 3 hydroxyl functionality respectively and designated as 1-OH(MMT), 2-OH(MMT) and 3-OH(MMT) respectively. The state of dispersion of clays was evaluated for preparation of polyurethane-clay nanocomposites via *in-situ* solution polymerization of 2-ethyl-1, 3-hexanediol and TDI. In addition, a thermoplastic polyurethanes (polycaprolactone diol and isophorone diisocyanate with butanediol as chain extender) /clay nanocomposites was also prepared using modified clays such as 1-OH(MMT)**,** 2-OH(MMT) and 3-OH(MMT).

Table 3.1: List of organoclays used and the structure of their modifiers

Organoclay	Structure of the modifier	Name of the modifier
Cloisite 25A	CH₃ — N⁺ — H₃C, CH₃, TH Where TH = hydrogenated tallow	*N*-(hydrogenated tallow)-*N,N,N*-trimethyl ammonium cation
Cloisite 30B	CH₃ — N⁺ — HO, OH, TH Where TH = hydrogenated tallow	*N,N*-bis(hydroxyethyl)-N-(hydrogenated tallow)-N-methyl ammonium cation
1-OH(MMT)	CH₃ — N⁺ — H₃C, OH, C₁₆H₃₃ **1**	N-(2-hydroxyethyl)-N,N-dimethyl-N-hexadecylammonium cation
2-OH(MMT)	CH₃ — N⁺ — HO, OH, C₁₆H₃₃ **2**	N,N-bis(2-hydroxyethyl)-N-methyl-N-hexadecylammonium cation
3-OH(MMT)	H₃C — N⁺ — HO, OH, OH, C₁₆H₃₃ **3**	N,N-bis(2-hydroxyethyl)-N-methyl-N-(2-(hydroxymethyl)octadecyl)ammonium cation
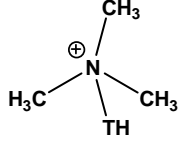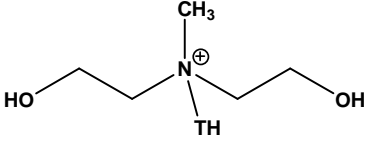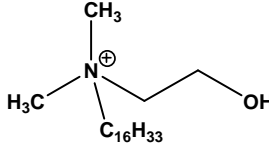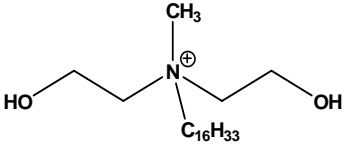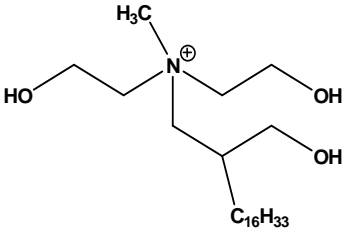
3.2   Experimental

3.2.1   Materials

Cloisite 30B and Cloisite 25A which are organo-modified Montmorillonites and Na⁺ Montmorillonite were obtained from Southern Clay Products, USA. They were dried by

subjecting the sample to azeotropic distillation with toluene and stored in a vacuum descicator. 2-ethyl-1,3-hexanediol, 1-hexadecyl bromide, *N,N*-bis(-2-hydroxyethyl)-*N*-methylamine, N-(2-hydroxyethyl)-N,N-dimethylamine and isophorone diisocyante were obtained from Aldrich Chemical Co., USA and used without further purification. 2-ethyl-2-(hydroxymethyl)propane-1,3-diol (TMP), 1,4- butanediol and dimethyl malonate were obtained from Sd fine chemicals, India and used as such. Toluene diisocyanate (mixture of 2,4 and 2,6 isomers in the ratio 20:80) were obtained from Narmada Chemicals, India. Polycaprolactone diol (CAPA 2077A, Mn: 750, PDI: 1.2) was kindly supplied by Solvay Chemicals, USA.

3.2.2 Preparation of *N*-(2-hydroxyethyl)-*N,N*-dimethyl-*N*-hexadecylammonium bromide (1)

N-(2-hydroxyethyl)-N,N-dimethyl amine (4.457 g, 50 mmol) was mixed with hexadecyl ammonium bromide (15.268 g, 50 mmol) in the stoichiometric ratio 1:1 and heated to 60 °C. White solid particles started forming immediately at 60 °C. Heating was continued for another six hours to ensure that the reaction was complete. 2-hydroxyethyl dimethyl hexadecylammonium bromide (**1**) (19.7 g) was obtained in a pure form and used without further purification. Yield: 75%. ^{1}H NMR: δ 0.88 (3H, t); 1.26 (26H, m); 1.76 (2H, m); 3.38 (6H, s); 3.55 (2H, m); 3.77 (2H, b); 4.14 (2H, b); 5.03 (1H, b).

3.2.3 Preparation N,N-bis(2-hydroxyethyl)-N-methyl-N-hexadecylammonium bromide (2)

Bis(hydroxyethyl)methyl amine (5.958 g, 50 mmol) was mixed with hexadecyl ammonium bromide (15.268 g, 50 mmol) in the stoichiometric ratio 1:1 and heated to 60 °C. White solid particles started forming 15 minutes after attaining the temperature of 60 °C and the heating was continued for another 8 hours to ensure completion of reaction. Obtained N,N-bis(2-hydroxyethyl)-N-methyl-N-hexadecylammonium bromide (**2**) (21.2 g) was used without further purification. ^{1}H NMR: δ 0.88 (3H, t); 1.26 (26H, m); 1.75 (2H, m); 3.33 (3H, s); 3.54 (2H, m); 3.73 (4H, b); 4.14 (4H, b); 5.03 (2H, b).

3.2.4 Preparation of N,N-bis(2-hydroxyethyl)-N-methyl-N-(2-(hydroxymethyl) octadecyl)ammonium bromide (3)

The hydroxy alkyl bromide was prepared from dimethyl malonate and hexadecyl bromide in three steps. The hydroxyalkyl bromide was used for the quartenization of bis(hydroxyethyl) methylamine. The reactions are depicted in Scheme 3.3.

3.2.4.1 Alkylation of dimethyl malonate with hexadecyl bromide

Clean dry sodium (2.0 g, 85 mmol) was placed in a three neck round bottom flask fitted with double surface codenser, dropping funnel and septum adapter. Dry methanol (100 mL) was added to sodium slowly under cooling. Sodium methoxide was formed with the evolution of hydrogen gas. Cooling was stopped after the evolution of hydrogen gas ceased. Dimethyl malonate (11.2 g, 85 mmol) was added under stirring and heated to gentle reflux. Hexadecyl bromide (24.4 g, 80 mmol) was taken in dropping funnel and added slowly into the contents of the round bottom flask over a period of 20 min and reflux continued for 12 hours. Progress of the reaction was monitored by TLC. The reflux was stopped when all the alkyl bromide was consumed. The crude reaction mixture was concentrated by evaporating methanol, diluted with ethyl acetate and washed with water several times until the washings was neutral to litmus. Pure dimethyl-2-hexadecyl malonate (18.5 g), was separated from the crude mixture by flash chromatography. Yield: 65%. ^{1}H NMR: δ 0.88 (3H, t); 1.26- (28H, m); 1.91 (2H, m); 3.36 (1H, t); 3.73 (6H, s).

3.2.4.2 Reduction of dimethyl-2-hexadecyl malonate to 2-(hydroxymethyl) octadecanol

Lithium aluminum hydride (LAH) (4.9 g, 130 mmol) was dispersed in 80 mL of dry tetrahydrofuran. Dimethyl-2-hexadecyl malonate (17.8 g, 50 mmol) was dissolved in 100 mL of dry THF and added slowly into LAH dispersion at 0 °C for 1 hour duration. After the addition was completed, temperature of the reaction mixture was brought to room temperature on its own and then heated to mild reflux for 6 hours. The reaction was monitored by TLC analysis and stopped when there was no starting material. Excess LAH was quenched by addition of ethyl acetate. The aluminum adduct formed was

cleaved by adding the reaction mixture slowly into hydrated sodium sulphate and the slurry was stirred for one hour and filtered over celite bed. The filtrate was concentrated to get the diol. Pure 2-(hydroxy methyl) octadecanol (9.8 g) was isolated by column chromatographic separation. Yield 65%. ^{1}H NMR: δ 0.88 (3H, t); 1.26-1.60 (30H, m); 1.75 (1H, m); 3.61 to 3.86 (4H, 2dd).

3.2.4.3 Monobromination of 2-(hydroxymethyl)octadecanol to 2-(hydroxymethyl) octadecyl bromide

2-(hydroxymethyl)octadecanol (**6**)(10 g, 33.3 mmol) and CBr_4 (13.28 g, 0.040 mol) was dissolved in dry tetrahydofuran (100 mL) and taken in a three-neck round bottom flask fitted with a dropping funnel, a condenser and a three-way stopcock. Triphenylphosphine (9.16 g, 35 mmol) was dissolved in tetrahydofuran and added to the reaction mixture at 0 °C dropwise over period of 30 minutes. Stirring was continued for an additional 4 hours at 0 °C. Progress of the reaction was monitored by TLC. The crude reaction mixture was concentrated by evaporating tetrahydrofuran and the residue dissolved in ethyl acetate and washed with water. 2-(hydroxymethyl)octadecyl bromide (9.7 g) was isolated in a pure form after column chromatography. Yield: 80 %. ^{1}H NMR: δ 0.88 (3H, t); 1.26 (28H, m); 1.60 (2H, m); 1.83 (1H, m); 3.47 to 3.74 (4H, 4dd).

3.2.4.4 Preparation of N,N-bis(2-hydroxyethyl)-N-methyl-N-(2-(hydroxymethyl) octadecyl)ammonium bromide (3)

N,N-Bis(2-hydroxyethyl)-*N*-methyl amine (2.98 g, 25 mmol) was mixed with hexadecyl ammonium bromide (9.1 g, 25 mmol) in the stoichiometric ratio 1:1 and heated to 60 °C in ethanol (65 mL). Progress of reaction was monitored by TLC anaysis. Even after 3 days the reaction did not go to completion, as evidenced by presence of unreacted alkyl bromide and amine. A white crystalline powder of N,N-bis(2-hydroxyethyl)-N-methyl-N-((2-hydroxymethyl)octadecyl)ammonium bromide (6.1 g) was obtained from the pasty crude reaction mixture by repeated recrystallization from ethyl acetate. Yield: 50%. ^{1}H NMR: δ 0.88 (3H, t); 1.26 to 1.44 (30H, m); 2.12 (1H, m); 3.07(1H,m); 3.33(1H,m); 3.45(1H, m); 3.28(3H, s); 3.76 (4H, b); 3.83 (1H, m); 4.12 (4H, b); 4.59 (1H, b), 4.89 (2H, b).

3.2.5   Model studies to assess the reactivity of 1, 2 and 3 with phenyl isocyanate

To demonstrate the reactivity of the hydroxyl groups of the organomodifiers **1, 2** and **3** with isocayanates, the modifier salt **1** (0.0985 g) was mixed with phenyl isocyanate (0.0297 g) at room temperature in toluene medium in presence of dibutyltin dilaurate as catalyst and heated at 60 °C for 2 hours. Subsequently, the solvent from the reaction mixture was evaporated in vacuo and the quantitative formation of phenyl carbamate was studied by ^{1}H NMR analysis. Similarly, **2** (0.106 g) was treated with phenyl isocyanate (0.0595 g) and **3** (0.1208 g) was treated with phenyl isocyanate (0.0893 g) to obtain the respective carbamates.

3.2.6   Preparation of organo-modified clays

The Na$^+$ montmorinollite (10 g) with CEC 92 meq/100 g, d spacing 12 Å was dispersed in water/methanol (300 mL) by stirring with an over head stirrer at room temperature for 2 hours. The modifier (11 meq) dissolved in methanol/water mixture was added slowly to the dispersion of clay and stirred for 24 hours at 65 °C. The reaction mixture was cooled, centrifuged and washed several times with distilled water and methanol until free of bromide ions. The organoclay obtained was freeze dried in vacuo. The organoclay was obtained as fine, dry powder. The interlayer d- spacing for the organomodified montmorillonite was measured from WAXD. The content of modifier was measured using thermogravimetric analysis performed at 900 °C.

3.2.7   Estimation of isocyanate content

The isocyanate content was estimated by adding known excess of dibutyl amine (DBA) in toluene and back titrating the excess amine with HCl using bromophenol blue as the indicator. The isocyanate solution to be estimated was taken in a conical flask and 10 mL of DBA (2 N) was added and stirred for one hour. Isopropanol (25 mL) was added followed by a few drops of bromothymol blue solution. Excess DBA was titrated with HCl (I N). The titre value was noted and the isocyanate content was calculated.

3.2.8 Preparation of prepolymer terminated with isocyanate from 2-ethyl-1,3-hexanediol (EHG) and toluene diisocyanate (TDI)

EHG (17.656 g) was dissolved in 180 mL of dry toluene. Dibutyltin dilaurate (DBTDL) (2.5 mL of 1 wt % solution) was added to the above solution. The mixture was cooled to 0 °C. TDI (29.348 g), was added slowly for 40 minutes. The temperature of the reaction mixture was maintained below 5 °C during the addition of TDI. After complete addition, the reaction mixture was allowed to come to room temperature. The reaction mixture was heated at 70 °C for one hour. The prepolymer solution thus obtained was transferred to a 250 mL volumetric flask fitted with a septum adapter through a cannula under a positive pressure of nitrogen. The level was made up to 250 mL by adding dry toluene through the cannula. The prepolymer solution was stored at room temperature under a nitrogen atmosphere. This solution was used for further studies and analysis. Isocyanate content of this prepolymer stock solution was estimated to be 9.17 wt %.

3.2.9 Preparation PU/organoclay nanocomposites using trimethylol propane

Various compositions of PU/organoclay nanocomposites prepared are shown in Figure 3.2

Table 3.2: Compositions PU/organoclay nanocomposites

Entry No.	Organoclay	Amount of TMP (g)	Amount of EHG (g)	Amount of Cloisite 30B (g)	Amount of prepolymer stock solution (mL)
A	Cloisite 30B	0.1423	0.0	0.130	10
B	Cloisite 30B	0.1067	0.0581	0.130	10
C	Cloisite 30B	0.0711	0.1163	0.130	10
D	Cloisite 30B	0.0356	0.1744	0.130	10
E	Cloisite 25A	0.1500	0.0	0.130	10
F	Cloisite 25A	0.1126	0.0581	0.130	10
G	Cloisite 25A	0.0711	0.1163	0.130	10
H	Cloisite 25A	0.0375	0.1744	0.130	10
I	Cloisite 25A	0	0.2325	0.130	10

Four two neck round bottom flasks fitted with a condenser and septum adapter were taken and to each flask 10 mL of dry toluene was transferred under nitrogen atmosphere through a cannula. To each of them 0.130 g of the organoclay was added and dispersed thoroughly by stirring with magnetic stirring bar. Varying amounts of trimethylolpropane and EHG was added (Table 3.2). The reaction mixture was stirred for 2 hours. Thereafter, 10 mL of prepolymer stock solution was added through a cannula to each flask at room temperature. The temperature was increased to 70 °C slowly and stirring continued for an additional four hours. Thereafter, the solvent was evaporated in vacuo. A fine powder was obtained which was subjected to analysis.

3.2.10 Preparation of PU/clay nanocomposites using clays having modifiers with varying hydroxyl functionality

Organoclays (0.130 g each), (1-OH(MMT), 2-OH(MMT) and 3-OH(MMT)),which are modified by ion exchange with various organoammonium cations **1, 2** and **3** having hydroxyl functionality of 1, 2 and 3 were dispersed in toluene medium separately in round bottom flasks by stirring at 70 °C. The prepolymer stock solution (10 mL) was added to the organoclay dispersion slowly at room temperature and after the addition was over the temperature was slowly raised to 70 °C for two hours. Then EHG (0.230 g) was added to the reaction mixture and continued stirring at 70 °C for another 4 hours to obtain PU nanocomposites.

3.2.11 Preparation of thermoplastic polyurethanes (TPU)

In the first step, isocyanate terminated prepolymer was prepared by reacting polycaprolactone diol (Mn: 750) with excess of isophorone diisocyanate (IPDI) in the mole ratio 1: 2.1. Calculated amount of IPDI was added slowly to the solution of polycaprolactone diol at 80 °C and stirred for 2 hours under nitrogen atmosphere in presence of dibutyltin dilaurate as catalyst. In the second step, the prepolymer was chain extended by addition of 1,4-butanediol and the modifier salt (either **1**, **2**, or **3**) with stirring at 80 °C for 4 hours. The composition of reactants are shown in Table 3.3

3.2.12 Preparation of TPU/clay nanocomposites

In the first step, isocyanate terminated prepolymer was prepared by reacting polycaprolactone diol (Mn: 750) with excess of isophorone diisocyanate (IPDI) in the mole ratio 1: 2.1. Calculated amount of IPDI was added slowly to the solution of polycaprolactone diol at 80 °C and stirred for 2 hours under nitrogen atmosphere in presence of dibutyltin dilaurate as catalyst. The reaction mixture containing the prepolymer was cooled down to room temperature. The organoclay was added and stirred at room temperature for 30 minutes to disperse the clay in the reaction mixture. The temperature was raised to 80 °C and stirred for an additional period of one hour. 1,4-butanediol was added as chain extender and continued the polymerization for another four hours. Thermoplastic polyurethane clay nanocomposites were obtained as films by pouring the reaction mixture onto a glass plate and casting the film by solvent evaporation under nitrogen flow at 55 °C. The amounts of each reactant taken were as shown in Table 3.3.

Table 3.3: Composition of reactants for preparation of TPU and nanocomposites

Entry No.	Organo-clay or modifier	Amount of organoclay or modifier		Poly(capro-lactone diol)		IPDI		1,4-Butanediol	
		(g)	(mmol)	(g)	(mmol)	(g)	(mmol)	(g)	(mmol)
1	**1**	0.185	0.469	7.55	10.07	4.85	21.83	0.895	9.94
2	**2**	0.195	0.458	7.58	10.11	4.84	21.77	0.874	9.69
3	**3**	0.230	0.477	7.51	10.02	4.76	21.43	0.826	9.17
4	1-OH (MMT)	0.656	0.469	7.59	10.12	4.84	21.77	0.875	9.71
5	2-OH (MMT)	0.656	0.458	7.56	10.08	4.84	21.77	0.857	9.51
6	3-OH (MMT)	0.7000	0.477	7.52	10.03	4.65	20.90	0.826	9.17

3.2.13 Analytical methods

Fourier-transformed infrared spectroscopy (FTIR) experiments were performed using Perkin Elmer FTIR spectrophotometer at a resolution of 4 cm^{-1}. The sample for FTIR study were prepared by taking the sample in nujol and mulled. The spectrum of the

mulled sample was obtained after being placed between two NaCl windows. ^{1}H NMR spectra were recorded in CDCl$_3$ solution with tetramethylsilane (TMS) as an internal standard using a Bruker DSX300 NMR spectrometer. The WAXD measurements were performed using Rigaku Dmax 2500 diffractometer fitted with a diffracted beam graphite monochromator. The system consists of a rotating anode generator and wide-angle power goniometer. The generator was operated at 40kV and 150 mA. The radiation was Ni-filtered Cu-Kα and samples were scanned between 2θ = 2 to 10° and the scan speed was 2°/min. The TGA-7 (Perkin-Elmer) thermal analysis system was used to determine the onset of degradation and the organic content in the organoclays. The samples were heated under a flow of nitrogen atmosphere from 50 to 900 °C at a heating rate of 10 °C/min, and the weight loss was recorded. The weight loss at 900 °C was taken as the % organic content in the organoclay. TEM imaging was done using a FEI-Tecnai G^2 transmission electron microscope operating at an accelerating voltage of 300 kV. The nanocomposite samples were sectioned into ultrathin slices (<100 nm) using a Leica Ultracut UCT microtome equipped with a diamond knife and then mounted on 200 mesh copper grids. PU nanocomposites samples based on EHG, TDI and TMP were sectioned at room temperature after embedding the nanocomposite powder in epoxy matrix. TPU nanocomposite sample films based on poly(caprolactone)diol were directly mounted on the microtome holder and sectioned at –120 °C. The density of clay particles was enough to produce contrast between polymer and clay stacks without any need for staining. Images were captured using charged couple detector (CCD) camera for further analysis using Gatan Digital Micrograph analysis software. The dyanamic mechanical properties of the samples were studied using Rheometrics Dyanamic Mechanical Analyzer, model DMTA IIIE. T$_g$ was measured as the temperature at which the maximum in tan δ appeared. The scans were carried out in rectangular sample tensile testing mode at a constant heating rate of 5 °C/min and a frequency of 1 Hz from -150 °C to 80 °C. The samples were cut (with span length of 10mm and thickness X width being 0.5 mm X 7 mm) from the sheets obtained by solvent casting at 55 °C after *in-situ* polymerization.

3.3   Results and discussion

3.3.1   Preparation of organomodifiers for the clay

Organomodifiers **1, 2,** and **3** were prepared according to Scheme 3.1, Scheme 3.2 and Scheme 3.3. The structure of the products was confirmed by ^{1}H NMR.
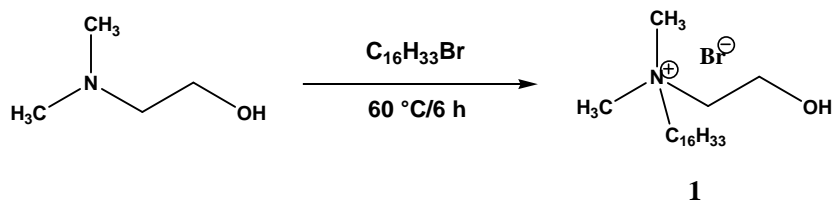
Scheme 3.1: Preparation of organo-modifier **1**
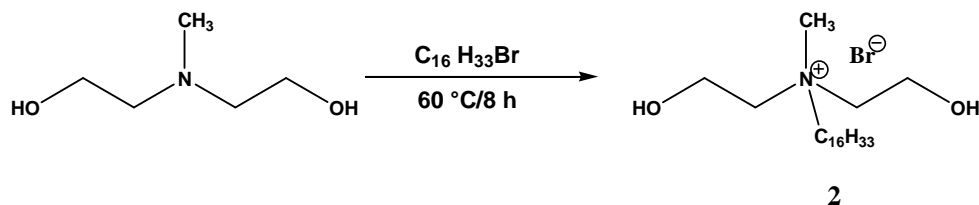
Scheme 3.2: Preparation of organo-modifier **2**
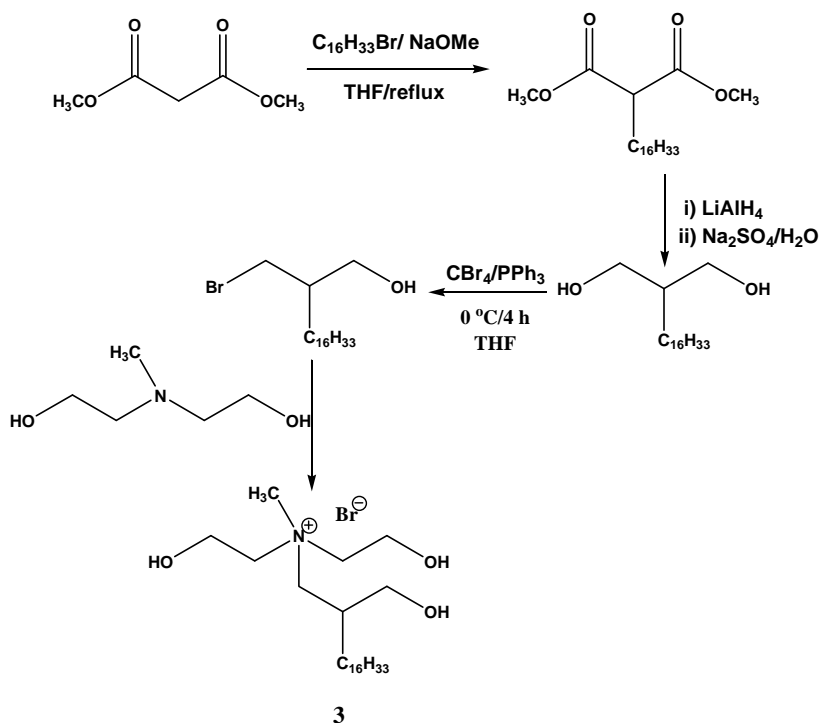
Scheme 3.3: Preparation of organo-modifier **3**

3.3.2 Reactivity of hydroxyl in the modifier 1, 2 and 3 with phenyl isocyanate

The reactivity of the hydroxyl groups present in the organomodifiers **1, 2** and **3** towards isocyanate group was studied by reacting them with phenyl isocyanate in presence of a catalyst DBTDL (Scheme 3.4) to form carbamates.
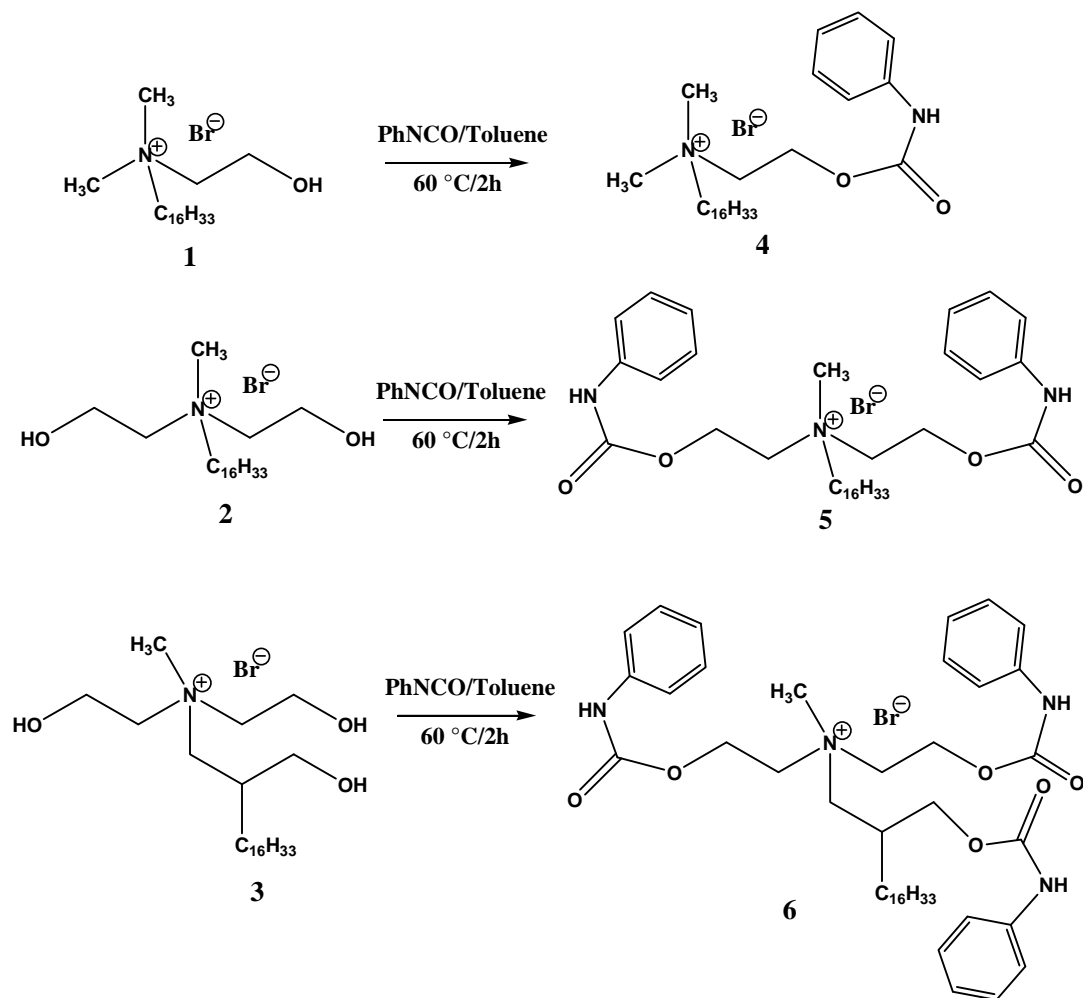
Scheme 3.4: Reaction of organo-modifiers **1, 2** and **3** with phenyl isocyanates

Extent of conversion of hydroxyl groups to phenyl carbamates was estimated using ^{1}H NMR analysis. The Figure 3.1(a), (b) and (c) show the ^{1}H NMR of **4, 5,** and **6,** the phenyl carbamates of **1, 2** and **3** respectively. Phenyl protons of the phenyl carbamate show characteristic chemical shift at δ 7.62, 7.26 and 7.02 ppm in the ratio 2:2:1. The ratio of integrated area of one of the ^{1}H signals due to the phenyl protons at 7.02 ppm with respect to the terminal methyl protons of the long alkyl chain at 0.88 ppm were

calculated. They showed the ratio of 1:3, 2:3 and 3:3 for the phenyl carbamates with one hydroxyl, two hydroxyls and three hydroxyls respectively. It is, thus, concluded that the hydroxyl groups of compounds **1, 2**, and **3** readily react with isocyanates quantitatively.
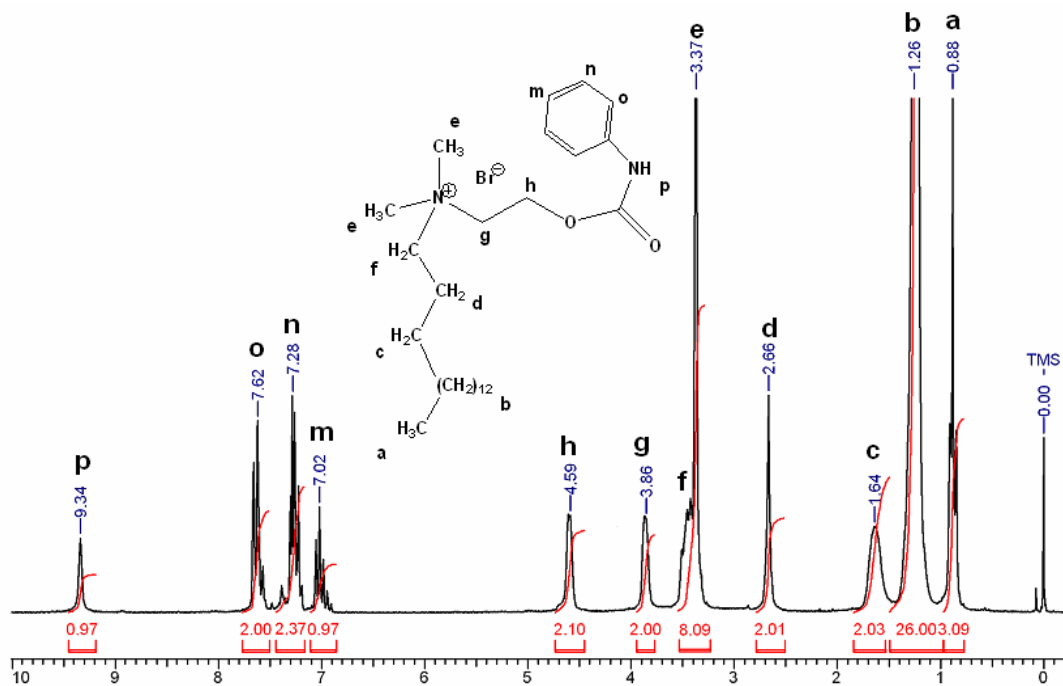
Figure 3.1 (a): ^{1}H NMR spectra of phenyl carbamate of **1**
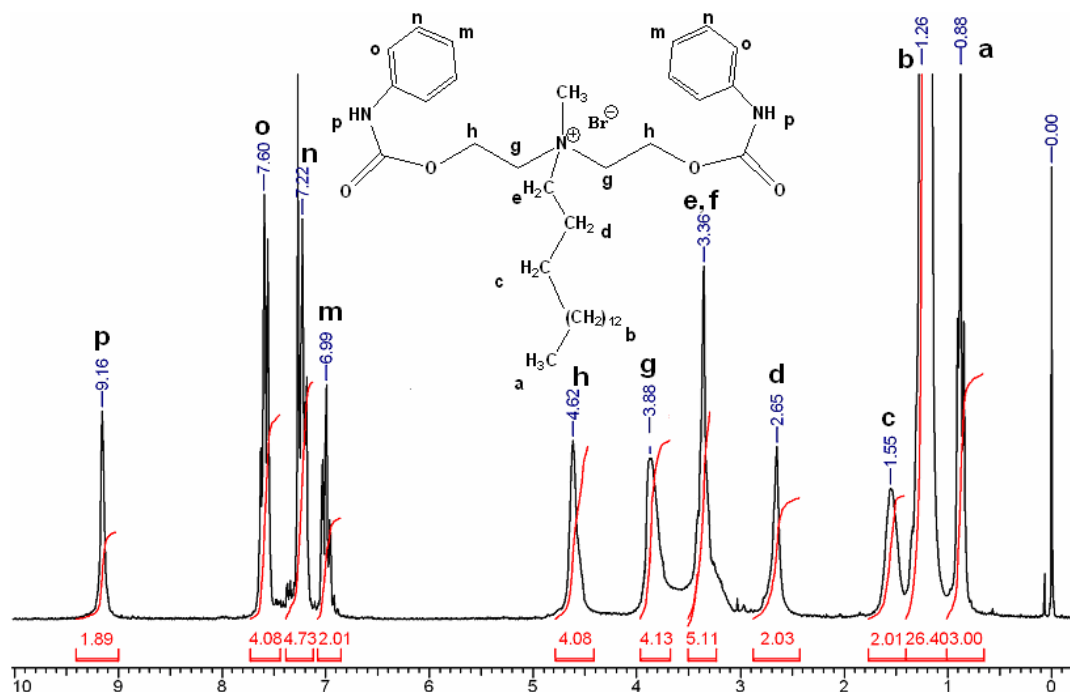
Figure 3.1 (b): ^{1}H NMR spectra of phenyl carbamate of **2**
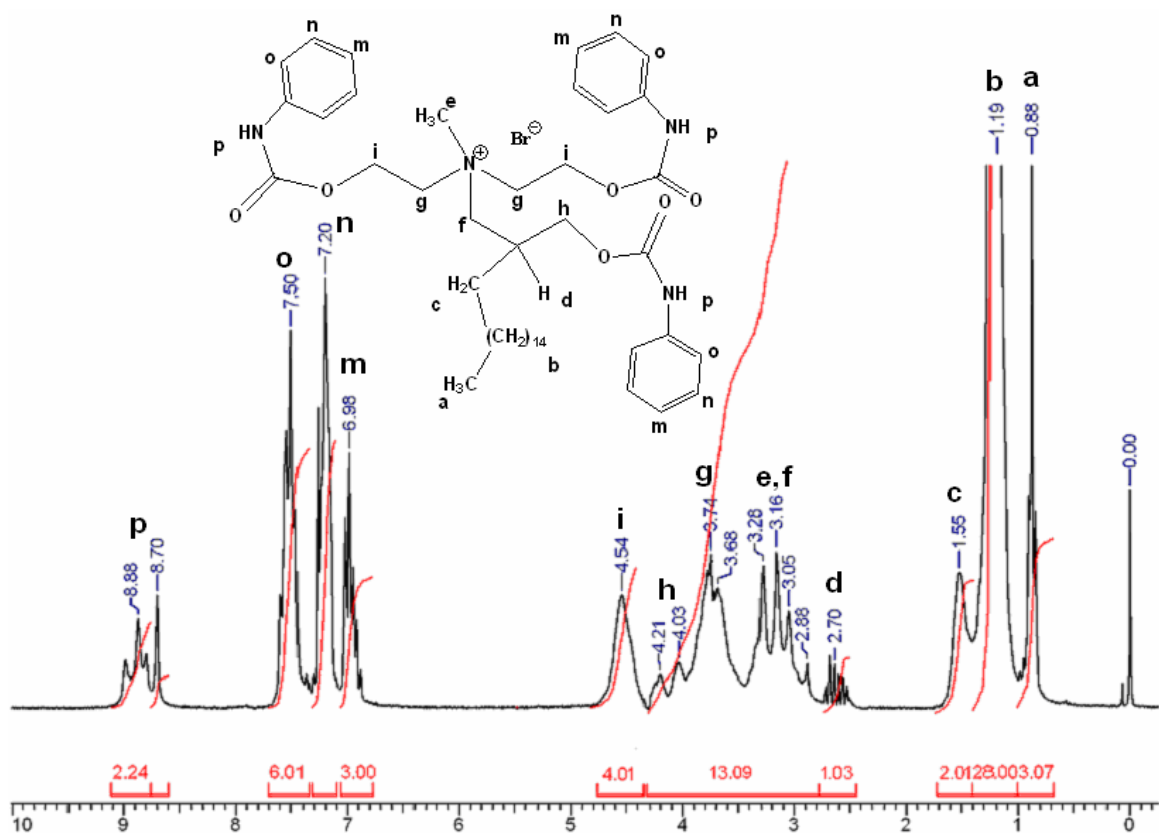
Figure 3.1 (c): ^{1}H NMR Spectra of phenyl carbamate of **3**

3.3.3 Preparation of organoclays with modifiers bearing varying hydroxyl functionality

Organoclays were prepared with the modifiers **1, 2** and **3** bearing varying hydroxyl functionalities. These organo-modified clay samples are designated as 1-OH(MMT), 2-OH(MMT) and 3-OH(MMT). The modified clay samples were characterized by WAXD (Figure 3.2). The WAXD patterns show 001 peak, which correspond to the interlayer d-spacing of the organoclay. The Table 3.4 shows the interlayer distance of the organoclays. The interlayer distance increases due to exchange of the larger organo-cation with Na$^+$ ion in the interlayer gallery. The larger increase in d-spacing for 3-OH(MMT) when compared to the other two clays, namely 1-OH(MMT) and 2 OHMMT can be attributed to the presence of slightly longer alkyl chain (18 C) in the case of **3** as compared to **1** and **2** (16 C). The organic content estimated from TGA was in agreement

with theoretically calculated value indicating quantitative exchange of the Na$^+$ with the quaternary ammonium ion.
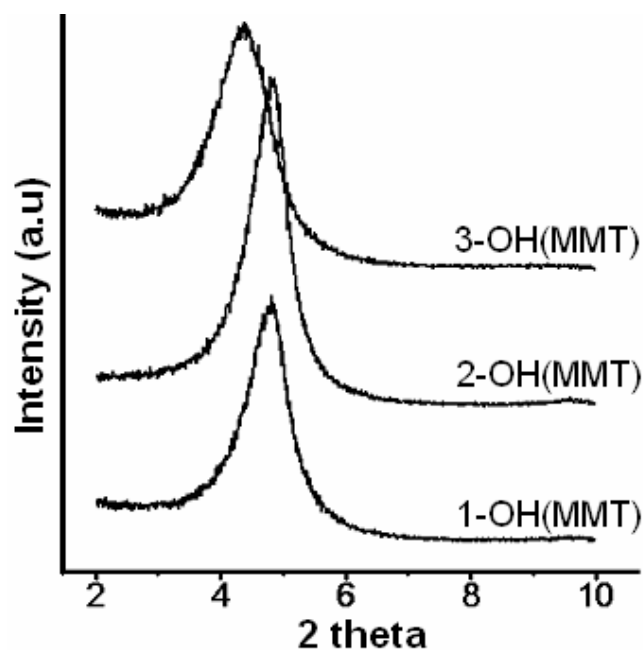
Figure 3.2: WAXD patterns for organoclays such as 1-OH(MMT), 2-OH(MMT) and 3-OH(MMT).

Table 3.4: The weight loss on charring at 900 °C from TGA and d- spacing for the organoclays from WAXD for the organoclays

Organoclay	Modifier	Weight loss on charring (%)		d-spacing for
		Theoretical	Experimental	clay, Å
1-OH(MMT)	**1**	22.7	22.8	18.5
2-OH(MMT)	**2**	24.5	24.6	18.5
3-OH(MMT)	**3**	27.5	27.7	20.2

3.3.4 Reactivity of hydroxyl of modifier in Cloisite 30B towards with isocyanate

The reactivity of hydroxyl group of the modifier in Cloisite 30B with isocyanate was examined by FTIR (Scheme 3.5). Cloisite 30B was mixed with phenyl isocyanate in dry toluene at 60 ºC for 6 hours. As a control an organoclay without hydroxyl group (Cloisite 25 A) was treated similarly and FTIR spectra was recorded. The FTIR spectra of Cloisite 30B/phenyl isocyanate and Cloisite 25A/phenyl isocyanate are shown in Figure 3.3.
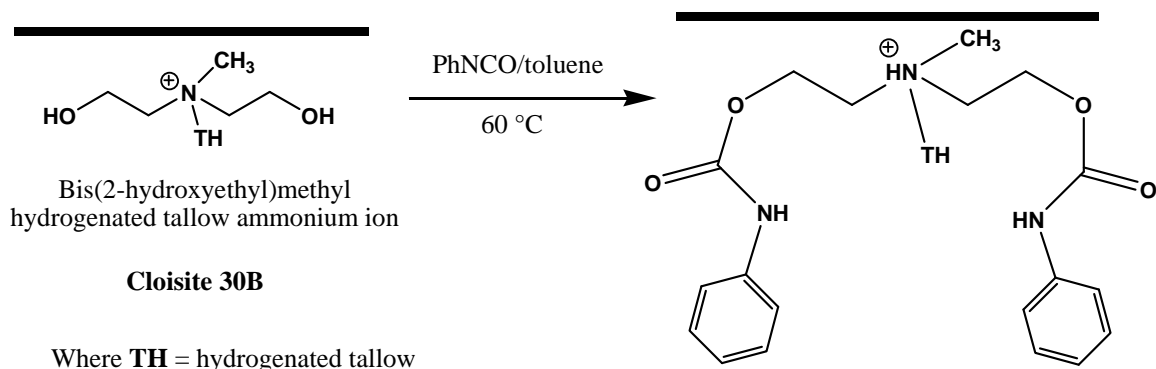
Scheme 3.5: Reaction of hydroxyl of the modifier in Cloistie 30B with phenyl isocyanate
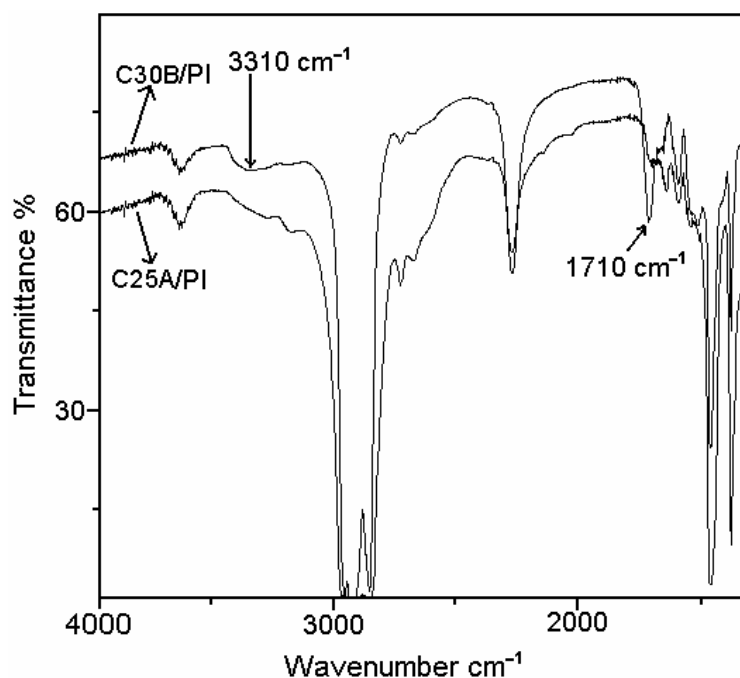
Figure 3.3: IR spectra of the product of the reaction of Cloisite 30B and Cloisite 25A with phenyl isocyanate

The hydrogen bonded carbonyl and the hydrogen bonded N-H bands from the urethane groups usually appeared at 1710 and 3310 cm^{-1}, respectively. There is no absorption peak observed at 1710 cm-1 or at 3310 cm^{-1} in the FTIR spectrum of Cloisite 25A/phenyl isocyanate, indicating that there is no reaction between Cloisite 25A and phenyl isocyante. This implies that the polyurethane is physically absorbed on the silicate surface. In case of Cloisite 30B/phenyl isocyanate, distinctive absorption bands were

observed at 1710 and 3310 cm^{-1} indicating presence of urethane group formed by the reaction of hydroxyl groups in Cloisite 30B with isocyanate group. Hence it is concluded that the polyurethane chain is chemically tethered to Cloisite 30B through the formation of urethane bonds.

3.3.5   Preparation of prepolymer terminated with isocyanate (7)

A urethane prepolymer terminated with isocyanate (**7**) was prepared by taking toluene diisocyanate with 2-ethyl-1,3-hexanediol (EHG) in a mole ratio 1: 1.4 in toluene. The obtained prepolymer contained 9.2 wt % isocyanate, which is close to the theoretically calculated value.

3.3.6   Effect of trimethylol propane (TMP) on the dispersion of clay in PU

The prepolymer **7** was reacted with Cloisite 30B and crosslinked using trimethylol propane (TMP). The effect of amount of branching agent used on the dispersion of clay was studied by scanning the WAXD patterns and TEM images of the obtained nanocomposites keeping the clay content constant by varying the amount of TMP (1.7, 3.4, 5.2, and 7.0 wt %). Figure 3.4 shows WAXD of the obtained PU-nanocomposites.
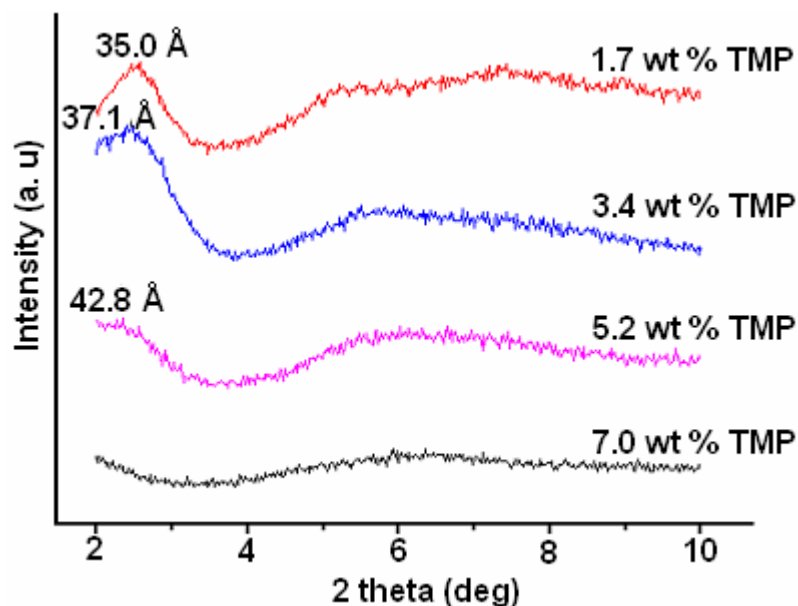
Figure 3.4: WAXD of PU/Cloisite 30B nanocomposites with varying amount of trimethylol propane

The interactions between silicate layers and polyurethane chains are demonstrated by a shift in peak assignable for 001 basal plane. It can be seen that with increasing content of TMP, the shift in peak to the small angle increases. For example, the d-spacing, corresponding to 001 plane, between the silicate layers was found to be 35.0 Å for the nanocomposites with 1.7 wt% of TMP, whereas, it was found to be 37.1 Å and 42.8 Å for the nanocomposites with 3.4 and 5.2 wt% of TMP, respectively.

(a)   (b)

(c)   (d)
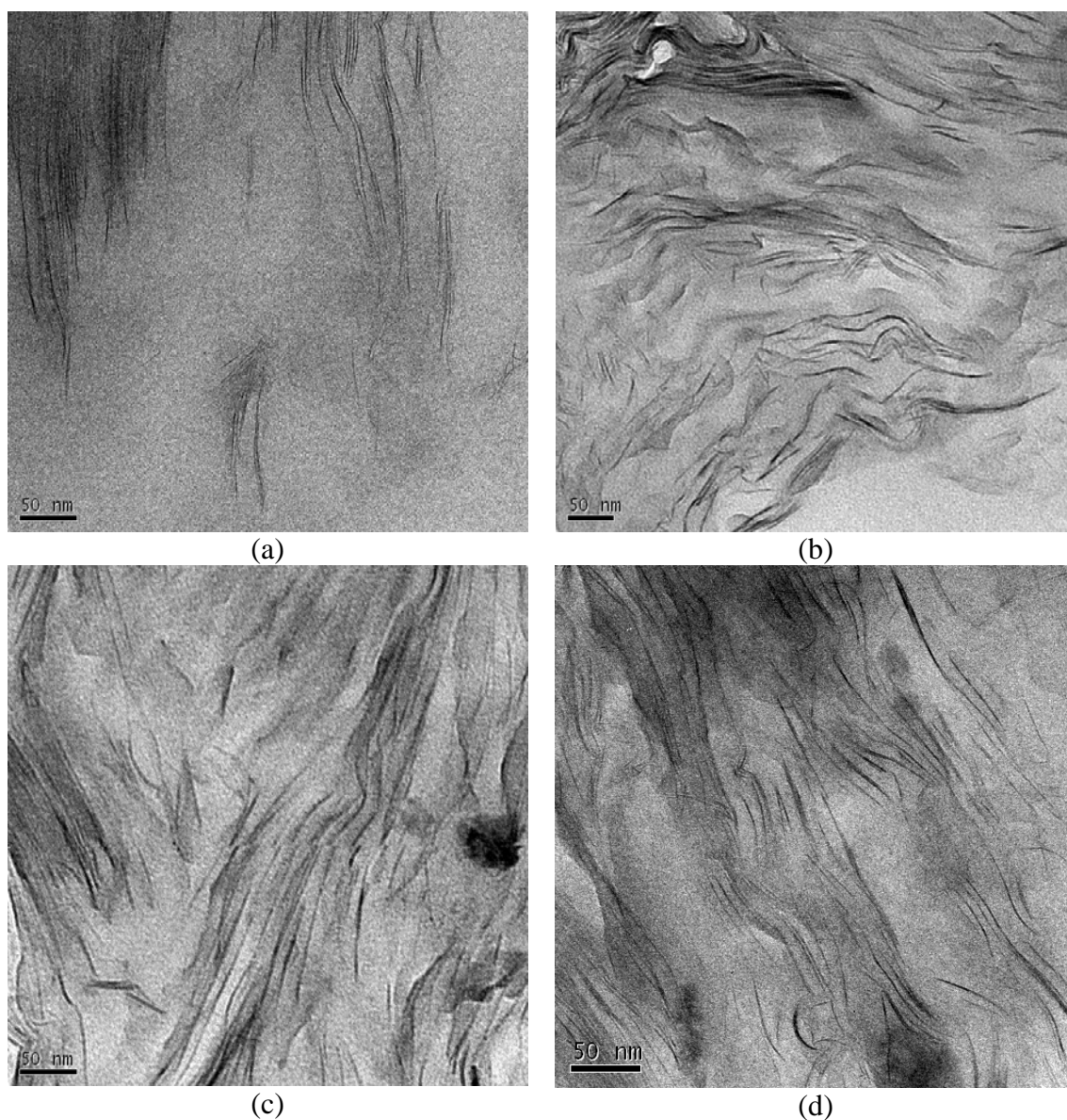
Figure 3.5: TEM images of PU/Cloisite 30B nanocomposite with (a) 1.7 wt% TMP (b) 3.4 wt% TMP (c) 5.2 wt% TMP and (d) 7.0 wt% TMP.

The increase in d-spacing with increasing content of TMP indicates better intercalation. It can also be seen that in case of the nanocomposites prepared using 7 wt % TMP, the peak of 001 basal plane completely disappear. This seems to indicate formation of exfoliated structures. Further evidence for this was found in the TEM images shown in Figure 3.5. It can be observed that with 1.7 wt% TMP, the obtained nanocomposites show intercalated structures (Figure 3.5(a)). The extent of intercalation appears to increase with increasing TMP content. Evidence for some exfoliated structures can also be deduced from TEM. Nanocomposites prepared using 7 wt% TMP show higher degree of exfoliated structures (Figure 3.5(d)). These observations are similar to that reported earlier with nanocomposites of polyurethane prepared using poly(propylene glycol) of functionality 3 as soft segment and 4,4'-methylene bis(cyclohexyl isocyanate) and 1,4-butanediol as hard segments[36]. Thus formation of tightly crosslinked PU networks in the gallery of clay results in exfoliation of the clay layers.

To understand the role of reactive hydroxyl groups on the clay surface, a similar composition of PU/clay nanocomposites was prepared by cross linking the urethane prepolymer with TMP using Cloisite 25A. The WAXD of the obtained are shown in Figure 3.6.
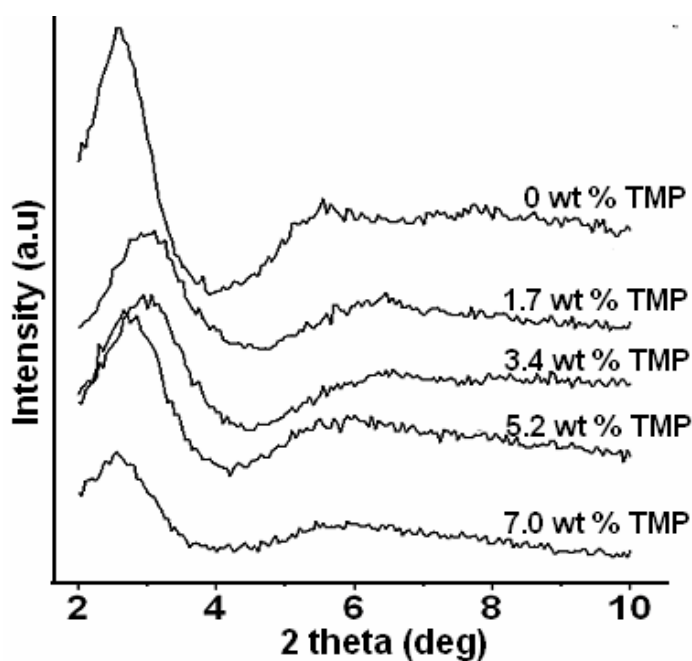
Figure 3.6: WAXD of PU/Cloisite 25A nanocomposites with varying amount of trimethylol propane (TMP)

No significant changes in the diffraction pattern are seen with increasing content of TMP. This observation is different from what was observed with Cloisite 30B, suggesting that the presence of reactive hydroxyl groups on the surface of the clay is critical to better dispersion of the organoclay. TEM images (Figure 3.7) of PU nanocomposites prepared using Cloisite 25A and with (7 wt %) and without branching agent confirm the formation of predominantly intercalated structures.

(a)   (b)
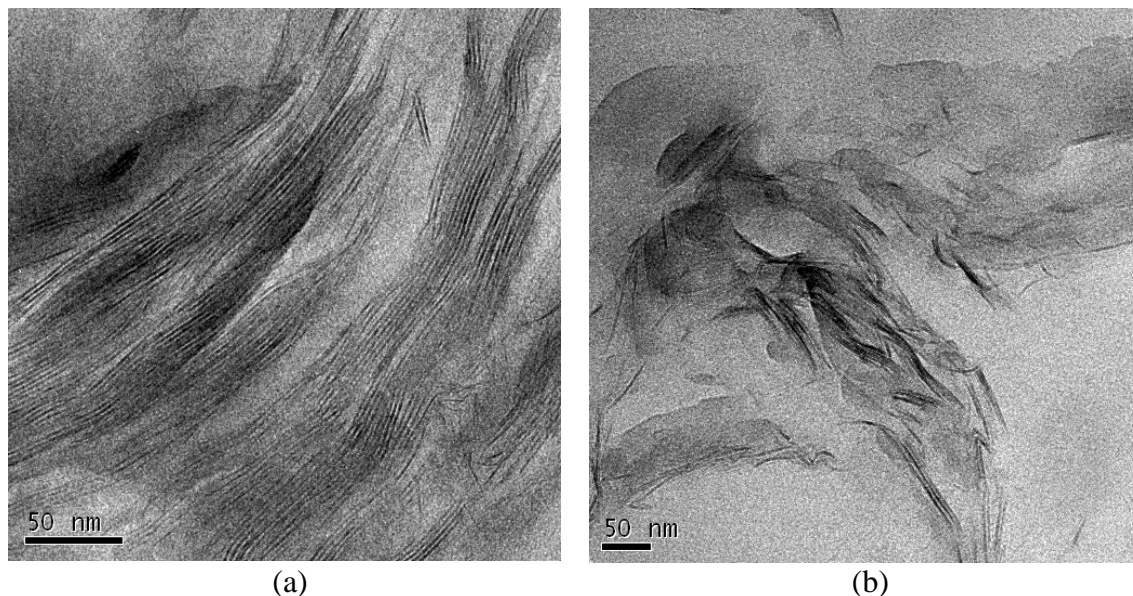
Figure 3.7: TEM pictures of PU/Cloisite 25A nanocomposites with (a) 0 wt% TMP and (b) 7.0 wt% TMP

Thus introduction of mere branch point in PU structure does not favor delamination of clay layers. Exfoliation is favored by the ability of the growing chain to chemically tether to the surface of the clay. Consequently, this study was further extended to include organomodifiers containing a graded number of hydroxyl functionality.

3.3.7   Effect of degree of functionality of the modifier on clay dispersion in PU nanocomposites

Three organoclays designated as 1-OH(MMT), 2-OH(MMT) and 3-OH(MMT) were prepared and used for the formation of PU/nanocomposites. It should be noted that the organoclays, Cloisite 30B and 2-OH(MMT) have similar structures except that the alkyl group present in the former is a hydrogenated tallow moiety which is a mixture of C-14, C-16 and C-18 alkyl chains while the alkyl group present in the latter case is only C-16

chain. As before an isocyanate terminated prepolymer was prepared from the reaction of EHG with TDI (Section 3.3.5). The isocyanate terminated prepolymer **7** was reacted with 1-OH(MMT), 2-OH(MMT) and 3-OH(MMT). No cross linker was added. WAXD of the obtained nanocomposites are shown in Figure 3.8. It is seen that the d-spacing for the clay increases from 18.5 Å (the organoclay) to 34.0 Å in the nanocomposites of 1-OH(MMT) and 2-OH(MMT), indicating the formation of intercalated structures.
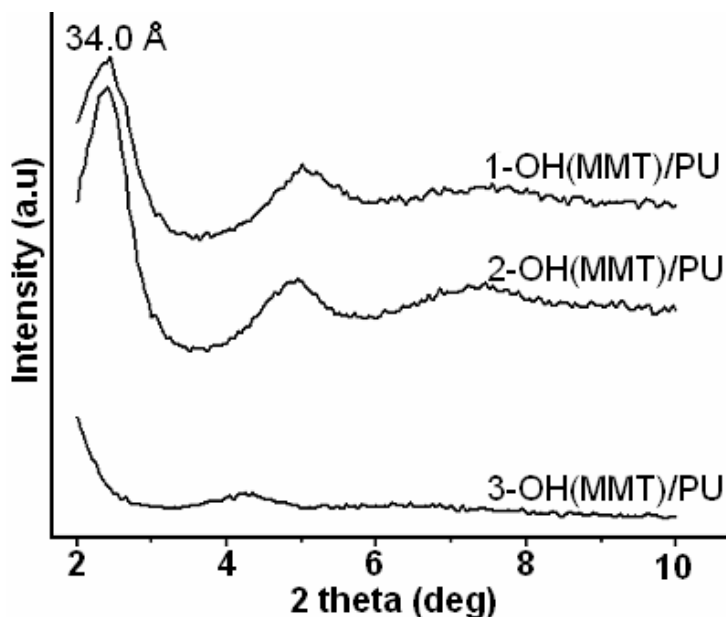
Figure 3.8: WAXD patterns of PU/clay nanocomposites with 1-OH(MMT), 2-OH(MMT) and 3-OH(MMT)

When the organoclay used was 3-OH(MMT), no peak for 001 basal plane was observed in the 2θ range of 2-4°. There can be two possibilities i.e. either the peak might have been shifted still lower angle region than 2° which is assignable for better/more intercalated nanostructures or the formation of exfoliated nanostructures. To clarify the interactions between the polymer and clay layers, the obtained nanocomposites were further characterized by TEM. Figures 3.8 (a), (b) and (c) show the TEM images of PU/clay nanocomposites based on 1-OH(MMT), 2-OH(MMT) and 3-OH(MMT), respectively. It is observed that in all the three nanocomposites the obtained morphologies appear to be intercalated ones, with a marginally higher degree of intercalation observed in case of the 3-OH(MMT)/PU nanocomposite.
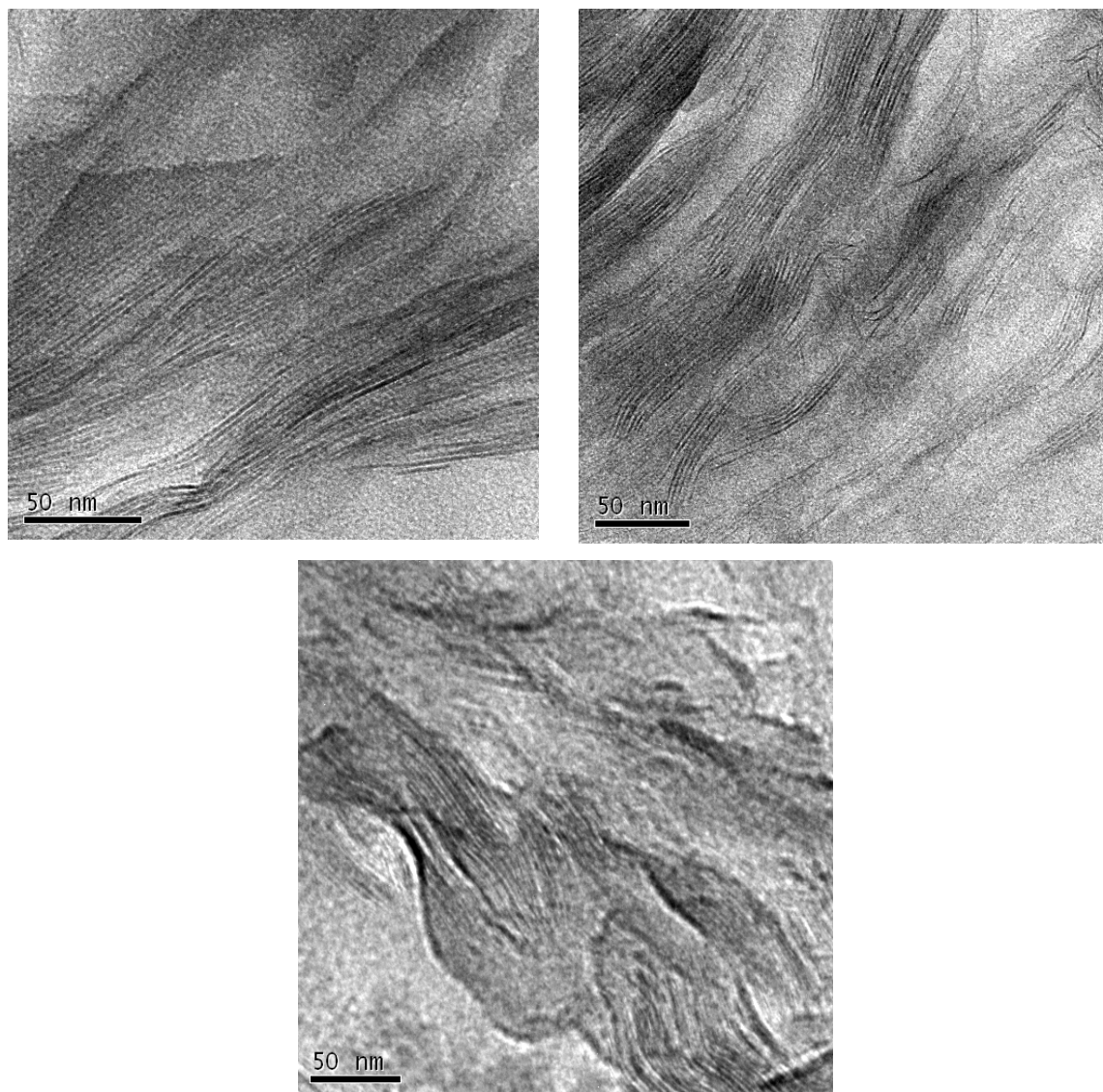
Figure 3.9: TEM pictures of (a) PU/1-OH(MMT), (b) PU/2-OH(MMT), (c)PU/3-OH(MMT), nanocomposites

3.3.8 Effect of degree of functionality of the modifier on the clay dispersion in thermoplastic polyurethane matrix

To further elucidate the role of functional modifiers in clay on the properties of PU/clay nanocomposites a thermoplastic polyurethane derived from poly(caprolactone diol) and isophorone diisocyanate (IPDI) was prepared and chain extended with 1,4-butanediol and reacted with 1-OH(MMT), 2-OH(MMT) and 3-OH(MMT). Figure 3.10 shows the WAXD of the obtained nanocomposites. Nanocomposites derived from 1-OH (MMT)

and 2-OH(MMT) showed an increase in d-spacing from 18.5 Å to 34.0 Å. In case of nanocomposites derived from 3-OH(MMT), the d-spacing further increased to 37.1 Å. This increase may be attributed either to the better dispersion of clay as a result of tethering of the polymer chain to the clay surface through the hydroxyls in the modifier or to the higher d-spacing of the clay incorporated. However, the d-spacing observed for these TPU based nanocomposites is lower than that observed for the nanocomposites of EHG and TDI based polyurethanes with the same organoclays.
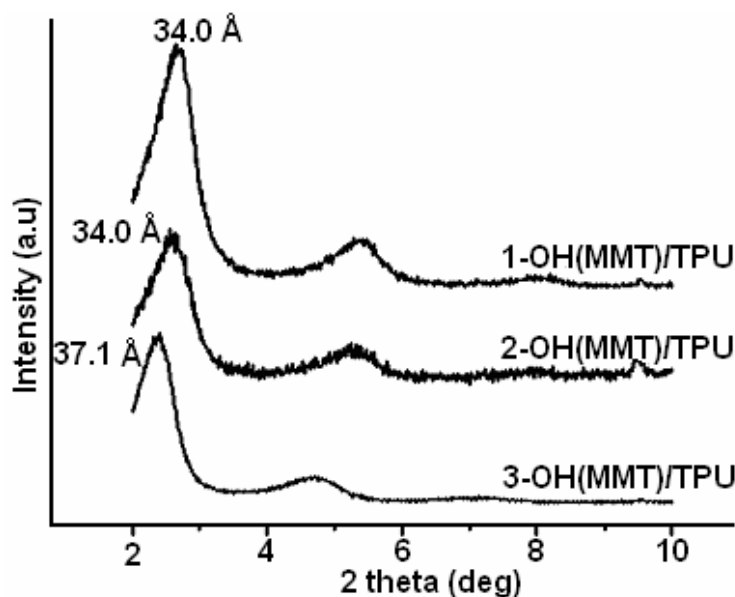
Figure 3.10: WAXD pattern of TPU/clay nanocomposites with 1-OH(MMT), 2-OH(MMT) and 3-OH(MMT)

The dispersion of clay in TPU was further examined by TEM (Figure 3.11). All the three composites show highly intercalated nanostructures and the interlayer distance is comparable to the d-spacing observed by WAXD. In comparison with nanocomposites of EHG-TDI based polyurethanes, the extent of intercalation or dispersion of clay is poorer in polycaprolactone diol based PU system. The better dispersion of silicate layers in polyurethanes containing harder segment can be attributed to the interactions imparted *via* higher density of hydrogen bonding between the polar groups of PU chains and the hydroxyl groups on the clay surface. In other words, the lower degree of intercalation in the thermoplastic polyurethane system containing poly(caprolactone diol) soft segments can be attributed to the lower polarity and density of hydrogen bonding. Presence of long

alkyl chains (C_{16} or C_{18}) does not appear to significantly enhance the compatibility of the polymer with the clay.

(a)   (b)

(c)
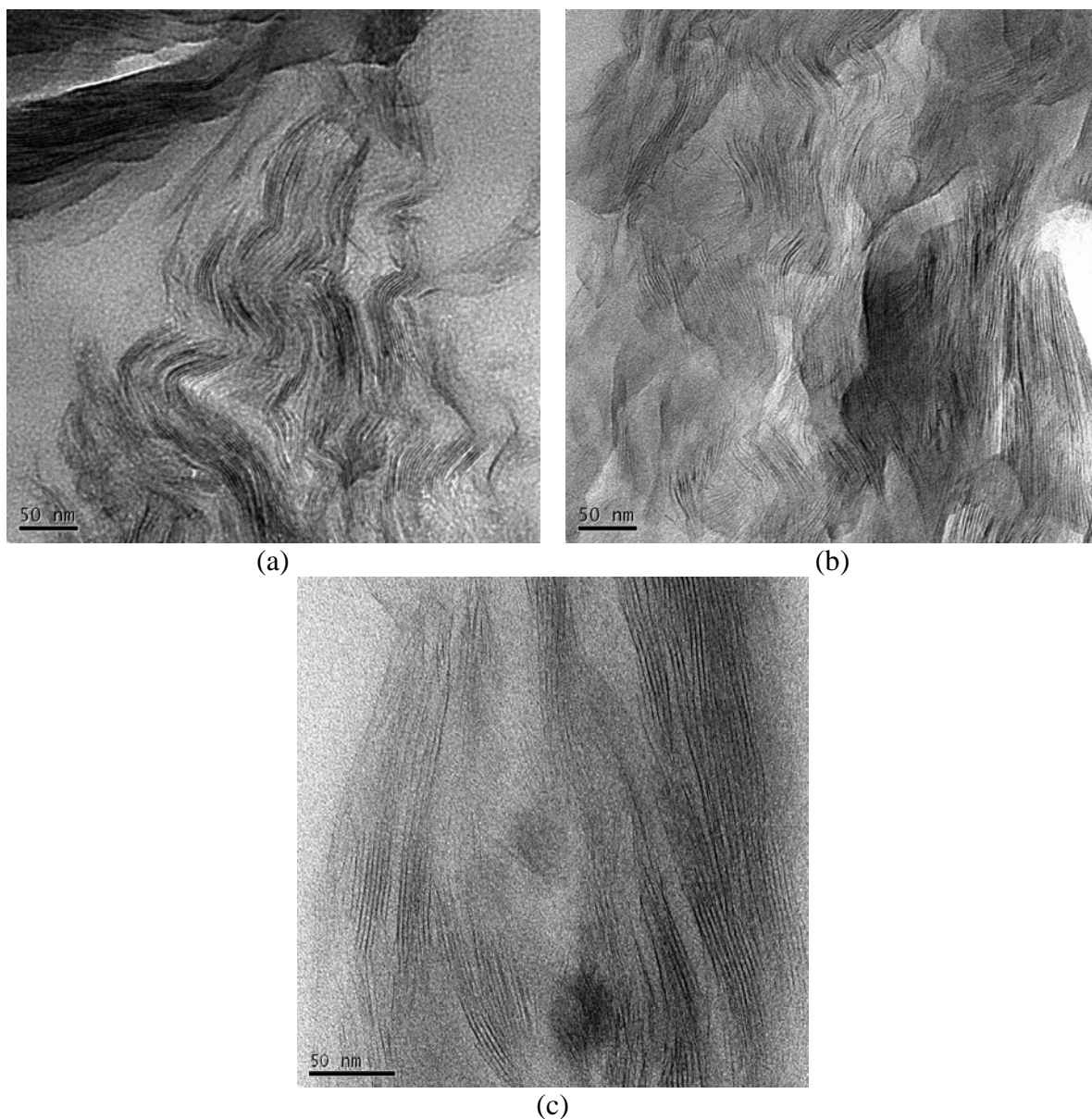
Figure 3.11: TEM pictures of nanocomposites based on TPU and (a) 1-OH(MMT), (b) 2-OH(MMT) and (c) 3-OH(MMT)

3.3.9   Dynamic mechanical properties

Temperature dependent dynamic mechanical property of the thermoplastic polyurethane nanocomposites was measured using DMA and compared with pristine polyurethanes

prepared using the same reactive modifiers. Figure 3.12 shows the storage moduli (G`) and the tan δ measured in the temperature range of –150 °C to 80 °C.
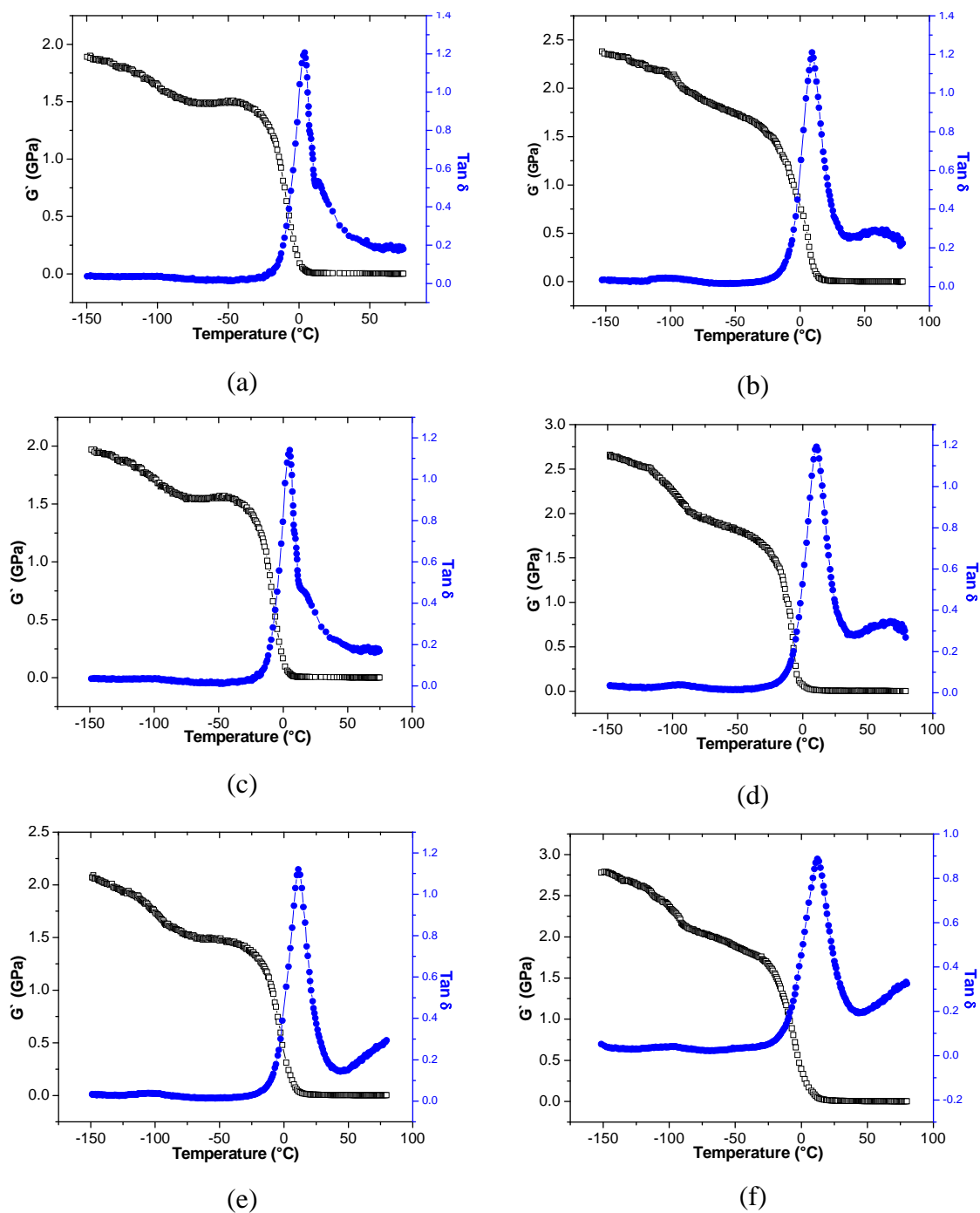
Figure 3.12: The temperature dependence of G` and tan δ of (a) pristine TPU-1OH, (b) pristine TPU-2OH, (c) pristine TPU-3OH, (d) 1-OH(MMT)/TPU) (e) 2-OH(MMT)/TPU and (f) 3-OH(MMT)/TPU

Figure 3.13 shows the storage modulus (G') plotted against temperature. Two transitions can be clearly observed. The first transition observed as broad peak at around –100 °C in the tan δ plot arises due to the relaxation arising from local mode motions of the methylene sequences in the poly(caprolactone) soft segment. The second transition was observed 5 to 10 °C range, which is due to glass transition.
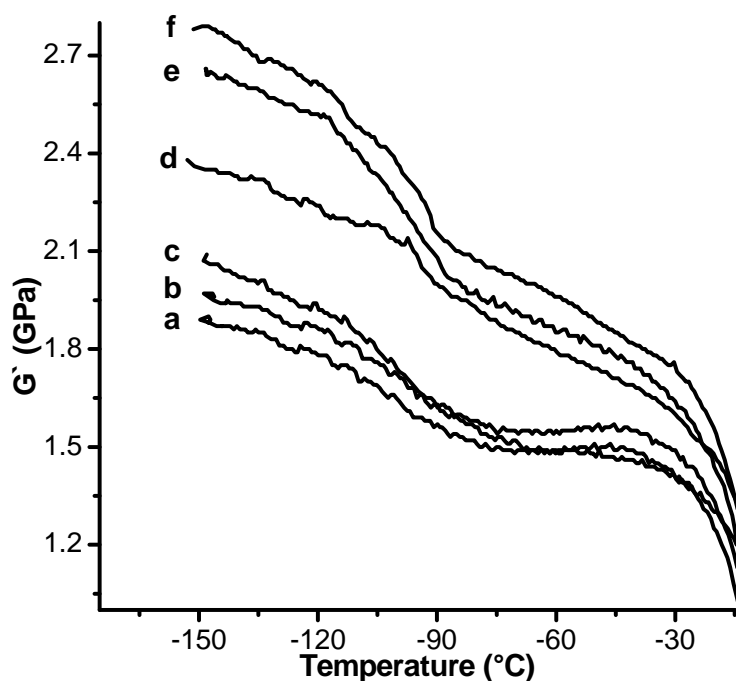
Figure 3.13: Tensile storage modulus (G`) of various samples measured by dyanamic mechanical analysis, (a) pristine TPU-1OH, (b) pristine TPU-2OH, (c) pristine TPU-3OH, (d) 1-OH(MMT)/TPU (e) 2-OH(MMT)/TPU, (f) 3-OH(MMT)/TPU.

It can be observed that for the nanocomposite samples the tensile storage moduli (G') was higher at all temperatures below the glass transition temperature. It should also be noted that the G` of the nanocomposite samples slowly reduces as the temperature increases at the temperature range below the glass transition temperature, whereas G` is constant for the pristine thermoplastic polyurethane samples. Another important observation is that with the increase in the degree of functionality of the modifier in the clay, the nanocomposites show higher G` values at all temperatures below glass transition temperature. This can be attributed to the improved interaction of the polymer chain with

the clay surface arising as a consequence of the chemical tethering of the polymer chains to the clay surface.

3.4   Conclusions

The results of this study lead us to conclude that for the preparation of completely exfoliated and well dispersed polyurethane/clay nanocomposites via *in-situ* polymerization, presence of tethering groups on the clay surface and an ability to form branched and crosslinked structure is necessary. Mere presence of either tethering functionalities in the organoclay or branched points in PU does not result in exfoliated structures. Incorporation of long alkyl chains in addition to tethering hydroxyl groups in the modifier structure of the clay did not significantly improve the compatibility of linear PU with the clay. Intercalated thermoplastic polyurethane/clay nanocomposites, prepared using poly(caprolactone diol) as soft segment and isophorone diisocyanate and 1,4-butanediol as hard segment show increase in storage tensile moduli at temperatures below glass transition temperature when compared to pristine polymers when functional groups capable of chemically reacting with the growing polymer chains are present in the clay modifier. This is indicative of improved interaction of the polymer with the clay surface.

References

1.   Meckel, W.; Goyert, W.; Wieder, W. in thermoplastic Elastomers, Hanser Munich **1987.**

2.   K. C. Frisch, Rubber Chem. Technol. **1980**, 126.

3.   Bayer, O.; Muller, E.; Petersen, S.; Piepenbrink, H. F.; Windemuth, E. *Angew. Chem.* **1950**, *62*, 57.

4.   Goda, H.; Frank, C. W. *Chem. Mater*. **2001**; *13*,2783.

5.   Furukawa, M.; Yokoyama, T. *J. Appl. Polym. Sci.* **1994**; *53*,1723.

6.   Dolui, S. K.; *J. Appl. Polym. Sci.* **1994**, *53*, 463.

7.   Feldman, D.; Lacasse, M. A. *J. Appl. Polym Sci.* **1994**, *51*,701.

8.   Otterstedt, E. A.; Ekdahl, J.; Backman, J. *J Appl Polym Sci* **1987,** *34*, 2575.

9.   Nunes RCR, Fonesca JLC, Pereira MR. *Polym Test* **2000**, *19,* 93.

10.   Hepburn, C. *Polyurethane elastomer*. London: Applied Science Publishers; **1982**.

11.   Wang, Z.; Pinnavaia, T. J. *Chem. Mater*. **1998**, *10*, 3769.

12.   Zilg, C.; Thomann, R.; Muelhaupt, R.;Finter J. *Adv. Mater.* **1999,** *11*, 49.

13.   Petrovic, Z. S.; Javni, I.; Waddon, A.; Banhegyi, G. *J Appl. Polym. Sc.* **2000**; *76,* 133.

14.   Chen, T. K.; Tien, Y. I.; Wei, K. H. *J. Polym. Sci. A: Polym. Chem.* **1999**, *37*, 2225

15.   Chen, T. K.; Tien, Y. I.; Wei, K. H. *Polymer* **2000,** *41,* 1345.

16.   Xu, R.; Manias, E.; Snyder, A. J.; Runt, J. *Macromolecules* **2001**; *34,* 337.

17.   Ma, J.; Zhang, S.; Qi, Z. *J Appl Polym Sci* **2001,** *82*, 1444.

18.   Tien, Y. I.; Wei, K. H. *Macromolecules* **2001**; *34*, 9045.

19.   Tien, Y. I.; Wei, K. H. *Polymer* **2001**; *42,* 3213.

20.   Hu, Y.; Song, L.; Xu, J.; Yang, L.; Chen, Z.; Fan, W. *Colloid Polym. Sci.* **2001**; *279*, 819.

21.   Yao, K.J.; Song, M.; Hourston, D. J.; Luo, D. Z. *Polymer* **2002**, *43*, 1017.

22.   Tien, Y. I.; Wei, K. H. *J. Appl. Polym. Sci.* **2002**, *86,* 1741.

23.   Chang, J. H.; An, Y. U.; *J. Polym. Sci., Part B: Polym. Phys.* **2002,** *40*, 670.

24.   Tortora, M.; Gorrasi, G.; Vittoria, V.; Galli, G.; Ritrovati, S.; Chiellini, E. *Polymer* **2002,** *43*, 6147.

25.   Zhang, X.; Xu, R.; Wu, Z.; Zhou, C. *Polym. Int.* **2003**, *5,* 790.

26.   Song, M.; Hourston, D. J.; Yao, K. J.; Tay J. K. H.; Ansarifar, M. A. *J. Appl. Polym. Sci.* **2003**, *90*, 3239.

27.   Mishra, J. K.; Kim, I.; Ha, C. S. *Macromol. Rapid Commun.* **2003,** *24*, 671.

28.   Chen, X.; Wu, L.; Zhou, S.; You, B. *Polym. Int*. **2003**; 790.

29.   Rhoney, I.; Brown, S.; Hudson, N. E.; Pethrik, R. A. *J Appl Polym Sci* **2003,** *91*, 1335.

30.   Osman, M. A.; Mittal, V. Morbidelli, M.; Suter, U.W. *Macromolecules* **2003**, *36,* 9851.

31.   Kojima, Y.; Usuki, A.; Kawasumi, M.; Okada, A.; Fukushima Y.; and Kurauchi, T. *J Mater Res* **1993,** *8*, 1185.

32.   Fukushima, Y.; Okada, A.; Kawasumi, M.; Kurauchi T.; Kamigaito, O. *Clay Miner.* **1998,** *23*, 27.

33.   Ni, P. ; Li, J.; Suo, J.S.; Li, S.B. *J. Appl. Polym. Sci.*, **2004** *94,* 534.

34.   Ni, P.; Wang, Q.L.; Li, J.; Suo, J.S.; and Li, S.B.;*J. Appl. Polym.Sci.*, **2006** *99*, 6.

35.   Singh, C.; Balazs, A. C.; *Polym. Int.* **2000**, *49*, 469.

36.   Xia, H. S.; Song, M. *Polym. International*, **2006**, 55, 229

37.   Imai, Y.; Nishimura, S.; Abe, E.; Tateyama, H.; Abiko, A.; Yamaguchi, A.; Taguchi, H. *Chem. Mater.* **2002**, *14*, 477.

38.   Moon S.-Y.; Kim, J.-K.; Nah, C.; Lee, Y.-S, *European Polym. J.* **2004**, *40*, 1615

39.   Chavarria, F.; Paul, D. R. *Polymer* **2006**, *47,* 7760

40.   Pattanayak, A.; Jana, S. C. *Polymer* **2005,** *46*, 3275.

41.   Pattanayak A., Jana S. C, Polymer **2005,** *46*, 3394.

42.   Pattanayak, A.; Jana, S. C. *Polymer* **2005,** *46***,** 5183.

43.   Pattanayak, A.; Jana, S. C.; *Polym. Eng. and Sci*. **2005,** *45*, 1532.

Chapter 4

Poly(carbonate)/Clay Nanocomposites via *in-situ*
Melt Polymerization

4.   Poly(carbonate)/clay nanocomposites via *in-situ* melt polymerization

4.1   Introduction

Poly(carbonate)s (PC) possess high impact strength, good optical clarity and high heat distortion temperature. However, it suffers from disadvantages of poor chemical resistance and low resistance to abrasion[1]. Thermal properties of polymers are known to be improved by addition of inorganic fillers[2]. However, use of traditional fillers often leads to loss of optical property. The possibility of further increasing heat distortion temperature and Tg of PC without impairing its ductility is a continuing research challenge.

Polymer-clay nanocomposites based on layered silicates like montmorillonite have been widely studied during the last ten years. Because of the high aspect ratio of this dispersed layered material as fillers dramatic improvements in the properties of the polymer can be achieved at very low filler levels[3-8]. Nanocomposites are prepared by three general methods. These are (a) intercalation of polymer or prepolymer from solution (b) *in-situ* intercalative polymerization and (c) melt intercalation[9]. The resulting structure may be agglomerated microcomposite or intercalated or exfoliated nanocomposite which depend critically on the organoclay, nature of the polymer and the method of its preparation. Of these, the *in-situ* intercalative polymerization method allows significant opportunities to alter the structure and morphology of nanocomposites.

Many attempts have been made towards the preparation of PC/clay nanocomposites. Brittain *et al* reported the preparation of partially exfoliated PC/clay nanocomposites using carbonate cyclic oligomers and ditallowdimethyl ammonium modified montmorillonite[10]. Cyclic oligomers when mixed with the organoclay at 180 °C in a Brabender mixer for 1 h resulted in exfoliated structures. Subsequent ring opening polymerization of the cyclic oligomers resulted in linear polymer matrix retaining the partially exfoliated structure for the nanocomposites[16]. Several reports are available for

the preparation of PC nanocomposites by melt mixing[11-26]. Paul and coworkers studied, the effect of organoclay structure and molecular weight of PC on morphology and properties of PC/clay nanocomposites using a variety of organoclays[11]. Higher molecular weight PC (M_n = 10,800, M_w = 32,000), which provide higher shear force during preparation by melt processing, were found to disperse the clay better than medium molecular weight PC (M_n = 8,500, M_w = 23,700). Several organoclays with a variety of modifier types were scanned. Best dispersion and consequently significant improvement in modulus was obtained with modifiers containing poly(oxyethylene) or octadecyl tails. Reduction in molecular weight for PC and color formation was observed during melt processing due to thermal degradation induced by the organoclay as well as the modifiers. The reduction in molecular weight and color formation was shown to be dependent on residence time in the extruder, chemical structure of the modifier and the iron content in the silicate clay[12]. Modifiers having ammonium cation with unsaturated alkyl chains, hydroxyethyl groups and tertiary ammonium groups had a larger effect on color. Reduced iron content in the clay (laponites) caused less degradation of polymer as compared to clays with higher Fe content (Montmorillonites). Studies on polymer blend/clay nanocomposites based on PC were explored to exploit the advantage of combining the properties of a nanocomposite with that of a blend[13-18]. PC/poly(caprolactone)(PCL)/organoclay nanocomposites based on the organoclay, Cloisite 30B, modified using bis(hydroxyethyl)methyltallow ammonium cation, were prepared by melt mixing and showed improved barrier properties and higher ductility compared to the pristine polymer[13]. However T_g decreased with addition of clay and PCL. Intercalated PC/poly(methyl methacrylate) (PMMA) blend (30/70 w/w)/organoclay nanocomposites based on organoclay, Cloisite 20A, a montmorillonite modified using dimethyl dihydrogenated tallow quaternary ammonium salt, was prepared by melt mixing[14]. The domain sizes of dispersed PC phase decreased considerably to give a transluscent PC/PMMA/organoclay nanocomposite while PC/PMMA blend was opaque. The tensile properties of the nanocomposites showed significant improvements. Thermal degradation behavior of PC/poly(acrylonitile-butadiene-styrene)(ABS)/organoclay nanocomposites was extensively studied and found that the nanocomposites show higher thermal stability and lower flammabilities compared to pristine PC/ABS blend[15-18]. Clay

layers were mostly found only in the ABS phase. Attempts were made to improve dispersion of clay in PC nanocomposites by use of compatibilizers[19-22]. Wu et al prepared PC/clay nanocomposites based on the organoclay, DK2 (a montmorillonite modified using bis(2-hydroxyethyl)methyl tallow ammonium ion), using a epoxy resin based on a bisphenol-A-diglycidyl ether as a compatibilizer[19]. It was observed that the extent of intercalation improved with the addition of the epoxy resin but did not lead to exfoliation. However, with increased epoxy resin content thermal stability of PC decreased leading to formation of dark color. This was attributed to a synergistic effect of organoclay and the epoxy resin. Guduri and Luyt prepared partially exfoliated PC/clay nanocomposites based on Cloisite 93A, a montmorillonite modified with methyl dihydogenated tallow alkyl ammonium salts, in presence of maleic anhydride-g-polypropylene (PPMA) as compatibilizer[20].   Tensile modulus and tensile strength showed considerable improvement as a result of increased exfoliation in presence of PPMA. However presence of some tactoids of clay clusters were observed which collapsed in the polymer matrix due to degradation of the modifier at the temperature of preparation of the nanocomposites. Okamoto and coworkers developed PC/clay nanocomposite foams based on organically modified fluorohectorite in presence of poly(styrene-co-maleic anhydride) as compatibilizer[21,22]. It was found that the PC/clay nanocomposites exhibit smaller cell size and larger cell density as compared to pristine PC foam. Hsieh and coworkers studied the mechanical response and the rheological behavior of PC/clay nanocomposites (Cloisite 25A), prepared by melt mixing[23]. The studies suggested the importance of proper selection of organo-modifiers to ensure thermal stability of PC and achieve the optimal mechanical properties of PC nanocomposites. Tribological properties of intercalated PC/clay nanocomposites based on an organo-ammonium modified clay, Bentone 2010 has been examined by Carrion and coworkers[24]. These nanocomposites showed a significant reduction of friction coefficient and wear. However, the nanocomposites exhibited lower Tg. This was attributed to the degradation of PC during preparation of nanocomposites. Lee et al prepared partially exfoliated PC nanocomposites based on organoclay, Cloisite 25A, by solid-state polymerization induced by microwave heating[27]. They first intercalated the prepolymer in the organoclay

followed by microwave induced solid-state polymerization to obtain partially exfoliated nanocomposites.

Most of the earlier studies on PC/clay nanocomposites used quaternary ammonium containing modifiers. However, at the temperature of preparation of PC by melt polycondensation, quaternary ammonium compounds are likely to decompose via Hoffman elimination reaction (Scheme 4.1), resulting in the formation of t-amines[28]. Amines are known to induce base catalyzed chain scission of PC leading to molecular weight reduction and color formation[11,12,29]. One approach to mitigate this problem is to use modifiers which are more thermally stable. Organocations based on phosphonium, imidazolium and tropylium cations are reported to be stable even at 300 °C[30-32]. Preparation of PC nanocomposites using phosphonium ion modified montmorillonite was repoted to lead to improvement in the thermal stability for PC/clay nanocomposites[33].
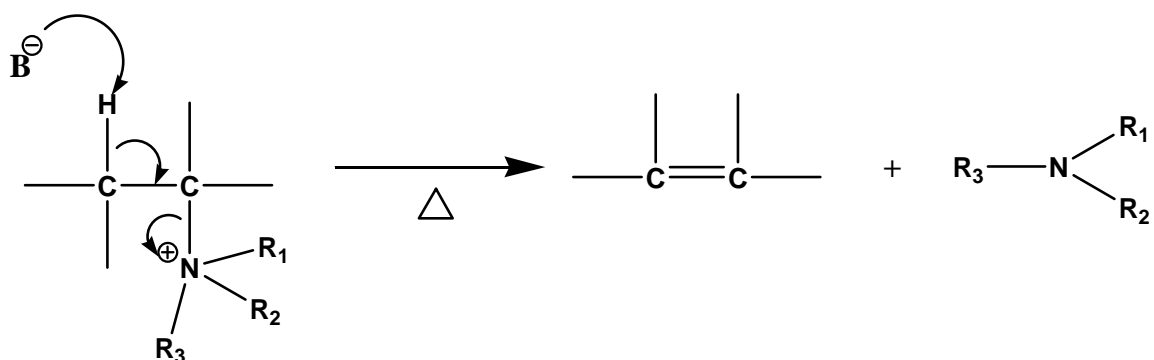
Scheme 4.1: Hoffman β- elimination reaction

It is generally recognized that the properties of the nanocomposite are enhanced when the interaction of the polymer chain with the surface of the clay layer is improved. This can be achieved by chemically tethering the polymer onto the surface of the clay layers, which are completely delaminated and fully exfoliated through out the polymer matrix. Many examples of hydrophobic modifiers possessing functional groups capable of co-polymerization or initiating polymerization have been recently reported with attendant improvement in the property of nanocomposites[34-39]. However there is no report in the literature of a similar approach for the preparation of PC/clay nanocomposites.

Therefore, the objective of the work described in this chapter is

- to prepare PC/clay nanocomposites via *in-situ* polymerization using thermally stable modifiers for the clay that contain the reactive bisphenol groups for polycondensation.

- to study the effect of organo-modification of the clay based on phosphonium and imidazolium cations on the molecular weights of polymer, structure and mechanical properties of nanocomposites obtained via *in-situ* polymerization and

- to compare the properties of the nanocomposites prepared using organoclays which are modified using thermally stable modifiers with and without reactive bisphenol groups for polycondensation.

4.2   Experimental

4.2.1   Materials

Na^+ Montmorillonite was obtained from Southern Clay products, USA. Methyl acetoacetate and phenol were obtained from Sd fine chemicals, Mumbai, India. 1,10-ecanediol, carbon tetrabromide, triphenylphosphine, lithium aluminum hydride, tetramethylammonium hydroxide (TMAH), 1,2-dimethyl imidazole and 1-hexadecyl bromide were obtained from Aldrich, USA and were used without further purification. Bisphenol-A and diphenyl carbonate were kindly provided by GE John F. Welch Technology Centre, Bangalore, India.

4.2.2   Analytical methods

^{1}H NMR spectra were recorded in $CDCl_3$ solution with tetramethylsilane (TMS) as an internal standard using a Bruker DSX300. Molecular weight and molecular weight distributions of polymers were determined using SEC (*Thermo separation products*) equipped with UV and RI detectors. Linear Polystyrene standards were used for calibration of the column. Chloroform filtered through 0.2 µL pore PTFE membranes was used. The sample concentration was 2 mg /mL and the injection volume was 50 µL. Samples for TEM were prepared by sectioning the samples into ultrathin slices (<100 nm) at room temperature using the microtome Leica Ultracut UCT equipped with a

diamond knife and then mounted on 200 mesh copper grids. The thermal properties of the samples were analyzed by TA instruments Q10 differential scanning calorimeter under standard conditions. The samples were heated to 280 °C and cooled to 50 °C and again reheated to 280 °C at a rate of 10 °C/min and the sample weight was about 5 mg and the Tg were measured from the second heating cycle. Dynamic mechanical properties of the samples were studied using Rheometrics Dynamic Mechanical Analyzer, model DMTA IIIE that provided storage modulus, loss modulus and loss tangent (tan δ) against temperature. The scans were carried out in single point cantilever bending mode at a constant heating rate of 2 °C/min and a frequency of 1 Hz from 35 °C to 170 °C. The samples were cut (with dimension of 25.0 X 6.0 X 1.0 mm^3) from the sheets obtained by compression molding at 260 °C. WAXD, TGA and TEM measurements were performed as per procedures described in Chapter 3.

4.2.3 Synthesis of modifiers for the clay

4.2.3.1 Synthesis of 10-bromodecanol (1) from 1,10-decanediol

To a mixture of 1,10-decanediol (35.73g, 0.205 mol) and toluene (700 mL) was added concentrated HBr (29 mL of 47% aqueous solution, 0.24 mol). The heterogeneous mixture was stirred and heated at reflux for 36 hours. TLC analysis indicated substantial amounts of 1,10-decanediol still remained. Therefore, a further quantity of HBr (15 mL, 0.12 mol) was added and the mixture was heated at reflux for a further period of 36 h, at which time TLC analysis showed no diol remaining. The reaction mixture was allowed to cool to room temperature and the phases were separated. The organic layer was concentrated by evaporating the toluene and diluted with ethyl acetate and washed with water, sodium bicarbonate and brine. Then the organic layer was dried over Na_2SO_4 and concentrated to a yellow liquid. Purification of the crude reaction mixture by column chromatography yielded pure 10-bromodecanol **1** (43.0 g). Yield: 90%. ^{1}H NMR: 1.2 to 1.8 (18 H, m); 3.43 (2H, t); 3.65 (2H, t).

4.2.3.2 Synthesis of methyl-(3-hydroxydecyl)acetoacetate (2)

Clean dry sodium (9.5 g, 0.413 mol) was placed in a three neck round bottom flask fitted with a double surface condenser, dropping funnel and septum adapter. Dry methanol (200

mL) was added on sodium slowly under cooling. Methyl acetoacetate (48.3 g, 0.416 mol) was added under stirring and heated to gentle heating. Potassium Iodide (5.6 g, 0.033 mol) was added. 10-Bromodecan-1-ol **1** (79 g, 0.33 mol) was taken in dropping funnel and added slowly into the contents of the round bottomed flask over a period of 60 min. Reflux was continued for 12 hours and the progress of the reaction was monitored by TLC. The reaction was terminated when all the bromodecanol was consumed. The crude reaction mixture was concentrated by evaporating methanol, diluted with ethyl acetate, washed with water several times until the washings were neutral to litmus. Methyl-(3-hydroxydecyl)acetoacetate **2** (58.3g), a pale yellow liquid, was separated from the crude product by flash chromatography. Yield: 65%. ^{1}H NMR: 1.26 to 1.8 (3H, s); 2.23 (3H, s); 3.43 (1H, t); 3.64 (2H, t); 3.74 (3H, s).

4.2.3.3 Synthesis of 13-hydroxytridecan-2-one (3)

Methyl-(3-hydroxydecyl)acetoacetate **2** (54.4 g, 0.20 mol) was dissolved in dimethyl sulfoxide (150 mL) in a round bottom flask and NaCl (15 g, 0.25 mol) was added to it along with distilled water (18 g, 1.0 mol). The above mixture was heated at 150 °C for 18 hours. The reaction was continued until all the starting material was consumed which was monitored by TLC. The product was poured into water and extracted with diethyl ether. The combined ether layer was washed with water, brine and then dried over sodium sulfate. The ether was evaporated to yield 13-hydroxytridecan-2-one **3** (32.1 g) as a white solid, which is then purified by recrystallization in hot petroleum ether. Yield: 75 %. Melting Point: 58 °C; ^{1}H NMR: 1.26 to 1.8 (18H m,); 2.14 (3H, s); 2.42 (2H, t); 3.64 (2H, t).

4.2.3.4 Synthesis of 2,2-bis(4-hydroxyphenyl)tridecanol (4)

13-Hydroxytridecan-2-one **3** (21.4 g, 0.10 mol) was mixed with phenol (56.4 g, 0.60 mol) and mercaptopropionic acid (0.106 g, 0.010 mol). Anhydrous HCl gas was bubbled into the reaction mixture. The reaction was continued under stirring for 12 hours at 45 °C. The reaction mixture was dissolved in ethyl acetate and was washed with water, $NaHCO_3$ and brine. The organic layer was dried over Na_2SO_4. Excess phenol in the reaction mixture was distilled out under vacuum at 60 °C. 2,2-Bis(4-hydroxyphenyl)tridecanol **4** (25.0 g)

was purified and isolated by column chromatography as a viscous liquid. Yield: 65 %. ^{1}H NMR: 1.14 to 1.53 (14H, m); 1.57 (3H, s); 1.63 (2H, m); 1.77 (2H, m); 2.00 (2H, m) 4.08 (2H, t); 6.68 (4H, d); 6.93 (4H, d).

4.2.3.5 Synthesis of 2,2-bis-(4-hydroxyphenyl)tridecyl bromide (5)

2,2-Bis(4-hydroxyphenyl)tridecanol **4** (22.37 g, 0.050 mol) and CBr_4 (19.92g, 0.060 mol) were dissolved in dry tetrahydofuran (100mL) and taken in three-neck round bottom flask fitted with a addition funnel, condenser and a three-way stopcock. Triphenylphosphine (14.41g, 0.055 mol) was dissolved in tetrahydofuran and added dropwise to the reaction mixture, kept at 0 °C over a period of 30 minutes. Stirring was continued for another 4 hours at 0 °C. The progress of reaction was monitored by TLC. After completion of the reaction the crude reaction mixture was concentrated by evaporating the solvent. The crude mass was dissolved in ethyl acetate and washed with water. 2,2-Bis(4-hydroxyphenyl)tridecyl bromide **5** (20.1 g) was isolated as a white solid after column chromatography. Yield: 90 %. Melting Point: 82 °C; ^{1}H NMR: 1.14 to 1.53 (16H, m); 1.55 (3H, s); 1.84 (2H, m); 1.98 (2H, m); 3.40 (2H, t); 6.68 (4H, d); 6.93 (4H, d).

4.2.3.6 Synthesis of 2,2-bis-(4-hydroxyphenyl)tridecyltriphenylphosphonium bromide (6)

Equivalent amounts of 2,2-bis-(4-hydroxyphenyl)tridecyl bromide (4.4746 g, 0.010 mol) and triphenylphosphine (2.631g, 0.010 mol) were mixed and heated at 100°C for 8 hours under an atmosphere of nitrogen. The melt mixture solidified after the reaction. 2,2-bis-(4-hydroxyphenyl)tridecyl triphenylphosphonium bromide **6** was obtained in a pure form as white solid and used without further purification. Melting point: 148 °C; ^{1}H NMR: 1.14 to 1.46 (16H, m); 1.50 (3H, s); 1.63 (2H, m); 1.93 (2H, m) 3.40 (2H, t); 6.68 (4H, d); 6.93 (4H, d); 7.72 to7.88 (15H, multiplet).

4.2.3.7 Synthesis of 2,2-bis-(4-hydroxyphenyl)tridecyl-(1,2-dimethylimidazolium) bromide (7)

Equivalent amounts of 2,2-bis-(4-hydroxyphenyl)tridecyl bromide (4.4746 g, 0.010 mol) and 1,2-dimethylimidazole (0.9613g, 0.010 mol) were mixed and heated at 100°C for 8

hours under an atmosphere of nitrogen. The melt solidified after the reaction. 2,2-bis-(4-hydroxyphenyl)tridecyl-(1,2-dimethylimidazolium) bromide **7** was obtained as a transparent yellow solid and used without further purification. Melting point: 78 °C; ^{1}H NMR 1.14 to 1.48 (16H, m); 1.56 (3H, s); 1.69 (2H, m); 2.01 (2H, m) 2.50 (3H, s); 3.75 (3H, s); 4.03 (2H, t); 6.68 (4H, d); 6.93 (4H, d); 7.42 (2H, m)

4.2.3.8 Synthesis of 1-hexadecyl triphenylphosphonium bromide (8)

Equivalent amounts of hexadecyl bromide (3.05 g, 0.010 mol) and triphenyl phosphine (2.631 g, 0.010 mol) were mixed and heated at 100°C for 8 hours under an atmosphere of nitrogen. The melt solidified after the reaction. Hexadecyl triphenylphosphonium bromide **8** was obtained as white solid and used without further purification. Yield: 100%. ^{1}H NMR: 0.88 (3H, t); 1.14 to 1.50 (24H, m); 1.63 (2H, m); 1.93 (2H, m) 3.40 (2H, t); 7.72 to7.88 (15H, multiplet).

4.2.3.9 Synthesis of 1-hexadecyl-2,3-dimethylimidazolium bromide (9)

Equivalent amounts of hexadecyl bromide (3.05 g, 0.010 mol) and 1,2-dimethylimidazole (0.9613 g, 0.010 mol) were mixed and heated at 100°C for 8 hours under an atmosphere of nitrogen. The melt solidified after the reaction. Hexadecyl-2,3-dimethylimidazolium bromide **9** was obtained as yellow solid and used without further purification. Yield: 100%. ^{1}H NMR: 0.88 (3H, t); 1.14 to 1.50 (24H, m); 1.65 (2H, m); 2.02 (2H, m) 2.50 (3H, s); 3.75 (3H, s); 4.02 (2H, t); 7.42 (2H, m).

4.2.4   Synthesis of organoclays.

Na montmorinollite (10 g) with a CEC of 92 meq/100 g, was dispersed in water/methanol (300 mL) by stirring with an over head stirrer at room temperature for 2 hours. The modifier (11 meq) was dissolved in methanol/water mixture was poured into a dispersion of clay dropwise and stirred for 24 hours at 65 °C. The reaction mixture was cooled, centrifuged and washed several times with distilled water and methanol until all the bromide ions were washed off. The organoclay obtained was freeze dried under vacuum overnight. The organoclay was obtained as fine, dry powder. The degree of exchange of Na^+ by the organic cation was > 99 %.

4.2.5   Synthesis of PC nanocomposites

Melt polymerization reactions were carried out in a three-neck tubular glass reactor equipped with a solid helical agitator (Figure 4.1). To remove any sodium from the surface of the glass, the reactor was soaked in 3N HCl for 24 hours followed by a soak in de-ionized water for 24 hours. The reactor was then dried in an oven overnight and stored covered until used. The temperature of the reactor was maintained using a salt bath with a PID controller and measured near the reactor and salt bath interface. The pressure over the reactor was controlled by a nitrogen bleed into the vacuum pump downstream of the distillate collection flasks and measured with a digital Pirani gauge.

Figure 4.1: Melt condensation reactor assembly.

The reactor was charged with bisphenol-A (BPA), diphenyl carbonate (DPC) and the organoclay in the desired ratios. The reactor was assembled, sealed and the atmosphere was exchanged with nitrogen three times. With the final nitrogen exchange the reactor

was brought to near atmospheric pressure and submerged into the molten salt bath, which was at 180° C. After five minutes agitation was begun at 100 rpm. Solution of TMAH (10^{-4} mol/mol of BPA) and NaOH (10^{-6} mol/mol of BPA) were added. After 30 minutes the temperature was ramped to 210 °C. The pressure was reduced slowly to 180 mbar at which time phenol started distilling out. After 30 minutes the pressure was further reduced to 100 mbar and maintained for 30 minutes. The temperature was then ramped to 240 °C and the pressure was lowered to 20 mbar. These conditions were maintained for 30 minutes. The temperature was then ramped to 260 °C and the pressure was lowered to 3.5 mbar. These conditions were maintained for 60 minutes. The temperature was then ramped to the final finishing temperature of 290 °C and the pressure was reduced to 0.030 mbar. After 4 hours the reactor was removed from the molten salt bath and cooled under vacuum. The nanocomposite was recovered by breaking the glass reactor.

4.2.6   Separation of PC from the nanocomposites

PC-nanocomposite (0.300 g) was dissolved in chloroform/tetrahydrofuran mixture (20/80 v/v, 20 mL) and 2 % solution LiCl in tetrahydrofuran (2 mL) was added slowly under stirring. The stirring continued for 24 h at room temperature. The clay was precipitated due to reverse ion exchange and separated by filtration. The filtrate was poured in to methanol to obtain the precipitate of polymer. The polymer obtained was filtered and dried in vacuo at 60 °C for 6 h and used for further analysis.

4.3   Results and discussion

4.3.1   Preparation of organomodifiers for the clay

Organic modifiers with reactive functional groups were prepared for this study. The reactive modifier had the following structural features: (a) presence of a functionality which can undergo polycondensation with bisphenol-A and diphenyl carbonate; (b) presence of a cationic group that can interact with the negatively charged silicate layer and   (c) an organic cation that is likely to be stable at the temperature of polycondensation. The synthetic approach to the chosen reactive modifiers is shown in the Scheme 4.2. For purposes of comparison, modifiers such as hexadecyltriphenylphosphonium bromide **8**, hexadecyl-2,3-dimethylimidazolium

bromide **9** were also prepared. These modifiers lack the reactive functional groups present in modifiers **6** and **7**.
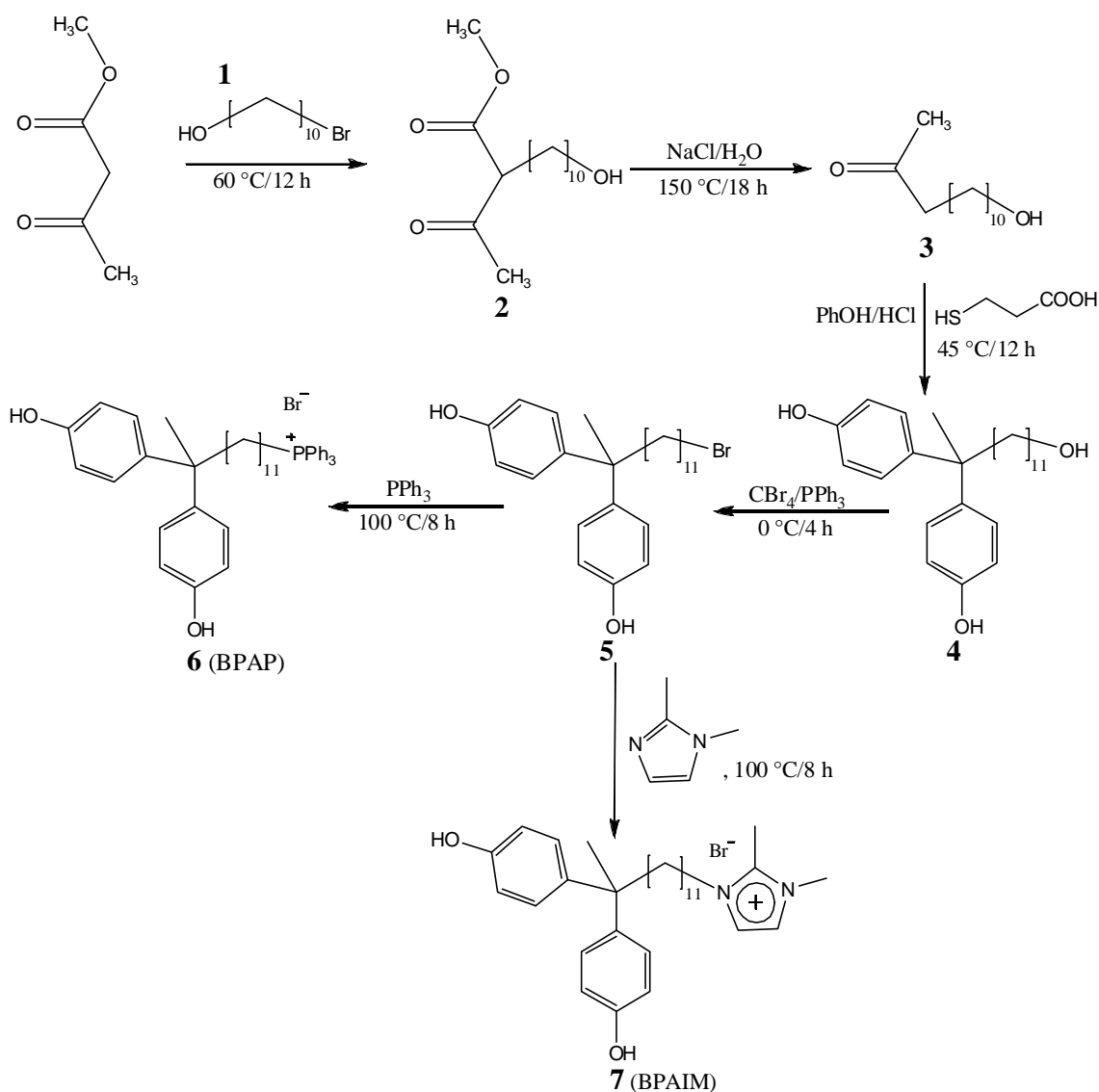
Scheme 4.2: Preparation of reactive modifiers

4.3.2 Preparation of organoclays

Four different organoclays were prepared by exchanging Na^+ ion in montmorillonite using 12,12-bis(4-hydroxyphenyl)tridecyltriphenylphosphonium bromide **6**, 12,12-bis(4-hydroxyphenyl)tridecyl-(2,3-dimethylimidazolium) bromide **7**, hexadecyltriphenyl phosphonium bromide **8** and hexadecyl-2,3-dimethylimidazolium bromide **8**, which are abbreviated as C16P-MMT, C16IMI-MMT, BPAP-MMT and BPAIMI-MMT,

respectively, using standard exchange reactions reported in the literature[40]. The interlayer d spacing for the organo-modified montmorillonite was measured from WAXD (Figure 4.2) and is shown in Table 4.1. The intercalation of onium ions in the interlayer gallery is evidenced by increase in d spacing after organo-modification.
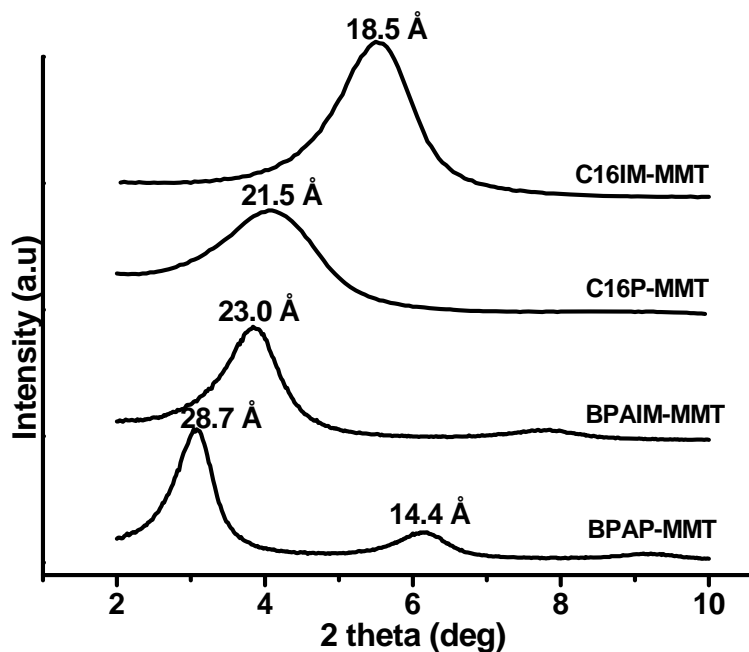
Figure 4.2: WAXD of various organoclays

Table 4.1: TGA and d- spacing for the organoclays[a]

Clay	Modifier	Onset of degradation (°C)	Weight loss on charring (%)		d-spacing for clay, Å
			Theoretical	Experimental	
BPAP-MMT	**6**	248	39	40	28.7
BPAIMI-MMT	**7**	240	31	32	23.0
C16P-MMT	**8**	300	33	33	21.5
C16IMI-MMT	**9**	300	25	26	18.5

[a] The unmodified clay had a d spacing of 12.3 Å.

4.3.2　Thermal analysis of organoclays

Figure 4.3(a)-(d) shows thermal analysis of the organo-modified clays performed using TGA. The organoclays degrade in multiple steps. The first onset of degradation for organoclays C16P-MMT and C16IMI-MMT is observed at 300 °C, whereas, organoclays BPAP-MMT and BPAIMI-MMT begin degrading at around 240 °C. The first step in degradation of BPAP-MMT and BPAIMI-MMT can be ascribed to either (a) the decomposition of the bisphenol group (Scheme 4.3) [41,42]. However, once the bisphenol is enchained in the polymer, this process of degradation becomes less significant.
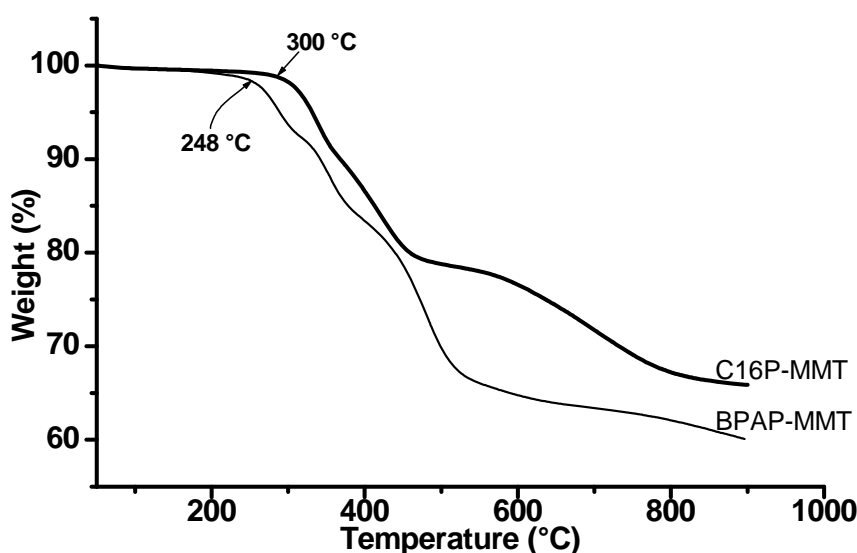
Figure 4.3(a): TGA of the organo-modified clays based on phosphonium ions
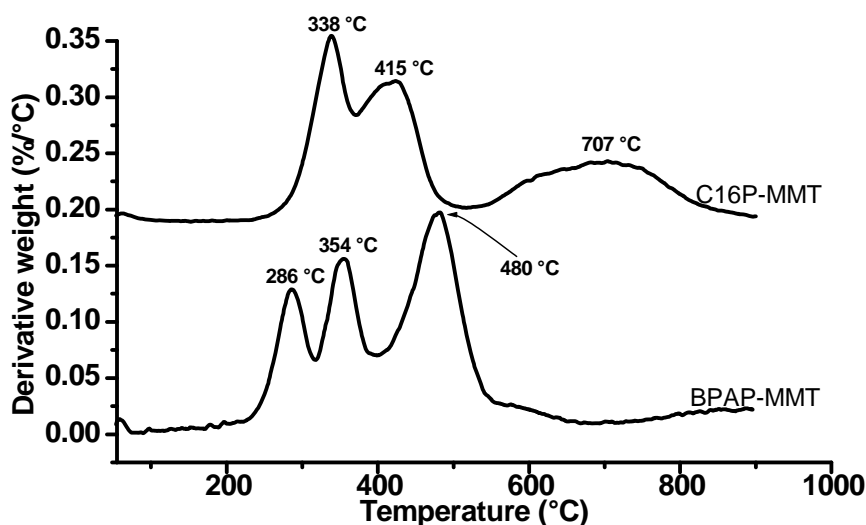
Figure 4.3(b): Derivative thermogram of the organo-modified clays based on phosphonium ions
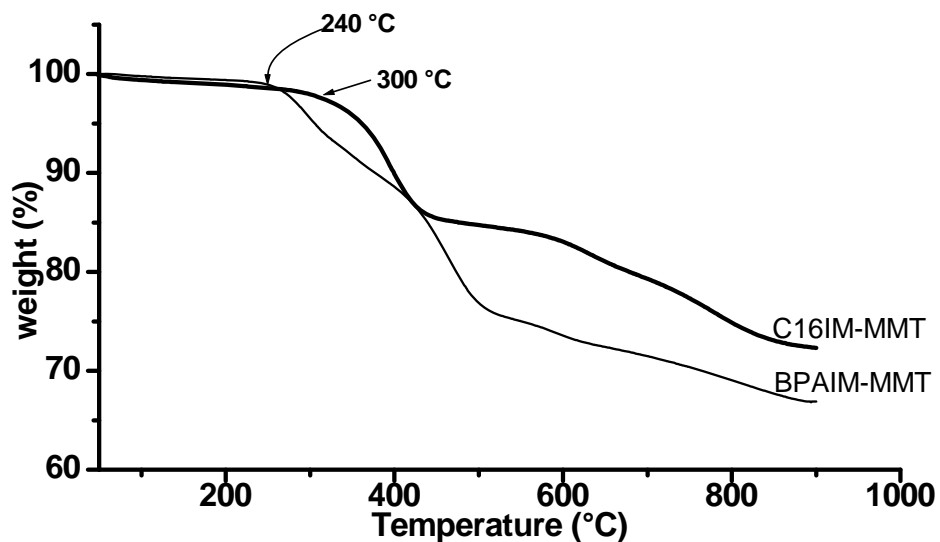
Figure 4.3(c): TGA of the organo-modified clays based on imidazolium ions
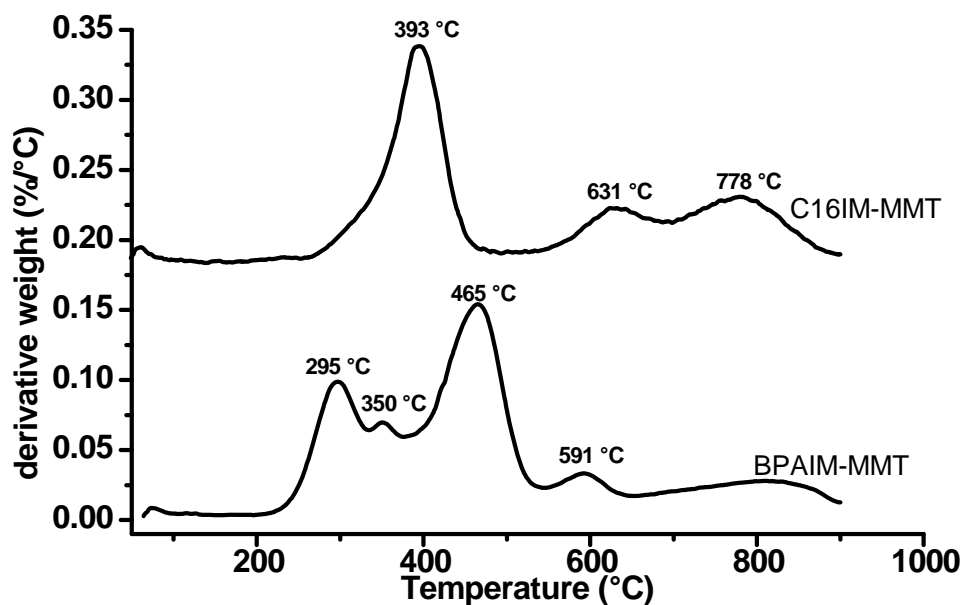
Figure 4.3(d): Derivative thermogram of the organo-modified clays based on imidazoilum ions

In general, the organomodifiers containing imidazolium cations have a higher onset temperature of degradation compared to phosphonium cations. Therefore, at the outset, it appears that these class of modifiers could be more suitable for the melt

polycondensation of BPA with DPC which is generally performed above 250 °C. The organic content was obtained from percentage of degradation (obtained from TGA, Figure 4.3) of the clays upon heating to 900°C. The organic content determined experimentally indicate that the exchange of Na^+ by the organic cation is > 99 %.
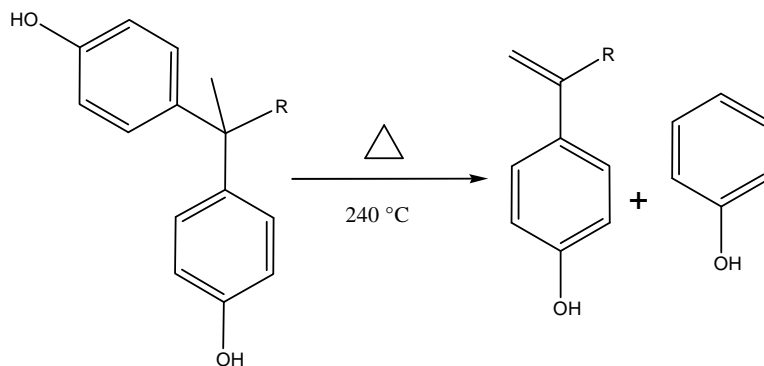
Scheme 4.3: Thermal decomposition of bisphenol group in the organomodifier

4.3.4 Preparation of PC/clay nanocomposites using phosphonium cations as modifiers

PC/clay nanocomposites were prepared via *in-situ* melt polycondensation by mixing the organoclay along with bisphenol A and diphenyl carbonate in presence NaOH/ tetramethylammonium hydroxide as catalyst. PC/clay nanocomposites were also prepared in the absence of catalyst. The final finishing temperature was kept at 290 °C to keep the degradation of the organomodifiers to the minimum. The compositions of the monomers, organoclay and the catalyst taken for the *in-situ* polymerization and the molecular weights of the polymer obtained are shown in the Table 4.2. Molecular weights of the polymer in the composites were measured after separating the polymer from the composite by selectively precipitating the clay by reverse ion exchange reaction using LiCl[43-45]. Bisphenol-A poly(carbonate)s prepared in presence of a catalyst comprising of TMAH and NaOH (Entry no: 1, Table 4.2) had a M_n of 22,100, M_w/M_n of 2.31 and T_g of 146 °C. of the This is similar to what has been previously reported in the literature for PC prepared under similar conditions[46-48].

Table 4.2: Melt polycondensation of bisphenol A with diphenyl carbonate in presence phosphonium cation-modified clay.

Entry	Organoclay	Catalyst [a]	Amount of organoclay (g)	BPA (g)	DPC (g)	Wt % of MMT	Mole ratio (DPC: BPA: BPA equivalents in organoclay)	T_g (°C)	Poly(carbonate)s [b]		
									T_g (°C)	M_n x 10^{-3} [c]	M_w/M_n [c]
1	-	TMAH/NaOH	-	15.00	15.22	-	108: 100: 0	146	-	22.1	2.31
2	BPAP-MMT	TMAH/NaOH	0.5079	15.00	15.27	1.8	108: 99.6: 0.45	124	122	4.4	1.93
3	BPAP-MMT	-	0.5079	15.00	15.27	1.8	108: 99.6: 0.45	145	144	24.5	1.74
4	BPAP-MMT	-	1.0204	15.00	15.34	3.6	108: 99.1: 0.91	144	138	20.7	2.26
5	BPAP-MMT	-	1.5384	15.00	15.42	5.3	108: 98.6: 1.36	145	134	25.0	2.77
6	C16P-MMT	-	0.6176	20.00	20.27	1.8	108: 100: 0	141	144	15.0	1.81
7	C16P-MMT	-	1.2352	20.00	20.27	3.6	108: 100: 0	143	142	16.5	1.76
8	C16P-MMT	-	1.8530	20.00	20.27	5.3	108: 100: 0	142	143	18.8	1.69

[a] TMAH: 10^{-4} mmol/mol of BPA, NaOH: 10^{-6} mmol/mol of BPA

[b] obtained from the nanocomposite after ion exchange with LiCl.

[c] by GPC in $CHCl_3$ and calculated with respect to polystyrene standards

Initially attempt was made to prepare a nanocomposites using BPAP-MMT in presence of TMAH/NaOH as catalyst (Entry No. 2, Table 4.2). However, under these conditions reverse reaction was favoured leading to depolymerization resulting in very low molecular weight PC. Avoiding the use of TMAH/NaOH, resulted in better result (Entry no. 3, table 4.2). Triarylphosphonium salts are reported to catalyze polycondensation reaction of BPA and DPC[49]. Additionally residual Na^+ cation or clay, can also act as catalyst for polycondensation. It is well known that more than optimum quantities of Na^+ ion can lead to reversal of the polycondensation reaction. Therefore, further studies were conducted in the absence of any externally added catalysts. In all the reactions, the ratio of reactants taken at the beginning of the reaction was BPA: DPC = 1: 1.08. An excess of DPC was always taken in the initial feed of the reaction to maintain the stoichiometric balance for the loss of DPC that might occur during the course of the reaction. For preparation of nanocomposites, the amount of BPA taken was corrected for the bisphenol equivalent present in the organoclay. In general, modifiers containing BPA group led to higher degree of polymerization (see entry no. 3 and 6, Table 4.2). The quantity of clay did not influence the degree of polymerization.

4.3.4.1 Structure of PC nanocomposites

The WAXD of PC nanocomposites using BPAP-MMT with varying amount of clay is shown in Figure 4.4.
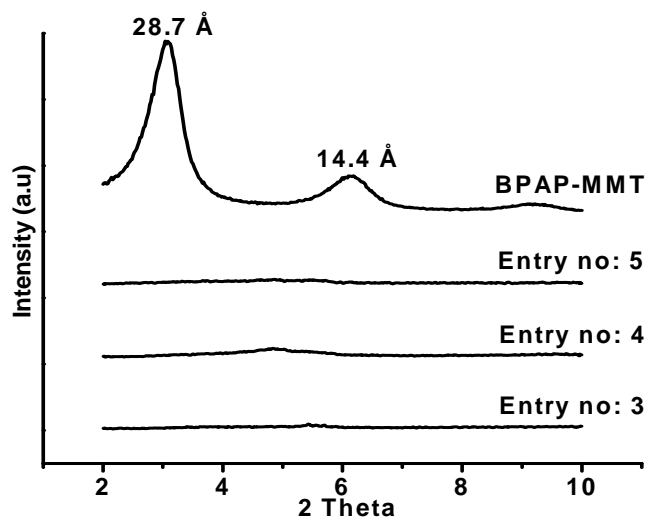
Figure 4.4: WAXD pattern of BPAP-MMT, and the PC nanocomposites (Entry nos: 2,3 and 4; Table 4.2)

TEM of PC nanocomposites using BPAP-MMT are shown in Figure 4.5. In all cases good dispersion of the clay is observed. The clay layers are well separated indicative of exfoliated structures. Thus WAXD and TEM taken together confirm delamination of clay layers with organo-modifier **6**.

(a)   (b)

(c)
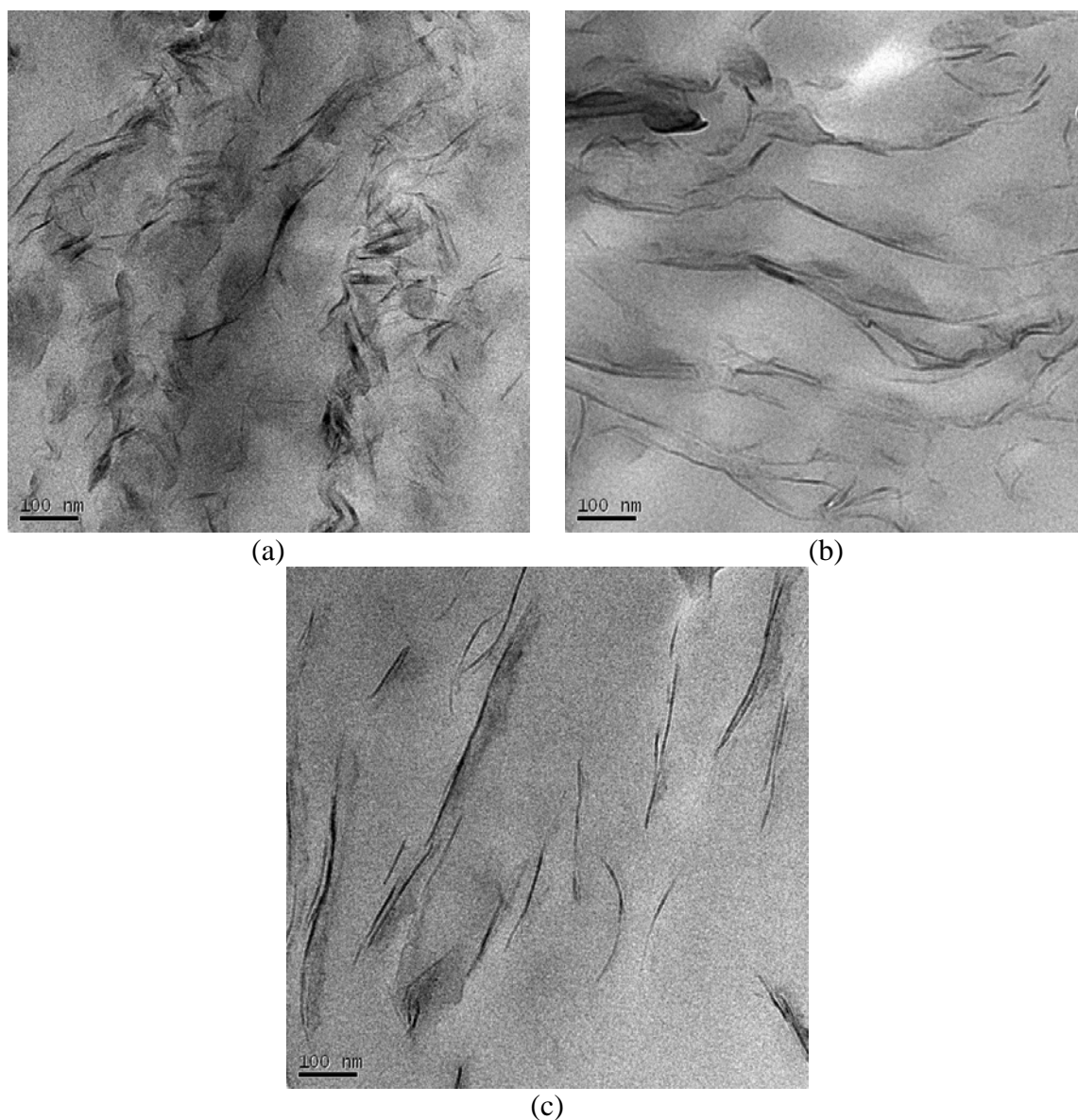
Figure 4.5: TEM pictures of PC nanocomposites with BPAP-MMT (a) Entry no: 3, (b) Entry no: 4 and (c) Entry no: 5; Table 4.2.

For purposes of comparison, PC nanocomposites were prepared using a clay modified by 1-hexadecyltriphenylphosphonium cation **8**. This modifier has no reactive functionality capable of undergoing polycondensation reaction. PC nanocomposites of C16P-MMT show lower d-spacing values (~17.8 Å) than the organoclay (21.5 Å) and was independent of the amount of clay.
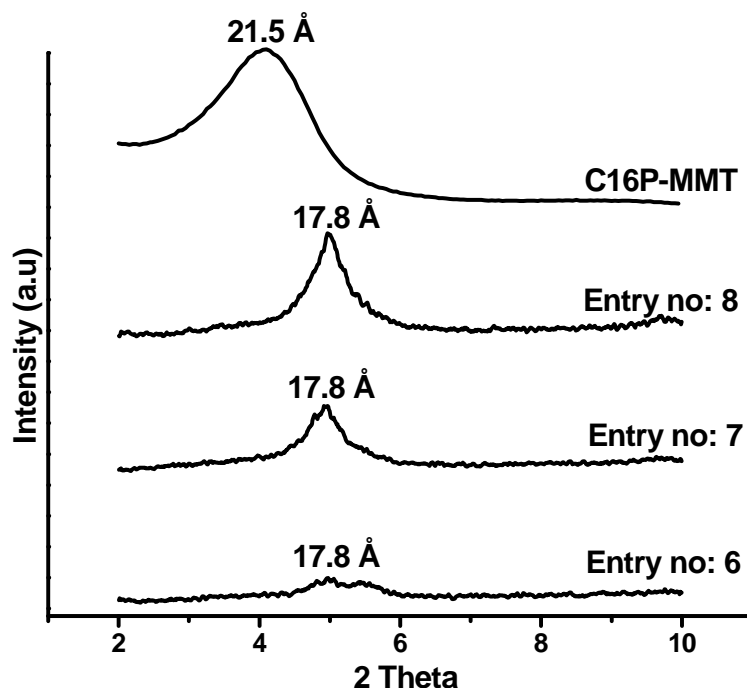
Figure 4.6: WAXD pattern of C16P-MMT, and the PC nanocomposites (Entry nos: 6, 7 and 8; Table 4.2)

This observation suggests formation of phase separated nanocomposites with a lower d-spacing than the modified clay. This may be due to either the deintercalation of modifiers during polymerization, or degradation of modifiers or penetration of polymer chains into the organoclay galleries accompanied with deintercalation of modifiers. Figure 4.7 show the TEM image of the C16P-MMT nanocomposites with 3.6% of clay content at different resolutions. The nanocomposites show intercalated structures. At higher magnification (Figure 4.7b), the silicate layers are seen to be arranged in an ordered array parallel to each other with an interlayer distance of 18 Å, comparable to that obtained from WAXD.

(a)   (b)
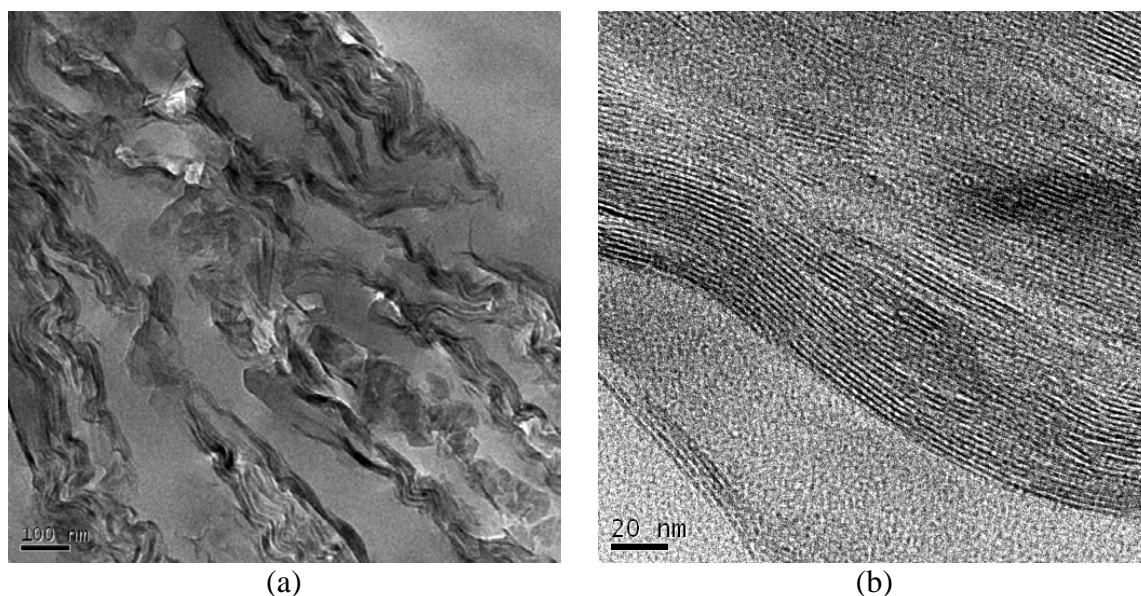
Figure 4.7: TEM pictures of PC Nanocomposite with C16P-MMT (Entry no: 7, Table 4.2) at different resolutions.

4.3.4.2 Glass transition temperatures

The effect of organo-modifiers on T_g of nanocomposites was examined. For purposes of comparison, the PC was separated from the corresponding nanocomposites using reverse ion exchange reaction and the T_g of the isolated PC determined. The results are shown in Table 4.2. It can be observed that the T_g of the polymer separated from the exfoliated nanocomposites based on BPAP-MMT is lower than that of the corresponding nanocomposites, especially at higher clay content. The lower T_g for the separated polymer may be attributed to the presence of a C_{11} alkyl group in the polymer. Based on the assumption that the entire modifier became enchained, the mole % modifier with C_{11} side chain in the PC is expected to be 0.45, 0.91 and 1.35 mole %, respectively, for polymer at entry no. 3, 4 and 5. On the other hand, no significant difference was observed in T_g for the matrix polymer and nanocomposites based on C16P-MMT since in this case the C16 alkyl group cannot become part of the polymer. The slightly lower T_g for these nanocomposites may be attributed to the plastisizing effect of the modifiers. Exfoliated nanocomposites, wherein, the polymer chains are anchored on the clay surface showed significantly higher T_g than PC. Agglomerated nanocomposites, wherein the polymer

chains are not anchored on the clay surface, showed slightly lower T_g compared to PC. This is indicative of some restricted chain mobility in case of exfoliated systems.

4.3.4.3 Dynamic mechanical behavior

Dynamic mechanical properties of PC nanocomposites using an organoclay modified with phosphonium cations were measured. Figure 4.8 (a) and (b) shows the temperature dependence of storage modulus (E') of nanocomposites based on BPAP-MMT and C16P-MMT, respectively.
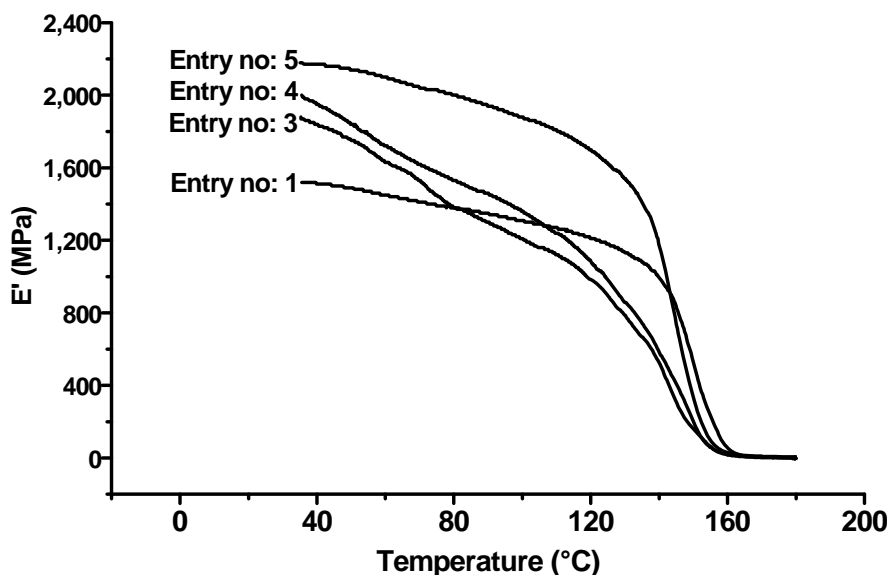
Figure 4.8 (a): Storage modulus (E') of PC nanocomposites with BPAP-MMT
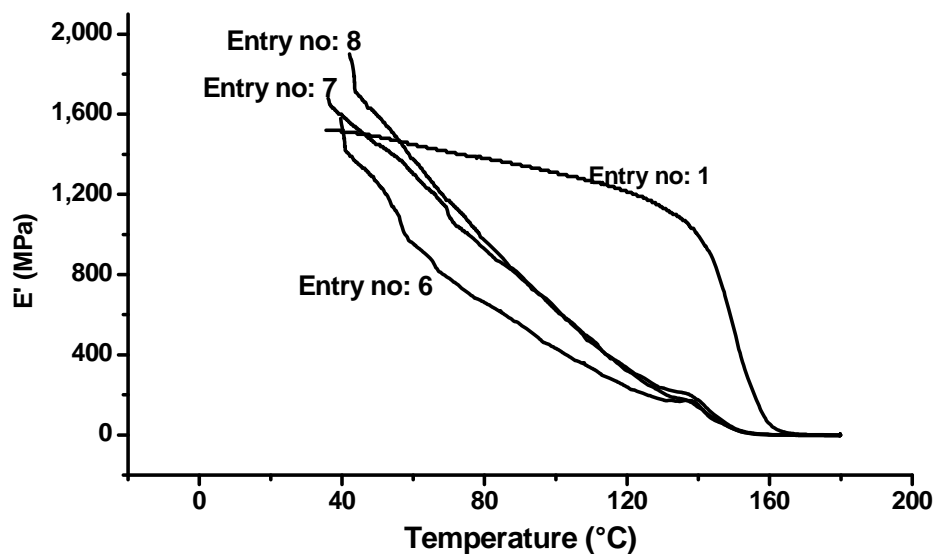
Figure 4.8 (b): Storage modulus (E') of PC nanocomposites with C16P-MMT

It can be observed that, at 35 °C, the nanocomposites exhibit higher storage modulus (E') than the pristine polymer and the increase is linear with the clay content. In comparison, the increase in storage modulus (E') is much higher for exfoliated nanocomposites obtained using BPAP-MMT than the their counterparts of agglomerated nanocomposites obtained using C16P-MMT.   However, It can also be seen that as the temperature increases, storage modulus keeps decreasing before the glass transition temperature (α-relaxation) regime. This rate of change in storage modulus is relatively faster in case of agglomerated nanocomposites based on C16P-MMT than the exfoliated nanocomposites based on BPAP-MMT. The faster relaxation may be attributed due to enhanced mobility of confined polymer chains at the interface polymer and silicate layers as reported by various groups[50-55]. According to the earlier reports, such relaxations are known to be limited to the nano-regime. The relatively slower relaxation behavior of the exfoliated nanocomposites can be attributed to the restricted mobility of polymer chains anchored on the clay surface[56,57]. The poor interfacial interactions can be ascribed for the faster relaxation behavior for the agglomerated nanocomposites based on C16P-MMT. This observation is in good agreement with the earlier reports[58,59].

4.3.4.4 Color of the nanocomposites

The color of PC/clay nanocomposites obtained via *in-situ* melt polymerization using phophonium modified organoclays of various compositions is shown in Figure 4.9. It is observed that nanocomposites prepared via *in-situ* polymerization using organoclays which are modified using phosphonium cations are found to be dark brown in color. Thus, a quaternary phosphonium modifier, whose temperature of degradation is slightly higher than the polycondensation temperature did not result in any improvement in color. The appearance of a dark coloration in PC is indicative of undesirable side reactions in PC leading to intensely absorbing chromophores[60]. Such reactions are known to be catalyzed by monovalant and divalent alkaline earths and transition metal ions. The clays used in the study were found to contain substantial amounts of Ca^{+2} (1.03 wt%) and Fe^{+3} (3.24 wt%). Apparently this causes the discoloration of PC.
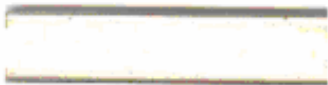
Figure 4.9: Appearance of various PC nanocomposites

4.3.5 Preparation of PC/clay nanocomposites using imidazolium cations as modifiers

PC/clay nanocomposites were prepared using imidazolium cation modified organoclays. However, extensive depolymerization was observed resulting in low molecular weight PC (Table 4.3). The results are indicative of decomposition of the modifier during polymerization resulting in free imidazole formation. Imidazoles in high concentration are known to be efficient depolymerization agents for PC. A plausible mechanism for free imidazole formation is shown in Scheme 4.4.

Table 4.3: Melt polycondensation of bisphenol A with diphenyl carbonate in presence imidazolium cation-modified clay.

Entry	Organoclay	Catalyst [a]	Amount of organo-clay (g)	BPA (g)	DPC (g)	Wt % of MMT	Mole ratio (DPC: BPA: BPA equivalents in organoclay)	T_g (°C)	Poly(carbonate)s [b]		
									T_g (°C)	M_n x 10^{-3} [c]	M_w/M_n [c]
9	BPAIM-MMT	TMAH/NaOH	0.9000	15.00	15.34	3.6	108: 99.1: 0.91	128	132	8.3	1.91
10	BPAIM-MMT	-	0.9000	15.00	15.34	3.6	108: 99.1: 0.91	126	131	8.2	1.94
11	C16IM-MMT	-	0.8165	15.00	15.22	3.6	108: 100: 0	132	138	10.3	2.05

[a] TMAH: 10^{-4} mmol/mol of BPA, NaOH: 10^{-6} mmol/mol of BPA

[b] obtained from the nanocomposite after ion exchange with LiCl.

[c] by GPC in $CHCl_3$ and calculated with respect to polystyrene standards.
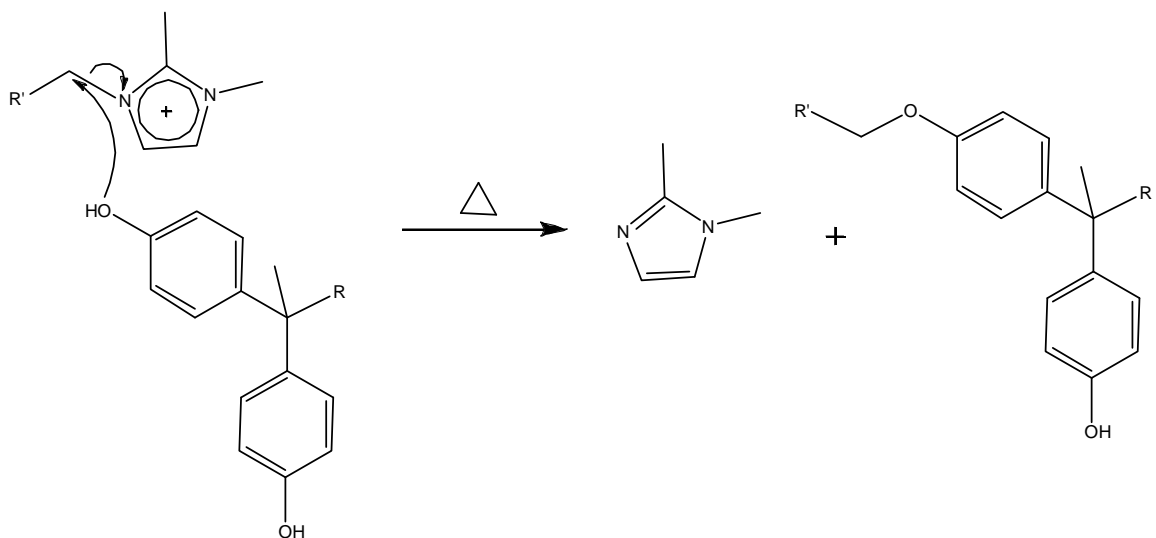
Scheme 4.4: Plausible mechanism for imidazole formation by decomposition of imidazolium ion modifier during polymerization

4.3.5.1 Structure of PC-nanocomposites

Figure 4.10 shows the WAXD of PC nanocomposites prepared using the organoclay, BPAIM-MMT (Entry no: 10, Table 4.3). The peak for the pristine organoclay at 23.0 Å completely disappeared in the nanocomposites indicating the formation of fully exfoliated structure.
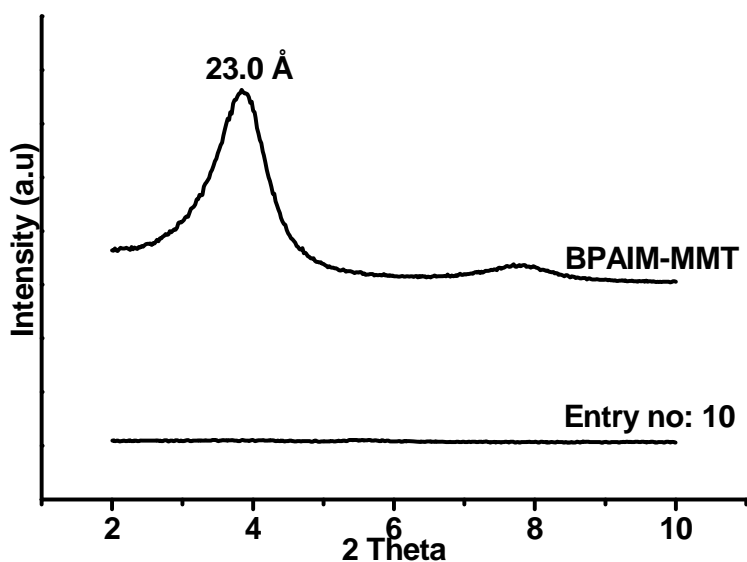
Figure 4.10: WAXD pattern of pristine BPAIM-MMT and the PC nanocomposite (Entry no: 10; Table 4.3)

TEM of PC nanocomposites using BPAIM-MMT (Entry no: 10, Table 4.3) at different resolutions are shown in Figure 4.11. The clay layers are well separated and thoroughly dispersed in the polymer matrix indicative of exfoliated structures. Thus WAXD and TEM taken together confirm formation of exfoliated PC/clay nanocomposites with organo-modifier **7**.

(a)   (b)
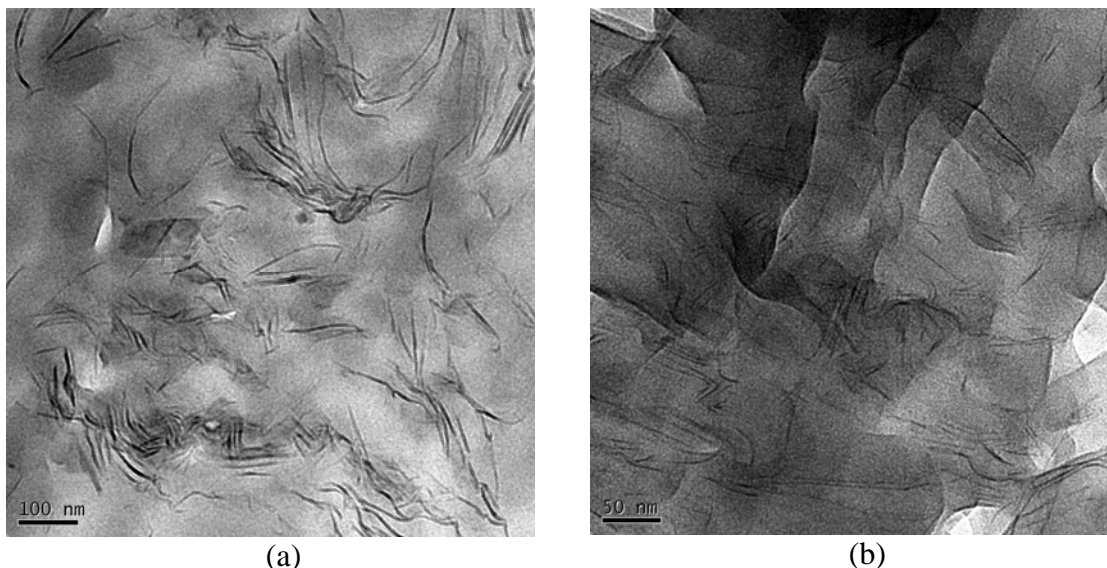
Figure 4.11: TEM pictures of PC nanocomposites with BPAIM-MMT (Entry no: 10; Table 4.3) at dfferent resolutions.

For purposes of comparison, PC nanocomposites were prepared using clay modified by 1-hexadecyl-2,3-dimethylimidazolium cation. This modifier has no reactive functionality capable of undergoing polycondensation reaction. Figure 4.12 shows the WAXD of nanocomposites prepared using C16IM-MMT (Entry no: 11, Table 4.3). The peak for the organoclay at 18.5 Å has shifted to 27.6 Å indicating the formation of intercalated structures.
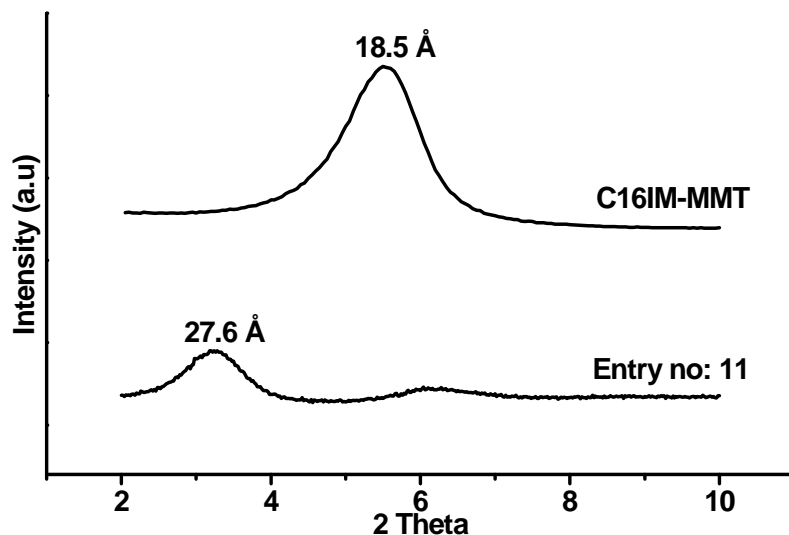
Figure 4.12: WAXD pattern of pristine C16IM-MMT and the PC nanocomposite (Entry no: 11; Table 4.3).

TEM of PC nanocomposites based on C16IM-MMT (Entry no:11 , Table 4.3) at different resolutions are shown in Figure 4.13. The silicate layers are seen to be arranged parallel to each other in stacks with interlayer distance of 28 Å, comparable to that obtained from WAXD which further confirms the formaton of intercalated structures.

(a)   (b)
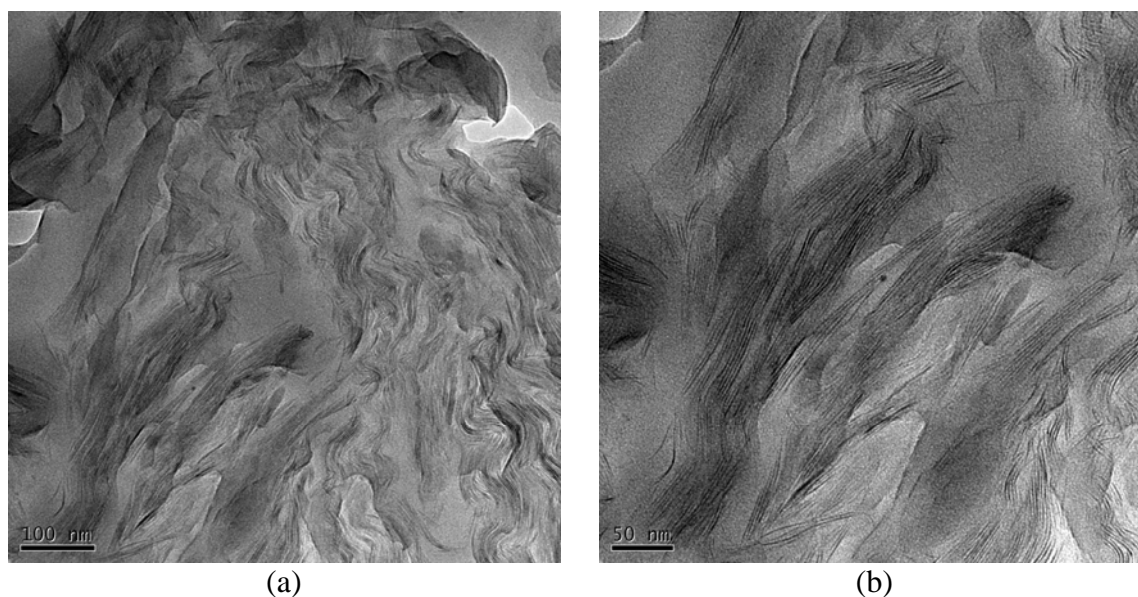
Figure 4.13: TEM pictures of PC nanocomposites with C16IM-MMT (Entry no: 11; Table 4.3) at different resolutions.

4.3   Summary and conclusions

- PC/clay nanocomposites were successfully prepared via *in-situ* intercalative melt-polycondensation using organoclays modified with quaternary phosphonium and imidazoilium cations based modifiers with and without reactive functionalities.

- In general, exfoliated PC/clay nanocomposites was obtained using an organoclay which contained a reactive bisphenol group in the modifier, whereas, only intercalated or phase separated structures were obtained with the organoclays which were modified using compounds having no reactive functionality.

- Organoclays modified using phosphonium cations presumably act as catalyst for polycondensation and produce high molecular weight PC in the absence of any additional base catalysts. Organoclays which are modified using imidazolium cations did not exhibit this behavior and resulted in low molecular weight polymers, indicative of competitive depolymerization. This was attributed to the formation of free imidazole base during polymerization.

- Exfoliated nanocomposites obtained using organoclays modified with phosphonium ions containing reactive bisphenol group, show slightly higher glass transtion temperature than the PC separated from the clay.

- Exfoliated nanocomposites showed superior storage modulus in the temperature range 25 °C to 140 °C when compared to intercalated or phase separated nanocomposites which is attributed to a stronger interaction of polymer with larger surface area provided by the exfoliated clay layers . A relaxation was observed below the glass transition temperature which is predominant in phase separated nanocomposites obtained with phosphonium ion modified organoclay bearing no reactive functional group. This is attributed to the increased mobility of polymer chains in a confined environment.

- Use of organomodifiers which had higher thermal stability than quaternary ammonium based modifiers did not cause any improvement in the color in PC nanocomposites. All PC/clay nanocomposites obtained in this study were dark brown in color. Formation of such color in PC is attributed to complex degradation reactions promoted by excess basic compounds or multivalant metal ions. The clays used in the present study had significant level of Fe^{+3}.

Thus it is demonstrated that well dispersed and exfoliated PC/clay nanocomposites can be prepared via in-situ melt polymerization using organoclays which are modified using phophonium cations containing reactive bisphenol functionality. Interaction between the polymer chains and the clay layers are enhanced as the polymer chains are anchored to clay surface through electrostatic forces. Such nanocomposites are expected to have superior thermal, mechanical and barrier properties. However, the color of the nanocomposites still needs considerable improvements if such nanocomposites have to find significant practical applications.

References

1.   LeGrand, D. G., Mechanical properties of polycarbonates. In "*Handbook of Polycarbonate Science and Technology*"**,** LeGrand, D. G.; Bendler, J. T., Eds.; Marcel Dekker, Inc.,: New York **2000** p 107.

2.   Friessell, W. J. In *Encyclopedia of Polymer Science and Technology*, Bikales, N. M., Ed.; John Wiley and Sons Inc: New York, 1967; Vol. 6, p 740.

3.   Usuki, A.; Kojima, Y.; Kawasumi, M,; Okada, A.; Fukushima, Y.; Kurauchi, T.; Kamigaito, O. *J. Mater. Res.* **1993**, *8*, 1179-1184.

4.   Kojima, Y.; Usuki, A.; Kawasumi, M.; Okada, A.; Fukushima, Y.; Kurauchi, T.; Kamigaito, O. *J. Mater. Res*. **1993**, *8,* 1185-1189.

5.   In *Polymer-Clay Nanocomposites*; Pinnavaia, T. J.; Beall, G. W.; Eds.; Wiley Series in Polymer Science; John Wiley & Sons Ltd: Chichester, England, **2000**.

6.   Giannelis, E. P. *Adv. Mater.* **1996**, *8*, 29-35.

7.   Carrado, K. A. *Appl. Clay Sci.* **2000**, *17*, 1-23.

8.   Porter, D.; Metcalfe, E.; Thomas, M. J. K. *Fire Mater.* **2000**, *24*, 45-52.

9.   Ray, S. S.; Okamoto, M. *Progress in Polymer Sci.,* **2003**, *28*, 1539-1641.

10.   Huang, X.; Lewis, S.; Brittain, W. J.; Vaia, R. A. *Macromolecules,* **2000,** *33* 2000-2004.

11.   Yoon, P. J.; Hunter, D. L.; Paul, D. R. *Polymer*, **2003,** *44*, 5323-5339.

12.   Yoon, P. J.; Hunter, D. L.; Paul, D. R. *Polymer,* **2003,** *44*, 5341-5354.

13.   Gonzalez, I.; Eguiazabal, J. I.; Nazabal, J., *Polym. Eng. Sci*. **2006**, *46*, 864.

14.   Ray, S. S.; Bousmina, M.; Maazaouz, A., *Polym. Eng. Sci*. **2006**, *46,* 1121.

15.   Wang, S.; Hu, Y.; Wang, Z.; Yong, T.; Chen, Z.; Fan, W. *Polym. Degrad. Stab*. **2003**, *80*, 157.

16.   Zong, R.; Hu, Y.; Wang, S.; Song, L. *Polym. Degrad. Stab*. **2004**, *83*, 423.

17.   Zong, R.; Hu, Y.; Liu, N.; Wang, S.; Liao, G., *Polym. Adv. Technol*. **2005**, *16*, 725.

18.   Wang, S.; Hu, Y.; Song, L.; Liu, J.; Chen, Z.; Fan, W. *J. Appl. Poly. Sci*. **2004**, *91*, 1457.

19.   Wu, D.; Wu, L.; Zhang, M.; Wu, L.; *European Polymer J*., **2007**, *43,* 1635-1644.

20.   Guduri, B. R.; Luyt, A. S.; J. *Nanosci. Nanotechnol*., **2008**, *8*, 1880-1885.

21. Mitsunaga, M.; Ito, Y.; Ray, S. S.; Okamoto, M.; Hironaka, K. *Macromol. Mater. Eng.* **2003,** *288***,** 543.

22. Ito, Y.; Yamashita, M; Okamoto, M.; *Macromol. Mater. Eng.* **2006,** *291,* 773.

23. Hsieh, A. J.; Moy, P.; Beyer, F. L.; Madison, P.; Napadensky, E.; Ren, J.; Krishnamoorti, R.; *Polym. Eng. Sci.* **2004,** *44*, 825-837.

24. Carrion, F-J.; Arribas, A.; Bermudez, M-D.; Guillamon, A. *European Polymer J.* **2008**, 44, 968.

25. Hu, X.; Lesser, A. J. *Polymer*, **2004**, *45,* 2333.

26. Lee, K. M.; Han, C. D. *Polymer*, **2003**, *44*, 4573.

27. Yoo, Y.; Choi, K.-Y.; Lee, J. H. *Macromol. Chem. Phys*. **2004**, *205*, 1863-1868.

28. Xie, W.; Pan W. -P.; Hunter, D.; Vaia, R. *Chem. Mater.,* **2001**,*13*, 2979.

29. Foldi, V. S.; Campbell, T. W.; *J. Polym. Sci*. **1962**, *56,* 1.

30. Xie, W.; Xie, R.C; Pan, W.P.; Hunter, D.; Koene B.; Tan L.S.; Vaia, R. *Chem. Mater.* **2002,** *14,* 4837.

31. Gilman, J. W.; Awad, W. H.; Davis, R. D.; Shields, J. Harris Jr., R. H.; Davis, C.; Morgan, A. B; Sutto, T. E.; Callahan, J.; Trulove, P. C.; DeLongr H. C. *Chem. Mater.* **2002,** *14*, 3776.

32. Awad, W. H; Gilman, J. W.; Nyden, M.; Harris Jr., R. H.; Sutto, T. E.; Callahan, J.; Trulove, P. C.; DeLongr H. C.; Fox, D. M. *Thermochimica Acta* **2004,** *40,* 3.

33. Severe, G.; Hsieh, A. J.; Koene, B. E.; *ANTEC 2000*, **2000**, *2,*1523-1526.

34. Imai, Y.; Nishimura, S.; Abe, E.; Tateyama, H.; Abiko, A.; Yamaguchi, A.; Taguchi, H. *Chem. Mater.*, **2002,***14***,** 477-479.

35. Messersmith, P. B.; Giannelis, E. P.; *Chem. Mater.*, **1993,** *5*, 1064-1066.

36. Weimer, M. W.; Chen, H.; Giannelis EP, Sugah DY, *J. Am. Chem. Soc*., **1999**, 121, 1615-1616.

37. Tyan, H. -L.; Liu, Y. -C.; Wei K. -H. *Chem. Mater.,* **1999**, *11*, 1942-1947.

38. Leu, C. -M.; Wu, Z.-W.; Wei K. -H. *Chem. Mater*., **2002**, *14*, 3016-3021.

39. Zeng, C.; Lee, L. J. *Macromolecules*, **2001**, *34*, 4098-4103.

40. Vaia, R. A.; Teukolsky, R. K.; Giannelis, E.P. *Chem. Mater*. **1994,** *6*, 1017.

41. Schnell, H.; Krimm, H. *Angew. Chem. Int. Ed. Engl*. **1963**, *2*, 373.

42. Dai, S. H.; Lin, C. Y.; Rao, D. V.; Stuber, F. A.; Carleton, P. S.; Ulrich, H. *J. Org. Chem*. **1985**, *50*, 1722-1725.

43. Messersmith, P. B.; Giannelis, E. P. *J. Polym. Sci. Part A: Polym. Chem.* **1995**, *33*, 1047.

44. Lepoittevin, B.; Pantoustier, N.; Devalckenaere, M.; Alexandre, M.; Kubies, D.; Calberg, C.; Jerome,R.; Dubois, P. *Macromolecules* **2002**, *35*, 8385.

45. Kubies, D.; Pantoustier, N.; Dubois, P.; Rulmont,A.; Jerome, R. *Macromolecules* **2002**, *35,* 3318.

46. McCloskey, P. J.; Burnell, T. B.; Smigelski, Jr. P. M. (General Electric Company). U. S. Patent 6,228,973, **2001.**

47. Lemmon, J. P.; McCloskey, P. J.; Siclovan, O. P. (General Electric Company). U. S. Patent 6,323,304, **2001.**

48. Lemmon, J. P.; McCloskey, P. J.; Siclovan, O. P. (General Electric Company). U. S. Patent 6,376,640, **2001.**

49. King, Jr. J. A.; McCloskey, P. J. (General Electric Company). U. S. Patent 6,376,640, **1995.**

50. Barut, G.; Pissis, P.; Pelster, R.; Nimtz, G. *Phys. Rev. Lett*. **1998**, *80*, 3543.

51. Schonhals, A.; Stauga, R.; J. *Chem. Phys.* **1998**,*112,* 5130.

52. Schonhals, A.; Stauga, R.; J. *Non-Cryst. Solids* **1998**, *235-237*,450.

53. Huwe, A.; Kremer, F.; Behrens, P.; Schwieger, W.; *Phys. Rev. Lett.* **1999**, *82*, 2338.

54. Baschnagel, J.; Mischler, C.; Binder, K.; *J. Phys.*, **2000**, *IV 10*, PR7, 9.

55. Huwe A.; *J. Phys.* **2000**, *IV 10*, PR7, 59.

56. Keddie, J. L.; Jones, R. A. L.; Cory, R. A. *Faraday Discuss.* **1994**, *98*, 219

57. Keddie, J. L.; Jones, R. A. L. *I. S. R. Chem. Soc.* **1995**, *35,* 21.

58. Forrest, J. A.; Dalnoki-Veress, K.; Dutcher, J. R. *Phys. Rev.* **1997**, *E 56***,** 5705.

59. Dalnoki-Veress, K.; Forrest, J. A.; Murray, C.; Gigault, C.; Dutcher, J. R. *Phys. Rev. E* **2001**, *63*, 31801.

60. Factor, A.; Degradation of bisphenol A polycarbonate by light and γ-ray irradiation. In "*Handbook of Polycarbonate Science and Technology*" New York **2000,** LeGrand, D. G.; Bendler, J. T., Eds.; Marcel Dekker, Inc.,: New York **2000** p 267.

Chapter 5

Syndiotactic Poly(styrene)/Clay Nanocomposites via Solvent Casting

5.   Syndiotactic Poly(styrene)/clay nanocomposites via solvent casting

5.1   Introduction

Syndiotactic poly(styrene) (sPS) is an engineering semicrystalline thermoplastic material showing high melting point (about 270 ^{o}C), heat and chemical resistance, rapid crystallization and good mechanical properties.[1-4] Dispersion of nanostructured clay in the sPS matrix is expected to enhance further the thermal and mechancal properties similar to many other polymer systems described[5-7].

Preparation of sPS/clay nanocomposites with enhanced thermal stability and mechanical properties relative to the virgin polymer was reported recently.[8,9] However, such reports are very few mainly because of the high melting temperature and, consequently, the high processing temperatures encountered with sPS. Furthermore, the low surface energy of sPS restricts its interactions with polar polymers[10] or with organoclay. When the surface energy of the polymer is too low, the interaction between the polymer and clay surfaces becomes difficult even if the clay surface is made organophilic. Introducing polar groups on the sPS backbone can enhance the surface energy of the polymers. Additionally conventional quaternary ammonium modified clays decompose at the processing temperatures[11-14]. To solve this problem Park *et al*[8,9] utilized stepwise mixing procedure by mixing the organoclay with functionalized amorphous styrenic polymer followed by blending with sPS. Thermally stable modifiers based on phoshonium and imidazolium cations have been reported in the literature[15-17]. Tseng *et al*[18,19] used a modifier for clay based on cetylpyridinium ion and Ghosh *et al*[20] used a modifier based on *N*-benzyl-*N,N*-dimethyl-*N*-(hydrogenated tallow) ammonium ion for the preparation of sPS nanocomposites via solvent casting. These authors claimed the formation of intercalated/exfoliated structures. However, careful analysis of the reported TEM reveals the presence of large quantity of phase separated clay in the polymer matrix.

Surface energy of semicrystalline polymers can be enhanced by introducing ionic groups in the polymer chains. Moore *et al* introduced sodium sulfonate groups on poly(ethylene

terephthalate)[21] and poly(butylene terephthalate)[22] back bone which when melt mixed with organoclay resulted in exfoliated structures. Nanocomposites prepared from ionomers of polypropylene[23], polyethylene[24,25] and variety of other nonpolar thermoplastics polymers[26-28] also reveal improved miscibility characteristics and higher degree of exfoliation of clay in the nanocomposites. However there are no reports on the use of sPS ionomers for the preparation of clay nanocomposites.

Therefore, the objective of the work presented in this chapter is

- to prepare sPS/organoclay nanocomposites by introducing ionic functional groups (metallic sulfonates) in the sPS chains;

- to evaluate the effect of degree of sulfonation (ranging from 0.5 to 3.8 mole%) and the nature of cations (H^+, Na^+, K^+ and Rb^+) on the structure and morphology of nanocomposites;

- to explore the use of a more thermally stable organic modifier, namely, 1-hexadecyl-2,3-dimethylimidazolium cation on the structure of nanocomposites and

- to study the effect of clay dispersion on the crystallization behavior of the nanocomposites.

5.2   Experimental

5.2.1   Materials

Syndiotactic poly(styrene) was kindly supplied by the Dow Chemical Company, USA. The weight average molecular weight was 2,75,000. 1,1,2-Trichloroethane (TCE) and rubidium hydroxide were obtained from Aldrich, USA. Potassium hydroxide, sodium hydroxide and chloroform were purchased from Merck, India. Na^+ Montmorillonite was obtained from Southern Clay Products, USA. All other reagents were of analytical grade and used as received. 1-hexadecyl-2,3-dimethylimidazolium bromide was prepared in the laboratory by quaternizing 1,2-dimethylimidazole with 1-hexadecyl bromide.

5.2.2   Preparation of organoclay

Organic modification of clay was performed using the standard exchange reaction.[29] Na^+ montmorillonite (10.0 g) with CEC 92 meq/100 g, d-spacing 12.3 Å was dispersed in water / methanol (60/40, v/v, 300 mL) under stirring using an overhead stirrer at room temperature for 2 hours. 1-Hexadecyl-2,3-dimethylimidazolium bromide (4.4 g, 11.0 mmol) in water / methanol mixture was poured in to the dispersion of clay dropwise and stirred for 24 hours at 65 °C. The reaction mixture was then cooled, centrifuged and washed several times with distilled water and methanol until all the bromide ions were washed off which was confirmed by testing the washings with $AgNO_3$. Organoclay thus obtained was freeze-dried under vacuum overnight to yield a fine, dry powder. The content of organics in the organoclay was determined using TGA analysis and found to be 25 wt%. The interlayer d-spacing for the organo-modified montmorillonite as measured from WAXD was found to be 18.5 Å.

5.2.3   Preparation of sulfonated sPS ionomers (SsPS)

5.2.3.1 Preparation of acetyl sulfate

Acetic anhydride (0.210 mol) was added to TCE/chloroform (50 mL, 60/40 v/v) mixed solvent. The solution was then cooled to below 10 °C using an ice-cold water bath. Concentrated sulfuric acid (0.70 mol) was slowly added under vigourous stirring. After the mixing was complete, the reaction mixture was diluted with the mixed solvent to 100 mL in a volumetric flask at room temperature.

5.2.3.2 Sulfonation of sPS

Sulfonation of sPS was performed as per the procedure reported elsewhere.[30-32] In a 1 L round bottom flask sPS (6.5 g) and TCE/chloroform (60/40, v/v) mixture (500 mL) were stirred at reflux temperature (ca. 115 °C) until all the sPS was dissolved. The solution was cooled to 70 °C and freshly prepared acetyl sulfate solution was added under vigorous stirring and stirring continued for 3 h. The amount of acetyl sulfate required was determined by the desired degree of sulfonation. Ethanol (10 mL) was added to arrest the reaction and the polymer was precipitated by pouring the solution in to diethyl ether (2 L), and filtered, washed with hot distilled water and dried in vacuo at 70 °C for 24 h. The

polymer was redissolved in TCE and precipitated in excess diethyl ether, filtered and dried in a vacuum oven at 70 °C for 24 h. The degree of sulfonation was determined by nonaqueous titration. The efficiency of sulfonation was around 45 %.

5.2.3.3 Preparation of SsPS ionomers

SsPS ionomers were prepared by fully neutralizing with addition of 20% excess methanolic alkali hydroxides (NaOH, KOH and RbOH). The neutralized polymer solution was precipitated in diethyl ether, washed with hot methanol and dried in vacuum at 70 °C for 24 hrs.

5.2.4   Preparation of SsPS ionomers / clay nanocomposites

SsPS ionomers/organoclay nanocomposites were prepared by solution technique. Pre–weighed SsPS ionomers were dissolved in TCE at 120 °C and then organoclay (8 wt%) was added and the solution maintained at 90 °C for 10 hrs under constant agitation. The solvent was evaporated to obtain a translucent film. The sample was dried under vacuum at room temperature.

5.2.5   Analytical measurements

Thermal properties of the samples were analyzed by TA instruments Q10 differential scanning calorimeter under standard conditions. The samples were heated under flowing nitrogen atmosphere from 0 °C to 300 °C at the rate of 10 °C/min and held for 1 minute at the maximum temperature. At the end of holding period the sample was cooled at the rate of 10 °C/min to record the crystallization exotherm. The sample weight was about 5 mg in all the experiments. TGA, WAXD measurements were performed as described in Chapter 3 and Section 3.2.13. ^{1}H NMR spectra were recorded in a mixture of CF_3COOD and $CDCl_3$ with tetramethylsilane (TMS) as an internal standard at room temperature using a Bruker DSX300 NMR spectrometer. Samples for TEM were sectioned using a Lieca Ultracut UCT microtome with thicknesses of 50-60 nm using a diamond knife at room temperature. The sections were collected from water on a 300 mesh carbon coated copper grids. TEM imaging was done using a JEOL 1200EX electron microscope operating at an accelerating voltage of 80 kV. The density of clay particles was sufficient

to produce contrast between polymer and clay stacks without a need for staining. Images were captured using charged couple detector (CCD) camera for further analysis using Gatan Digital Micrograph analysis software.

5.3   Results and discussion

5.3.1   Preparation of sulfonated sPS and its ionomers

sPS was sulfonated to different levels (0.5, 2.0, 3.2 and 3.8 mol%). The sulfonation procedure was similar to that reported by Li *et al* [31] and which is a modified procedure of Moore *et al* [30] (Scheme 5.1). Alkali salts of sPS (i.e., NaSsPS, KSsPS, and RbSsPS) were prepared by fully neutralizing the sulfonic acid groups with the corresponding hydroxides. The degree of sulfonation was determined by nonaqueous titration.
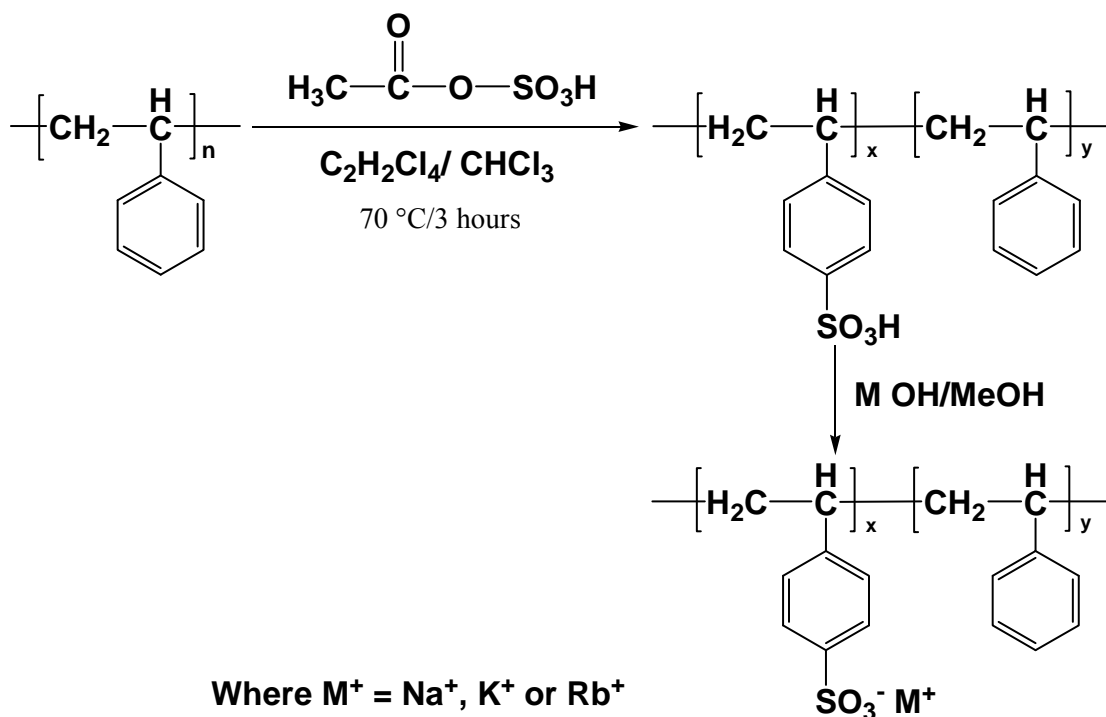
Scheme 5.1: Preparation of sulfonated sPS ionomers.

FTIR spectra of sPS and SsPS samples containing 3.8 mol% sulfonic acid group are shown in Figure 5.1. Absorption bands at 1097 cm^{-1} and 1175 cm^{-1} were observed only for sulfonated samples while the sPS sample did not show these bands. The absorption

band at about 1097 cm^{-1} is attributed to the in-plane skeletal vibrations of the disubstituted benzene rings. The absorption band at 1174 cm^{-1} was assigned to symmetric stretching vibration of the sulfonic acid group in poly(styrene).
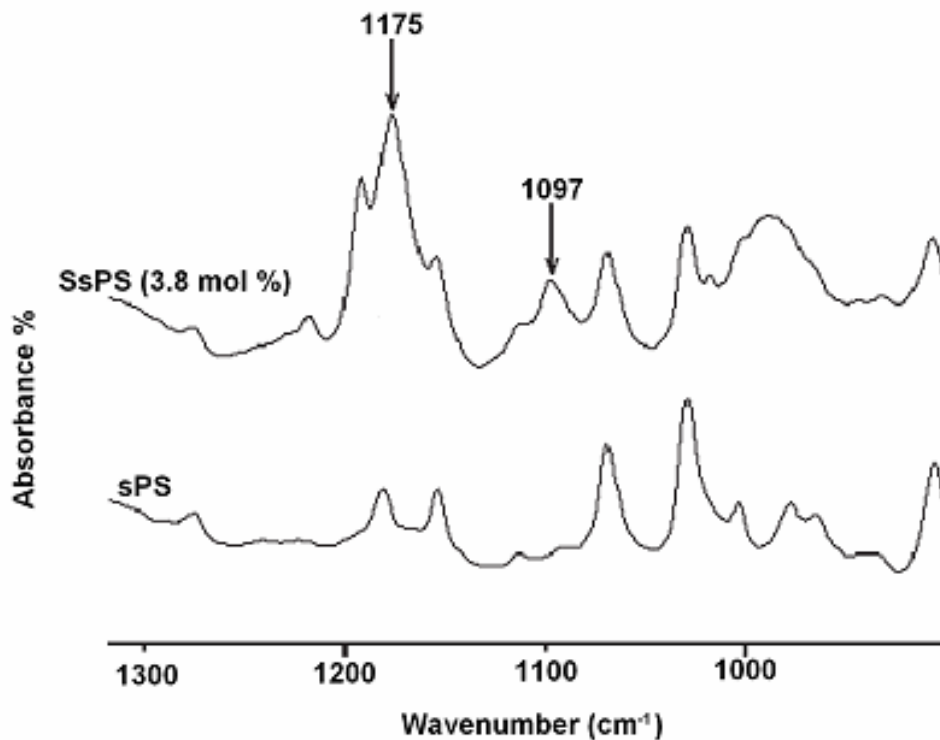
Figure 5.1: FTIR spectra of sPS and SsPS (3.8 mole % sulfonation).

Figure 5.2 compares the ^{1}H-NMR spectra of sulfonated sPS (3.8 mole %) with that of neat sPS. The spectra exhibit peaks at about 1.3 ppm for CH_2 (a) and 1.8 ppm for CH (b) protons. The ortho-protons (c) appear at 6.5 ppm. The meta and para-protons (d) of the unsubstituted aromatic ring appear at about 7.0 ppm. The meta-protons (e) of the substituted aromatic ring appear at about 7.5 ppm for the sulfonated sample but were absent in the sPS spectrum.
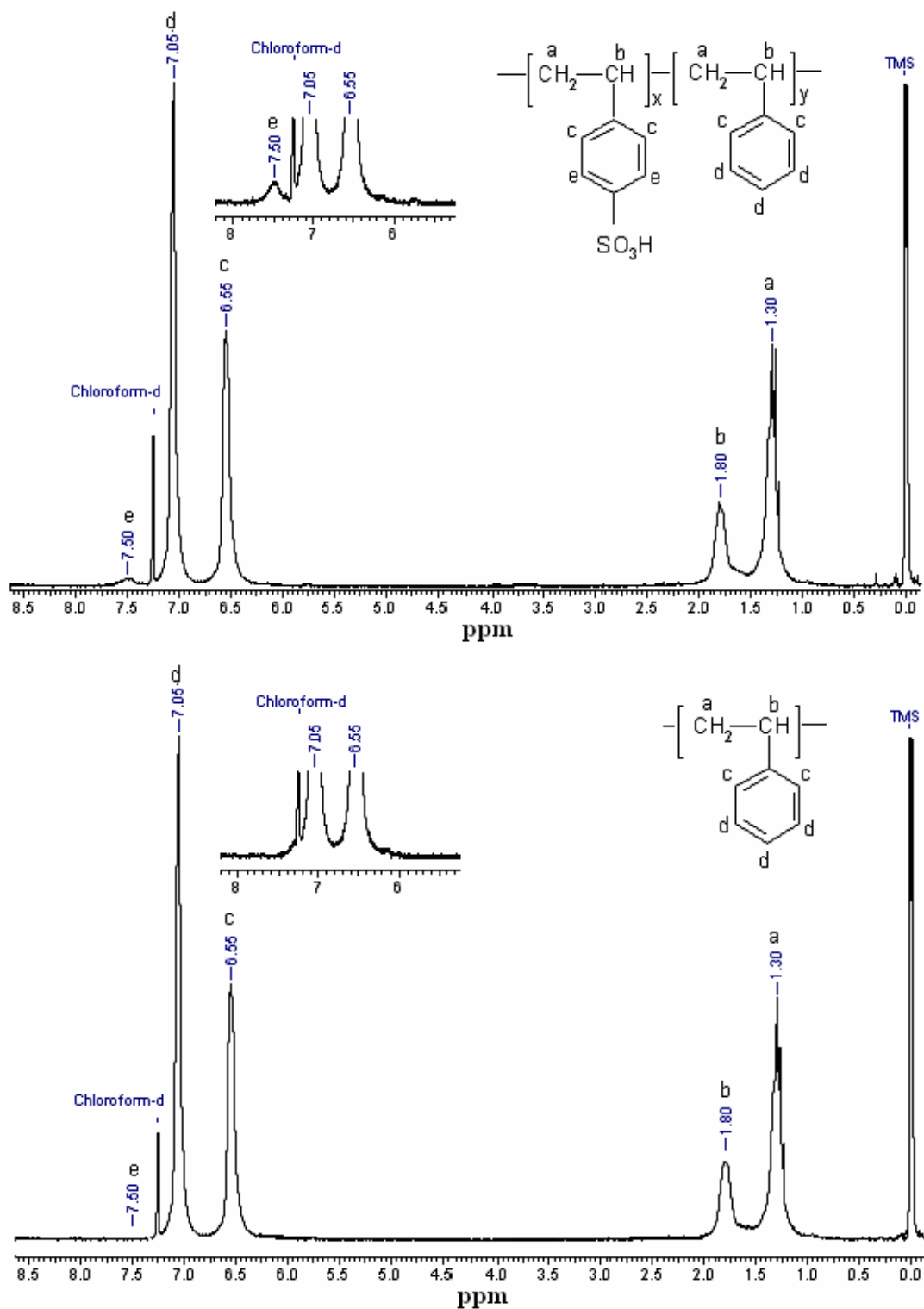
Figure 5.2: ^{1}H NMR spectra of sPS and sulfonated sPS (3.8 mole % sulfonation).

5.3.2   Thermal stability of the organoclay and the nanocomposites

Organoclay used in the present study was obtained by modification of pristine Na^+ montmorillonite with 1–hexadecyl-2,3–dimethylimidazolium cation. Figure 5.3 shows the TGA thermograms of the (a) organoclay, (b) RbSsPS (3.8 mole% sulfonation)/organoclay nanocomposites and (c) RbSsPS (3.8 mole% sulfonation).
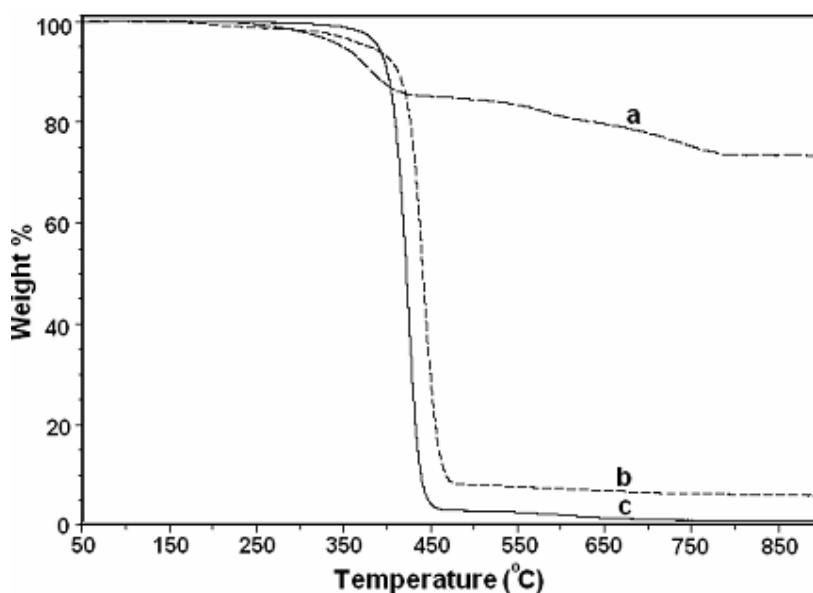
Figure 5.3: TGA thermogram of (a) organoclay (modified with 1-hexadecyl-2,3-dimethylimidazolium cation), (b) RbSsPS (3.8 mole% sulfonation)/organoclay nanocomposite and (c) RbSsPS (3.8 mole% sulfonation).

The organic content in the organoclay was found to be 25 wt%, obtained as the weight loss at 900 °C. This value was in agreement with the calculated value assuming 100% efficiency of cation exchange. The onset of degradation of the modifier in the organoclay (295 °C, 2% weight loss) was higher than the melting temperature of sPS. The nanocomposite also exhibited thermal stability up to 300 °C. Imidazolium based modifier was chosen for the study, because of its thermal stability upto 295 °C which is close to the processing temperature of sPS (290 °C). Conventional organo-ammonium modified clays are not expected to be stable at such temperatures.

5.3.3   Structure of sPS/organoclay nanocomposites

Figure 5.4a shows the WAXD pattern for the unmodified clay, modified clay, sPS and the sPS/organoclay nanocomposite. For the unmodified clay the inter-gallery distance is 12.4 Å which upon modification increases to 19.0 Å. The sPS/clay nanocomposite shows two peaks due to clay at $2\theta = 4.20°$ and at $4.65°$ and the d-spacings are 21.0 Å and 19.0 Å respectively. This indicates that in the nanocomposite, the sPS penetrates into a fraction of the clay galleries and the gallery expands to 21.0 Å.
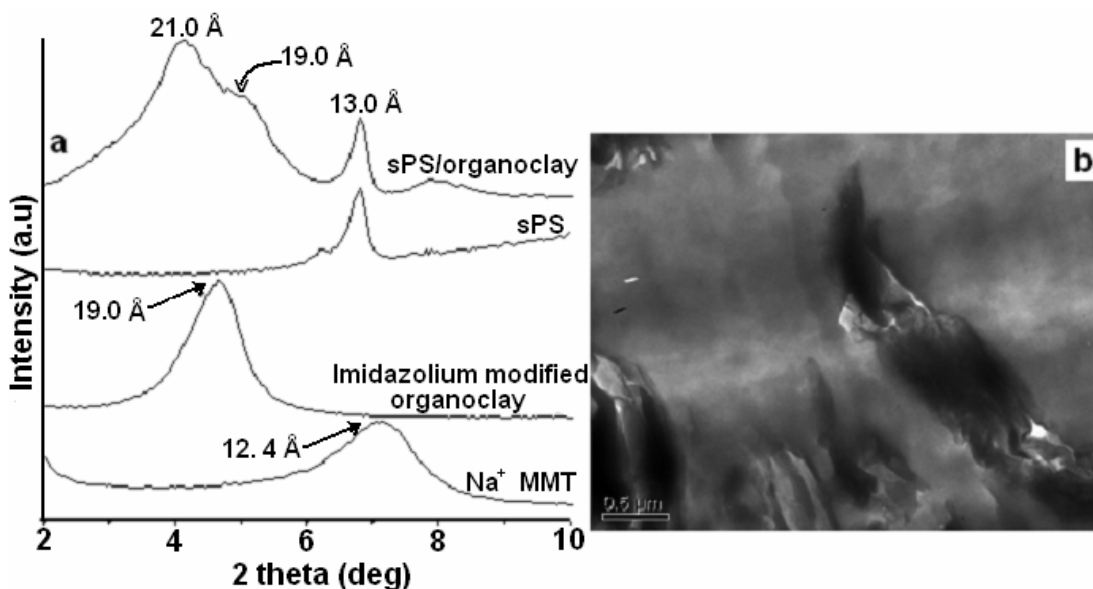
Figure 5.4: a) WAXD of Na$^+$ Montmorillonite (Na$^+$ MMT), imidazolium cation modified organoclay, sPS and sPS/organoclay nanocomposite. b) TEM micrograph of sPS/organoclay nanocomposite.

The presence of a peak at $4.65°$ indicates that some amount of organoclay remains without intercalation. The peak at around $2\theta = 6.8°$ in the sPS and sPS/organoclay nanocomposite is due to the 110 reflection of the α crystalline form. The nanocomposites prepared by the solution technique exhibit δ form but on heating above 200 ^{o}C, all the samples exhibited only the α form. Such a behavior has been previously observed for sPS[33]. Tseng *et al*[18,19] observed a peak at $6.3°$ for the sPS/organoclay nanocomposite prepared via solvent casting and which was attributed to the formation of β crystalline form. However formation of β crystalline form is not possible under the conditions

reported (solvent evaporation by freeze drying and annealing in vacuo at 140 °C). β crystalline form can be obtained only at higher crystallization temperatures (230 °C)[34]. Therefore, the peak appearing at 6.3° can be attributed to the presence of phase separated clay structures in the polymer matrix. Figure 5.4b shows the TEM of sPS/organoclay nanocomposites. The structures appear phase separated implying that the organoclay tactoids remain intact and no substantial intercalation has occurred. This observation can be attributed to the limited interaction of sPS with the organoclay layers in view of the low surface energy of the sPS.

5.3.4   Structure of SsPS ionomer/organoclay nanocomposites

5.3.4.1 Effect of ionomer content

Converting the sPS into sPS ionomers improves the interaction of the sPS with organoclay and Figure 5.5 shows the X-ray diffraction pattern of SsPS ionomer/organoclay nanocomposites with various degrees sulfonation and different cations (H^+, Na^+, K^+ and Rb^+). Table 5.1 shows the gallery height of the clays for various ionomer/organoclay nanocomposites.

Table 5.1: Interlayer distance from WAXD data of SsPS ionomers/clay nanocomposites

Sulfonation level (%)	Clay gallery height (Å)			
	H^+	Na^+	K^+	Rb^+
0.5	18.4	19.0	26.3	27.2
2.0	22.0	29.4	*	*
3.2	26.0	31.5	*	*
3.8	29.0	34.0	*	*

* Exfoliated

WAXD patterns in Figure 5.5a show that as the extent of sulfonation in sPS increases from 0.5 to 3.8 mole %, the interlayer d-spacing of the organoclay increases gradually from 19.0 to 29.0 Å, demonstrating that higher sulfonation levels lead to higher degree of intercalation in the nanocomposites.
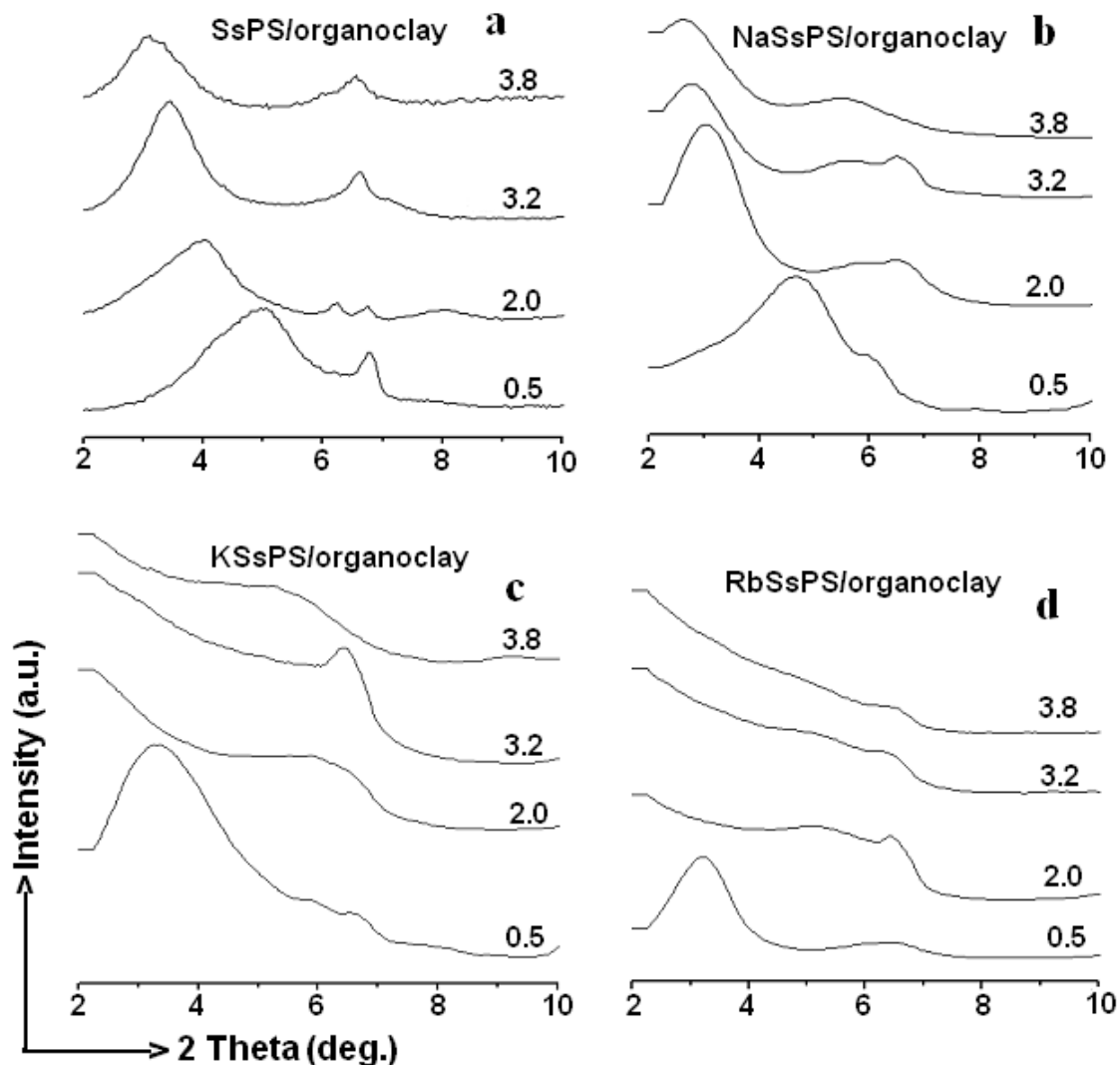
Figure 5.5: WAXD pattern of SsPS ionomer/organoclay nanocomposites with different ionomer content and cation type (a) H^+, (b) Na^+, (c) K^+ and (d) Rb^+.

Similarly Figure 5.5b shows that for the sodium salt of SsPS ionomer (NaSsPS)/organoclay nanocomposites, 0.5 mole% ionomer content shows little intercalation, while the extent of intercalation gradually increased with the increase in the ionomer content to 3.8 mole%. SsPS/organoclay nanocomposites prepared with K^+ and Rb^+ ionomers show intercalation of polymer chains in to the organoclay gallery at lower levels of sulfonation (0.5 mole%), while at higher levels of sulfonation complete

disappearance of the peaks due to clay is observed (Figure 5.5(c), 5.5(d)). This is indicative of complete delamination of clay in the nanocomposites. Thus, irrespective of the cation type, the extent of dispersion of the organoclay in the polymer matrix improves with an increase in the degree of sulfonation.

5.3.4.2 Effect of type of ionomer

It is interesting to note that the extent of interaction of the SsPS ionomer with organoclay depends on the type of cation in the SsPS ionomers. Even for low level of sulfonation i.e. with 0.5 mole% sulfonation of SsPS, with the change of cations from H^+ to Rb^+ in the SsPS ionomer/organoclay nanocomposites, the WAXD patterns show systematic changes in the intergallery distance. The distance increases marginally from 18.4 Å to 19.0 Å when H^+ is changed to Na^+. However, when the cation is changed to K^+ and Rb^+ the intergallery distance increases to 26.3 and 27.2 Å respectively, indicating high level of intercalation. Similarly, when the ionomer content was higher (2 to 3.8 mole%), for H^+ and Na^+ cations in the SsPS ionomer/organoclay nanocomposites, the WAXD pattern shows an increase in the organoclay d-spacing indicating that the polymer chains have penetrated into the organoclay interlayer gallery. On the other hand, for K^+ and Rb^+ cations in the SsPS ionomer/organoclay nanocomposites, the WAXD patterns show disappearance of the peak due to the organoclay, indicating exfoliation of organoclay in the polymer matrix. Here too, it can be noted that the extent of intercalation increased with the change in the cation type from H^+ to Na^+ and leads to exfoliations in the case of K^+ and Rb^+.

The structure of the nanocomposites with various cations was further confirmed by TEM analysis. Typical TEM micrographs of SsPS ionomer/organoclay nanocomposites with an ionomer content of 3.8 mole % with various cations are shown in the Figure 5.6. The parallel lines observed in the micrograph in Figure 5.6a and 5.6b indicate that intercalated nanocomposites were obtained with H^+ and Na^+ SsPS/organoclay nanocomposites and the distance between the parallel lines measured from TEM micrographs are comparable with the d-spacing obtained from WAXD. Figure 5.6c and 5.6d shows the TEM micrograph of SsPS ionomers/organoclay nanocomposite with K^+ and Rb^+ cations

revealing that the clay layers are completely delaminated and exfoliated in the polymer matrix.
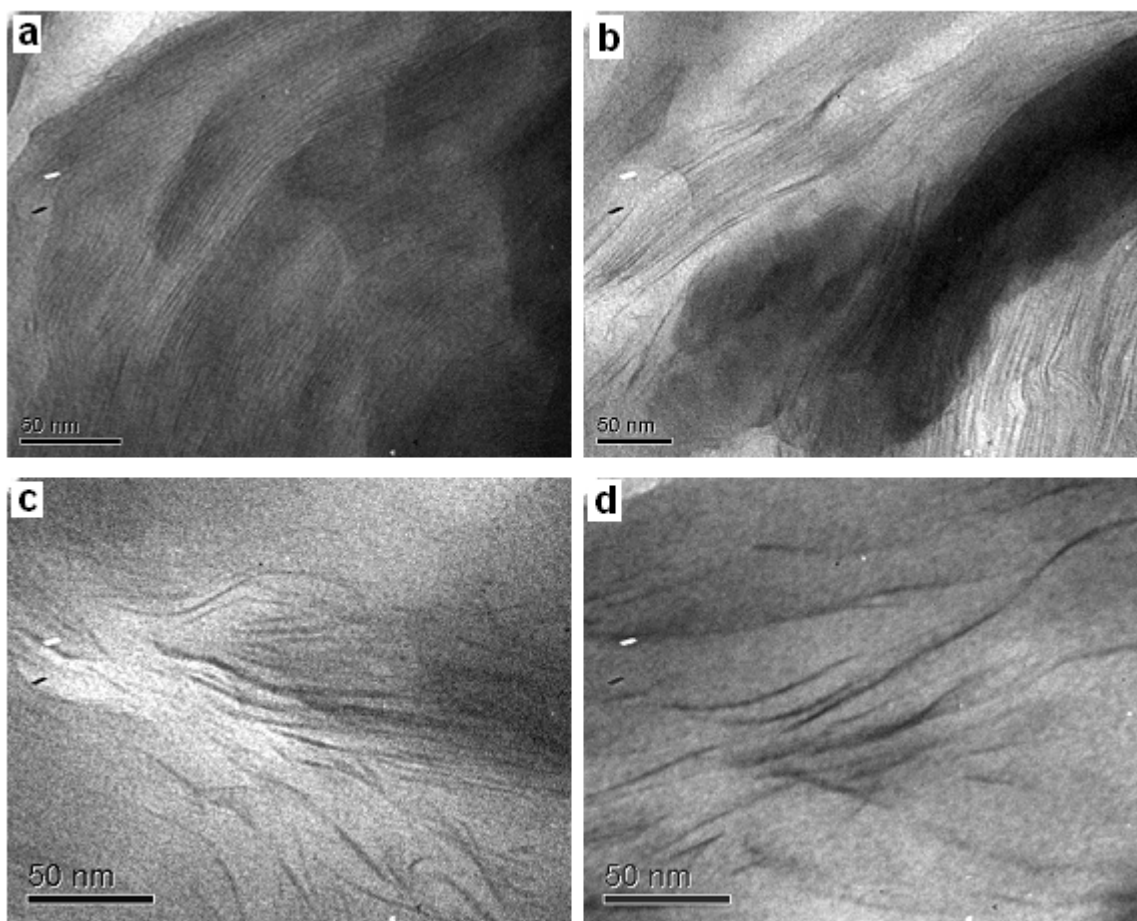
Figure 5.6: TEM micrographs of SsPS ionomers 3.8 mole %/organoclay nanocomposites (a) SsPS, (b) NaSsPS, (c) KSsPS and (d) RbSsPS

The extent of intercalation/exfoliation of the polymer with the organoclay depends on the extent of interaction of the polymer with the organoclay surface. The ionomers, which are anionic polymers, can interact with the clay surface through various mechanisms[35,36]. The anionic groups on the polymer may form strong ionic and/or hydrogen bonding interaction with edge hydroxyl groups of clay layers; or may coordinate with multivalent cations present at the basal surface. As expected, with increase in sulfonation content, the polarity of the polymer was improved and, hence, the interaction between clay and ionomer improved. As the size of the cation is increased from Na^+ to Rb^+, the ionic

potential decreases. This is expected to cause a decrease in the interaction of the ionomer with clay surface. However, the observed results are contrary to this expectation as evidenced by the exfoliated structures obtained with K^+ and Rb^+ ionomers. Theng et al[35,37] observed such anomalous behavior during adsoption of polyanions on clay surface which were saturated by various cations in aqueous medium and attributed this behavior to the stronger ion-dipole interaction with higher polarizable cations (softer cations) which can act as a bridge between negatively charged clay layers and the polyanion.

5.3.5   Structure of SsPS ionomer/Na$^+$ Montmorillonite nanocomposites
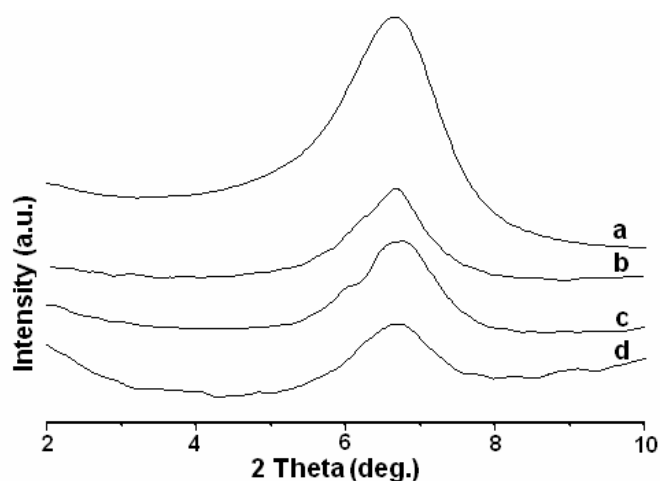
Figure 5.7: WAXD pattern of 3.8 mole% SsPS ionomers/Na$^+$ Montmorillonite nanocomposites with ionomers containing different cations: (a) cloisite Na$^+$ (b) NaSsPS/Na$^+$ Montmorillonite (c) KSsPS/Na$^+$ Montmorillonite (d) RbSsPS/Na$^+$ Montmorillonite

It is also of interest to see whether the increased surface energy of the polymer is sufficient to intercalate/exfoliate the unmodified clay. To that end nanocomposites of various ionomers with a maximum ionomer content of 3.8 mole% were prepared with unmodified clay. WAXD pattern is shown in Figure 5.7. In all the samples the clay peak shows no significant shift, indicating the absence of intercalation of the polymer in to the gallery. These results indicate that merely increasing the surface energy of the polymer is

not sufficient and organic modification of clay is also necessary. Such an observation has been made earlier.[34]

5.3.6   Crystallization behavior of SsPS ionomer/organoclay nanocomposites

The interaction of the polymer with clay layers has profound influence on the melt crystallization of the sPS ionomer. Crystallization peak temperature (T_{CC}) on cooling from melt was taken as a measure of crystallization rate.[38] High T_{CC} during cooling in non-isothermal experiments indicates higher crystallization rate. Table 5.2 gives the T_{CC} on cooling from the melt for various samples. T_{CC} decreases with increasing degree of sulfonation indicating inhibition in crystallization. Crystallization was further inhibited when the H^+ ion was replaced by different cations like Na^+, K^+ and Rb^+. At higher degree of sulfonation, ca 3.8 mole%, most of the samples do not crystallize upon cooling from the melt. The reduction in the crystallization rate can be attributed to the ionic aggregation arising due to the coulombic interactions between the ion pairs which impedes chain mobility[39]. The coulombic interactions between the ion pair become weaker with increasing size of the alkali ions.[40,41] Hence RbSsPS samples exhibit better crystallization rate compared NaSsPS, while the KSsPS show an intermediate behavior.

Table 5.2: Crystallization temperature on cooling from the melt for various samples

Sulfonation level (%)	Crystallization temperature (^{o}C)							
	Without clay				Nanocomposite			
	H^+	Na^+	K^+	Rb^+	H^+	Na^+	K^+	Rb^+
0.5	234	233	233	232	234	236	236	236
2.0	225	199	189	193	228	209	218	223
3.2	222	183	183	194	222	205	215	222
3.8	212	*	*	*	212	163	184	198

* Do not crystallize on cooling from the melt

Clay layers apparently do not influence the crystallization of the sPS samples (Table 5.2). On the other hand, clay layers enhance the crystallization rate of the samples having

alkali metal ions. A sample with a degree of sulfonation of 3.8 % and neutralized with K^+ does not crystallize upon cooling and remains amorphous. However, in the nanocomposite the same material crystallizes at 184 °C indicating that the crystallization rate has improved. In the case of samples with lower degree of sulfonation, the crystallization peaks appear at higher temperatures than the samples without clay, indicating faster crystallization rates in the case of nanocomposites. These results suggest that clay layers modified with 1-hexadecyl-2,3-dimethylimidazolium cation reduce the tendency of ions to aggregate causing the crystallization rate to increase. Exfoliated nanocomposites show a better crystallization rate than the intercalated ones because of the uniformly dispersed clay layers in the polymer matrix in the former (Table 5.2).

5.4.   Conclusions

Exfoliated sPS ionomer/organoclay nanocomposites were successfully prepared via solvent casting. The interaction of sPS with organoclay was evaluated by introducing polar ionic functional groups such as metallic sulfonates with varying degree of sulfonation (ranging from 0.5 to 3.8 mole%) and differing nature of cations (H^+, Na^+, K^+ and Rb^+). Higher degree of sulfonation leads to better interaction with the polar silicate surface of the organoclay resulting in better intercalation/exfoliation. Increase in the size and polarizability of the cation ($Na^+<K^+<Rb^+$) result in higher degree of intercalation/exfoliation even at low degrees of sulfonation. Nanocomposites prepared using more thermally stable 1-hexadecyl-2,3-dimethylimidazolium cation modified clay are amenable to being processed at temperatures upto 300 °C without any appreciable degradation. The dispersed silicate clay layers partially restores the reduced crystallization rates of sPS ionomers by disrupting the ionic aggregation. Thus, it can be purported that fully exfoliated nanocomposites of poly(styrene) can be prepared by functionalizing the polymer chains with ionic groups.

References:

1. LeBaron, P. C.; Wang, Z.; Pinnavaia, T. J. *Appl. Clay Sci.* **1999**, *15*, 11.

2. Alexander, M.; Dubois, P. *Mater. Sci. Eng.* **2000**, *28*, 1.

3. Ray, S. S.; Okamoto, M. *Prog. Polym. Sci.* **2003**, *28*, 1539.

4. Woo, E. M.; Sun, Y. S.; Lee, M. L., *Polymer* **1999**, *40,* 4425.

5. Vittoria, V.; Filho A. R; De Candia, F. *J. Macromol. Sci. – Phys.* **1990**, *B29,* 411.

6. Cimmino, S.; Pace, E. Di; Martuscelli, E; Silvestre, C. *Polymer* **1991**, *32,* 1080.

7. De Rosa, C.; Rapacciuolo, M; Guerra, G.; Petraccone, V. *Polymer* **1992**, *33,*1423.

8. Molner, A.; Eisenberg, A. *Polym Eng and Sci*. **1992**, *32*, 1665.

9. Xie, W.; Gao, Z.; Pan, W.-P.; Vaia, R.; Hunter, D.; Singh, A. *Polym. Mater. Sci. Eng.* **2000**, *83*, 284.

10. Xie, W.; Goa, Z.; Lui, K.; Pan, W.P.; Vaia, R.; Hunter, D.; Singh, A. *Thermochim. Acta*. **2001**, *367*, 339.

11. Jones, M.; *Jr. Organic Chemistry*, 2nd ed.; W. W. Norton & Co. Inc.: New York, **2000**; p 258.

12. Wright, A. C.; Granquist, W. T.; Kennedy, J. V. *J. Catal.* **1972**, *25*, 65.

13. Park, C. I.; Park, O. O.; Lim, J. G.; Kim, H. J. *Polymer* **2001**, *42*, 7465.

14. Park, C. I.; Choi, W. M.; Kim, M. H.; Park, O. O. *J Polym. Sci. Polym. Phys.* **2004**, *42*, 1685.

15. Zhu, J.; Morgan, A. B.; Lamelas, F. J.; Walkie, C. A. *Chem. Mater*. **2001**, *13*, 3774.

16. Gilman, J. W.; Awad, W. H.; Davis, R. D.; Shields, J.; Harris Jr. R. H.; Davis, C.; Morgan A. B.; Sutto, T. E.; Callahan, J.; Trulove, P. C.; DeLong, H. C.; *Chem. Mater.* **2002**, *14*, 3776

17. Xie, W.; Xie, R.; Pan, W.; Hunter, D.; Koene, B.; Tan, L.; Vaia, R. *Chem. Mater*. **2002**,*14*, 4837.

18. Tseng, C. R.; Wu, J. Y.; Lee, H. Y.; Chang, F. C. *Polymer* **2001**, *42*, 10063**.**

19. Tseng C. R.; Lee, H. Y.; Chang, F. C. *J. Polym. Sci.*, *Part* B: Polym. Phys. **2001**, *39*, 2097.

20. Ghosh, A. R.; Woo, E. M. *Polymer* **2004**, *45*, 4749.

21. Barber, G. D.; Calhoun, B. H.; Moore, R. B. *Polymer* **2005**, *46*, 6706.

22.   Chisholm, B. J.; Moore, R. B.; Barber, G.; Khouri, F.; Hempstead, A.; Larsen, M.; Olson, E.; Kelley, J.; Balch, G.; and Caraher, J. *Macromolecules* **2002**, *35*, 5508.

23.   Wang, Z. M.; Nakajima, H.; Manias, E.; Chung, T. C. *Macromolecules* **2003**, *36*, 8919.

24.   Shah, R. K.; Paul, D. R. *Macromolecules* **2006**, *39*, 3327.

25.   Lee, J. A.; Kontopoulou, M.; Parent, J. S. *Polymer* **2005**, *46*, 5040.

26.   Start, P. R.; Mauritz, K. A. *J. Polym. Sci. Polym. Phys.* **2003**, *41*, 1563.

27.   Kovarova, L.; Kalendova, A.; Malac, J.; Vaculik, J.; Malac, Z.; Simonic, J. *Annu. Tech. Conf. Soc. Plast. Eng.* **2002**, *60ᵗʰ*, 2291.

28.   Barber, G. D.; Carter, C. M.; Moore, R. B. *Annu. Tech. Conf. Soc. Plast. Eng.* **2000**, *58ᵗʰ*, 3763.

29.   Vaia, R. A.; Teukolsky, R. K.; Giannelis, E. P. *Chem. Mater.* **1994**, *6*, 1017.

30.   Govindaiah, P.; Avadhani, C. V.; Ramesh, C. *Macromol. Symp.* **2006**, 241, 88.

31.   Orler, E. B.; Yontz, D. J.; Moore., R.B. *Macromolecules* **1993**, *26*, 5157.

32.   Li, H. M.; Liu, J. C.; Zhu, F. M.; Lin, S. A. *Polym. Int.* **2001**, *50*, 421.

33.   Gowd, E. B.; Nair, S. S.; Ramesh, C., *Macromolecules* **2002**, *35*, 8509.

34.   Woo, E. M.; Sun, Y.S.; Yang, C. P. *Prog. Polym. Sci.* **2001,** *26*, 945.

35.   Theng, B. K. G., *Formation and Properties of Clay-Polymer Complexes*, Elsevier Scientific Publishing Co. Amsterdam, The Netherlands, **1979**. pp-290

36.   Greenland, D. J. *Soil Science* **1971**, *111*, 34.

37.   Theng, B. K. G.; Scharpenseel, H. W. *Proceedings of International Clay Conference*, Mexico City, **1975,** pp. 643-653.

38.   Pilati, F.; Toselli, M.; Messori, M.; Manzoni, C.; Turturro, A.; Gattiglia, E. G. *Polymer* **1997**, *38,* 4469.

39.   Orler, E. B.; Moore, R. B. *Macromolecules* **1994**, *27*, 4774.

40.   Lu, X.; Steckle, W. P.; Weiss, R. A. *Macromolecules* **1993**, *26*, 5876.

41.   Hird, B.; Eisenberg, A. *Macromolecules* **1992**, *25*, 6466.

Chapter 6

Poly(propylene)/Clay Nanocomposites via Melt Mixing

6.   Polypropylene/clay nanocomposites via melt mixing

6.1   Introduction

Polypropylene (PP) is a fast growing thermoplastic and dominates the industrial applications due to its attractive combination of properties such as low density, high thermal stability, resistance to corrosion etc. and low cost. Yet, there is a continuing interest to further improve its physical properties especially for applications in the automotive industry[1]. It has been shown that reinforcement with dispersed clay in the polymer matrix enhances the mechanical properties without significantly affecting the density of the polymer[2]. Therefore, efforts have been made to efficiently disperse the clay in the PP matrix. However such dispersions are hard to prepare in view of the non polar nature of PP. Generally practiced organo-modification of clay does not sufficiently lower the surface energy of the clay for favorable interaction with PP chains. Unmodified PP lack the intrinsic thermodynamic affinity with currently available organoclays to form well dispersed nanocomposites[3]. It is necessary to improve the surface energy of PP chains. In one such successful effort it was found that PP could be intercalated into clay gallery by using a PP oligomer containing hydroxyl groups[4]. Later, studies on preparation and properties of PP/organoclay nanocomposites were extensively performed using functionalized PP as compatibilizeres[5-12]. Majority of the studies uses maleated PP as compatibilzer although the resultant nanocomposites show intercalated or mixture of intercalated/exfoliated structures. Liu *et al* and Zhang *et al* prepared PP/organoclay nanocomposites by using a new kind of co-intercalation organophilic clay which could tether to the PP backbone by a process of grafting[13,14]. Tudor *et al* and Sun and coworkers have reported the preparation of PP/organoclay nanocomposites by *in-situ* intercalation polymerization [15,16].

Many researchers introduced ionic groups in nonpolar polymers, thereby, improving the surface energy of the polymer to obtain exfoliated polymer/clay nanocomposites[17-25]. Wang *et al*[19] demonstrated that exfoliated PP/clay nanocomposites can be prepared using ammonium terminated PP. They prepared the nanocomposites by static melt intercalation technique which involves annealing the clay with ammonium terminated PP at 190 °C for

2 hours. The ammonium terminated PP used for the above study was prepared by a metallocene polymerization/chain transfer reaction. Inspired by the idea that ammonium terminated PP could be a better compatibilizer for PP/clay nanocomposites, Lili and Paul[26], prepared ammonium functionalized PP from maleated PP by reactive melt extrusion and evaluated them as compatibilizers for PP clay nanocomposites. However, ammonium functionalized PP prepared as above failed to enhance the dispersion of clay in the PP matrix as compared to maleated PP.

The effect of molecular weight of the matrix PP on the dispersion of clay has been studied[27-30]. It has been reported that low molecular weight PP (with high melt flow index) could disperse clay better than high molecular weight PP (lower MFI). In the absence of any favorable polar forces, delamination is driven by diffusion of polymer chains, the lower molecular weight polymer possessing higher diffusivity. This is contrary to the results obtained for the PA-6/clay nanocomposites, wherein, high molecular weight PA-6 showed better dispersion of clay and better property enhancements compared to low molecular weight PA-6. This was attributed to the assisted delamination process induced by larger shear stress provided by higher melt viscosity of polymer[31]. This difference in behavior between PP and PA-6 might be due to the polar nature of PA-6 causing favorable interaction with clay surface through hydrogen bonding.

More recently, when our work was in progress, Nguyen *et al*[32] reported the preparation of polypropylene clay nanocomposites using polypropylene ionomers to improve the dispersion of clay in PP. PP ionomers were prepared by neutralizing maleated PP dissolved in xylene/butanol with KOH to obtain ionomers with 50% and 75% neuatralization. Masterbatch of PP ionomers with Cloisite 20A (6 wt%) were prepared using co-rotating twin screw extruder at 220 °C. PP/clay nanocomposites were prepared by melt mixing PP (M_n = 8,500 and M_w = 85,900) with the masterbatches in a twin screw extruder. The study revealed that the use of PP ionomer led to improved dispersion of the organoclay in the nanocomposites, best result being obtained with an ionomer of 75%

neutralization. PP/clay nanocomposites showed large increase in Young's modulus (from 371 mPa for PP to 806 mPa for PP/clay nanocomposite)

In view of above, it was decided to explore the efficiency of PP ionomers to compatibilize higher molecular weight PP in clay. In general, preparation of well exfoliated PP/clay nanocomposites with low MFI (high molecular weight) PP has been found to be difficult with a conventional compatibilizer such as PPMA. It was also of interest to examine the effect of well dispersed clay in PP matrix on the crystallization behavior of PP.

6.2   Experimental

6.2.1   Materials

Polypropylene homopolymer, REPOL H034SG (MFI = 3.2 g/10 min, measured at 230 °C with a load of 2.16 Kg; Mn = 80,000 and Mw = 570,000) was obtained from Reliance Industries Ltd. Mumbai. Maleated polypropylene (PPMA), FUSABOND M613-05 (MFI = 120 g/10 min, measured at 190 °C at a load of 2.16 Kg) containing 0.65 wt% maleic anhydride group was obtained from DuPont, USA. The organoclay, Cloisite 20A, containing dimethyl dihydrogenated tallow quaternary ammonium, $M_2(HT)_2$ as the organic modifier and Na^+ montmorillonite (Na^+ MMT) were provided by Southern Clay Products Inc., USA. CEC of the clay was 95 meq per 100 grams of dry clay. The percentage of weight loss on ignition (LOI) was 38 wt%. 1,2 - dichlorobenzene was obtained from LOBA Chemie Pvt Ltd., Mumbai, India and used as such.

6.2.2   Preparation of potassium succinate grafted polypropylene ionomer

Maleated polypropylene (PPMA) was dissolved in 1, 2- dichlorobenzene at 120 °C. One drop of phenolphthalein indicator was added into the solution. 0.2 N base (KOH) prepared in methanol was added drop by drop to the solution until the color of the solution changes to light pink. This was then heated for another half an hour to ensure the persistence of pink color and to ensure complete neutralization (~100%). The ionomer was precipitated in excess methanol and washed with hot methanol, filtered and dried at 65 °C to get an ionomer (K^+ form) in white color.

6.2.3   Preparation of nanocomposites

Nanocomposites were prepared by a melt mixing using a twin-screw extruder, DSM Micro 5 having a net barrel capacity of 5 cc with a screw speed of 100 rpm, barrel temperature of 190 °C and a residence time of 10 min. Various compositions prepared and their sample codes are listed in the Table 6.1.

Table 6.1: Various compositions by weight for the nanocomposites and their sample codes

S. No	Sample code	PP	PPMA	KPPSA	CLOISITE 20A
1	PP	100	-	-	-
2	PPMA15	80	15	-	-
3	PPMA20	75	20	-	-
5	PPMA25	70	25	-	-
5	KPPSA15	80	-	15	-
6	KPPSA20	75	-	20	-
7	KPPSA25	70	-	25	-
8	PPMA95C-D	-	95	-	5
9	KPPSA95C-D	-	-	95	5
10	PPMA15C-D	80	15	-	5
11	PPMA20C-D	75	20	-	5
12	PPMA25C-D	70	25	-	5
13	PPMA15C-M	80	15	-	5
14	PPMA20C-M	75	20	-	5
15	PPMA25C-M	70	25	-	5
16	KPPSA15C-D	80	-	15	5
17	KPPSA20C-D	75	-	20	5
18	KPPSA25C-D	70	-	25	5
19	KPPSA15C-M	80	-	15	5
21	KPPSA20C-M	75	-	20	5
22	KPPSA25C-M	70	-	25	5

Nanocomposites were prepared with different concentrations of compatibilizer keeping the organoclay concentration at 5 wt%. For comparison matrix polymer compositions

without clay were also prepared. Nanocomposites were prepared by two different methods. In the first method, PP, compatibilizer and Cloisite 20A were melt mixed directly in a single step. In the second method, compatibilizer was mixed with the organoclay to form a masterbatch which was then mixed with PP in the second step. Various compositions prepared were coded in such a way that the number in the code after the compatibilizer name indicates the percentage of the respective compatibilizer, C for 5 wt% organoclay, and the method of preparation indicated in the sample code by D for direct mixing and M for masterbatch route. For e.g., the sample name KPPSA25C-M represents the nanocomposites with composition of 25 wt% KPPSA, 70 wt% PP and 5 wt% Cloisite 20A which are prepared by masterbatch route. Pristine matrix polymer blends are named without C, D or M. For e.g., PPMA25 represents the composition of 25 parts by weight of PPMA and 70 parts by weight of PP.

6.2.4   DSM micro extruder and injection molder

Various compositions of nanocomposites and the matrix polymer were prepared using the DSM microcompounder. A brief overview of the Micro Extruder & Injection Molder is described using Figure 6.1. The system comprises of four primary components: the micro-extruder (1); the feeder (2); mini-injection molder (3) and the transfer cylinder (4). Materials to be processed are weighed and placed in the feeder hopper (5). The plunger (8) transfers the materials through the tube (7) into the extruder barrel (6). Inside the barrel, the two co-rotating screws mix, melt and force the material downward. When the material reaches the bottom of the barrel the melt is directed into the recirculation canal (11) where it travels upward and enters the main barrel cavity. This process can be repeated as long as the operator desires, typical mixing and recirculation times are 2-10 minutes. At the conclusion of the mixing and recirculation process, T gate (10) is closed and the melt stream is directed out through the die orifice (9) where it immediately enters the heated transfer cylinder (13). As the melt fills the cylinder, the plunger (14) is pushed out of the cylinder. Gate (10) is closed, and the cylinder is placed in the molder cradle (16) of the injection-molding unit. A pneumatic ram (15) pushes the plunger forward, which forces the melt into the mold (17) where it is cooled and solidified.

Figure 6.1: DSM Micro Extruder & Injection Molder

Opened split molds for stiffness beams and disks are shown in (18). This system allows the processing of small amounts of polymers and composites into specimens suitable for physical and mechanical property testing.

6.2.5   Analytical methods

Spherulitic morphology of the samples prepared was studied by OLYMPUS polarized optical microscope (POM) attached with a Mettler Toledo FP82HT hot stage under

crossed polarizer. Thin slices were cut from the injection molded samples, inserted between two microscope cover glasses, melted at 200 °C. The slides were then transferred to the hot stage and melted at 200 °C then slides were held for one minute to ensure uniform melting. In subsequence, samples were cooled to room temperature at a constant rate of 10 °C/min. After cooling to room temperature, the photomicrographs of the sample were recorded using Olympus digital camera. The flexural modulus of nanocomposites was tested with Instron 4204 model universal testing machine. The test specimen bars were obtained using DSM micro-injection molding machine with a barrel temperature set at 210 °C and mold temperature at 35 °C. The injection molding pressure and holding pressure were both set at 30 bar. The dimensions of the flexural specimens were $3.20 \times 12.15 \times 71.0$ mm. The test was conducted with a load of 1 KN at a cross head speed of 2.8 mm/min and the span length was kept at 40 mm. WAXD, TEM, TGA and DSC measurements were performed as mentioned in the Chapters 3. Samples for TEM were prepared by sectioning the samples into ultrathin slices (<100 nm) at –60 °C using the microtome Leica Ultracut UCT equipped with a diamond knife and mounted on 200 mesh copper grids.

6.3   Results and discussion

6.3.1   Preparation of potassium succinate grafted polypropylene

Potassium succinate grafted polypropylene (KPPSA) was prepared by simultaneous hydrolysis and neutralization of a solution of PPMA in 1,2-dichlorobenzene at 120 °C with methanolic KOH in a single step (Scheme 6.1). Formation of the potassium salt of succinate-grafted polypropylene from PPMA was confirmed by FT-IR analysis. The FTIR spectrum of PPMA and KPPSA are shown in Figure 6.2. The strong absorbance peaks at 1784 cm^{-1} and 1711 cm^{-1} observed for carbonyl group of the anhydride in PPMA disappeared and new peaks appeared at 1700 cm^{-1} and 1570 cm^{-1} corresponding to the symmetric and asymmetric stretching of the carbonyl of carboxylate anion showing the formation of the potassium succinate functionality.
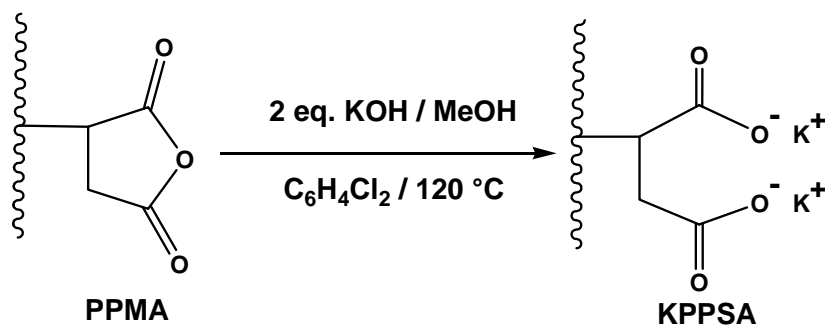
Scheme 6.1: Preparation of potassium succinate-g-polypropylene.
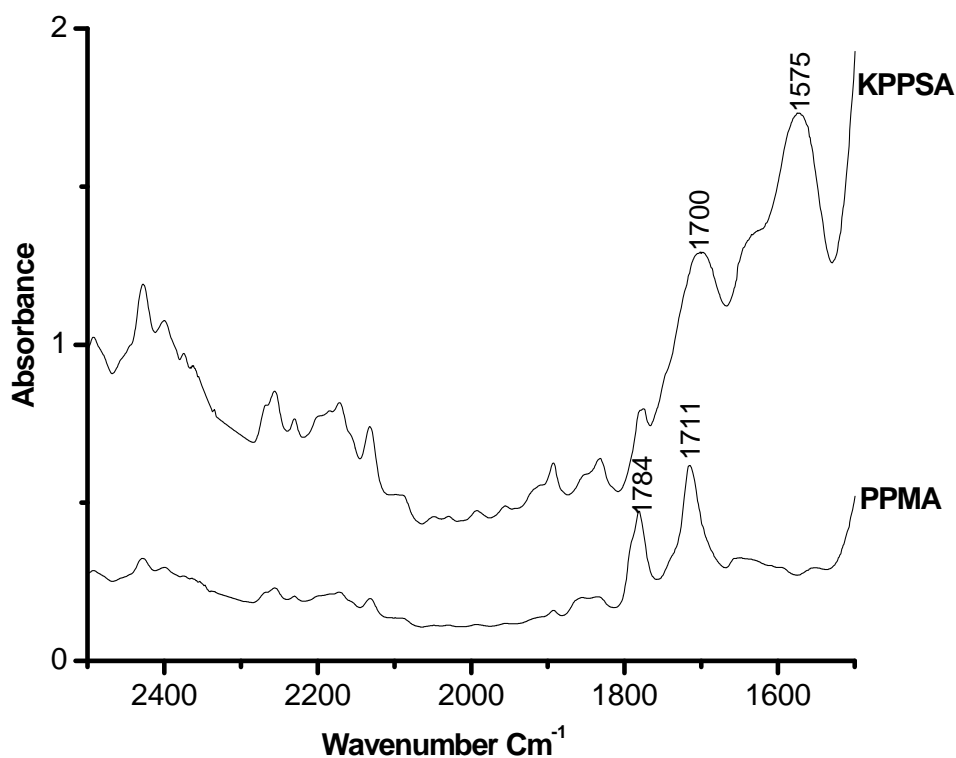
Figure 6.2: FTIR spectrum of PPMA and KPPSA

6.3.2   Structure of the nanocomposites

Cloisite 20A was chosen as the organoclay to be dispersed in the PP matrix. Binary composites containing 95 wt% KPPSA and 5 wt% Cloisite 20A were prepared by melt mixing using DSM micro compounder at 190 °C for 10 minutes with a screw speed of 100 rpm. The product was characterized by WAXD. The WAXD pattern (Figure 6.3a) of KPPSA/Cloisite 20A showed no peak for the organoclay indicating that the organoclay was completely delaminated and exfoliated in the KPPSA matrix. PPMA/Cloisite 20A

blend, however, showed a broad low intensity peak with a d-spacing of 38 Å indicating the presence of intercalated tactoids. The above result confirms the beneficial effect of KPPSA and the contribution of polar ionic functional groups. KPPSA is superior to PPMA as a compatibilizer. The latter is commonly used for the preparation of PP nanocomposites.
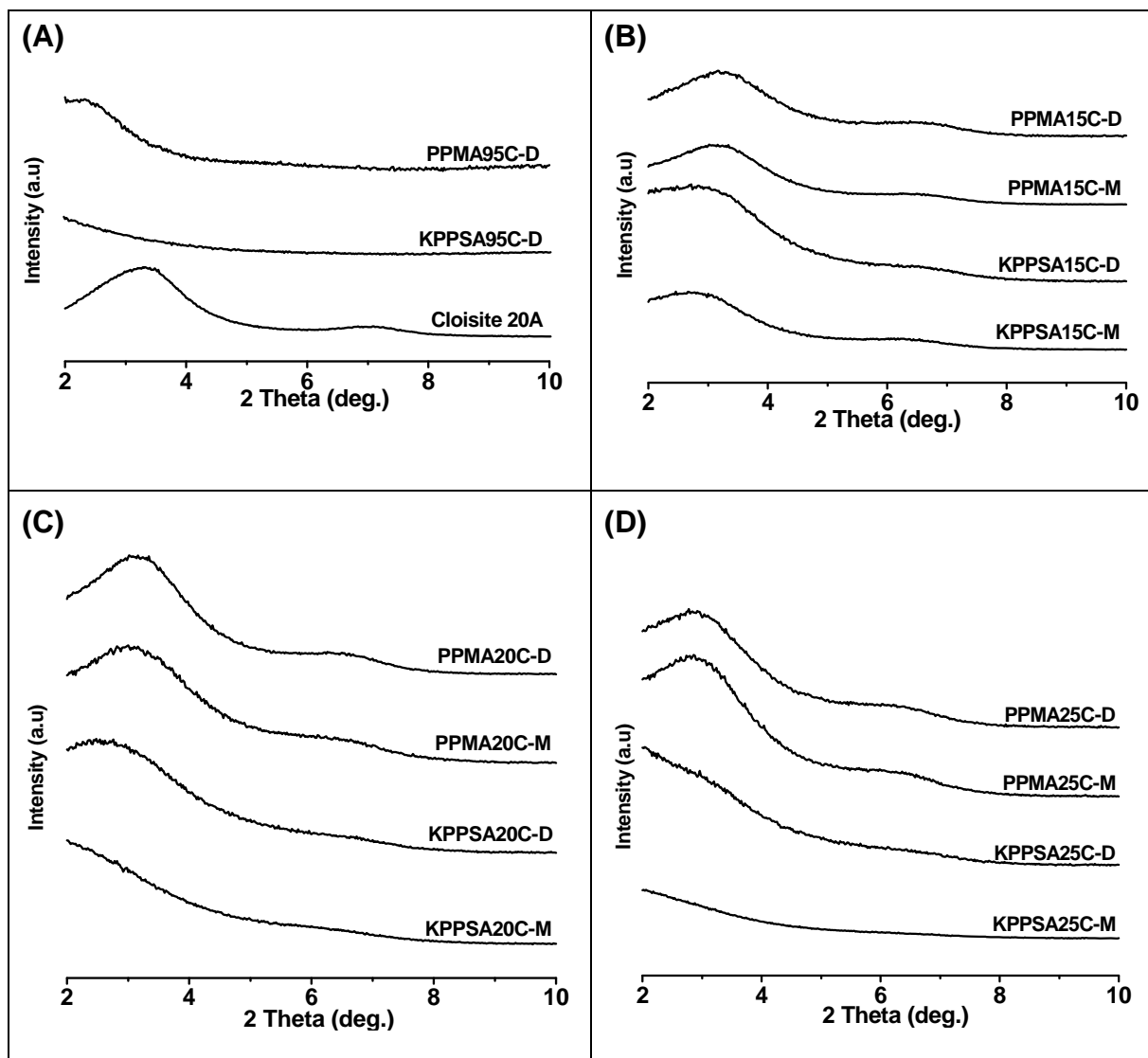
Figure 6.3: WAXD of   nanocomposites of (A) binary composites (B) 15 wt% of the compatibilizers (C) 20 wt% of the compatibilizers (D) 25 wt % of the compatibilizers; In the sample code, the number indicates wt% of the compatablizer, C indicates 5 wt% cloisite 20A, D for the samples prepared by direct mixing route and M for the samples prepared by masterbatch route.

It is pertinent to note the results of Paul *et al*[26] who prepared binary composites using an ionomer based on ammonium functionalized PP which showed complete disappearance of peak for the clay in WAXD and complete exfoliation of clay layers as observed by TEM. However, PP nanocomposites prepared using this ammonium functionalized PP as compatibilizer did not improve the dispersion of clay as compared to PPMA[26]. The ratio of compatibilizer to organoclay used was 1:1. Nguyen *et al*[32] showed that use of higher concentration of potassium succinate grafted polypropylene as compatibilizer improved the dispersion of clay in PP. Therefore, in the present study, nanocomposites were prepared by varying the concentration of the compatibilizer keeping the concentration of the organoclay, Cloisite 20A constant. Two different mixing routes were used to prepare the nanocomposites. In the first route, the organoclay, compatibilizer and the matrix polymer were mixed together directly in a single step. In the second route, the organoclay was mixed with the compatibilizer in the first step to form a masterbatch followed by mixing it with the matrix PP in the second step. The properties of the nanocomposites obtained were compared with the nanocomposites prepared using PPMA as compatibilizer under identical conditions. The WAXD patterns for the nanocomposites prepared are shown in Figure 6.3(B)-(D) and their d-spacings corresponding to the clay interlayer distance are tabulated (Table 6.2).

Table 6.2: d - spacing of nanocomposites and organoclay

Sample	d-spacing (Å)			
	15 wt% of the compatibilizer	20 wt% of the compatibilizer	25 wt% of the compatibilizer	95 wt% of the compatibilizer
PPMA-C-D	27.7	28.8	31.0	38.0
PPMA-C-M	28.8	29.4	31.3	-
KPPSA-C-D	30.4	33.7	a	a
KPPSA-C-M	32.2	a	a	-
C20A	24.2 Å			

a – no peaks observed for the clay (exfoliated)

It can be observed that irrespective of the method of preparation with increasing PPMA concentration the peak position shifts towards lower angles indicating improvement in

the extent of intercalation of the polymer into the organoclay gallery. These results are similar to earlier reports[13, 32,33-35].
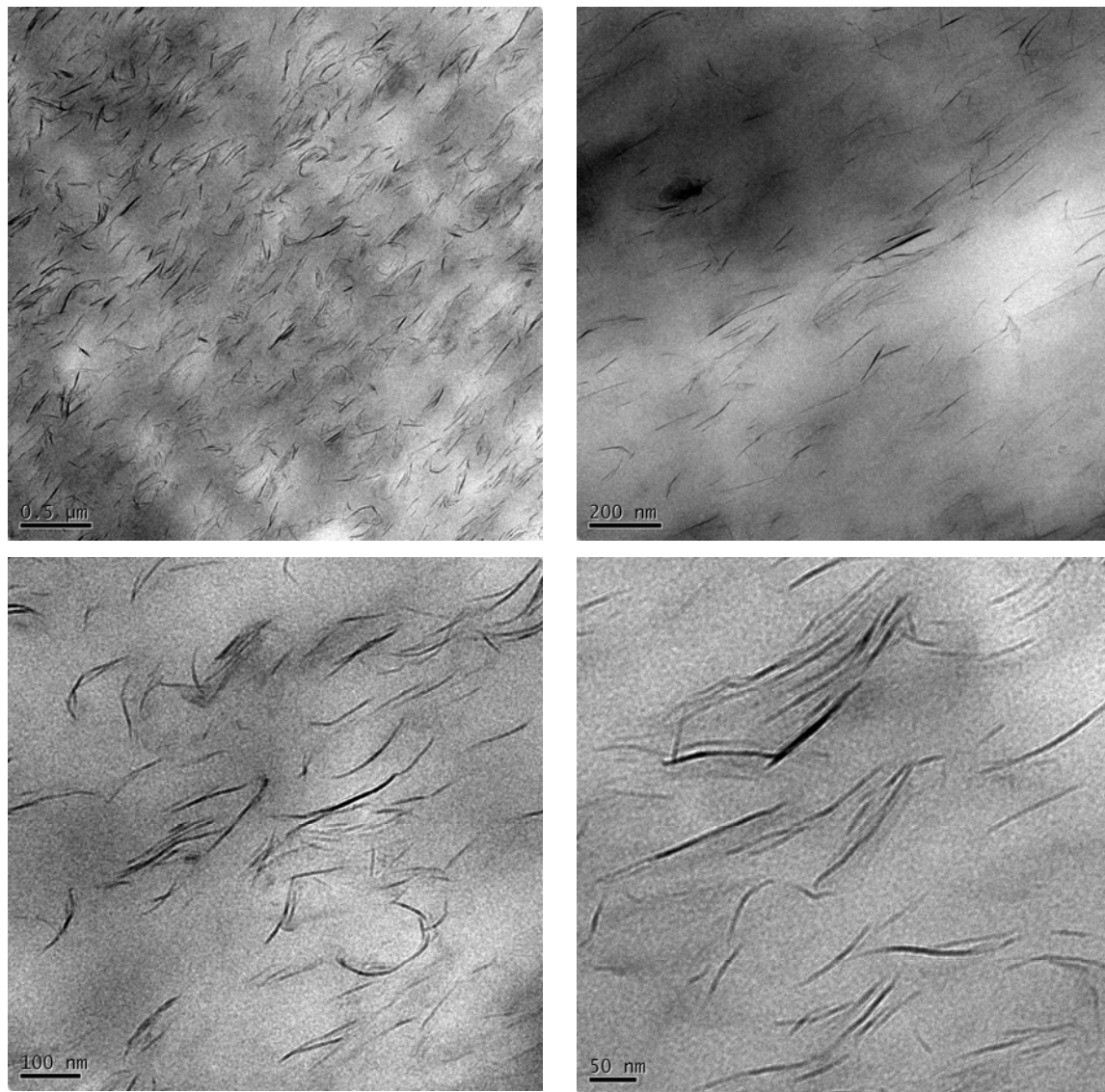
Figure 6.4: TEM micrographs of KPPSA25C-M at different resolutions

When the nanocomposites were prepared by direct mixing route and KPPSA was used as compatibilizer, the WAXD patterns show higher d-spacing for the clay as compared to that observed with the nanocomposites prepared using PPMA. When the nanocomposites were prepared by masterbatch route with KPPSA as compatibilizer, larger d-spacing was observed at 15 wt% concentration of the compatibilizer and at 20 wt% and 25 wt% concentrations complete exfoliation of the clay layers was observed. In case of

nanocomposites prepared using PPMA only intercalated structures were observed. Typical TEM micrographs of the nanocomposites prepared by masterbatch route with 25 wt% KPPSA and with 25 wt% PPMA are shown in Figure 6.4 and Figure 6.5. It is evident from the TEM pictures that the nanocomposites prepared with 25 wt% KPPSA as compatibilizer show exfoliated structures where the clay layers are completely delaminated and dispersed homogeneously in the polymer matrix while the nanocomposites prepared with 25 wt% PPMA as compatibilizer showed clusters of clay layers suggesting intercalated structures.
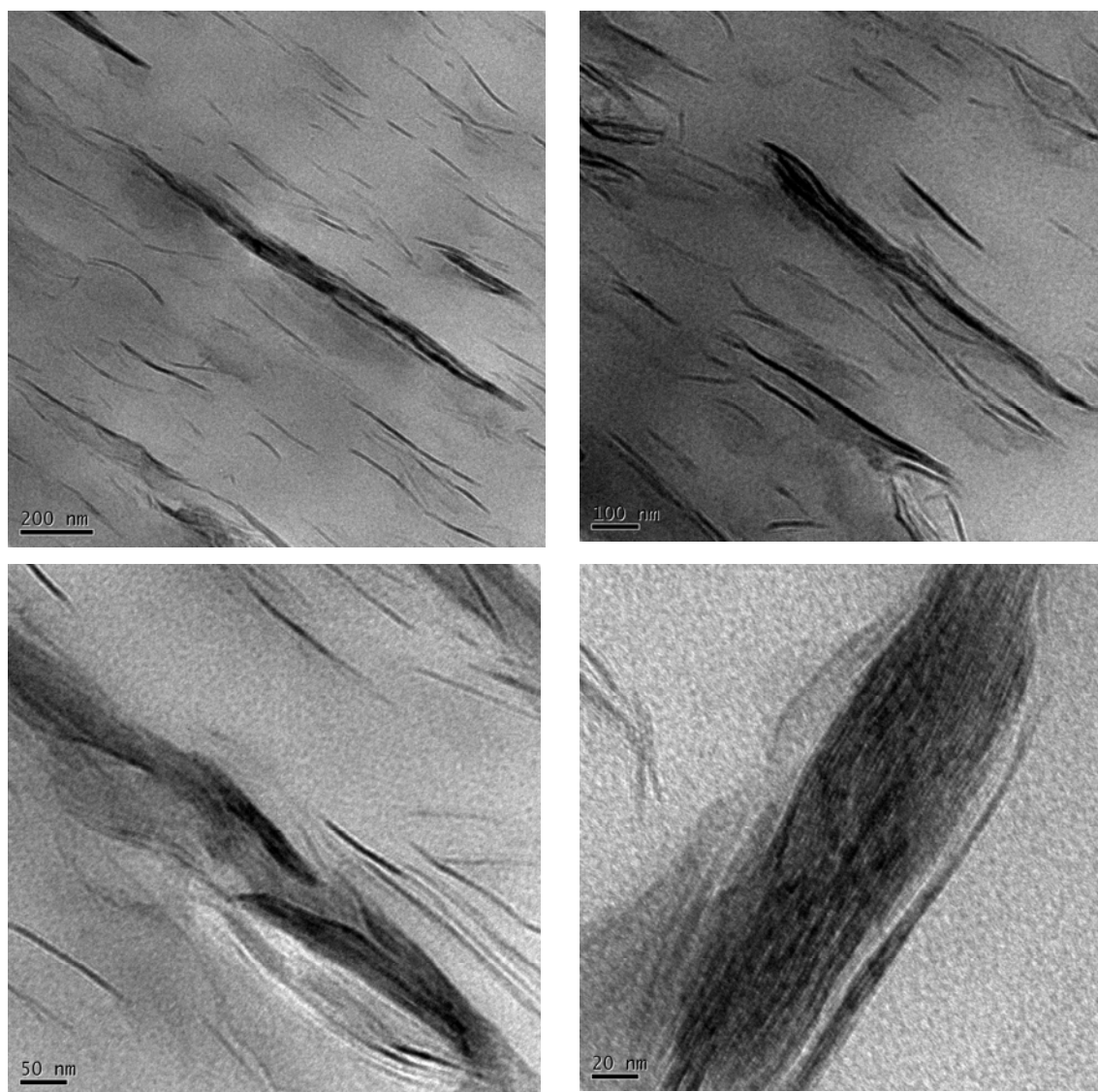
Figure 6.5: TEM micrographs of PPMA25C-M at different resolutions

Although Nguyen *et al*[32] stated that increasing concentration of ionomer resulted in better dispersion of clay, their study was limited to a concentration of 14 wt% ionomer. They observed partial exfoliation with some intercalated structures. However, in the present study the concentration range was extended to 20 wt% and 25 wt% of KPPSA which resulted in completely exfoliated nanocomposites. Generally, dispersion of clay in a high molecular weight PP is found to be difficult using a compatabilizer such as PPMA[27-30]. Some examples of the PP/clay nanocomposites reported in the literature which demonstrates the effect of molecular weight (MFI) on the dispersion of clay is provided in Table 6.3.

Table 6.3: PP/clay nanocomposites: Effect of molecular weight (MFI) on clay dispersion

PP grade	MFI (g/10 min)	PPMA (wt%)	Organoclay (5 wt%)	d-spacing (Å)	Ref.
LG HI-Prene M710PP copolymer	0.6	20	DK2	25.7	27
HopeleneY130PP homopolymer	4.0	10	DK1N	27.8	
SK H380F homopolymer	25	5	DK4	36.5	
HostalenPPYD50G homopolymer	0.5	7	Cloisite 20A	26.0	28
Moplen HP 501 L homopolymer	6	7	Cloisite 20A	25.2	
Moplen HP 400 R homopolymer	25	7	Cloisite 20A	25.2	
Moplen HP 500J homopolymer	3.2	7	Cloisite 15A	31.0	29,
Moplen HP 500N homopolymer	12	7	Cloisite 15A	31.0	30

Gianelli *et al*[28] prepared a series of PP/clay nanocomposites with 5 wt% Cloisite 20A in presence of PPMA (7 wt%) using a series of PP homopolymers with varying MFI (0.5 g/10 min, 6.0 g/10 min and 25 g/10 min) using a corotating intermeshing twin screw extruder. They found that the dispersion of clay was better in higher MFI as compared to lower MFI PP. A PP sample of MFI = 25 g/10 min was found to have better dispersion of clay compared to a PP of MFI = 0.6 g/10 min. However, in both these samples, presence of intercalated tactoids was observed. Dong and Bhattacharya[27] employed a statistical analysis method to evaluate the significant factors that affect the morphology of PP nanocomposites using a series of PP with varying MFI (0.6, 4.0 and 25 g/10 min).

Nanocomposites were prepared via melt blending in a co-rotating intermesh twin screw extruder. Molecular weight of PP was found to be significant factor in determining the extent of dispersion of clay. TEM showed that PP/clay nanocomposites prepared with a PP homopolymer of MFI = 4.0 g/10 min and PPMA as compatibilizer had poor dispersion. Causin *et al*[29,30] prepared PP/clay nanocomposites based on Cloisite 15A using two PP grades of MFI = 3.2 g/10 min and 12 g/10 min in presence of 7 wt % compatibilizer using a reciprocating single screw extruder. Dispersions were found to be better in case of PP with MFI = 12 g/10 min as compared to PP with MFI = 3.2 g/10 min was evidenced by TEM analysis. WAXD of nanocomposites obtained with both the PP samples showed a diffraction peak for clay which clearly indicated the presence of intercalated structures. However, an ionomer such as KPPSA was found to be an efficient compatiblizer even for a high molecular weight PP resulting in the formation of exfoliated nanocomposites.

6.3.3   Thermogravimetric analysis

All the nanocomposites were prepared with 5 wt% organoclay in the feed. Typical thermograms and their derivatives are shown in the Figure 6.6(a) and 6.6(b).
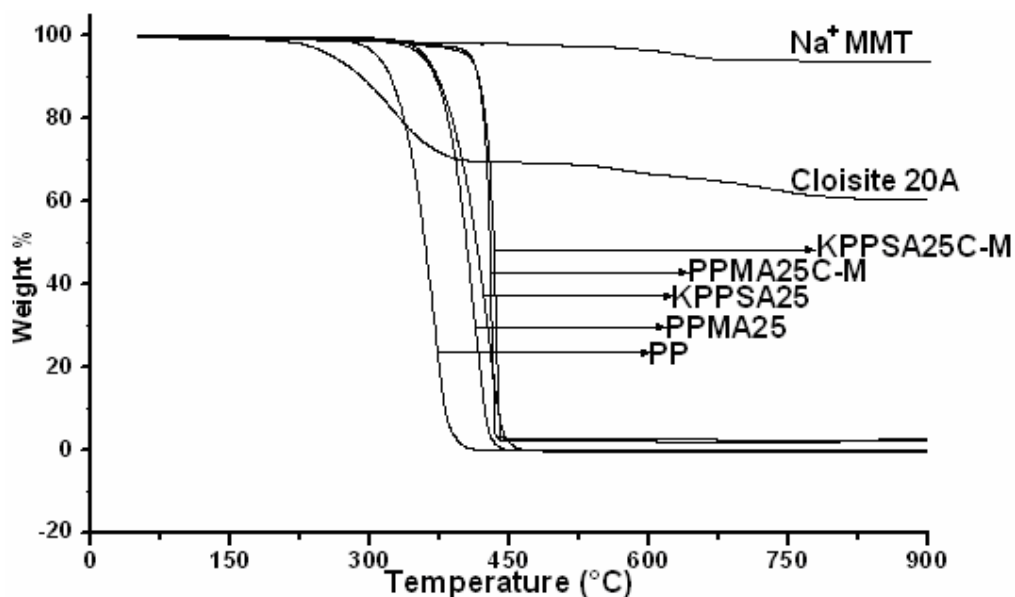
Figure 6.6(a): Thermograms of Na^{+}MMT, Cloisite 20A, PP, PPMA25, KPPSA25, PPMA25C-M and KPPSA25C-M
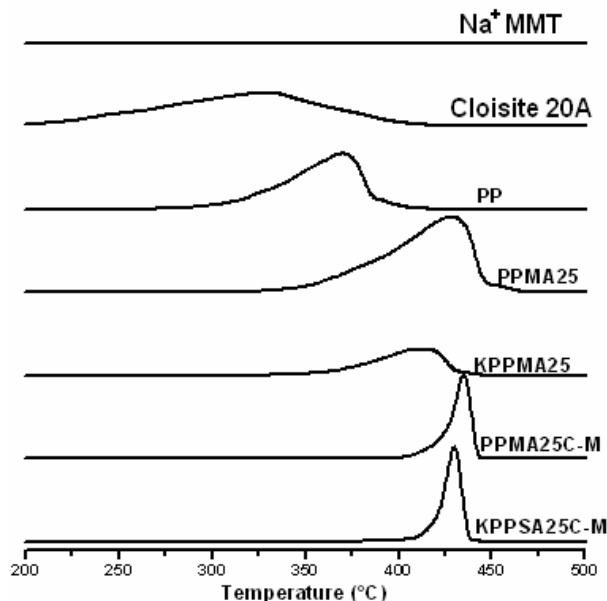
Figure 6.6(b): Derivative thermograms of Na$^+$MMT, Cloisite 20A, PP, PPMA25, KPPSA25, PPMA25C-M and KPPSA25C-M

MMT silicate content in the nanocomposites was obtained from thermogravimetric analysis as reported by Paul *et al* using the formula [31,36].

$$\text{Percentage MMT content} \quad = \quad \frac{\text{MMT}_{char}\text{ of nanocomposite}}{0.935}$$

In the above equation 0.935 is the char fraction of the pristine montmorillonite.

Percentage of organoclay present in the nanocomposites was calculated using a simplified formula shown below:

$$\text{Percentage organoclay content} \quad = \quad \frac{\%\text{ MMT}_{char}\text{ of nanocomposite}}{\%\text{ MMT}_{char}\text{ of organoclay}} \times 100$$

The onset of degradation and the maximum degradation temperature of the selected samples are listed in Table 6.4. TGA results of the nanocomposites showed MMT $_{char}$ contents of 3.0 wt% at 900 °C which corresponds to 3.2 wt% MMT content.

Table 6.4: Thermal degradation behavior of PP matrix and its nanocomposites

Sample	Onset degradation Temperature °C (T_{onset})	Maximum degradation temperature °C (T_{max})
PP	282	370
PPMA25	329	428
KPPSA25	349	412
PPMA25C-M	398	435
KPPSA25C-M	398	429

The onset of degradation (T_{onset}) for all the nanocomposites show an increase of about 110 °C as compared to pristine PP. To ascertain the enhancement of T_{onset} due to nanocomposite formation, T_{onset} of the matrix polymer containing the compatibilizers were also measured. Results indicate an enhancement of about 50 °C when PPMA was used as compatibilizer, whereas, with KPPSA an enhancement by more than 65 °C was observed. However, all nanocomposites show a uniform increase in T_{onset} irrespective of the compatibilizer used. The presence of clay increases the temperature of thermal decomposition of the polymer in all the samples. Such a behavior of uniform increase in T_{onset} irrespective of the extent of dispersion is similar to the observation made by earlier workers and was attributed to a labyrinth effect slowing down the diffusion rate of degradation products from the bulk of the polymer to the gas phase[28]. The fact that similar behavior is found for all nanocomposites independent of their morphology indicates the effectiveness of the ablative reassembling process in providing the high temperature protective ceramised surface[28].

6.3.4   Crystallization behavior

Crystallization behavior of various nanocomposites obtained was studied using DSC and polarized optical microscopy. Typical DSC thermogram curves obtained for various

nanocomposites, the matrix polymers and the pristine polypropylene during cooling from the melt at 10 °C/min are shown in Figure 6.7. The crystallization peak temperature (Tcc) on cooling from the melt is taken as a measure of crystallization rate[37]. High Tcc during cooling from the melt in non-isothermal experiments indicates higher crystallization rate. Table 6.5 shows the Tcc for the various samples.
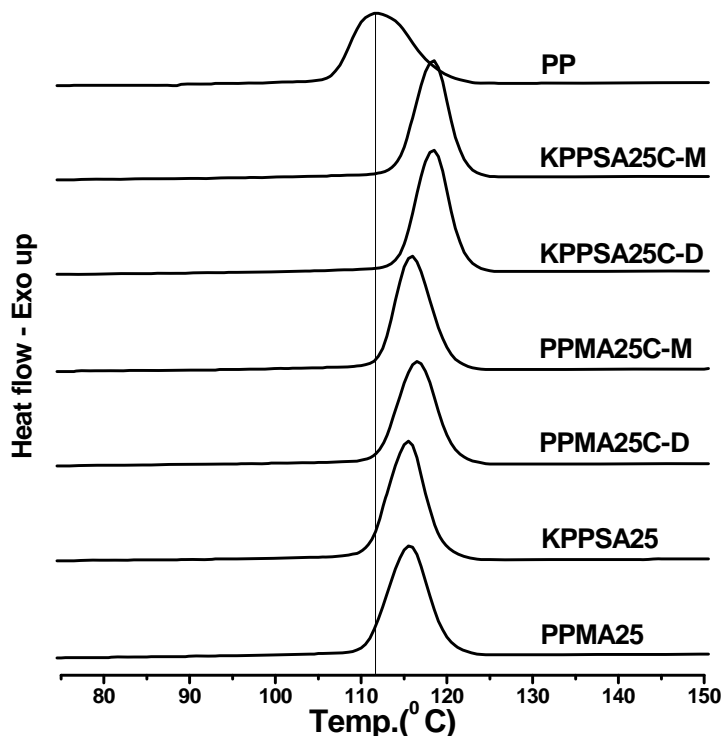
Figure 6.7: DSC thermogram of the matrix polymers and the nanocomposites upon cooling from the melt at 10°C/min.

Table 6.5: Crystallization temperature of various samples upon cooling from melt

Sample	Tcc (° C)
PP	112
PPMA25	114
KPPSA25	114
PPMA25C-D	116
PPMA25C-M	116
KPPSA25C-D	118
KPPSA25C-M	118

Nanocomposites are known to exhibit higher crystallization rates than the corresponding homopolymers due to nucleation by clay layers[12,38-41]. Exfoliated clay nanocomposites obtained with 25 wt% KPPSA showed marginally enhanced crystallization rates as compared to intercalated nanocomposites obtained with 25 wt% PPMA. In the exfoliated nanocomposite the clay layers are completely delaminated providing a larger surface for nucleation resulting in higher Tcc.
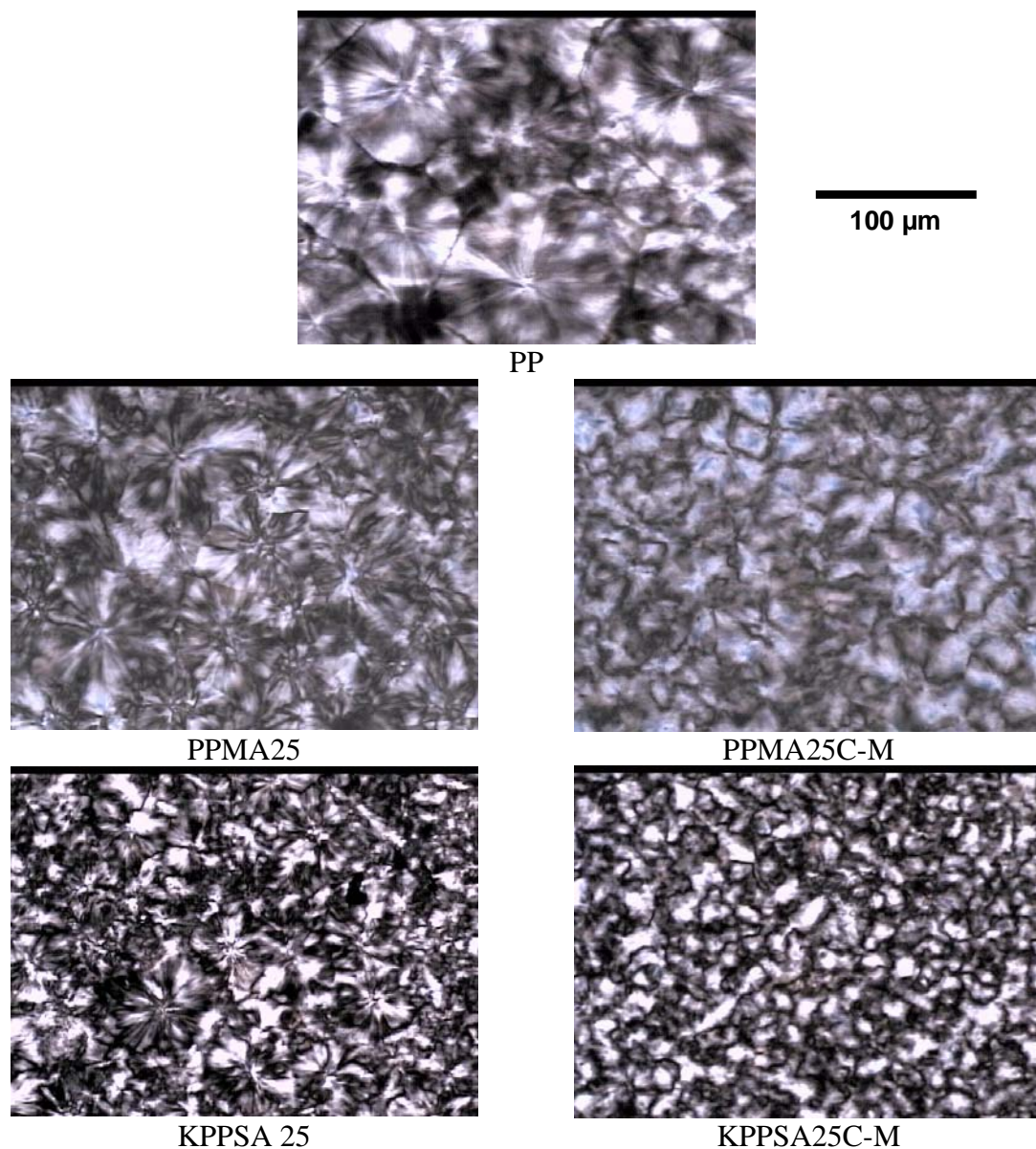
Figure 6.8: Polarized optical microscope pictures of PP, PP/compatibilizer and PP/compatibilizer/organoclay nanocomposites obtained at room temperature after cooling from melts at 10°C/min.

Spherullite structures of the nanocomposites and the matrix polymers at room temperature were determined from polarized optical microscopy (POM) after cooling the samples from the melt at 10 °C/min. The POM pictures (Figure 6.8) showed smaller spherullite size (less than 35 µm) for the exfoliated nanocomposites obtained with 25 wt% KPPSA as compared to 40 to 60 µm for the intercalated nanocomposites obtained with 25 wt% PPMA. PP homopolymer shows a spherullite size of 75 to 100 µm. Decrease in spherullite size with increase of clay content in PP nanocomposites have been observed earlier and can be attributed to the increased number of nucleation centers[12,40-43]. At equivalent clay concentration, smaller spherullitic sizes were observed for exfoliated nanocomposite compared to that observed with intercalated nanocomposites. This is due to larger number of nucleation sites provided by exfoliated clay layers.

6.3.5 Mechanical properties

Flexural moduli of the nanocomposites measured are shown in Table 6.6. For purposes of comparison binary blends of compatibilizer/PP were also prepared and their properties measured.

Table 6.6: Flexural modulus of the PP homopolymer and the nanocomposites

Sample	Flexural modulus (MPa) with compatibilzer composition of		
	15 wt%	20 wt%	25 wt%
PPMA	747	710	691
KPPSA	738	759	788
PPMA-C-D	842	840	834
KPPSA-C-D	840	852	863
PPMA-C-M	862	852	845
KPPSA-C-M	888	895	937
PP	804		

It is observed that there is a small decrease in the flexural moduli when PPMA is mixed with PP which further decreases with increase in the concentration of PPMA. This behavior can be attributed to the blending of low molecular weight PPMA in PP. When the compatibilizer KPPSA is melt mixed with PP homopolymer the flexural modulus is initially lowered; however the flexural modulus increases marginally with increase in concentration of KPPSA from 15 wt% to 25 wt%. This behavior can be attributed to the aggregation phenomenon of the ionomers at higher concentration. Flexural moduli of all the nanocomposite samples showed improvement over that of the PP homopolymer. Best results were obtained in the case of KPPSA25C-M which contains 25 wt% KPPSA and prepared by a masterbatch route. For a given concentration of compatibilizer, irrespective of the compatibilizer type, the improvements in flexural moduli were better for samples prepared by masterbatch route compared to that prepared by direct mixing route. Nanocomposites prepared using PPMA as compatibilizer did not show any significant change in the flexural moduli with a change in concentration for either of the two methods of preparation. Paul and coworkers observed a similar behavior which they attributed to the dilution effects by a lower molecular weight PPMA[44]. Therefore, they suggested the use of 1:1 ratio of organoclay: PPMA to obtain maximum improvement in flexural moduli. Nanocomposites prepared using KPPSA as compatibilizer by direct mixing route showed a slight increase in flexural moduli with increase in the concentration of KPPSA from 15 wt% to 25 wt%. The increase was larger when the samples were prepared using the masterbatch route. However, the degree of enhancement in the flexural moduli of the high molecular weight PP/clay nanocomposites of the present study appear to be lower than that observed for low molecular weight PP/clay nanocomposites reported earlier[32].

6.4   Conclusions

The efficiency of a PP ionomer based on potassium succinate grafted PP (KPPSA) as compatibilizer for the preparation of high molecular weight PP/clay nanocomposites by melt mixing was evaluated and compared with a well known compatibilizer namely maleated PP (PPMA). The dispersion of the organoclay was found to be superior with KPPSA when the nanocomposites were prepared by a two step masterbatch route.

Exfoliated nanocomposites could be obtained with KPPSA at concentrations of 20 wt% and 25 wt%, while, only intercalated structures were obtained with PPMA as compatibilizer. Thermal stability of the nanocomposites is not influenced by the dispersion of clay or by the type of compatibilizer used. Well dispersed clay platelets act as nucleation centers resulting in enhanced crystallization rates and reduced spherullite size. Flexural modulus of the exfoliated nanocomposites prepared using an ionomer as compatibilizer showed significant improvements compared to intercalated nanocomposites prepared using PPMA. Use of higher molecular weight ionomers and higher ionic functionality may be desirable for obtaining further improvements in the flexural properties. Thus, an ionomer such as KPPSA is a better compatibilizer for the preparation of well-dispersed PP/organoclay nanocomposites and is found to be effective even with high molecular weight PP.

References

1. Usuki, A.; Hasegawa, N.; Koto, M. *Adv. Polym. Sci.* **2005**, *179*, 135.

2. Pinnavaia, T. J.; Beall, G. W. *Polymer-Clay Nanocomposites*, Wiley series in polymer science, **1997**.

3. Manias, E.; Touny, A.; Wu, l.; Strawhecker, K.; Lu, B.; Chung, T. C. *Chem. Mater.* **2001**, *13*, 3516.

4. Kato, M.; Usuki, A.; Okada, A. *J. Appl. Polym. Sci*. **1997**, *66*, 1781.

5. Kawasumi, M.; Hasegawa, N.; Kato, M.; Usuki, A.; Okada, A. *Macromolecules* **1997**, *30*, 6333.

6. Hasegawa, N.; Kawasumi, M.; Kato, M.; Usuki, A.; Okada, *A. J. Appl. Polym. Sci.* **1998**, *67*, 87.

7. Reichert, P.; Nitz, H.; Klinke, S.; Brandsch, R.; Thomann, R.; Mulhaupt, R. *Macromol. Mater. Engg.* **2000**, *275*, 8.

8. Ishida, H.; Campbell, S.; Blackwell, J. *Chem. Mater*. **2000**, *12*, 1260.

9. Varela, C.; Rosales, C.; Perera, R.; Matos, M.; Poirier, T.; Blunda, J. *Polymer Composites,* **2006**, *27*, 451.

10. Lopez-Quintanilla, M.L.; Sanchez-Valdes S.; Ramos de V.L.F.; Guedea, M. R. *Polymer Bulletin* **2006**, *57*, 385.

11. Galgali, G.; Ramesh, C.; Lele, A. *Macromolecules*, **2001**, *34,* 852.

12. Maiti, P.; Nam, P. H.; Okamoto, M.; Hasegawa, N.; Usuki, A. *Macromolecules* **2002**, *35,* 2042.

13. Liu, X.; Wu, Q. *Polymer* **2001**, *42*,10013.

14. Zhang Y-Q, Lee J-H, Rhee J. M., Rhee K. Y. *Composites Science and Technology* **2004**, *64*, 1383.

15. Tudor, J.; Willington, L.; O'Hare, D.; Royan, B. *Chem Commun* **1996***,* 2031.

16. Sun, T.; Garces, J. M. *Adv. Mater*. **2002**, *14***,** 128.

17. Barber, G. D.; Calhoun, B. H.; Moore, R. B. *Polymer* **2005**, *46*, 6706.

18. Chisholm, B. J.; Moore, R. B.; Barber, G. D.; Khouri, F.; Hempstead, A.; Larsen, M.; Olson, E.; Kelley, J.; Balch, G.; Caraher, J. *Macromolecules* **2002**, *35*, 5508.

19. Wang, Z. M.; Nakajima, H.; Manias, E.; Chung, T. C. *Macromolecules* **2003**, *36*, 8919.

20.   Shah, R. K.; Paul, D. R. *Macromolecules* **2006**, *39*, 3327.

21.   Lee, J. A.; Kontopoulou, M.; Parent, J. S. *Polymer* **2005**, *46*, 5040.

22.   Start, P. R.; Mauritz, K. A. *J. Polym. Sci., Polym. Phys.* **2003**, *41*,1563.

23.   Kovarova, L.; Kalendova, A.; Malac, J.; Vaculik, J.; Malac, Z.; Simonic, J. *Annu. Tech. Conf. Soc. Plast. Eng.* **2002**, *60*, 2291.

24.   Barber, G. D.; Carter, C. M.; Moore, R. B. *Annu. Technol. Conf. Soc. Plast. Eng.* **2000**, *58*, 3763.

25.   Govindaiah, P.; Mallikarjuna, S. R.; Ramesh, C. *Macromolecules* **2006,** *39,* 7199.

26.   Lili C.; Paul, D. R. *Polymer* **2007**, *48,* 1632.

27.   Dong, Y.; Bhattacharya, D. *Composites: Part A* **2008,** *39*, 1177

28.   Gianelli, W.; Ferrara, G.; Camino, G.; Pellegatti, G.; Rosenthal, J.; Thrombini, R. C. *Polymer* **2005**, *46*, 7037.

29.   Benetti, E. M.; Causin, V.; Marega, C.; Marigo, A.; Ferrara, A.; Ferraro, A.; Consalvi, M.; Fantinel, F. *Polymer* **2005**, *46,* 8275.

30.   Causin, V.; Marega, C.; Saini, R.; Marigo, A.; Ferrara, *J. Thermal. Anal. Cal.*, **2007**, *90*, 849.

31.   Fornes, T. D.; Yoon, P. J.; Keskkula H.; Paul, D. R. *Polymer* **2001**, *42*, 9929.

32.   Nguyen, V. K.; Jin, S. H.; Lee, S. H.; DAI SOO Lee, D. S.; Choe, S. *Composite Interfaces* **2006,** *13*, 299

33.   Marchant, D.; Jayaraman, K. *Ind. Eng. Chem. Res.* **2002**, *41*, 6402.

34.   Tjong, S. C.; Meng, Y. Z.; Hay, A. S. *Chem. Mater.* **2002**, *14*, 44.

35.   Kotek, J.; Kelnar, I.; Studenovsky, M.; Baldrian, J. *Polymer* **2005,** *46*, 4876.

36.   Fornes, T. D.; Yoon, P. J.; Keskkula, H.; Paul, D. R. *Polymer* **2002**, *43*, 2121.

37.   Pilati, F.; Toselli, M.; Messori, M.; Manzoni, C.; Turturro, A.; Gattiglia, E. G. *Polymer* **1997**, 38*,* 4469.

38.   Hambir, S.; Bulakh, N.; Kodgire, P.; Kalgaokar, R.; Jog, J. P. *J. Polym. Sci., Polym. Phys.* **2001**, *39*,446

39.   Kodgire, P.; Kalgaokar, R.; Hambir, S.; Bulakh, N.; Jog, J. P. *J. Appl. Polym. Sci.* **2001**, *81*, 1786.

40.   Maiti, P.; Nam, P. H.; Okomoto, M.; Kotaka, T.; Hasegawa, N.; Usuki, A. *Polym. Eng. Sci*. **2002**, *42*, 9.

41. Nam, P. H.; Maiti, P.; Okomoto, M.; Kotaka, T.; Hasegawa, N.; Usuki, A. *Polymer* **2001**, *42*, 9633.

42. Svoboda, P.; Zeng, C.; Wang, H.; Lee, J.; Tomasko, L. *J. Appl. Poly. Sci*. **2002**, *85*, 1562.

43. Ma, J.; Zhang, S.; Qi, Z.; Li, G.; Hu, Y. *J. Appl. Poly. Sci*. **2002**, *83*, 1978.

44. Kim, D. H.; Fasulo, P.D.; Rodgers, W. R.; Paul, D. R. *Polymer* **2007,** *48*, 5308.

Chapter 7

Conclusions

7. Conclusions

Various strategies were explored to obtain improved dispersion of clay layers in selected polymers such as poly(urethane)s, poly(carbonate)s, syndiotactic poly(styrene)s and poly(propylene)s. The resultant property enhancements of the nanocomposites were correlated with structure of the nanocomposites. The salient conclusions are as summarized below.

For the preparation of completely exfoliated and well-dispersed polyurethane/clay nanocomposites via *in-situ* polymerization, presence of tethering groups on the clay surface and an ability to form branched and crosslinked structure is necessary. Mere presence of either tethering functionalities in the organoclay or branch points in PU does not result in exfoliated structures. Incorporation of long alkyl chains, in addition to tethering hydroxyl groups, in the modifier structure of the clay did not significantly improve the compatibility of linear PU with the clay. Intercalated thermoplastic polyurethane/clay nanocomposites, prepared using poly(caprolactone diol) as soft segment and isophorone diisocyanate and 1,4-butanediol as hard segment show increase in storage tensile moduli at temperatures below glass transition temperature when compared to corresponding poly(urethane)s when functional groups capable of chemically reacting with the growing polymer chains are present in the clay modifier. This is indicative of improved interaction of the polymer with the clay surface.

Well dispersed and exfoliated PC/clay nanocomposites were prepared via in-situ melt polymerization using organoclays modified using phophonium cations containing reactive bisphenol functionalities. Interaction between the polymer chains and the clay layers are enhanced due to the enchainment and attachment of the polymer to clay surface through electrostatic forces. Such nanocomposites can be expected to have superior thermal, mechanical and barrier properties. However, the color of the nanocomposites still needs considerable improvements if such nanocomposites have to find significant practical applications.

Exfoliated sPS ionomer/organoclay nanocomposites were prepared via solvent casting. The interaction of sPS with organoclay was evaluated by introducing polar ionic functional groups such as metallic sulfonates with varying degree of sulfonation (ranging from 0.5 to 3.8 mole%) and differing nature of cations (H^+, Na^+, K^+ and Rb^+). Higher degree of sulfonation leads to better interaction with the polar silicate surface of the organoclay resulting in better intercalation/exfoliation. Increase in the size and polarizability of the cation ($Na^+ < K^+ < Rb^+$) result in higher degree of intercalation/exfoliation even at low degrees of sulfonation. Nanocomposites prepared using more thermally stable 1-hexadecyl-2,3-dimethylimidazolium cation modified clay are amenable to being processed at temperatures upto 300 °C without any appreciable degradation. The dispersed silicate clay layers partially restores the reduced crystallization rates of sPS ionomers by disrupting the ionic aggregation. Thus, it can be purported that fully exfoliated nanocomposites of polystyrene can be prepared by functionalizing the polymer chains with ionic groups.

The efficiency of a PP ionomer based on potassium succinate grafted PP (KPPSA) as compatibilizer for the preparation of high molecular weight PP/clay nanocomposites by melt mixing was evaluated and compared with a well known compatibilizer namely maleated PP (PPMA). The dispersion of the organoclay was found to be superior with KPPSA when the nanocomposites were prepared by a two step masterbatch route. Exfoliated nanocomposites could be obtained with KPPSA at concentrations of 20 wt% and 25 wt%, while, only intercalated structures were obtained with PPMA as compatibilizer. Thermal stability of the nanocomposites is not influenced by the dispersion of clay or by the type of compatibilizer used. Well dispersed clay platelets act as nucleation centers resulting in enhanced crystallization rates and reduced spherullite size. Flexural modulus of the exfoliated nanocomposites prepared using an ionomer as compatibilizer showed significant improvements compared to intercalated nanocomposites prepared using PPMA. Use of higher molecular weight ionomers and higher ionic functionality may be desirable for obtaining further improvements in the flexural properties. Thus, an ionomer such as KPPSA is a better compatibilizer for the

preparation of well-dispersed PP/organoclay nanocomposites and is found to be effective even with high molecular weight PP.

Thus, it has been demonstrated that when the interaction of the polymer chains with the layered silicate clay is improved either by modifying the surface of the clay to suitably interact with polymer or upon modifying the polymer by functionalization a better dispersion of clay in the polymer can be obtained. Improved intercalation and exfoliation behavior is observed when the polymer chains are anchored on the surface of the clay through the modifier or the polymer chains are sufficiently functionalized with polar groups such as ionomers. Properties of the resultant nanocomposites show good correlation with extent of clay dispersion in the polymer matrix.